Order Number 8821123

Singular solutions and an indirect boundary integral formulation for spherical shells

Simos, Nikolaos, Ph.D.

City University of New York, 1988

U·M·I
300 N. Zeeb Rd.
Ann Arbor, MI 48106

PLEASE NOTE:

In all cases this material has been filmed in the best possible way from the available copy. Problems encountered with this document have been identified here with a check mark __✓__.

1. Glossy photographs or pages _____
2. Colored illustrations, paper or print _____
3. Photographs with dark background _____
4. Illustrations are poor copy _____
5. Pages with black marks, not original copy __✓__
6. Print shows through as there is text on both sides of page _____
7. Indistinct, broken or small print on several pages __✓__
8. Print exceeds margin requirements _____
9. Tightly bound copy with print lost in spine _____
10. Computer printout pages with indistinct print _____
11. Page(s) _____ lacking when material received, and not available from school or author.
12. Page(s) _____ seem to be missing in numbering only as text follows.
13. Two pages numbered _____. Text follows.
14. Curling and wrinkled pages _____
15. Dissertation contains pages with print at a slant, filmed as received _____
16. Other _____

_____

_____

SINGULAR SOLUTIONS AND AN INDIRECT BOUNDARY INTEGRAL FORMULATION FOR SPHERICAL SHELLS

by

NIKOLAOS SIMOS

A dissertation submitted to the Graduate Faculty in Engineering in partial fulfillment of the requirements for the degree of Doctor of Philosophy, The City University of New York.

1988

This manuscript has been read and accepted for the Graduate Faculty in Engineering in satisfaction of the dissertation requirement for the degree of Doctor of Philosophy.

3/1/88
Date

Ali M. Sadegh
Chair of Examining Committee

3/1/88
Date

Jacques E. Benveniste
Executive Officer

Prof. Ali M. Sadegh (Chair)

Prof. Feridun Delale

Prof. Benjamin Been-Ming Liaw

Prof. Jacques Benveniste

Prof. David Hoetzel

Prof. Mumtaz Kassir
Supervisory Committee

The City University of New York

ABSTRACT

SINGULAR SOLUTIONS AND AN INDIRECT BOUNDARY INTEGRAL FORMULATION FOR SPHERICAL SHELLS

by

Nikolaos Simos

Adviser: Professor Ali M. Sadegh

Despite the various mathematical descriptions of the shell element, the analysis of practical engineering shell problems remains complex and rigorous. The development of numerical techniques has assisted such analyses to a great extend. However, the limits of applicability of the various computational techniques are not clearly delineated as yet and as a consequence new approaches and mathematical models continue to be introduced.

This investigation consists of three major parts. First, the singular solutions of a non-shallow spherical shell are derived in closed form. Such solutions correspond to the state of deformation and stress in a complete spherical domain under the action of surface point loads along the normal or tangential directions and concentrated surface moments. The singular loads involved apply in a

self-equilibating fashion. The mathematical analysis is performed for both classical and improved theories.

Next, an Indirect Boundary Integral Method is formulated by utilizing the derived singular solutions. The method is built upon the superposition principle and it involves the embedding of a partial spherical shell of arbitrary boundary and surface traction onto a complete sphere of which the singular solutions are known. The introduction of a set of uknown fictitious line vectors along the boundary, equal in number to the prescribed boundary conditions, and their incorporation into the coupled integral equations will ensure the satisfaction of the specified constraints along the boundary. The advantage of such approach over other methods is the reduction of the problem dimension by one.

Finally, the performance of the introduced technique is evaluated through the solution of a number of spherical shell problems under various types of surface loading and different sets of boundary constraints such as fixed, simply supported, free to move in the normal direction and free. Further, problems associated with stress concentration as well as a case of a spherical shell with a through crack are solved with the Boundary Integral Method. The results obtained are compared with the available analytical solutions and also with the Finite Element solutions and they demonstrate excellent agreement while at the same time project computational efficiency over the Finite Element Method.

AKNOWLEDGEMENTS

I wish to express my sincere appreciation to my adviser Professor Ali M. Sadegh for his support and guidance throughout the course of this research.

I also wish to extend my gratitude to all the members of my doctoral committee and especially to Professors Feridun Delale and Benjamin Been-Ming Liaw for numerous suggestions and discussions which helped me in the completion of the dissertation. My thanks also extend to the Department of Mechanical Engineering at the City College for providing me with financial support and teaching experience. Partial support of this research was provided from two grants, 6-63249 and 6-64237, from the Professional Staff Gongress of the City University of New York and it is deeply appreciated.

I want to thank Mr. and Mrs. John Sklavos for their love and support through all good and difficult times. Their tender caring will always mean a great deal to me.

I am thankfull to my wife Karen for standing by me in every step of the way. Her love and devotion made the completion of this work possible.

TABLE OF CONTENTS

Page

Page

Page

LIST OF TABLES

LIST OF FIGURES

Figure Page

Figure Page

Figure Page

Figure Page

LIST OF APPENDICES

CHAPTER I

INTRODUCTION

I.1 THE GENERAL SHELL PROBLEM

The elastic nature of thin shells presents a variety of properties useful to a designer interested in supporting large loads in constructions where light weight is a vitally important factor. This particular characteristic of thin shells is readily utilized in the aerospace, nuclear and marine industries. Their broad range of applications as well as their mathematical appeal, which is a consequence of their reliance upon the theory of space curves and differential geometry postulates, resulted in an extensive variety of solutions of both theoretical and engineering interest. In addition, the development and formulation of such solutions contributed to the construction of the foundations of the theory of thin shells upon which these solutions are based.

The theory of shells forms a part of the theory of elasticity associated with the study of the stress and displacement fields under the influence of given loads. In the three dimensional theory of elasticity the fundamendal equations are complicated and thus certain simplifying assumptions, which provide a reasonable description of the behavior of a thin elastic shell, had to be incorporated. The adoption of such assumptions led to the formulation of different

shell theories. The basic equations of thin shells have been derived by Love[31], and together with the assumptions upon which they are based, form the first approximation theory. Love's fundamental analysis had the greatest impact in the development of additional improved theories and the establishment of the broad theory of shells which, despite the simplifying postulates, remains mathematically rigorous.

The present analysis is concerned with the study of spherical shell domains in both theoretical and computational descriptions. The spherical shell, because of the unique geometry of its middle surface, represents a very distinct class of shells combining not only technical but also unmatched, compared to the surfaces of its kind, mathematical interest. The equations of the general shell theory are significantly simplified and still retain all the characteristics of a shell in their simplest form. They also display a number of properties of the flat plate. It is thus reasonable to suggest that the study of the behavior of shells in general should begin with the study of the analogous spherical shell problem. The study of the spherical shell in this investigation consists of the the discussion of solutions of various classes of problems through the utilization of the so called classical and improved theories. Furthermore, the integration and implementation of such analyses into innovative numerical techniques, necessary for the evaluation of complex physical systems with practical expectations, is emphasized and applied.

The exact and approximate solutions of particular shell problems derived over the years, in an effort to describe the state of stress and deformation in a shell, overwelmingly refer to a class of problems with convenient and symmetric geometric properties. The goal of these solutions was primarily to demonstrate the typical behavior of thin elastic shells and to that extent the goal has been accomplished. However, the study and analysis of arbitrary shell geometries under the influence of arbitrary loading functions departs from the guidelines set by the closed-form exact or approximate solutions and more rigorous mathematical approaches must be incorporated. Interest in studying practical physical problems, which constitute the rule rather than the exception, sets the stage for the integration of numerical techniques into the analysis of such problems that could arise within the framework of the theory of thin elastic shells.

In treating complex practical shell problems over the years three numerical methods were commonly used: the method of finite differences, the stepwise integration method and the finite element method. The recent developments and expansion of the range of applicability of the finite element method undoubtedly makes it the most attractive of the above three. However, the use of the shell element, as well as the interaction of many shell parameters and variables with the formulation of the solution, results in considerable ammount of computation time needed for the evaluation. In an effort to reduce computer time, an alternative numerical method made its way into the computational mechanics community. The so

called Boundary Integral or Boundary Element Method,(BIM or BEM), demonstrates a direct relation to the solution of the governing system of equations of the particular domain. BIM is based upon the implementation of the superposition principle as well as the Green's second identity and Betti's reciprocal theorem. Its mathematical integration with the physical problem is associated with the state of stress and deformation resulting from the action of concentrated excitations over the domain of interest. Such excitations, in the case of a shell, correspond to concentrated forces and moments applied at its middle surface. It is important to note that in the recent years BIM has been applied in the entire area of mechanics. The advantages of the method are the flexibility of its use and the characteristic requirement relating it to only the boundary of the domain. This characteristic is translated into treatment of only the boundary rather than the whole extend of the domain. Furthermore, the solution is fully continuous throughout the domain. The above features demonstrate the uniqueness of BIM among the possible alternatives. In the course of the development of the new treatment, two major directions which originate at a common origin have appeared. The Indirect Boundary Integral Method (IBIM) on one hand expresses the integral equations in terms of a unit singular solution of the governing differential equations. This solution is distributed over the boundary of the domain of interest in the form of a set of line vectors, which for the theory of elasticity correspond to load and moment vectors, enforcing the satisfaction of the boundary constraints. These unit singular solutions are also referred to as "free-space" Green's functions or Fundamental solutions of the

governing differential equations. The introduced vectors over the boundary are fictitious and they have no physical significance. Their evaluation from the integral equations, however, will lead to the evaluation of the field variables inside the domain by a simple integration process. One main characteristic of this approach is a consequence of its dependence onto the solution of the infinite domain which includes the particular problem. The embedding of the real domain onto the infinite region for which the Fundamental solutions have been derived for is often the way of applying the IBIM to particular problems and thus avoiding the derivation of the unit singular solutions for every distinct case.

In the Direct Boundary Integral Method (DBIM) the unknown functions that are incorporated into the integral equations are the physical variables of the problem. In elastostatics, for example, the integral equations will evaluate the displacement and stress fields at the boundary directly and consequently their counterparts inside the domain will be obtained from the boundary values by integration. Even though the two approaches utilize the same singular solutions, there are differences between them. Their basic difference is that while IBIM is based upon the principle of superposition, implying the linearity requirement, DBIM is closely related to Green's second identity and Betti's reciprocal theorem. The dependence of DBIM on these two principles consequently requires a more sophisticated approach which in turn requires more computational effort. Despite their differences, the two formulations are considered to be equivalent in terms of the accuracy of the solution attempted.

I.2 LITERATURE REVIEW

The governing differential equations of shells have been derived by several people, thus reflecting the interest as well as the effort to simplify the complex nature of the governing system. The amount of literature associated with the shell theory is nearly overwhelming. As mentioned earlier, the equations of the theory of thin shells have been first derived by Love[31]. His fundamental postulates, combined with the ones introduced by Kirchhoff, formed the basis for most of the theories that followed. The description of the postulates is given in the following statements:

1. Points which lie on one and the same normal to the undeformed middle surface also lie on one and the same normal to the deformed surface.
2. The effect of the normal stress on surfaces parallel to the middle surface may be neglected in the stress-strain relations.
3. The displacements in the direction of the normal to the middle surface are approximately equal for all points on the same normal

These assumptions eliminated some of the complexities of the system equations. The shell problem, however, is still quite laborious and the results of the analysis are not easy to obtain. Considerable simplification of the analysis have been achieved with the introduction of the assumption of shallowness. Such simplifications are due to the neglect of the of the contribution of the transverse

shearing stress resultants to the equilibrium of forces in the meridional and tangential directions, and the neglect of the contributions of the "stretching" displacements u_r and u_θ to the change of curvature expressions. Because of the order of simplification most published work is associated with shallow shells. On the other hand inclusion of additional parameters into the construction of the theory, such as transverse shear effect, add to the complexity of the problem by increasing the order of the governing equations. As a result, the literature supporting such theories is limited.

Attention is focused on the part of literature studying the effects of concentrated loads onto shell domains and on the derivation and construction of appropriate Green's functions or Fundamental solutions associated with the theory of shells. The application of the Boundary Integral formulation, and in particular its indirect approach, are also considered. Finally, some publications incorporating the transverse shear effect on shell and plate domains containing cracks are referred to.

E. REISSNER[1,2], using the shallow shell approach to a rotationally symmetric spherical cap, obtained closed-form solutions for the displacement and stress functions. His solution that resulted from two simultaneous fourth order equations was reduced to two independent second order equations. The introduction of auxiliary variables into the general system of equations of either shallow or non-shallow shells is used extensively and appears to be the most

effective approach in reducing the primary system of governing equations. With his solution he facilitated three rotationally symmetric problems which can provide "exact" solution results in the immediate area of the concentrated load applied at the pole. It is apparent that Reissner's solution is only valid within the limits of the shallow region in a shell. In addition, Reissner was able to compare his results with the corresponding results for a flat plate by utilizing the same general solution. The above has been attempted by several authors in investigations of shallow spherical shell problems. It is not only because the spherical shell displays the characteristics of a shell in the simplest manner but also because it retains a number of properties of the flat plate that makes its study so attractive.

In [3], Reissner considered the unsymmetrical deformation of shallow spherical shells due to a tilting moment and a side force acted upon a rigid insert around the pole. The significance of that report is owed to the finding that univalued stress functions and axial displacement components give rise to multivalued expressions for radial and circumferential displacement components. The introduction of additional multivalued stress functions results in univalued displacement functions. In addition he found that the nature and form of the side force solution differs in important respects from the corresponding known solution of a flat plate.

S. LUKASIEWICZ [15] considered stress and displacements due to concentrated loads and obtained simple solutions corresponding to a

normal force, a tangential force and a bending moment applied at the pole of a shallow spherical cap. In deriving his solutions he assumed that the components of stress and displacement are small at some distance from the loading point while the effect of the boundary conditions is limited to a small area near the edge of the shell and it was neglected. His method of solution involved the application of Fourier integrals to the shallow shell equations and the stress and displacement expressions were obtained in closed form. His results can be used as reference to the behavior of the shell region near the pole where the loads apply.

G.N. CHERNYSHEV [16] provided a complete study of the effect of concentrated forces and moments on elastic thin shells of arbitrary plan form. He derived the singular solutions for the shallow class of shells and he examined the nature of peculiarities of the stress and displacement functions in the neighborhood of the point load. For the solution of the general problem he made use of the fundamental solutions of partial differential equations of the elliptic type and he obtained the explicit form of the principle singularities of the displacement and stress resultant functions. He succeeded in showing the relation of the kernels of a unit normal force and a unit normal moment applied onto the shell surface. That relation, which is associated with the principle singularities of the kernels, will be discussed extensively in the section where the concentrated moment kernels are to be derived.

J.L. SANDERS [10] obtained similar singular solutions for shallow shells of arbitrary plan form. His theoretical investigation focused onto multivalued singular solutions of the shallow shell equations that physically correspond to concentrated loads and dislocations. The multivalued solutions are the result of multivalued stress functions. By using the shell equations in complex form he made a unified treatment of the load and the dislocation problem possible. He also discussed the difficulties associated with the defining of the uniqueness of the fundamental singular solutions in the neighborhood of the singular point and the application of conditions on the behavior of the solutions in the neighborhood of infinity. The behavior of the singular solution at infinity is of critical importance to a shallow shell which theoretically extends to infinity. Finally complete closed-form solutions of a shallow sphere are deduced from the general solution.

A more detailed solution derived by utilizing the findings of the previous analysis [10] was presented by J.L. SANDERS and J.G. SIMMONDS [8]. Solutions for the normal displacement and the two tangential displacements for a shallow cylindrical shell subjected to concentrated forces were investigated. The results for the displacements were expressed in terms of elementary functions and modified Bessel functions while the Fourier series form, used by several investigators, was avoided. When the Fourier series form is used , it is very difficult to obtain numerical results because of poor convergence, and it is virtually impossible to gain any insight into the true nature of the solution.

J.G. SIMMONDS and C.G. TROPF [9] presented a complete characterization for the fundamental solution of the complex-valued differential operator governing the linear behavior of a shallow, elastically isotropic hyperbolic paraboloidal shell. The fundamental solution is expressed in the form of a Fourier series. It should be noted that the approach used above could serve, to their remarks, other classes of shells when the parameter λ (ratio of the radii of curvature), which is a parameter in the differential operator, is appropriately adjusted.

K. FORSBERG and W. FLUGGE [12] developed solutions for non-axially symmetric shallow shells that have the form of an elliptic paraboloid near their vertex. In the case of a spherical shallow cap the singular solutions can be expressed in closed form while in the case of non-axisymmetric domain the solutions have infinite-series representation. The rapid convergence of the series is a function of the geometric properties of the particular shell. Detailed graphical results are also presented for the stress and radial displacement of a shell subjected to a point load at its vertex.

W. FLUGGE and R.E. ELLING [13] developed solutions for non-symmetric shallow shells subjected to normal surface loading and thermal loading. The singular solutions were identified by a consistent limiting process applied to the complete set of singular solutions. Numerical results were presented for the case of the normal concentrated load acting on shallow shells with negative, zero or positive Gaussian curvature. The solution is expressed in the form of

a rapidly converging harmonic series. The limiting process mentioned earlier utilizes the solution of a shell with distributed loading over a finite area by reducing the area of loading while maintaining the load resultant constant.

R.P. NORDGREN [17] applied the method of Green's function to the quasi-static thermoelastic theory of shallow shells. In addition, the effect of transverse shear deformation with reference to an unlimited shallow spherical shell under specified temperature field and normal surface traction. The solution was obtained through the Green's function and the character of the singularities was compared with the corresponding classical theory solutions.

Thus far singular solutions associated with the theory of shallow shells were considered. As already mentioned, all of the above solutions are valid in the part of the shell domain where the shallowness assumption is retained. However, the nature of the singularities and their behavior around the point of application is preserved and thus making the comparison of shallow and non-shallow solution kernels possible.

In the area of the non-shallow theory of shells, where the present investigation is confined, singular solutions have also been studied in an effort to obtain a complete solution. The particularly simple geometry of the spherical shell suggested that if such a solution was attainable, it would best be demonstrated in a spherical shell.

W.T. KOITER[18] obtained closed form solutions for the case of a complete sphere under point loads at its poles. The evaluation of his solution led to a complete verification of the membrane theory at some distance from the poles and to a virtually complete verification of Reissner's results near the poles. The most important discrepancy with Reissner's results is that not only the bending moments, but also the stress resultants have singularities at the poles. He also found that the relative error of shallow shell theory on the normal deflection at the pole is of order h/R ln(h/R), i.e.,slightly larger than the relative error of order h/R which is inherent in the basic shell equations.

J.G. SIMMONDS[7] derived the "free space" Green's functions for two uncoupled, second order operators acting onto two complex-valued functions in terms of which the field equations were reduced. The fundamental solutions of the two operators are of a closed spherical shell under arbitrary, self-equilibrated surface loads. The non-shallow fundamental solutions were compared against the corresponding solutions of the shallow shell theory and Koiter's observation on the order of the error introduced, h/R ln(h/R), was reconfirmed.

J.G. BERRY[19] applied the classical non-shallow theory approach to solve two example shell problems. The first example was that of a complete hemispherical shell subjected to concentrated edge moments. The concentrated moments were distributed over the edge in the form of a series and became boundary conditions for the problem. The second example considered was that of a hemisphere with a

concentrated load at the appex and supported at two points. In an effort to hold the tangential displacements single-valued, Berry ommited certain terms from his analysis and thus regarding his solution approximate. Results of his approximate solution are compared to similar results obtained from the shallow solution of Reissner. The reduction of the general equations in this investigation for the classical theory approach follows the same guidlines used by Berry.

J.P. WILKINSON and A. KALNINS[23,24] obtained an exact solution for the Green's function of an open rotationally symmetric spherical shell subjected to any consistent boundary conditions. Their fundamental solution corresponds to a concentrated normal load solution in the shell domain and is accompanied by a regular solution in the form of an infinite series. The general solution was obtained within the scope of the improved theory addressed by Naghdi[6], in which not only the transverse shear but also rotatory inertia was included. An example problem was solved and the singularities due to the concentrated normal load for the three different theories, classical, improved and shallow were examined. In [24] they derived solutions for the deformation of thin open spherical shells explicitly in terms of Legendre functions. In these solutions the effects of transverse shear and rotatory inertia were fully accounted for. Results were obtained for an open spherical shell with a rigid insert subjected to horizontal force and/or moment and compared with similar results of the shallow theory of shells. In addition, the solution to the problem of a concentrated lateral force and moment at

the shell appex was obtained from the general formulation and the singularities of the dependent variables were identified.

The effect of transverse shear deformation has already been mentioned and included in the investigations [23,24]. The principal result of the implementation of the above effect into the analysis of the above effect is the upgrading, in terms of the order, of the system of differential equations governing the deformation and stress matrices of the problem. With the new system it is possible and necessary to satisfy five boundary conditions along a shell boundary instead of the four conditions which Kirchhoff has established for the classical theory.

The role of transverse shear was first discussed by E. REISSNER[3] on bending of elastic plates. The inaccuracies of the classical theory of plates associated with the treating of problems of stress concentration around holes when compared to experimental results and on the other hand the substantial agreement of the improved theory results with the same experiment, confirmed the need of the new theory for the treatment of such problems. His assumption of the parabolic variation of the transverse shear stresses over the thickness of the plate led to the introduction of the tracer $k_s^0 = 6/5$ that identifies the shear deformation terms in the analysis. The same transverse shear stress variation, $\tau_{iz} = \frac{V_i}{2\ h/3}\left[\ 1 - \left(\ \frac{\zeta}{h/2}\ \right)^2\ \right]$, is also used in shell theory analysis resulting in the same value for the shear coefficient K_s^0.

Explicit solutions on the effect of transverse shear deformability on stress concentration factors were obtained by E. REISSNER and F.Y.M. WAN [4] for the problems of transverse twisting and tangential shearing of shallow spherical shells with a small circular hole.

P.M. NAGHDI[5] deduced a system of differential equations for thin shallow elastic shells with small displacements that include the effect of transverse shear deformation. Naghdi's general equations, when applied to spherical coordinates, formulated the governing system for the works of Wilkinson and Kalnins[23,24]. The most interesting point in Naghdi's analysis is that with the introduction of an Airy's stress function he obtained an eighth-order differential equation in the normal displacement. Different approaches to the reduction of the primary system in the theory of shells have usually resulted in a sixth-order equation governing the radial displacement.

C. PRASAD[25] dealt with the vibrations of a non-shallow spherical shell with both the effect of the transverse shear and rotatory inertia accounted into the analysis. A suitable choice of auxiliary variables reduced the primary system of five second-order partial differential equations to a secondary system of three equations: an uncoupled sixth-order differential equation in the transverse displacement W, an uncoupled second-order equation in an auxiliary variable Λ, and a coupled equation in Λ and another auxiliary variable Ψ. Prasad's reduction procedure was used in this investigation to deduce the secondary system of equations after neglecting the rotatory inertia terms.

A step further from the work of Reissner and Wan [4] on concentration factors is the incorporation of the shear effect into the analysis of shell problems that include cracks inside their domain. F. DELALE and F. ERDOGAN[29] applied the improved theory of shallow shells in a thin spherical cap containing a through crack. A specially orthotropic as well as an isotropic material was considered. The results found for the shells were quite similar to those of flat plates. Thus as expected, the angular distribution of bending and membrane stress resultants around the crack surface are invalid when obtained through the classical theory analysis. The above statement was confirmed by F. ERDOGAN and J.J. KIBLER[27] who derived stress intensity factors around a meridional crack in a shallow spherical shell using the classical theory approach.

The use of boundary integral equation procedures in elastic analysis is rather extensive. The intricacies and the different approaches to the method are well comprehended by P.K. BANERJEE and R. BUTTERFIELD[36]. However the use of the Indirect Boundary Integral Method on plate and shell problems is limited.

A.M. SADEGH and N.J. ALTIERO [33,34] applied the IBIM to the problem of a finite, plane, linear-elastic region containing a crack or an arbitrarily shaped hole.They developed the Green's function of the problem in the form of two complex potential functions. Their method involved the embedding of the region of interest in an infinite plane and the application of a layer of body force onto the boundary contour. The satisfaction of the appropriate boundary conditions led to the desired solution within the domain.

Similar methods were used by N.J. ALTIERO and D.L. SIKARSKIE[35] on thin plate problems. Their method involved the embedding of the real plate in a fictitious plate for which the Green's function is known. An unknown load vector, in the form of transverse line load and normal boundary moment, was introduced around the contour of the real boundary. The satisfaction of the boundary constraints of the real plate led to a vector integral equation in terms of the unknown boundary loads. Several example cases were considered and the inaccuracies of the indirect method near the boundary were addressed.

I.3 GOAL AND EXTEND OF PRESENT RESEARCH

The main goal of this research is to derive the singular solutions of the governing differential system and also to provide a complete formulation of the Indirect Boundary Integral Method with application on spherical shell problems. It has already been mentioned that extensive interest in the response of a shell due to concentrated excitation led to different forms of singular solutions, the overwhelming majority of which refer to the shallow approach. Our intention in this investigation is to derive a new form of the singular solutions, Green's functions, that would not only reflect the nonshallow treatment of the shell but most importantly these solutions to be of closed form. Further reasons that led to the undertaking of this effort, despite the existence and wide use of other numerical techniques, have been briefly addressed earlier in this chapter. However, the particularities of this class of problems,

the complexity of the governing system and lastly the broad applicability of the theory of shells in general in modern technology, do provide space for new methods that combine reliability, accuracy and efficiency. The fundamental principle that the new method is formed upon is that of superposition and therefore it can only be applied to linear or incrementally linear systems. As a general picture, a very limited class of problems solvable by finite element methods cannot be solved at least as efficiently by BIM. It is the property of BIM which reduces the dimensions of the problem by one that has such an effect on the efficiency aspect of the comparison. Thus for two-dimensional problems the analysis will be the one of a one-dimensional boundary integral equation and for three-dimensional problems only two-dimensional surface integrals will be incorporated. We should also note that when dealing with problems involving surface tractions(given),i.e. in a two-dimensional problem, the domain as well as the boundary must be discretized and it so seems that the advantage of dimension reduction is no longer valid. However, even in those cases the effect of the surface vectors will not increase the order of the system. Further, for a very large class of engineering problems only the boundary needs to be manipulated. The coefficient matrix of the system, in general, is fully populated when generated by BIM while banded when constructed by finite element methods. Nevertheless, significant ammount of computer time is required to arrive to the final banded form of the FEM global stiffness matrix. To conlude the comparison of the two techniques we must stress the fact that it is the computational time required for the analysis of a problem that becomes the critical

factor in choosing one technique over the other. In this investigation comparisons will be performed in terms of the accuracy as well as the efficiency of these two methods. The purporse of the comparison, however, is not to discredit any of the two methods but rather to give an insight that would eventually combine the advantages of both techniques into a powerful engineering tool.

The indirect character of the BIM approach and the finite geometric extent of the domain of interest, closed sphere, requires the derivation of very carefully chosen fundamental solutions which will not only satisfy all the conditions that a singular fundamental solution must satisfy but also insure equilibrium of the complete domain. In Chapter II the new form of the singular solutions is derived by utilizing the idea of a self-equilibrated complete sphere. The common ground with the previous analyses is in the general governing system of equations. The final form of the governing system, adjusted to the needs and the scope of the present analysis, is derived in Appendix A. The governing differential equations are utilized and solved in Chapter II to provide the singular solutions for concentrated normal loads, concentrated tangential loads and concentrated surface moments. All the above solutions are obtained for both the classical and the improved theory of shells and a detailed study of their singular behavior and their differences is also presented.

The new formulation of the Boundary Integral scheme for spherical shell is presented in Chapter III. The unique approach of the method,

incorporated in this investigation, is based upon the principle of superposition and the embedding of the spherical shell problem onto a complete sphere. Such principles have only been applied, so far, to plane and plate problems. The method itself can be viewed according to the following sequense of steps:

a. The domain of interest is embedded onto the complete sphere for which the fundamental solutions have been derived.

b. A fictitious boundary is introduced, not necessarily over the closed line that corresponds to the real boundary, and a set of integral equations is formed that will satisfy the boundary constraints.

c. The solution of the system provides the complete stress and displacement matrices over the real domain.

The fictitious boundary line is introduced away from the real boundary line that bears the constraint requirement only for the reason of avoiding integrations over singular points. Such approach has a noticable impact not only in the amount of computational time required but also on the smoothening of the dependent variable functions in the vicinity of the boundary.

In Chapter IV a set of shell problems are solved in order to justify the validity of the mathematical analysis that produced the singular solutions and the performance and accuracy of the developed Boundary

Integral numerical scheme. The choice of example problems presented reflect our interest in demonstrating the response of a spherical shell when subjected to different sets of boundary constraints and different types of surface loading. Our intentions also are to discuss and evaluate the differences between the two shell theories through actual shell problem solutions. Thus problems with clamped, simply supported, free to move in the normal direction and free boundaries are solved and compared with the available analytical solutions as well as the FEM solutions obtained with the ANSYS code. The problems evaluated reveal on one hand the effect of concentrated loads and the influence of the boundary conditions and on the other hand demonstrate the excellent agreement of the proposed numerical approach, IBIM, with the analytical and FEM solutions. Further, in order to test the limitations of IBIM, a shell problem containing a through crack is evaluated and compared with the available analytical solution. The advantages of the Indirect Boundary Integral formulation in terms of computation time become apparent in the treatment of rather complex systems. In addition, the different sets of boundary constraints, such as conditions of free edge, make possible a thorough and complete study of the stress concentration fields around openings as well as stress intensities in the neighborhood of cracks. The advantage of studying such cumbersome systems with the IBIM is that no particular effort is needed other than the usual procedure of solving any shell problem.

It is these advantages of BIM that project the future of the technique and its participation in the modern engineering practices.

However, a number of aspects of the shell theory still need to be analyzed and incorporated into the boundary integral code for it to become a complete and fully effective tool. Nevertheless, the goal of the present effort has been achieved by successfully demonstrating, through the solution of a wide class of shell problems, the effectiveness of the technique in its interaction with complex physical systems.

CHAPTER II

DERIVATION OF THE FUNDAMENTAL SINGULAR SOLUTIONS

II.1 CLASSICAL THEORY

Love's first approximation to the theory of thin elastic shells and its closely related versions constitute what is known as the classical theory of shells. The basic equations which describe the behavior of a thin shell are derived on the basis of the well known and already introduced Love-Kirchhoff postulates. These simplifying assumptions were incorporated into the equations of equilibrium of a thin shell element (see Appendix A). In addition, the introduction of an auxiliary stress function F, which relates to the stress resultants of the element as shown in Eqns.(A.18), led to the the secondary or reduced system of governing equations for the spherical nonshallow shell domain. The symmetric stress resultant $N_{\alpha\beta}$, stress couple $M_{\alpha\beta}$, bending strain $k_{\alpha\beta}$ and extensional strain $\epsilon_{\alpha\beta}$ tensors are reduced to a system of two coupled equations in terms of the radial displacement W and the stress function F. For the particular case of a shell domain under the action of normal surface traction q_n, the uncoupled form of the governing system takes the following form [also recorded as Eqns. A.21,22]:

$$(\nabla^2 + 2)\left[\nabla^4 + 2\nabla^2 + \frac{EhR^2}{D}\right] W = \frac{R^4}{D}[\nabla^2 + 1 - \mu)\, q_n \qquad (2.1)$$

and

$$(\nabla^2 + 2)\, F = \frac{D}{R}\left[\frac{R^4}{D} q_n - (\nabla^2 + 2)^2 W\right]. \qquad (2.2)$$

Eqn. 2.1 governs the normal displacement W of a spherical shell loaded with normal surface traction. It should be pointed out that, within the scope of Love's postulates, the equations above correspond to the exact solution. The shallow shell treatment gives a very good approximation to this solution whenever the assumption of shallowness is valid.

A basic problem in the linear theory of elastic shells is the construction of the fundamental solutions or "free space" Green's functions for the governing differential system. By definition the Green's function of a system can be expressed in the form

$$G = G_s + G_r \qquad (2.3)$$

where G is a dependent variable of a solution state, G_s corresponds to a singular solution state, or known as fundamental solution, and G_r represents a regular solution state.

The determination of the singular state G_s for various shell plan forms has been the topic of several investigations indicative of the extensive literature on the subject. In the course of the derivation of a fundamental singularity, several questions arise as to what conditions or relations such a singular solution must satisfy at the pole. The two obvious conditions, which imply that the fundamental singularity must be (a) a solution of the governing differential equation, and (b) singular at the pole, are usually not sufficient. For a spherical shell in particular, the fundamental singularity corresponds to an axisymmetric concentrated load solution and it is reasonable to demand that such a solution, in the limit as the load point is approached, satisfies (a) equilibrium normal to the middle surface, (b) the vanishing of the meridional displacement u at the pole, $\lim_{\phi \to 0} u_\phi = 0$, and also the vanishing of the rotation of the normal β according to $\lim_{\phi \to 0} \beta_\phi = 0$. In addition the fundamental singularity is required to satisfy the Green's identity (reciprocal theorem) everywhere in the region.

However, when constructing the fundamental singularity, the physical conditions of equilibrium and vanishing of displacement vectors at the pole which result from axisymmetry, should not be imposed as priori. Such approach could lead to the incorrect form of the Green's function. The only requirement that needs to be satisfied and incorporated into the differential operator is the existence of a concentrated singular load which produces the singular field.

II.1.1.1 FUNDAMENTAL SOLUTION OF NORMAL SURFACE TRACTION

We shall obtain the fundamental solutions associated with a unit concentrated load applied at an arbitrary point $\underset{\sim}{x}'(\phi',\theta')$ of the middle surface of a complete sphere. When constructing the "free space" Green's function, in addition to the requirements mentioned earlier, we should also require that the equilibrium of the shell domain be preserved. This is due to the fact that the domain of interest is of finite extend. When dealing with shallow shells or infinite plates such requirement need not to be met simply because load vectors at infinity can satisfy equilibrium without effecting the solution in the neighborhood of the pole.

The equilibrium requirement is accomplished through the application of an equilibrating normal surface traction, axisymmetric with respect to the axis that pierces the point $\underset{\sim}{x}'(\phi',\theta')$ where the unit concentrated load is applied. The fundamental solution will be the solution of the differential operators of Eqns. 2.1, 2.2 subject to the loading conditions described above and it will be constructed from their complimentary as well as their particular integrals. Again, this solution is required to have a definite singularity at a single point and to satisfy the Green's identity everywhere in the domain.

The unit concentrated load is applied at point $\underset{\sim}{x}'(\phi',\theta')$ in the form of a two-dimensional Dirac Delta distribution $\delta(\underset{\sim}{n} - \underset{\sim}{n}')$ where $\underset{\sim}{n}'$ is

the unit normal vector at $\underset{\sim}{x}'(\phi',\theta')$ and $\underset{\sim}{n}$ is the unit normal vector at an arbitrary field point $\underset{\sim}{x}(\phi,\theta)$ of the middle surface. The two unit vectors can be related in terms of the surface coordinates (ϕ,θ) through the expression

$$\underset{\sim}{n} \cdot \underset{\sim}{n}' = \cos\gamma = \cos\phi\cos\phi' + \sin\phi\sin\phi'\cos(\theta - \theta') \tag{2.4}$$

where γ is the angle between the two unit vectors as shown in Fig. 2-1.

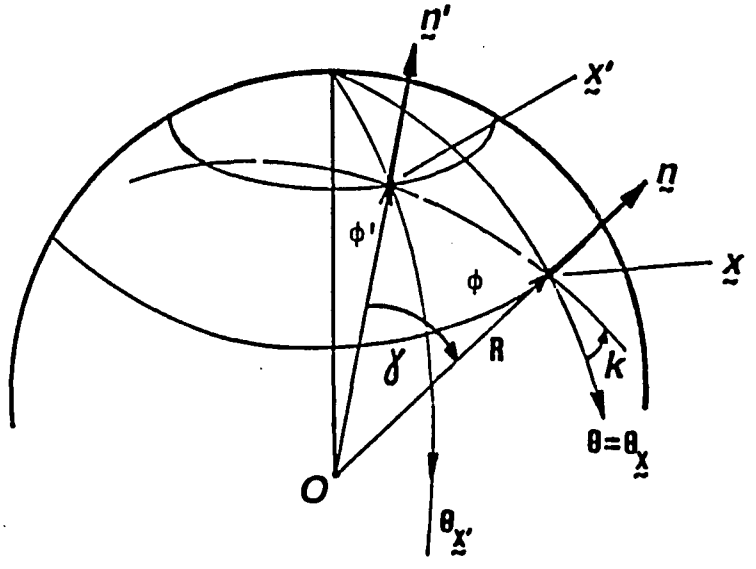

Figure 2-1. Global and local spherical surface coordinates.

We introduce a geographical coordinate system (γ,η) with the north pole $\gamma = 0$ coinciding with the unit vector $\underset{\sim}{n}'$. The two-dimensional

Delta function in the new system will also be axisymmetric and, since it is applied at its pole, will take the form

$$\delta (\underset{\sim}{n} - \underset{\sim}{n}') = \frac{\delta (\gamma)}{2 \pi R^2 \sin\gamma}. \qquad (2.5)$$

The axisymmetrically distributed normal surface traction denoted as $q_{n'}$ must be of such form as to produce a unit resultant force opposing the resultant generated by the Delta function. Its distribution over the whole surface will be of the form

$$q_{n'} = - \frac{3}{4\pi R^2} \cos \gamma. \qquad (2.6)$$

Thus, we seek a solution to the Eqn.(2.1) with

$$q_n = \frac{1}{R^2} \left[\frac{\delta (\gamma)}{2 \pi \sin \gamma} - \frac{3}{4 \pi} \cos\gamma \right]. \qquad (2.7)$$

The symmetry of the domain suggests that the operators in Eqns. 2.1, 2.2 are invariant to rotations and that their solution must be a function only of the surface coordinate γ. Substitution of Eqn. 2.7 into 2.1 leads to

$$(\nabla^2 + 2) [\nabla^2 + \nu (\nu + 1)] [\nabla^2 + \lambda (\lambda + 1)] W =$$

$$= \frac{R^2}{D} (\nabla^2 + 1 - \mu) \left[\frac{\delta(\gamma)}{2\pi \sin \gamma} - \frac{3}{4\pi} \cos \gamma \right] \qquad (2.8)$$

where ν and λ are complex conjugate parameters and relate to the shell constants according to the following relations

$$\nu\ (\nu + 1) + \lambda\ (\lambda + 1) = 2 \tag{2.9a}$$

$$\nu\ (\nu + 1) \cdot \lambda\ (\lambda + 1) = \frac{EhR^2}{D} \tag{2.9b}$$

and

$$\nu\ (\nu + 1) = 1 + i \tan \psi \tag{2.9c}$$

$$\lambda\ (\lambda + 1) = 1 - i \tan \psi \tag{2.9d}$$

such as,

$$\chi \cos\psi = 1 \tag{2.9e}$$

$$\chi^2 = \frac{EhR^2}{D}. \tag{2.9f}$$

The Laplacian operator ∇^2 in the new axisymmetric coordinate system (γ,η) will take the form

$$\nabla^2 = \frac{d^2}{d\gamma^2} + \cot\gamma \frac{d}{d\gamma}. \tag{2.10}$$

Let the normal displacement function $W(\underset{\sim}{x};\underset{\sim}{x}')$ in Eqn. 2.8 be written in the following equivalent form

$$W(\underset{\sim}{x};\underset{\sim}{x}') = W_1(\underset{\sim}{x};\underset{\sim}{x}') + W_2(\underset{\sim}{x};\underset{\sim}{x}') \tag{2.11}$$

and (2.8) can be written as

$$(\nabla^2 + 2) + [\nabla^2 + \nu\ (\nu + 1)]\ [\nabla^2 + \lambda\ (\lambda + 1) \begin{pmatrix} W_1 \\ W_2 \end{pmatrix} =$$

$$= \frac{R^2}{D}\ (\nabla^2 + 1 - \mu) \begin{pmatrix} \frac{\delta(\gamma)}{2\pi \sin\gamma} \\ -\frac{3}{4\pi} \cos\gamma \end{pmatrix}. \qquad (2.12)$$

The particular solution of Eqn. 2.12, associated with the distributed surface traction $q_{n'}$, leads to the following expression

$$W_2\ (\underset{\sim}{x};\underset{\sim}{x}') = -\frac{\mu + 1}{4\pi\ Eh}\ [\ 1 + \cos\gamma\ \ln(1 - \cos\gamma)\ ] \qquad (2.13)$$

We observe a singular character of the particular solution at $\gamma = 0$ eventhough it is introduced by a nonsingular loading function. However, the singularity is retained since the complete solution of Eqn. 2.12 would require the presence of such singularity.

In order to obtain the particular integral that is introduced by the Delta function distribution, we incorporate a scalar function $U_s(\underset{\sim}{x};\underset{\sim}{x}')$ which relates to $W_1(\underset{\sim}{x};\underset{\sim}{x}')$ according to the relation

$$W_1\ (\underset{\sim}{x};\underset{\sim}{x}') = \frac{R^2}{D}\ (\nabla^2 + 1 - \mu)\ U_s(\underset{\sim}{x};\underset{\sim}{x}'), \qquad (2.14)$$

provided that the function U_s satisfies the differential operator

$$(\nabla^2 + 2)[\nabla^2 + \nu(\nu + 1)]\ [\nabla^2 + \lambda(\lambda + 1)]\ U_s(\underset{\sim}{x};\underset{\sim}{x}') = \frac{\delta(\gamma)}{2\pi\ \sin\gamma}. \qquad (2.15)$$

Because of the distribution form of the Delta function we would expect that away from the singular point, $\gamma = 0$, $U_s(\underset{\sim}{x};\underset{\sim}{x}')$ is the homogeneous solution of Eqn.(2.15), while in the vicinity of the singularity such solution must satisfy the existence of the Delta function distribution. That will be accomplished through the singular character of the homogeneous solution that will be retained. Thus, in order to arrive at the general form of the homogeneous solution of Eqn.(2.15), we express U_s in the following equivalent form

$$U_s\ (\underset{\sim}{x};\underset{\sim}{x}') = U_1\ (\underset{\sim}{x};\underset{\sim}{x}') + U_2\ (\underset{\sim}{x};\underset{\sim}{x}') + U_3\ (\underset{\sim}{x};\underset{\sim}{x}') \tag{2.16}$$

such as

$$(\ \nabla^2 + 2\ )\ U_1\ (\underset{\sim}{x};\underset{\sim}{x}') = 0 \tag{2.17a}$$

$$[\nabla^2 + \nu\ (\nu + 1)]\ U_2\ (\underset{\sim}{x};\underset{\sim}{x}') = 0 \tag{2.17b}$$

$$[\nabla^2 + \lambda\ (\lambda + 1)]\ U_3\ (\underset{\sim}{x};\underset{\sim}{x}') = 0. \tag{2.17c}$$

The solution of Eqns.(2.17) lead to the following general expressions

$$U_1\ (\underset{\sim}{x};\underset{\sim}{x}') = A_1\ P_1\ (\cos\gamma) + B_1\ Q_1\ (\cos\gamma) \tag{2.18a}$$

$$U_2\ (\underset{\sim}{x};\underset{\sim}{x}') = A_2\ P_\nu\ (\cos\gamma) + B_2\ Q_\nu\ (\cos\gamma) \tag{2.18b}$$

$$U_3 (\underset{\sim}{x};\underset{\sim}{x}') = A_3 P_\lambda (\cos\gamma) + B_3 Q_\lambda (\cos\gamma) \qquad (2.18c)$$

where $P_{1,\nu,\lambda} (\cos\gamma)$ and $Q_{1,\nu,\lambda} (\cos\gamma)$ are the Legendre functions of the first and second kind respectively.

According to Eqn. 2.16 all six independent solutions obtained above will constitute the general expression of the homogeneous solution $U_s(\underset{\sim}{x};\underset{\sim}{x}')$. However, since the solution is required to be singular at a single point on the complete spherical surface and because $Q_1(\cos\gamma)$, $Q_\nu(\cos\gamma)$ and $Q_\lambda(\cos\gamma)$ present singularities at two points of the domain ($\gamma = 0$ and $\gamma = \pi$), their contribution toward the construction of the fundamental solution must be eliminated. On the other hand, $P_1(\cos\gamma)$ is regular everywhere in the domain while $P_\nu(\cos\gamma)$ and $P_\lambda(\cos\gamma)$ present a singularity at $\gamma = \pi$. Because the solution that survives will be evaluated upon the existence of a singular effect at $\gamma = 0$, the regular function $P_1(\cos\gamma)$ can be ignored for the moment since it can only lead to rigid body displacements. Thus the final form of the singular homogeneous solution of $U_s(\underset{\sim}{x};\underset{\sim}{x}')$ is expressed as

$$U_s (\underset{\sim}{x};\underset{\sim}{x}') = A_2 P_\nu (\cos\gamma) + A_3 P_\lambda (\cos\gamma) \qquad (2.19a)$$

or, in order for the singular character to appear at $\gamma = 0$, equivalently

$$U_s(\underset{\sim}{x};\underset{\sim}{x}') = A_2 P_\nu(-\cos\gamma) + A_3 P_\lambda(-\cos\gamma). \qquad (2.19b)$$

Because of the complex conjugacy between the parameters ν and λ, it also follows that $P_\nu(-\cos\gamma)$ and $P_\lambda(-\cos\gamma)$ are complex conjugates and so must be the two arbitrary constants A_2 and A_3. The conjugacy requirement is imposed so that the scalar function $U_s(\underset{\sim}{x};\underset{\sim}{x}')$ is real since it relates to the displacement function $W_1(\underset{\sim}{x};\underset{\sim}{x}')$ that, in turn, describes a real parameter. The satisfaction of the existence of the Delta function at $\gamma = 0$ will lead to the evaluation of the two arbitrary constants A_2 and A_3.

To evaluate the singular solution we proceed by introducing the function $f(\underset{\sim}{x};\underset{\sim}{x}')$ which satisfies the relation

$$(\nabla^2 + 2)\ [\nabla^2 + \lambda(\lambda + 1)]\ U_s(\underset{\sim}{x};\underset{\sim}{x}') = f(\underset{\sim}{x};\underset{\sim}{x}') \qquad (2.20)$$

everywhere in the domain, and it also satisfies

$$[\nabla^2 + \nu(\nu + 1)]\ f(\underset{\sim}{x};\underset{\sim}{x}') = 0 \qquad (2.21)$$

away from the pole $\gamma = 0$, while

$$[\nabla^2 + \nu(\nu + 1)]\ f(\underset{\sim}{x};\underset{\sim}{x}') = \frac{\delta(\gamma)}{2\pi \sin\gamma} \qquad (2.22)$$

is representative of its behavior in the vicinity of the pole. Substitution of the expression of $U_s(\underset{\sim}{x};\underset{\sim}{x}')$ into Eqn. 2.20 leads to

$$f(\underset{\sim}{x};\underset{\sim}{x}') = -2i\tan\psi\,(1 - i\tan\psi)\,A_2\,P_\nu(-\cos\gamma). \tag{2.23}$$

To evaluate the constant A_2 we apply the divergence theorem in a circular contour $C(\gamma = \gamma_0)$ around the pole $\gamma = 0$. The theorem is expressed in the form

$$\iint_\sigma \nabla^2 f(\underset{\sim}{x};\underset{\sim}{x}')\,d\sigma = \int_C \frac{\partial f(\underset{\sim}{x};\underset{\sim}{x}')}{\partial \underset{\sim}{n}}\,dC \tag{2.24}$$

where σ denotes the surface area not enclosed by the contour C and $\underset{\sim}{n}$ refers to the on-surface normal direction along C.

With reference to Eqn. 2.22 we can write the following

$$\nabla^2 f(\underset{\sim}{x};\underset{\sim}{x}') = \frac{\delta(\gamma)}{2\pi R^2 \sin\gamma} - \nu(\nu+1)\,f(\underset{\sim}{x};\underset{\sim}{x}'). \tag{2.25}$$

Thus

$$\iint_\sigma \nabla^2 f(\underset{\sim}{x};\underset{\sim}{x}')\,d\sigma = \iint_\sigma \frac{\delta(\gamma)}{2\pi R^2 \sin\gamma}\,d\sigma - \nu(\nu+1)\iint_\sigma f(\underset{\sim}{x};\underset{\sim}{x}')\,d\sigma \tag{2.26a}$$

or

$$\int_C \frac{\partial f(\underset{\sim}{x};\underset{\sim}{x}')}{\partial \underset{\sim}{n}}\, dC = \iint_\sigma \frac{\delta(\gamma)}{2\pi R^2 \sin\gamma}\, d\sigma \; - \nu(\nu+1) \iint_\sigma f(\underset{\sim}{x};\underset{\sim}{x}')\, d\sigma \qquad (2.26b)$$

But

$$\frac{\partial f(\underset{\sim}{x};\underset{\sim}{x}')}{\partial \underset{\sim}{n}} = \frac{df(\underset{\sim}{x};\underset{\sim}{x}')}{d\gamma} = 2\, i\, \tan\psi\, (1 - i\, \tan\psi)\, A_2\, P_\nu^1(-\cos\gamma) \qquad (2.27)$$

and

$$d\sigma = R^2 \sin\gamma\, d\gamma\, d\eta \qquad (2.28a)$$

$$dC = R \sin\gamma\, d\eta. \qquad (2.28b)$$

From the definition and the fundamental property of the Delta function we observe that as the contour C shrinks, approaching $\gamma = 0$, the following relation holds

$$\lim_{\gamma\to 0} \iint_\sigma \frac{\delta(\gamma)}{2\pi R^2 \sin\gamma}\, d\sigma = 1. \qquad (3.30a)$$

Also from the limiting behavior of the Legendre functions (see Appendix C for details) we observe the following as $\gamma_0 \to 0$

$$\lim_{\gamma\to 0} P_\nu(-\cos\gamma) = \frac{2}{\pi} \sin\nu\pi \lim_{\gamma\to 0} \left[\frac{1}{2} \log(1 - \cos\gamma) + \text{const.} \right]$$

$$\lim_{\gamma\to 0} P_\nu^1(-\cos\gamma) = -\frac{2}{\pi}\sin\nu\pi \lim_{\gamma\to 0}\left[\frac{1}{\gamma} - \right.$$

$$\left. -\gamma\,\nu\,(\nu+1)\left[\frac{1}{2}\log(1-\cos\gamma) + \text{const.}\right]\right] \qquad (2.30b)$$

$$\lim_{\gamma\to 0}\int_0^{2\pi} \sin\gamma\,\left[\frac{1}{\gamma} - \text{logarithmic term} - \text{const.}\right] d\eta = 2\pi. \qquad (2.30c)$$

From the limiting behavior shown above we observe that

$$\lim_{\gamma\to 0}\iint_\sigma f(\underset{\sim}{x};\underset{\sim}{x}')\, d\sigma = 0 \qquad (2.30d)$$

and finally Eqn.(2.26) can be written in the form

$$\lim_{\gamma\to 0}\int_C \frac{\partial f}{\partial \underset{\sim}{n}}\, dC = \lim_{\gamma\to 0}\int_0^{2\pi}\frac{df}{d\gamma}\sin\gamma\, d\eta = -8\,i\tan\psi\,(1-i\tan\psi)\sin\nu\pi. \qquad (3.30d)$$

Thus when the limit is applied onto both sides of Eqn. 2.26 we obtain for the arbitrary constant A_2

$$A_2 = -\left[\,8\,i\,\tan\psi\,(1 - i\,\tan\psi)\sin\nu\pi\,\right]^{-1} \qquad (2.31)$$

and consequently

$$A_3 = \text{CONJ}\,[\,A_2\,]. \qquad (2.32)$$

By utilizing Eqn.(2.14) we obtain

$$W_1\ (\underset{\sim}{x};\underset{\sim}{x}') = \frac{R^2}{D}\ (\nabla^2 + 1 - \mu)\ U_s\ (\underset{\sim}{x};\underset{\sim}{x}')$$

$$- \frac{R^2}{D}\ \Big[\ (1-\mu-i\tan\psi)\ A_2\ P_\nu(-\cos\gamma) + (1-\mu+i\tan\psi)\ A_3\ P_\lambda(-\cos\gamma)\ \Big],$$

or equivalently

$$W_1\ (\underset{\sim}{x};\underset{\sim}{x}') = 2\ \frac{R^2}{D}\ \mathrm{Re}\ \Big[\ (1 - \mu - i\ \tan\psi)\ A_2\ P_\nu(-\cos\gamma)\ \Big]. \qquad (2.33)$$

Finally, the complete solution of the normal displacement function W $(\underset{\sim}{x};\underset{\sim}{x}')$ will be expressed in the form

$$W\ (\underset{\sim}{x};\underset{\sim}{x}) = 2\ \frac{R^2}{D}\ \mathrm{Re}\ \Big[\ (1 - \mu - i\ \tan\psi)\ A_2\ P_\nu\ (-\cos\gamma)\ \Big]$$

$$- \frac{1 + \mu}{4\pi\ Eh}\ [\ 1 + \cos\gamma\ \ln(1 - \cos\gamma)\ ]. \qquad (2.34)$$

We recall that the second part of $W(\underset{\sim}{x};\underset{\sim}{x}')$ was the result of the axisymmetric surface traction chosen in the form $q_{n'} = -\frac{3}{4\pi R^2}\cos\gamma$ to equilibrate the effect of the Dirac Delta function. To insure the uniqueness of such equilibrating function we refer to an argument on this particular point presented by Courant (see ref. [40] pp.351-358) of general validity. Courant discusses the need for the chosen function to be orthogonal to the eigenvalues of the operator as well as the particular orthogonality condition that must be imposed onto the system in order for the final solution to correspond to the

correct Green's function for the operator. In addition, because of the application of the equilibrating traction, the construction of the fundamental solution for our analysis falls under the so called Generalized Green's function process. The condition that must be satisfied by our Generalized Green's function can be viewed in the form of an integral over the entire domain

$$\iint_R W(\underset{\sim}{x};\underset{\sim}{x}')\ \Xi\ (\underset{\sim}{x};\underset{\sim}{x}')\ dR\ = 0 \tag{2.35}$$

where $\Xi(\underset{\sim}{x};\underset{\sim}{x}')$ is the introduced equilibrating function. We can write Eqn. 2.35 in the equivalent form

$$\iint_R W\ (\underset{\sim}{x};\underset{\sim}{x}')\ \cos\gamma\ dR = 0. \tag{2.35b}$$

The above condition can be satisfied only when $W\ (\underset{\sim}{x};\underset{\sim}{x}')$ takes the form

$$W(\underset{\sim}{x};\underset{\sim}{x}') = 2\mathrm{Re}[\ A\ P_\nu(-\cos\gamma)\ ] - \frac{1+\mu}{4\pi\ Eh}\ [1 + \cos\gamma\ \ln(1 - \cos\gamma) + B\ \cos\gamma] \tag{2.36}$$

where

$$A = \frac{R^2}{D}\ (1 - \mu - i\ \tan\psi)\ A_2$$

$$B = \frac{4}{3} - \ln(\ 2\ ) \tag{2.37a}$$

It is thus apparent that the regular homogeneous solution $A_1 P_1(\cos\gamma)$, which was eliminated from the construction of the singular solutions, is in fact reactivated in order for the orthogonal condition of Eqn. 2.35 to be satisfied. Subsequently we can write for the arbitrary constant A_1

$$A_1 = - \frac{1 + \mu}{4\pi\, Eh} B. \tag{2.37b}$$

So finally expression 2.36 corresponds to the fundamental solution or "free space" Green's function of the transverse displacement function W due to the the effect of self-equilibrated normal surface traction.

The description of the complete field, however, requires the fundamental solution of the auxiliary stress function $F(\underset{\sim}{x};\underset{\sim}{x}')$. By refering to the governing system of equations, Eqns. A.22, $F(\underset{\sim}{x};\underset{\sim}{x}')$ can be deduced from the operator

$$(\nabla^2 + 2)\, F(\underset{\sim}{x};\underset{\sim}{x}') = R^3\, q_n - \frac{D}{R} (\nabla^2 + 2)^2\, W(\underset{\sim}{x};\underset{\sim}{x}'). \tag{2.38}$$

We express the solution of Eqn. 2.38 as

$$F(\underset{\sim}{x};\underset{\sim}{x}') = F_1(\underset{\sim}{x};\underset{\sim}{x}') + F_2(\underset{\sim}{x};\underset{\sim}{x}') \tag{2.39}$$

such as

$$F_1(\underset{\sim}{x};\underset{\sim}{x}') = -\frac{D}{R}(\nabla^2 + 2)\, W(\underset{\sim}{x};\underset{\sim}{x}') \tag{2.40}$$

and

$$(\nabla^2 + 2)\, F_2(\underset{\sim}{x};\underset{\sim}{x}') = R^3\, q_n. \tag{2.41}$$

We again consider for q_n the self-equilibrated normal surface traction in the form

$$q_n = \frac{1}{R^2}\left[\frac{\delta(\gamma)}{2\pi \sin\gamma} - \frac{3}{4\pi}\cos\gamma\right]. \tag{2.7'}$$

The function $F_1(\underset{\sim}{x};\underset{\sim}{x}')$ can be obtained directly from the evaluation of the right side of Eqn. 2.40 by utilizing the properties of the operator. Accordingly, F_1 will take the form

$$F_1(\underset{\sim}{x};\underset{\sim}{x}') = 2\,\mathrm{Re}[\,A'\,P_\nu(-\cos\gamma)\,] + C_1\cos\gamma \tag{2.43}$$

where

$$A' = -\frac{D}{R}[2 - \nu(\nu + 1)]\,A \tag{2.44a}$$

and

$$C_1 = -\frac{3\,D\,(1+\mu)}{4\,\pi\,E\,h\,R}. \tag{2.44b}$$

We also need to construct the generalized Green's function for the operator (∇^2+2) governing F_2 in Eqn. 3.41. Such function will be the particular solution of the equation

$$(\nabla^2 + 2)\, F_2(\underset{\sim}{x};\underset{\sim}{x}') = R\,\left[\, \frac{\delta(\gamma)}{2\pi \sin\gamma} - \frac{3}{4\pi}\cos\gamma \,\right]. \qquad (2.45)$$

The homogeneous solution of the operator above leads to two eigenvalues one of which, $P_1(\cos\gamma)$, is regular everywhere in the region and the second, $Q_1(\cos\gamma)$, is singular at two points in the domain. Thus, to proceed, we solve Eqn. 2.45 for an influence function $\theta(\underset{\sim}{x};\underset{\sim}{x}')$ which corresponds to the particular solution of

$$(\nabla^2 + 2)\, \theta(\underset{\sim}{x};\underset{\sim}{x}') = -\frac{3R}{4\pi}\cos\gamma, \qquad (2.46)$$

with the condition that it satisfies the orthogonality condition

$$\iint_R \theta(\underset{\sim}{x};\underset{\sim}{x}')\cos\gamma\, dR = 0. \qquad (2.47)$$

The particular integral of Eqn. 2.46 is of the form

$$F_2(\underset{\sim}{x};\underset{\sim}{x}') = \frac{R}{4\pi}\,[1 + \cos\gamma\, \ln(1 - \cos\gamma) + B\cos\gamma) \qquad (2.48)$$

where, as noted earlier, $B = 4/3 - \ln 2$.

Finally, the complete expression of the "free space" Green's function for the auxiliary variable $F(\underset{\sim}{x};\underset{\sim}{x}')$ is

$$F(\underset{\sim}{x};\underset{\sim}{x}') = 2\mathrm{Re}\{A' P_\nu(-\cos\gamma)\}$$

$$+ C_2 [1 + \cos\gamma \ln(1 - \cos\gamma) + B \cos\gamma] + C_1 \cos\gamma \qquad (2.49)$$

where

$$C_2 = \frac{R}{4\pi}.$$

From the stress function - stress resultants relations given by Eqns. A.18 we obtain the fundamental solutions of the stress resultants as seen by the surface coordinate system (γ,η)

$$N_\gamma = \frac{1}{R^2}\left[\cot\gamma \left[2\,\mathrm{Re}\{ - A' P_\nu^1(-\cos\gamma) \} \right] - C_1 \cos\gamma \right.$$

$$\left. + C_2 \left(1 + \frac{\cos^2\gamma}{1 - \cos\gamma}\right) \right] \qquad (2.50)$$

and

$$N_\eta = \frac{1}{R^2}\left[2\,\mathrm{Re}\{ - A' \frac{d}{d\gamma} P_\nu^1(-\cos\gamma) \} - C_1 \cos\gamma \right.$$

$$\left. + C_2 \left[1 - 2(1 + \cot\gamma) - \frac{\cos\gamma}{1 - \cos\gamma}\right] \right] \qquad (2.51)$$

while, due to axisymmetry of the field in the (γ,η) coordinate frame, we obtain

$$N_{\gamma\eta} = 0. \qquad (2.52)$$

To compute the meridional displacement u_γ we apply the stress-displacement relation which, for axisymmetry reasons, is expressed as

$$\frac{1}{E\,h}\left(N_\gamma - \mu\, N_\eta \right) = \frac{1}{R}\left(\frac{du_\gamma}{d\gamma} + W \right) \qquad (2.53a)$$

or equivalently

$$u_\gamma = \frac{R}{E\,h}\int \left(N_\gamma - \mu\, N_\eta \right) d\gamma \; - \int W\, d\gamma. \qquad (2.53b)$$

We express N_γ and N_η in the form

$$N_\gamma = \frac{1}{R^2}\Bigg[2\,\mathrm{Re}\Big\{ -\frac{d^2}{d\gamma^2}\left[A'\, P_\nu(-\cos\gamma) \right] - \nu\,(\nu+1)\, A'\, P_\nu(-\cos\gamma) \Big\}$$

$$- C_1 \cos\gamma + C_2\left[1 + \cos\gamma\, \ln(1-\cos\gamma) + (B+3)\cos\gamma\right]$$

$$+ C_2 \frac{d^2}{d\gamma^2}\left[1 + \cos\gamma\, \ln(1-\cos\gamma) + B\cos\gamma\right] \Bigg]$$

and

$$N_\eta = \frac{1}{R^2}\left[2\,\mathrm{Re}\left\{ \frac{d^2}{d\gamma^2}\left[A'\, P_\nu(-\cos\gamma) \right] \right] - C_1 \cos\gamma \right.$$

$$\left. + C_2 \left(1 + \frac{d^2}{d\gamma^2}\right)\left[1 + \cos\gamma\, \ln(1-\cos\gamma) + B\cos\gamma\right] \right].$$

When the modified forms of N_γ and N_η, together with the transverse displacement function W, are introduced into Eqn. 2.53b and after noticing that

$$- \frac{\mu + 1}{E\ h\ R}\ C_2 + \frac{\mu + 1}{4\pi\ Eh} = 0 \qquad (2.54a)$$

and

$$- \frac{1}{EhR}\ 2\ \mathrm{Re}\{\ \nu\ (\nu + 1)\ A'\} - 2\ \mathrm{Re}\{\ A\ \} = 0, \qquad (2.54b)$$

we obtain for u_γ the expression

$$u_\gamma = \frac{1 + \mu}{EhR} \left[2\ \mathrm{Re}\{\ A'\ P_\nu^1\ (-\cos\gamma)\ \} - C_2\ [\ -\sin\gamma\ \ln(1 - \cos\gamma) \right.$$

$$\left. + \frac{\cos\gamma\ \sin\gamma}{1 - \cos\gamma} - B\ \sin\gamma\ ] \right] - \frac{1}{EhR}\ [\ C_1\ (1 - \mu) + 3\ C_2\ ]\ \sin\gamma \qquad (2.55)$$

while

$$u_\eta = 0. \qquad (2.56)$$

The moment resultants are deduced from the moment-curvature relations

$$M_\gamma = D\ (\ k_\gamma^0 + \mu\ k_\eta^0\ ) + \frac{h^2}{12R}\ N_\gamma$$

and

$$M_\eta = D\ (\ k_\eta^0 + \mu\ k_\gamma^0\ ) + \frac{h^2}{12R} \qquad (2.57)$$

where

$$k_\gamma^0 = - \frac{1}{R^2}\ (\ \frac{d^2W}{d\gamma^2} + W\ )$$

$$k_\eta^0 = - \frac{1}{R^2}\ (\ \cot\gamma\ \frac{dW}{d\gamma} + W\ ) \qquad (2.58)$$

and

$$M_{\gamma\eta} = 0. \tag{2.59}$$

The transverse shearing stress resultant Q_γ is related to the transverse displacement W through the relation

$$Q_\gamma(1 + \frac{h^2}{12R^2}) = - \frac{D}{R^3} \frac{d}{d\gamma} \left[(\nabla^2 + 2) W \right] \tag{2.60}$$

which leads to

$$Q_\gamma = \frac{D}{R^3} \left[2 \, \mathrm{Re}([2 - \nu(\nu + 1)] A P_\nu^1(-\cos\gamma)) + \frac{3 (1 + \mu)}{4 \pi E h} \sin\gamma \right] \tag{2.61}$$

after setting $1 + \frac{h^2}{12R^2} \approx 1$. For the same axisymmetry reasons

$$Q_\eta = 0. \tag{2.62}$$

With the evaluation of the shearing stress resultants, the fundamental solution matrix of the normal surface traction acting on a closed sphere has been completed.

II.1.1.2 IDENTIFICATION OF THE SINGULARITIES

In the beginning of this chapter we discussed the need that a fundamental singularity must satisfy certain physical conditions such

as equilibrium and axisymmetry which is translated into the vanishing of the meridional displacement and rotation of the normal vectors. Further, the true physical nature of the fundamental solution is viewed through the character of the singularities in the stress and displacement kernel functions.

We first consider the limiting value of the meridional displacement function u_γ which as $\gamma \to 0$, takes the form

$$\lim_{\gamma\to 0} u_\gamma = \frac{1+\mu}{EhR} \lim_{\gamma\to 0} \left[2\,\mathrm{Re}\, A'\, P_\nu^1(-\cos\gamma) - C_2 \frac{\cos\gamma \sin\gamma}{1-\cos\gamma} \right]$$

$$= -\frac{1+\mu}{EhR} \lim_{\gamma\to 0} \left[2\,\mathrm{Re}\left(\frac{R(\tan\psi - i\mu)}{8 \tan\psi \sin\nu\pi} \left(-\frac{2}{\pi}\sin\nu\pi\right) \right) \frac{1}{\gamma} - \frac{R}{4\pi}\frac{2}{\gamma} \right] \qquad (2.63)$$

and equivalently

$$\lim_{\gamma\to 0} u_\gamma = 0. \qquad (2.64)$$

Also from the rotation function

$$\beta_\gamma = \frac{1}{R}\left(u_\gamma - \frac{dW}{d\gamma} \right)$$

we obtain for $\gamma \to 0$,

$$\lim_{\gamma\to 0} \beta_\gamma = -\frac{1}{R} \lim_{\gamma\to 0} \left(\frac{dW}{d\gamma} \right) \qquad (2.65)$$

$$= -\frac{1}{R}\lim_{\gamma\to 0}\left[\frac{2R^2}{D}\,\mathrm{Re}\{\,-(1-\mu-i\tan\psi)\,A_2\,P_\nu^1(-\cos\gamma)\,\}-\frac{1+\mu}{4\pi\,Eh}\,\frac{\cos\gamma\,\sin\gamma}{1-\cos\gamma}\right].$$

However,

$$\frac{2R^2}{D}\,\mathrm{Re}\left[(1-\mu-i\tan\psi)\,A_2\left(-\frac{2}{\pi}\sin\nu\pi\right)-\frac{1+\mu}{2\pi\,Eh}\right]=0 \qquad (2.67)$$

and consequently

$$\lim_{\gamma\to 0}\beta_\gamma = 0. \qquad (2.68)$$

Further

$$\lim_{\gamma\to 0}Q_\gamma = \frac{2D}{R^3}\lim_{\gamma\to 0}\left[\mathrm{Re}\{\,[2-\nu\,(\nu+1)]\,A\,P_\nu^1\,(-\cos\gamma)\,\}\right]$$

$$= \frac{2D}{R^3}\lim_{\gamma\to 0}\left[\mathrm{Re}\{\,(2-\nu\,(\nu+1)\,A\left(-\frac{2}{\pi}\sin\nu\pi\right)\,\}\,\frac{1}{\gamma}\right]$$

or

$$\lim_{\gamma\to 0}Q_\gamma = -\frac{1}{2\pi R}\lim_{\gamma\to 0}\left(\frac{1}{\gamma}\right). \qquad (2.69)$$

We next examine the response of the shell in the radial direction addressed by the limiting value of the displacement W. Thus

$$\lim_{\gamma\to 0} W = \lim_{\gamma\to 0} \left[\frac{2R^2}{D} \mathrm{Re}\{ (1 - \mu - i \tan\psi) A_2 P_\nu(-\cos\gamma) \right.$$

$$\left. - \frac{1 + \mu}{4\pi Eh} (1 + \cos\gamma \ln(1 - \cos\gamma) + B \cos\gamma) \right].$$

After utilizing Eqn. 2.67 the above can be written as

$$\lim_{\gamma\to 0} W = \frac{1 + \mu}{2\pi Eh} \lim_{\gamma\to 0} \left[(1-\cos\gamma) \ln[\sin(\gamma/2)] - \frac{1 + \mu}{4\pi Eh} [1 + (B+\ln 2) \cos\gamma] \right]$$

$$+ \frac{1}{2\pi Eh} \mathrm{Re}\left[1 + \mu + i \left(\frac{\tan^2\psi - \mu}{\tan\psi} \right) \left(\psi(\nu + 1) + C + \frac{\pi}{2} \cot\nu\pi \right) \right]. \tag{2.70}$$

We observe that

$$\lim_{\gamma\to 0} (1 - \cos\gamma) \ln[\sin(\gamma/2)] = 0 \tag{2.71}$$

which implies that the response of the shell in the vicinity of the point load in the radial direction is finite. This finding agrees with results obtained by Reissner[1], Koiter[18], Kalnins[23] and Nordgren[17] for the classical theory approach of shallow or nonshallow shells.

The kernels of the stress and moment resultants are also singular at $\gamma = 0$. Thus in the limit as $\gamma\to 0$,

$$\lim_{\gamma\to 0} N_\gamma = \lim_{\gamma\to 0} [\ a_1 \ln[\ \sin(\gamma/2) + b_1\ ], \tag{2.72}$$

$$\lim_{\gamma\to 0} N_\eta = \lim_{\gamma\to 0} [\ a_1 \ln[\ \sin(\gamma/2) + b_2\ ] \tag{2.73}$$

where

$$a_1 = \frac{2}{R^2}\,\mathrm{Re}\{\ \frac{\sin\nu\pi}{\pi}\ \nu\ (\nu+1)\ A'\ \}$$

$$b_1 = -\frac{1}{R^2}\left[\ \mathrm{Re}\{\ \frac{\sin\nu\pi}{\pi}\ A'\ \nu\ (\nu+1)\ CP_1(\nu)\ \} + C_1 - C_2\ \right] \tag{2.74}$$

$$b_2 = \frac{1}{R^2}\left[\ 4\ \mathrm{Re}\{\ \frac{\sin\nu\pi}{\pi}\ A'\ \nu\ (\nu+1)\ [\ CP_0(\nu) - CP_1(\nu) - C_1 - 3\ C_2\ \right]$$

$$CP_0(\nu) = \psi(\nu+1) + C + \frac{\pi}{2}\cot\nu\pi - \frac{1}{2}\ln 2$$

$$CP_1(\nu) = [\ \pi\cot\nu\pi + \psi(\nu+2) + \psi(\nu) + 2\ C - 1 - \ln 2\ ]/4.$$

Further the moment resultant kernels M_γ and M_η also present logarithmic behavior at the vicinity of the point load. This is in agreement with the predictions of the shallow theory of Reissner[1] as well as the nonshallow theory of Koiter[18] and Kalnins[23]. On the other hand, Reissner predicted finite response in the stress resultants N_γ and N_η, while all nonshallow theories predicted logarithmic behavior at $\gamma = 0$.

A closer evaluation of the kernels in the vicinity of the singular point reveals that, while for a positive load the moment resultants approach $+\infty$, the stress resultants approach $-\infty$ in a manner shown in Fig. 2-2.

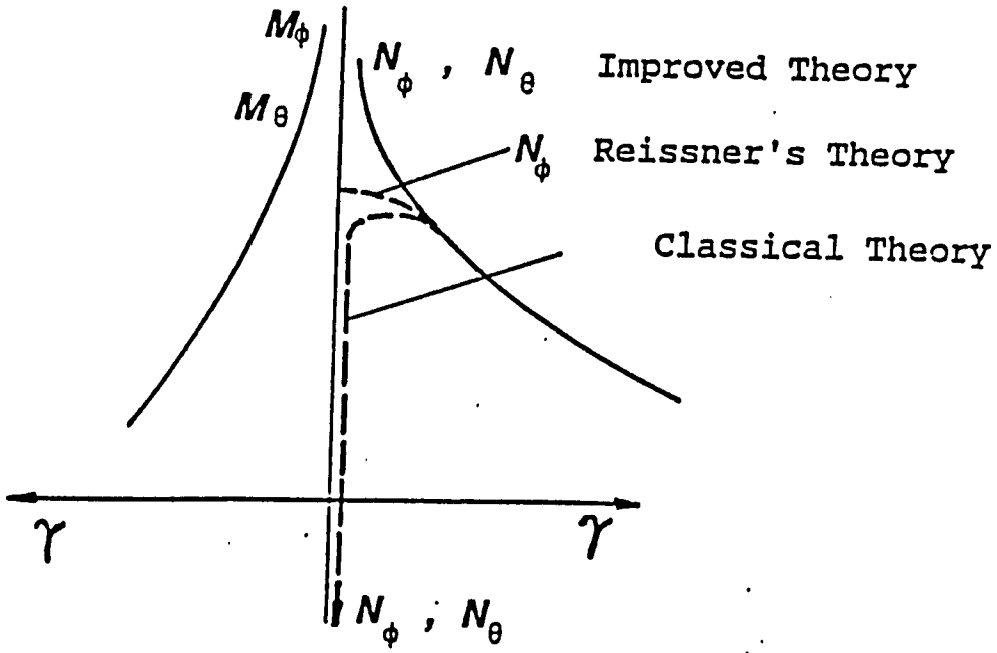

Figure 2-2. Stress and moment resultant behavior in the vicinity of a normal point load.

This prediction coincides with findings by Kalnins[23] and Koiter[18] (the derivation and predictions of the improved theory are obtained in later section of this chapter). Koiter discussed the above peculiar behavior under the reasoning that according to the mathematical model of the classical theory, the normal at the load point is forced to remain normal. The bending moments necessary to inforce the requirement, put the vicinity of the load in compression, as indicated by the sign of the stress kernels in that region. The

apparent mismatch between the shallow and the nonshallow theories, as seen from the membrane stress resultants, is negligible in the theory of thin shells since the region over which it occurs is negligible too. Because of the correlation between the stress and moment resultants the presence of the singularity in the stress resultant implies that the neutral surface at the pole is shifted outward over a distance $\frac{h^2}{12\ R}$, considered as negligible in shell theory.

Lastly, the equilibrium requirement is examined by taking the limiting value of the resultant force around the edge of a contour C ($\gamma = \gamma_0$). The resultant force opposite in direction to the unit load can be expressed in the form of the following limiting integral

$$\lim_{\gamma \to 0} \int_0^{2\pi} \left[Q_\gamma \cos\gamma + N_\gamma \sin\gamma \right] R \sin\gamma \, d\eta =$$

$$- \lim_{\gamma \to 0} \int_0^{2} \left(- \frac{1}{2\pi R} \left(\frac{1}{\gamma} \right) \cos\gamma + \sin\gamma \left[a_1 \ln(\sin \frac{\gamma}{2}) + b_1 \right] \right) R \sin\gamma \, d\eta$$

$$= - 1 \qquad (2.75)$$

which clearly indicates that equilibrium around the pole is satisfied.

II.1.2.1 CONCENTRATED TANGENTIAL LOAD SOLUTION

In deriving a solution of the governing system of equations that would correspond to the solution for a concentrated unit tangential load applied arbitrarily, one must consider solution forms which have no axial symmetry. The objective is to consider a unit tangential load applied at an arbitrary point $\underset{\sim}{x}(\phi';\theta')$ of the middle surface equilibrated in some fashion with either distributed surface traction or a singular load state. If one chooses to equilibrate the complete sphere with traction over the surface should have in mind that such a system cannot represent a self-equilibrated system of tangential forces on the spherical surface. The above was satisfied in the normal unit load solution because the function describing the distributed traction was itself an eigenvalue of the differential equation. On the other hand, if one chooses to equilibrate the complete sphere by applying a suitable set of singular forces, then he departs from the restrictive condition which requires that the fundamental solution should demonstrate singular behavior at only one point in the domain. Such restrictions, however, are eliminated when the shallow shell approach is to be applied, clearly because such shell extends to infinity. Nevertheless, a singular solution state with double-singularity kernels, even though it cannot strictly correspond to a "free-space" Green's function for the domain, can accurately represent the singular solution state in the region around the concentrated tangential load. Thus, the utilization of such

singular solution in the Boundary Integral scheme is still possible by restricting the domain of application of such solution.

A solution in which the unit concentrated load was equilibrated by a distributed surface traction was first attempted. That solution though failed to satisfy the vanishing of the surface traction accompanying a set of self-equilibrated systenm of tangential loads. This very important finding prevented the solution from being incorporated into the numerical scheme.

We begin the construction of the singular solution by considering the traction-free version of Eqns. 2.1 and 2.2 (we set $q_n = 0$) as well as the nonsymmetric form of their homogeneous solution. It becomes apparent that the solution, due to the type of loading shown in Fig. 2-3, can no longer be axissymetric around the point of application.

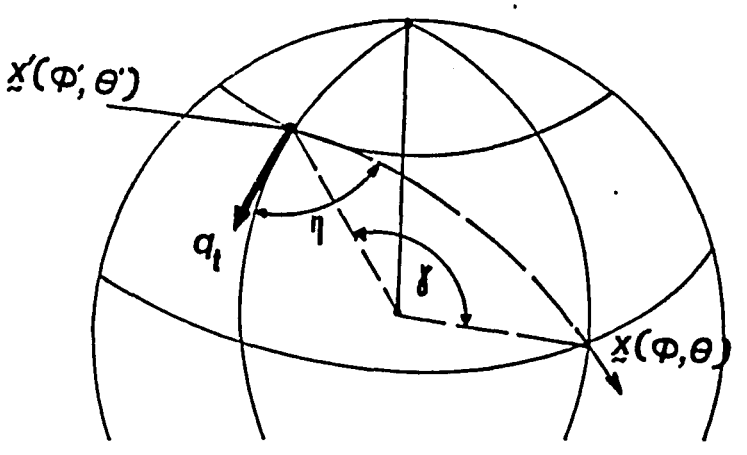

Figure 2-3. Orientation of a tangential load on the spherical surface.

We consider the general form of solution of the transverse displacement function $W(\underset{\sim}{x};\underset{\sim}{x})$ as

$$W(\underset{\sim}{x};\underset{\sim}{x}') = \sum_{m=1}^{\infty} \Big[h_1^m P_\nu^m(\cos\gamma) + h_2^m P_\nu^m(-\cos\gamma) + \bar{h}_1^m P_\lambda^m(\cos\gamma) + \bar{h}_2^m P_\lambda^m(-\cos\gamma) + C_0^m P_1^m(\cos\gamma) + C^m P_1^m(\cos\gamma) \Big] \cos m\eta \qquad (2.76)$$

where h_1^m, h_2^m, $\bar{h}_1^m$, $\bar{h}_2^m$, C_0^m and C^m are arbitrary constants and the only restriction that they bear is that h_1^m, h_2^m and $\bar{h}_1^m$, $\bar{h}_2^m$ are complex conjugates respectively. The form of the solution chosen for the transverse displacement function W implies that the state of deformation, due to the action of the concentrated effects shown in Fig. 2-3, will be symmetric with respect to the point $\eta = 0$.

Also the stress function $F(\underset{\sim}{x};\underset{\sim}{x}')$, in the absense of surface tractions would, according to Eqn. 2.2, obtain a general solution form from the modified governing system

$$(\nabla^2 + 2)\, F_1(\underset{\sim}{x};\underset{\sim}{x}') = 0 \qquad (2.77)$$

$$F_2(\underset{\sim}{x};\underset{\sim}{x}') = -\frac{D}{R}(\nabla^2 + 2)\, W(\underset{\sim}{x};\underset{\sim}{x}') \qquad (2.78)$$

such as

$$F_1(\underset{\sim}{x};\underset{\sim}{x}') + F_2(\underset{\sim}{x};\underset{\sim}{x}') = F(\underset{\sim}{x};\underset{\sim}{x}'). \qquad (2.79)$$

The general solution, after operating on the relations above and considering the same symmetry about $\eta = 0$, will take the form

$$F(\underset{\sim}{x};\underset{\sim}{x}') = \sum_{m=1}^{\infty} \Big[H_1^m P_\nu^m(\cos\gamma) + H_2^m P_\nu^m(-\cos\gamma) + \overline{H}_1^m P_\lambda^m(\cos\gamma) + \overline{H}_2^m P_\lambda(-\cos\gamma) + D_0^m P_1^m(\cos\gamma) + D^m Q_1^m(\cos\gamma) \Big] \cos m\eta \qquad (2.80)$$

where D_0^m and D^m are two additional constants introduced by $F_1(\underset{\sim}{x};\underset{\sim}{x}')$ into the system, while

$$\begin{aligned} H_1^m &= -\frac{D}{R}[2 - \nu(\nu+1)]\, h_1^m \\ H_2^m &= -\frac{D}{R}[2 - \nu(\nu+1)]\, h_2^m \\ \overline{H}_1^m &= -\frac{D}{R}[2 - \lambda(\lambda+1)]\, \overline{h}_1^m \\ \overline{H}_2^m &= -\frac{D}{R}[2 - \lambda(\lambda+1)]\, \overline{h}_2^m. \end{aligned} \qquad (2.81)$$

The general solutions for $W(\underset{\sim}{x};\underset{\sim}{x}')$ and $F(\underset{\sim}{x};\underset{\sim}{x}')$, expressed in the forms of infinite series, can be simplified further by considering the physical problem they must correspond to. The application of a tangential load along $\eta = 0$ suggests that the symmetry of the resulting field can be preserved with $m = 1$. Furthermore, because of

the two singularities that we require to be present in the solution, at $\gamma = 0$ and $\gamma = \pi$, the independent solutions $P_1(\cos\gamma) = \sin\gamma$ can be ignored with no loss of generality by simply setting

$$C_0 = D_0 = 0. \tag{2.83}$$

We also note that

$$Q_1^1(\cos\gamma) = -\frac{1}{2}\sin\gamma \log\frac{1+\cos\gamma}{1-\cos\gamma} - \cot\gamma. \tag{2.84}$$

Thus, the general solution form for $W(\underset{\sim}{x};\underset{\sim}{x}')$ and $F(\underset{\sim}{x};\underset{\sim}{x}')$, upon which the singular solution state will be constructed, can now be written as

$$W(\underset{\sim}{x};\underset{\sim}{x}') = \Big[h_1 P_\nu^1(\cos\gamma) + h_2 P_\nu^1(-\cos\gamma) + \bar{h}_1 P_\lambda^1(\cos\gamma) + \bar{h}_2 P_\lambda^1(-\cos\gamma) + C^1 Q_1^1(\cos\gamma) \Big] \cos\eta \tag{2.85}$$

$$F(\underset{\sim}{x};\underset{\sim}{x}') = \Big[H_1 P_\nu^1(\cos\gamma) + H_2 P_\nu^1(-\cos\gamma) + \bar{H}_1 P_\lambda^1(\cos\gamma) + \bar{H}_2 P_\lambda^1(-\cos\gamma) + D^1 Q_1^1(\cos\gamma) \Big] \cos\eta. \tag{2.86}$$

By utilizing the stress function- stress resultant expressions, given by Eqns. A.16, the stress resultant variables are obtained and introduced into the following stress-displacement relations

$$\frac{1}{Eh} \left(N_\gamma - \mu N_\eta \right) = \frac{1}{R} \left(\frac{\partial u_\gamma}{\partial \gamma} + W \right) \qquad (2.87a)$$

$$\frac{1}{Eh} \left(N_\eta - \mu N_\gamma \right) = \frac{1}{R} \left(\csc\gamma \frac{\partial u_\eta}{\partial \eta} + u_\gamma \cot\gamma + W \right). \qquad (2.87b)$$

We express

$$N_\gamma - \mu N_\eta = \frac{1}{R^2} \Bigg[- \frac{d^2}{d\gamma^2} \left[(\mu + 1) F(\gamma) \right] - (\mu + 1) D^1 Q_1^1 (\cos\gamma)$$

$$- \nu (\nu + 1) \left[H_1 P_\nu^1 (\cos\gamma) + H_2 P_\nu^1 (-\cos\gamma) \right]$$

$$- \lambda (\lambda + 1) \left[\bar{H}_1 P_\lambda^1 (\cos\gamma) + \bar{H}_2 P_\lambda^1 (-\cos\gamma) \right] \Bigg] \cos\eta \qquad (2.88a)$$

and

$$N_\eta - \mu N_\gamma = \frac{1}{R^2} \Bigg[- \frac{d^2}{d\gamma^2} \left[(\mu + 1) F(\gamma) \right] + (\mu + 1) D^1 Q_1^1 (\cos\gamma)$$

$$+ \mu \Bigg[\nu (\nu + 1) \left[H_1 P_\nu^1 (\cos\gamma) + H_2 P_\nu^1 (-\cos\gamma) \right]$$

$$+ \lambda (\lambda + 1) \left[\bar{H}_1 P_\lambda^1 (\cos\gamma) + \bar{H}_2 P_\lambda^1 (-\cos\gamma) \right] \Bigg] \Bigg] \cos\eta \qquad (2.88b)$$

where $F(\gamma)$ satisfies $F(\underline{x};\underline{x}') = F(\gamma,\eta) = F(\gamma) \cos\eta$.

When expressions 2.88 are introduced into 2.87 , after integration we obtain for the two tangential displacement components

$$u_\gamma = \frac{1}{EhR} \Bigg[- (\mu + 1) \frac{d}{d\gamma} F(\gamma) - (\mu + 1) D^1 Q_1^1 (\cos\gamma)$$

$$- \nu\,(\nu+1)\,[\,H_1\,P_\nu(\cos\gamma) - H_2\,P_\nu(-\cos\gamma)\,]$$

$$- \lambda\,(\lambda+1)\,[\,\bar{H}_1\,P_\lambda(\cos\gamma) - \bar{H}_2\,P_\lambda(-\cos\gamma)\,] - h_1\,P_\nu(\cos\gamma) + \qquad (2.89)$$

$$h_2\,P_\nu(-\cos\gamma) - \bar{h}_1\,P_\lambda(\cos\gamma) + \bar{h}_2\,P_\lambda(-\cos\gamma) - C^1\,Q_1(\cos\gamma)\,\Big)\,\cos\eta + f(\eta)$$

and

$$u_\eta = -\frac{1+\mu}{EhR}\csc\gamma\,\frac{\partial}{\partial\eta}F(\gamma,\eta) + \Big[\cos\gamma\,\Big[\,\frac{1+\mu}{EhR}\,D^1\,Q_1(\cos\gamma) + C^1\,Q_1(\cos\gamma)\Big]$$

$$- \sin\gamma\,\Big[\,\frac{1+\mu}{EhR}\,D^1\,Q_1^1\,(\cos\gamma) + C^1\,Q_1^1\,(\cos\gamma)\,\Big]\,\Big)\,\sin\eta$$

$$- \cos\gamma\int f(\eta)\,d\eta \quad + \quad g(\gamma) \qquad (2.90)$$

where $f(\eta)$ and $g(\gamma)$ are arbitrary functions of integration.

We proceed by observing the following relation that holds between the functions and the arbitrary constants

$$\frac{1}{EhR}\Big(\,- \nu\,(\nu+1)\,[\,H_1\,P_\nu(\cos\gamma) - H_2\,P_\nu(-\cos\gamma)\,]$$

$$- \lambda\,(\lambda+1)\,[\,\bar{H}_1\,P_\nu(\cos\gamma) - \bar{H}_2\,P_\nu(-\cos\gamma)\,]\,\Big) \qquad (2.91)$$

$$- h_1\,P_\nu(\cos\gamma) + h_2\,P_\nu(-\cos\gamma) - \bar{h}_1\,P_\nu(\cos\gamma) + h_2\,P_\nu(-\cos\gamma) = 0$$

which allows Eqn. 2.89 to be written in the form

$$u_\gamma = - \frac{1 + \mu}{EhR} \left[\frac{d}{d\gamma}F(\gamma) + D^1 Q_1(\cos\gamma)\right] \cos\eta - C^1 Q_1(\cos\gamma) + f(\eta) \quad (2.92)$$

while the expression for u_η remains unchanged.

In order to evaluate the form of the arbitrary functions of integration $f(\eta)$ and $g(\gamma)$, we utilize the third of the stress-displacement relations expressed as

$$\frac{2\ (1 + \mu)}{Eh}\ N_{\gamma\eta} = \frac{1}{R}\left[\frac{\partial u_\eta}{\partial\gamma} - \cot\gamma\ u_\eta + \csc\gamma\ \frac{\partial u_\gamma}{\partial\eta}\right]. \quad (2.93)$$

When the appropriate expressions of the variables are introduced and operated on in the above relation, we observe that on the right side of the equal sign the following additional terms, expressed as Ω, with no counterparts remain:

$$\Omega = \left[\frac{1 + \mu}{EhR} D^1 + C^1\right]\left(- \sin\gamma \frac{d}{d\gamma} Q_1^1\ (\cos\gamma) + \cos\gamma\ Q_1^1\ (\operatorname{coc}\gamma)\right) \sin\eta$$

$$+ \sin\gamma \int f(\eta)\ d\eta + \csc\gamma \frac{d}{d\eta} f(\eta) + \frac{d}{d\gamma} g(\gamma)$$

$$- \cot\gamma \left[g(\gamma) - \cos\gamma \int f(\eta)\ d\eta \right]. \quad (2.94)$$

But

$$- \sin\gamma \frac{d}{d\gamma} Q_1^1\ (\cos\gamma) + \cos\gamma\ Q_1^1\ (\cos\gamma) = - \frac{2}{\sin\gamma}$$

and thus

$$\Omega = -2\left[\frac{1+\mu}{EhR}D^1 + C^1\right]\csc\gamma\,\sin\eta + \csc\gamma\left[\frac{d}{d\eta}f(\eta) + \int f(\eta)\,d\eta\right] + \frac{d}{d\gamma}g(\gamma) - \cot\gamma\,g(\gamma). \tag{2.94a}$$

Since $\frac{d}{d\gamma}g(\gamma) - \cot\gamma\,g(\gamma)$ is completely independent of η we can require that

$$\frac{d}{d\gamma}g(\gamma) - \cot\gamma\,g(\gamma) = 0 \tag{2.95}$$

which leads to

$$g(\gamma) = a'\sin\gamma \tag{2.96}$$

where a' is an arbitrary constant.

Further, by setting $f(\eta) = A_0\,\eta\,\sin\eta$, we observe that

$$\frac{d}{d\eta}f(\eta) + \int f(\eta)\,d\eta = 2A_0\sin\eta \tag{2.97}$$

and the expression for Ω becomes

$$\Omega = -2\left[\frac{1+\mu}{EhR}D^1 + C^1\right]\csc\gamma\,\sin\eta + 2A_0\csc\gamma\,\sin\eta = 0. \tag{2.98}$$

If we set

$$A_0 = \frac{1+\mu}{EhR}D^1 + C^1 \tag{2.99}$$

then $\Omega = 0$ and the third of the stress-displacement relations is satisfied. However, because of the form of the the function $f(\eta)$,

the displacement functions u_γ and u_η will be multivalued. Since the present analysis deals with the complete spherical domain, such multivalued functions must be suppressed by setting the arbitrary constant of the function

$$A_0 = 0 \tag{2.100a}$$

and consequently in order for $\Omega = 0$ to still hold we deduce

$$\frac{1+\mu}{EhR} D^1 = C^1. \tag{2.100b}$$

The above choice satisfies all the stress-displacement relations and leads to the following expressions for the components of the tangential displacement

$$u_\gamma(\underset{\sim}{x};\underset{\sim}{x}') = -\frac{1+\mu}{EhR} \frac{\partial}{\partial\gamma} F(\underset{\sim}{x};\underset{\sim}{x}') \tag{2.101a}$$

and

$$u_\eta(\underset{\sim}{x};\underset{\sim}{x}') = -\frac{1+\mu}{EhR} \csc\gamma \frac{\partial}{\partial\eta} F(\underset{\sim}{x};\underset{\sim}{x}') + a' \sin\gamma. \tag{2.101b}$$

However, since $g(\gamma)$ is independent of η, it can be viewed as rigid body displacement and with no loss of generality, due to the absense of singularity in its kernel, set $a' = 0$ and write for u_η

$$u_\eta(x;x') = -\frac{1+\mu}{EhR} \csc\gamma \frac{\partial}{\partial\eta} F(\underset{\sim}{x};\underset{\sim}{x}'). \tag{2.102}$$

To this point, the dependent variables through which the complete field can be described in its general form have been derived. The unknown arbitrary constants that accompany their general expressions must be evaluated in a manner which will reflect the particular physical situation. The singularities in all the dependent variables, which exist at $\gamma = 0$ and $\gamma = \pi$, need to be examined as to what they actually correspond to in the complete spherical domain. Such an evaluation is accomplished by cutting an adjacent parallel circle near each pole and obtaining the resultant force as well as the resultant moment of the state of stress around the edge of the contour. Such state, singular in its character, is the result of the unbounded expressions of the stress and moment resultant kernels in the vicinity of the two poles.

The resultant force, along $\eta = 0$, of the stresses over the contour can be viewed in the form of the following integral expression

$$F_r = \lim_{\substack{\gamma \to 0 \\ \gamma \to \pi}} \int_0^2 \left[(N_\gamma \cos\gamma + Q_\gamma \sin\gamma) \cos\eta - N_{\gamma\eta} \sin\eta \right] R \sin\gamma \, d\eta \qquad (2.103)$$

and the resultant moment along the same direction can be viewed as

$$M_r = \lim_{\substack{\gamma \to 0 \\ \gamma \to \pi}} \int_0^{2\pi} R \left[M_\gamma \cos\eta - M_{\gamma\eta} \cos\gamma \sin\eta \right.$$

$$\left. - R \sin\gamma \cos\eta \, [\, Q_\gamma \cos\gamma - N_\gamma \sin\gamma \,] \right] \sin\gamma \, d\eta \qquad (2.104)$$

with

$$Q_\gamma = - \frac{D}{R^3} \frac{\partial}{\partial \gamma} (\nabla^2 + 2)\, W(\underset{\sim}{x};\underset{\sim}{x}') \tag{2.105}$$

and M_γ, M_η, $M_{\gamma\eta}$ deduced from Eqns. A.15.

When the appropriate expressions are introduced into the two integrals above and the limiting values of the Legendre functions are incorporated, we obtain the following interesting results:

$$F_r = \lim_{\substack{\gamma \to 0 \\ \gamma \to \pi}} \int_0^{2\pi} [\ \ldots\ ]\, R \sin\gamma\, d\eta = - \frac{2\pi}{R} D^1 \tag{2.106}$$

$$M_r = \lim_{\substack{\gamma \to 0 \\ \gamma \to \pi}} \int_0^{2\pi} [\ \ldots\ ]\, R \sin\gamma\, d\eta = \lim_{\substack{\gamma \to 0 \\ \gamma \to \pi}} \left[\ 2\, \pi\, D^1 \cos\gamma\ \right]. \tag{2.107}$$

It is apparent from the results shown above that the only term of the general solution that contributes to both integrals is the one accompanied by the arbitrary constant D^1. Furthermore, if the constant D^1 is given the value

$$D^1 = \frac{R}{2\,\pi}, \tag{2.108}$$

the general solution that has been developed corresponds, under the light of Eqns. 2.106 and 2.107, to the physical problem shown in Fig. 2-4 below.

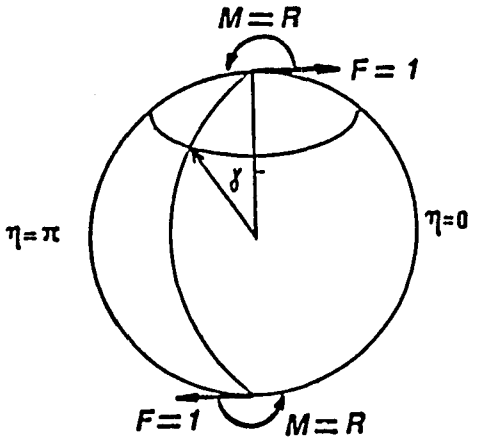

Figure 2-4. Self equilibrated force system A

It is interesting to observe that the overall equilibrium of the complete spherical shell is identically satisfied. However, a singular solution that will describe the stress and displacement fields due to a unit concentrated tangential load in a self-equilibrated complete sphere would be one that corresponds to the singular load arrangement shown in Fig. 2-5.

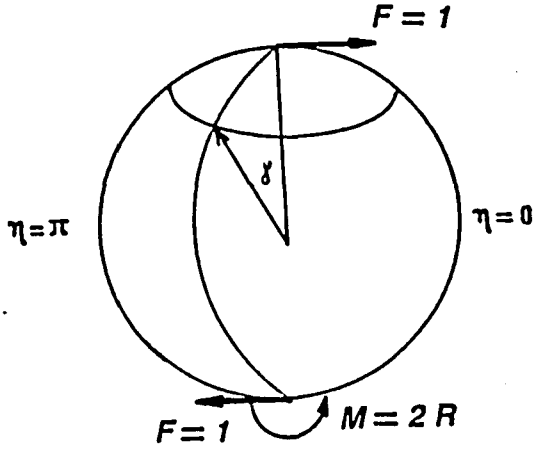

Figure 2-5. Self-equilibrated force system B

Obviously an additional solution described in Fig. 2-6 must be superimposed onto the already derived solution in order for the desired physical state of Fig. 2-5 to be deduced.

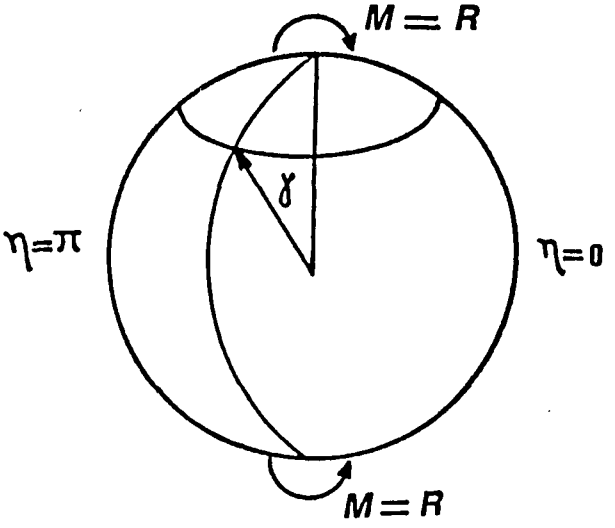

Figure 2-6. Self-equilibrated moment pair.

Such solution that describes the problem of Fig. 2-6 is in itself singular at $\gamma = 0$ and $\gamma = \pi$. However, as noted previously in the evaluation of the resultant integrals around the two poles, the general solution was only able to provide the physical problem of Fig. 2-4 and also incorporate one arbitrary constant in the analysis of the problem. Thus, it becomes inevitable to seek additional solutions of the governing system which would fill the need of the evaluation of the required physical state described in Fig. 2-6.

We return to the general system of equations and we seek a solution to the equation

$$(\nabla^2 + 2)\ F^*\ (\underset{\sim}{x};\underset{\sim}{x}') = 0 \qquad (2.109)$$

where the auxiliary variable $F^*\ (\underset{\sim}{x};\underset{\sim}{x}')$ is no longer expressed in terms of the Legendre fuctions of the homogeneous solution of Eqn. 2.109, which have already been incorporated into the previous analysis, but in the form of any multivalued function which satisfies the differential equation. We should point out that even though multivalued displacement and stresses are not allowed in the analysis, multivalued stress functions can in fact be permitted for as long as they lead to single-valued displacements and stresses in the domain of interest.

Such multivalued form of the solution of Eqn. 2.109 can be expressed as

$$F^*\ (\underset{\sim}{x};\underset{\sim}{x}') = A^*\ [\ \sin\gamma\ \eta\ \sin\eta\ -\ \csc\gamma\ \cos\eta\ ]. \qquad (2.110)$$

From the stress function-stress resultant relations we obtain the following single-valued expressions for the stress resultants:

$$N^*_\gamma = \frac{2\ A^*}{R^2}\ \frac{\cos\eta}{\sin^3\gamma}$$

$$N^*_\eta = -\ \frac{2\ A^*}{R^2}\ \frac{\cos\eta}{\sin^3\gamma} \qquad (2.111)$$

$$N^*_{\gamma\eta} = \frac{2\,A^*}{R^2} \quad \frac{\cos\eta}{\sin^3\gamma} \sin\eta.$$

When the singular solution is evaluated in the vicinity of the two poles according to the same two integrals of the force and moment resultants, we observe that the force resultant integrand vanishes identically due to

$$N^*_\gamma \cos\gamma - N^*_{\gamma\eta} = 0, \tag{2.112}$$

while the moment integral, by choosing the following value for the arbitrary constant

$$A^* = - D^1, \tag{2.113}$$

leads to the solution state described by Fig. 2-6.

The additional stress resultant components of Eqns. 2.111 will introduce new components of the tangential displacement functions u^*_γ and u^*_η which, in turn, must be single-valued. These new components will be obtained from the stress-displacement relations which are of the form

$$\frac{1}{E\,h} \left[N^*_\gamma - \mu\, N^*_\eta \right] = \frac{1}{R} \frac{\partial u^*_\gamma}{\partial\gamma}$$

$$\frac{1}{E\,h}\left[\,N_{\eta}^{*}-\mu\,N_{\gamma}^{*}\,\right]=\frac{1}{R}\left[\,\frac{\partial u_{\eta}^{*}}{\partial\eta}\csc\gamma+\cot\gamma\,u_{\gamma}^{*}\,\right] \qquad (2.114)$$

$$\frac{2\,(1+\mu)}{E\,h}\,N_{\gamma\eta}^{*}=\frac{1}{R}\left[\,\frac{\partial u_{\eta}^{*}}{\partial\gamma}-\cot\gamma\,u_{\eta}^{*}+\csc\gamma\,\frac{\partial u_{\gamma}^{*}}{\partial\eta}\,\right].$$

Integration of the first two of the relations above leads to the following expressions of the displacement functions u_{γ}^{*} and u_{η}^{*}:

$$u_{\gamma}^{*}=-\frac{2(1+\mu)}{EhR}\,D^{1}\left[\,\frac{1}{2}\ln\left[\,\tan\tfrac{1}{2}\gamma\,\right]-\frac{1}{2}\,\frac{\cos\gamma}{\sin^{2}\gamma}\,\right]\cos\eta \qquad (2.115)$$

$$u_{\eta}^{*}=\frac{2(1+\mu)}{EhR}\,D^{1}\left[\,\cos\gamma\left(\,\frac{1}{2}\ln[\tan_{2}^{1}\gamma]+\frac{1}{2}\,\frac{\cos\gamma}{\sin^{2}\gamma}\,\right)+1\,\right]\sin\eta \qquad (2.116)$$

Furthermore, when the above expressions are introduced into the third of the stress-displacement relations, the relation is identically satisfied.

With the analysis associated with the multivalued stress variable F^{*} we arrived at the complete stress and displacement field description corresponding to the physical problem of Fig. 2-6. Thus, while the transverse dispacement function W was uneffected by the introduction of F^{*}, the tangential displacement components are now expressed as

$$u_{\gamma}=-\frac{1+\mu}{EhR}\,\frac{\partial}{\partial\gamma}\,F(\underset{\sim}{x};\underset{\sim}{x}')+u_{\gamma}^{*} \qquad (2.117)$$

$$u_\eta = - \frac{1 + \mu}{EhR} \csc\gamma \frac{\partial}{\partial \eta} F(\underset{\sim}{x};\underset{\sim}{x}') + u^*_\eta. \qquad (2.118)$$

The stress and moment resultants will also contain the contribution of their starred counterparts introduced by the multivalued stress function as well as their expressions derived from Eqns. A.18 and A.15 respectively. The shearing stress resultants, however, being only a function of the transverse displacement W will not experience any change in their forms.

To complete the analysis, the remaining arbitrary constants must now be evaluated from physical requirements imposed at the two poles where the singular loads apply. These requirements are closely related to the way these loads act onto the middle surface of the complete sphere.

The first of these requirements is expressed in the form of the following integral

$$\lim_{\substack{\gamma\to 0 \\ \gamma\to\pi}} \int_0^{2\pi} \left[W \cos\gamma - u_\gamma \sin\gamma + R \sin\gamma \, \beta_\gamma \right] R \sin\gamma \cos\eta \, d\eta = 0 \qquad (2.122)$$

which implies that the net displacement in the normal direction vanishes since there is no net force acting in that direction. By introducing the expression of the rotation β_γ

$$\beta_\gamma = \frac{1}{R} \left(u_\gamma - \frac{\partial W}{\partial \gamma} \right) \tag{2.123}$$

into Eqn. 2.122, we obtain the equivalent expression

$$\lim_{\substack{\gamma \to 0 \\ \gamma \to \pi}} \left[W \cos\gamma - \sin\gamma \frac{\partial W}{\partial \gamma} \right] \sin\gamma = 0. \tag{2.122a}$$

The singular behavior of the Legendre functions is incorporated into the above limiting relation and two relations between the arbitrary constants are deduced.

Hence, as $\gamma \to 0$

$$\frac{2}{\pi} \left[\sin\nu\pi \, h_2 + \sin\lambda\pi \, \bar{h}_2 \right] + C^1 = 0 \tag{2.124}$$

and, as $\gamma \to \pi$

$$\frac{2}{\pi} \left[\sin\nu\pi \, h_1 + \sin\lambda\pi \, \bar{h}_1 \right] - C^1 = 0 \tag{2.125}$$

where $C^1 = - \frac{1 + \mu}{EhR} D^1$ and $D^1 = \frac{R}{2\pi}$.

The second requirement reflects the physical condition which implies that the net displacement component along the axis lying on the horizontal tangent plane and being perpendicular to the direction of the unit tangent load must vanish. Such condition is expressed in the

form of a similar integral, as in the previous case, which in turn, leads to the following limiting value of its integrand:

$$\lim_{\substack{\gamma\to 0\\ \gamma\to\pi}} \left[u_\gamma \cos\gamma + W \sin\gamma + u_\eta \right] \sin\gamma = 0. \qquad (2.126)$$

Two additional limiting relations are deduced from the above and which in terms of the arbitrary constants are expressed as follows:

as $\gamma\to 0$

$$\sin\nu\pi\ H_2 + \sin\lambda\pi\ \bar{H}_2 = 0 \qquad (2.127)$$

and as $\gamma\to\pi$

$$\frac{\sin\nu\pi}{\pi} H_1 + \frac{\sin\lambda\pi}{\pi} \bar{H}_1 - \frac{D^1}{2} = 0. \qquad (2.128)$$

The solution of the system of Eqns. 2.124-128, together with the constants C^1 and D^1 which have already been evaluated, will lead to the complete evaluation of the stress and displacement kernels which describe the state of stress and deformation in a complete sphere under the influence of the system of self-equilibrated singular loads shown in Fig. 2-5.

We should note that the region around $\gamma = 0$ predominantly experiences the effect of the unit tangential load and thus the singularities present in the kernels are purely due to that load.

II.1.2.2 IDENTIFICATION OF THE SINGULARITIES

Evaluation of the singularities in the kernels at the appex of the shell ($\gamma = 0$) leads to the following limiting values of the displacement and stress functions:

a. The normal displacement function W is zero at the load point

b. Both tangential displacement components u_γ and u_η experience logarithmic singularity

c. The stress and moment resultants have a stronger singularity of the order ($\frac{1}{\gamma}$) in their kernel functions.

d. The transverse shearing stress resultants Q_γ and Q_η have a very strong singular behavior of the order ($\frac{1}{\gamma^2}$).

The character of the singularities associated with the present analysis completely agrees with the order and character of singularities in the respective kernels obtained by Kalnins[24]. The shallow shell solution, however, presented by Luckasiewicz[15] revealed that the moment resultants are zero at the point of application of the load.

II.1.3.1 FUNDAMENTAL SOLUTIONS OF A UNIT CONCENTRATED MOMENT

A unit moment is defined as the effect of a definite distribution of normal loading. It can best be described as the derivative of the Delta function distribution with respect to the surface coordinate along which the unit moment is to be acting. For a given shell represented by means of the orthogonal surface coordinates (α,β), the intensities of unit concentrated moments directed along α and β axes can be expressed in the form

$$\frac{1}{AB^2}\frac{\partial\delta}{\partial\beta} \quad , \quad -\frac{1}{A^2B}\frac{\partial\delta}{\partial\alpha} \tag{2.129}$$

respectively, where A and B are the coefficients of the first quadratic form of the middle surface of the shell. Thus for the particular case of a spherical shell described by the surface coordinates (ϕ,θ)

$$A = R \quad , \qquad B = R\sin\phi \tag{2.130}$$

and the intensities of the unit moments along ϕ and θ will be

$$-\frac{1}{R^3\sin\phi}\frac{\partial\delta(\underset{\sim}{n}-\underset{\sim}{n}')}{\partial\phi} \quad , \quad \frac{1}{R^3\sin^2\phi}\frac{\partial\delta(\underset{\sim}{n}-\underset{\sim}{n}')}{\partial\theta} \tag{2.131}$$

respectively.

From the theory of generalized functions it is known that if Φ is a fundamental solution of the equation $L\,\Phi = \delta(\underset{\sim}{n}-\underset{\sim}{n}')$, where L is a differential operator, then $\frac{\partial \Phi}{\partial \alpha}$ is a solution of the equation $L\,\Phi = \frac{\partial \delta}{\partial \alpha}$.

It follows from the above that the principle parts of the moment kernels can be obtained by simple differentiation on the principle parts of the corresponding kernels of the unit normal load solution.

Let primed quantities correspond to coordinates of an arbitrary point where a concentrated load or moment applies and unprimed ones to coordinates of an arbitrary field point in the domain. The displacement field produced by a unit moment, applied at (ϕ',θ') along either ϕ or θ axes, at the field point (ϕ,θ) is obtained by differentiating onto the displacement functions $W(\underset{\sim}{x};\underset{\sim}{x}')$ and $u(\underset{\sim}{x};\underset{\sim}{x}')$ with the respective coordinate. Thus, for a moment directed along ϕ axis, the singular solutions of the displacement components would be

$$W^m(\underset{\sim}{x};\underset{\sim}{x}') = -\frac{1}{R}\,\frac{\partial W(\underset{\sim}{x};\underset{\sim}{x}')}{\partial \phi'} \quad , \quad u^m(\underset{\sim}{x};\underset{\sim}{x}') = -\frac{1}{R}\,\frac{\partial u(\underset{\sim}{x};\underset{\sim}{x}')}{\partial \phi'} \qquad (2.132)$$

while for a moment directed along the θ axis, the displacement functions would be

$$W^m(\underset{\sim}{x};\underset{\sim}{x}') = \frac{1}{R\,\sin\phi'}\,\frac{\partial W(\underset{\sim}{x};\underset{\sim}{x}')}{\partial \theta'} \quad , \quad u^m(\underset{\sim}{x};\underset{\sim}{x}') = \frac{1}{R\,\sin\phi'}\,\frac{\partial u(\underset{\sim}{x};\underset{\sim}{x}')}{\partial \theta'}. \qquad (2.133)$$

The same would be also true for every other kernel function associated with the domain.

However, as mentioned earlier, the differentiation process above can represent a moment solution state when only applied onto the principle singularities of the normal load kernels. This will be the case of the construction of the fundamental singularity for a shallow shell whose singular solution is expressed only in terms of the principle singularity.

A numerical evaluation of different moment solutions was performed in an effort to best describe such concentrated effect. These solutions were derived (a) from the differentiation of the normal load kernels as described above, (b) from the superposition of two tangential load solutions applied in such a manner as to introduce two unit concentrated moments at the poles(see Fig. 2-6), and (c) from a pair of two concentrated normal loads with opposite directions approaching each other at the pole and corrected by a concentrated tangential load.

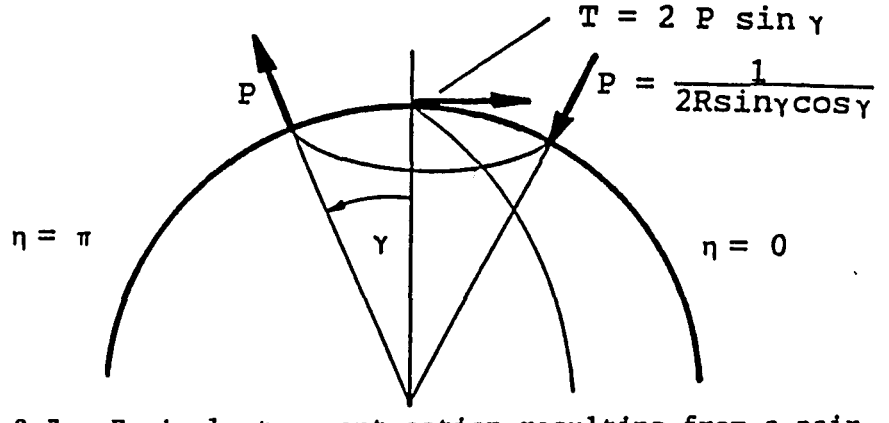

Figure 2-7. Equivalent moment action resulting from a pair of normal point loads.

The magnitude of the applied forces, shown in Fig. 2-7 , insure a unit moment effect at each of the poles. The evaluation revealed that approaches (b) and (c) provide the exact same answers while the differentiation procedure, case (a), fails to represent the solution in the vicinity of the pole.

Thus, the comparison of the above different unit moment solutions has proven that the argument stated earlier about the role of differentiation on principle singularities of the kernels is in fact critical. Furthermore, it has proven that an exact moment singular solution can be represented by the superposition of two appropriate tangential load solutions derived in the previous section. An alternative exact solution could have been derived by using the same procedure utilized in the tangential load analysis, by simply requiring that the singularities at the two poles, introduced by the general solution, together with the condition on the transverse displacement function $W(\underset{\sim}{x};\underset{\sim}{x}')$

$$W(\gamma,\eta) = W(\pi-\gamma,\eta) \tag{2.134}$$

are justified due to the presence of two concentrated unit moments applied there.

II.1.3.2 IDENTIFICATION OF THE SINGULARITIES

The character of the singularities in the kernels is the same with the tangential load solution. Thus, the radial displacement W is zero

at the pole while both tangential displacement components u_γ and u_η have logarithmic singular behavior. The stress and moment resultants have singularities of order ($1/\gamma$), while the transverse shearing stress resultants Q_γ and Q_η present strong singularities of order ($1/\gamma^2$).

II.2 IMPROVED THEORY

In the improved theory of shells the effect of the transverse shear is incorporated into the equations of equilibrium of the thin shell element. Even though the basic equations of equilibrium are the same for both theories, as noted in Appendix-A, the independent role of the angular rotations of the normal β_i will introduce two additional variables which in turn will upgrade the order of the governing differential system. This is because transverse shearing strains do not vanish in the improved theory analysis and, therefore, the rotations β_i can no longer be expressed in terms of the displacement component functions W, u_ϕ and u_θ. Furthermore, the shearing stress resultants Q_ϕ and Q_θ are now the direct effect of the nonvanishing shear stress and no longer a requirement for the overall equilibrium of the shell element. The natural boundary conditions that need to be satisfied along a boundary edge increase to five, and thus, along a boundary segment of constant s, the stress resultant N_{ns}, the twisting moment M_{ns} and the transverse shearing resultant Q_n cannot be combined into Kirchhoff's effective shearing boundary forces $Q_n + \frac{\partial M_{ns}}{\partial s}$ and $N_{ns} + \frac{M_{ns}}{R_s}$, but stand as independently prescribed boundary conditions.

The equations of the nonshallow spherical shell are uncoupled with the introduction of the auxiliary variables U, Ψ, Γ and Λ, see

Eqns. A.29-30, which relate to the displacement vector as well as the angular rotations of the normal. The primary system of equations is reduced to a secondary system of equations in terms of the introduced variables and the transverse displacement function W. This secondary system, for the case of only normal surface traction q_n being present, is uncoupled into a set of two differential equations:

$$\nabla^6 W + p_4 \nabla^4 W + p_2 \nabla^2 W + p_0 W + L_0 q_n = 0 \qquad (2.135)$$

where p_0, p_2, p_4 are defined in Eqns. (A.39) and the differential operator L_0 is given by Eqn. (A.40) and

$$(\nabla^2 + 2)\left[\nabla^2 + 2 - \frac{1}{\xi k_s^0}\right] \Psi = 0 \qquad (2.136)$$

where $k_s^0 = \frac{6}{5}$ and corresponds to the coefficient of shear as defined by Reissner[3] and Naghdi[5].

The remaining auxiliary variables Λ, U and Γ are governed by the system of equations (A.31), (A.33) and (A.35) which relates them, through differential operators, to the functions W and Λ.

The construction of the fundamental solutions for the differential operators of Eqns. 2.135-136 will follow a procedure similar to the one adopted in the classical theory analysis.

II.2.1.1 FUNDAMENTAL SOLUTIONS OF NORMAL SURFACE TRACTION

In constructing the fundamental singular solution we should again require that such solution must satisfy the differential operator and demonstrate singular behavior at a unique point on the complete sphere. Also, with the same argument used in the classical theory, the condition of equilibrium in the vicinity of the pole and the vanishing of the tangential displacement and the rotation vector at the pole must be satisfied by the fundamental solution without being introduced as a priori.

The self equilibrated normal surface traction which will again lead to the "free space" Green's function takes the same form as previously

$$q_n = \frac{1}{R^2}\left[\frac{\delta(\gamma)}{2\pi \sin\gamma} - \frac{3}{4\pi}\cos\gamma\right]. \qquad (2.137)$$

We consider Eqn. 2.135 in the form

$$L_1[\,W\,] = L_0[\,q_n\,] \qquad (2.138)$$

where

$$L_1 = \nabla^6 + p_4\,\nabla^4 + p_2\,\nabla^2 + p_0$$

and

$$p_4 = 3 - \mu - k_s\,(1 - \mu^2)$$

$$p_2 = \frac{1 - \mu^2}{\xi} + 2\,(1 - \mu) + k_s\,(1 - \mu^2)\,(\mu - 3) \qquad (2.139)$$

$$p_0 = \frac{2\,(1 - \mu^2)}{\xi} - 2\,(1 - \mu)\,(1 - \mu^2)\,k_s$$

$$L_0 = \frac{R^4}{D}\,(\nabla^2 + 1 - \mu)\left[\,1 - \frac{k_s\,(1 - \mu^2)\,D}{EhR^2}\,(\nabla^2 + 1 - \mu)\,\right]$$

$$k_s = \frac{2\,k_s^0}{1 - \mu}.$$

We express operator L_1 in its equivalent form

$$L_1 = (\nabla^2 - r_1)\,(\nabla^2 - r_2)\,(\nabla^2 - r_3) \qquad (2.140)$$

provided that r_i (i=1,2,3) are the roots of the cubic equation

$$r_i^3 + p_4\,r_i^2 + p_2\,r_i + p_0 = 0. \qquad (2.141)$$

The three roots can be obtained by using the formulas

$$r_1 = A + B - \frac{p_4}{3}$$

$$\begin{Bmatrix} r_2 \\ r_3 \end{Bmatrix} = -\frac{1}{2}\,(A + B) - \frac{p_4}{3} \pm \frac{i\sqrt{3}}{2}\,(A - B) \qquad (2.142)$$

where

$$\begin{pmatrix} A \\ B \end{pmatrix} = \left[\frac{1}{2} \left[-q \pm \left(\frac{\Delta}{27} \right)^{\frac{1}{2}} \right] \right]^{\frac{1}{3}} \tag{2.143}$$

$$q = p_0 - \frac{p_4 p_2}{3} + \frac{2 p_4^3}{27}$$

$$p = p_2 - \frac{p_4^2}{3} \tag{2.144}$$

$$\Delta = 27 q^2 + 4 p^2.$$

The nature of the roots r_i is governed by the determinant Δ, and thus if,

$\Delta > 0$: one root is real and two are complex conjugates

$\Delta = 0$: all roots are real and two are equal

$\Delta < 0$: all roots are real and unequal.

When Δ is evaluated for our particular case it is found positive and the three roots can be written as

$$r_1 = c_1 \quad , \quad \begin{pmatrix} r_2 \\ r_3 \end{pmatrix} = c_2 \pm i\, c_3 \tag{2.145}$$

where c_1, c_2 and c_3 are real numbers.

A numerical evaluation of the three roots above proves that root r_1 has the value of -2 and it is independent of the choice of the shell parameters and constants. Thus the equivalent form of the operator L_1 coincides with the product form of the operator of Eqn 2.1. The significance of the value of root r_1 will be discussed later in this section.

With one real root and two complex conjugate roots we express L_1 in the form

$$L_1 = (\nabla^2 + 2)\,[\nabla^2 + \nu\,(\nu + 1)]\,[\nabla^2 + \lambda\,(\lambda + 1)] \qquad (2.146)$$

where

$$r_1 = -2, \quad -r_2 = \nu\,(\nu + 1), \quad -r_3 = \lambda\,(\lambda + 1) \qquad (2.147)$$

or

$$\nu = -\frac{1}{2} \pm \left(\frac{1}{4} - r_2\right)^{\frac{1}{2}}$$

$$\lambda = -\frac{1}{2} \pm \left(\frac{1}{4} - r_3\right)^{\frac{1}{2}} \qquad (2.148)$$

Obviously ν and λ are complex conjugate parameters.

The component $\nabla^2 + 2$ of the operator L_1 represents the membrane solution of a loaded spherical shell. It is interesting to note that for both theories, classical and improved, the contribution of the

membrane solution is somewhat decoupled from the bending solution which dominates in the vicinity of the pole.

The complete form of Eqn. 2.135 can now be expressed as

$$(\nabla^2 + 2)\,[\nabla^2 + \nu\,(\nu + 1)]\,[\nabla^2 + \lambda\,(\lambda + 1)]\,W(\underset{\sim}{x};\underset{\sim}{x}') =$$

$$= \frac{R^4}{D}\,(\nabla^2 + 1 - \mu)\left(1 - \frac{k_s\,(1 - \mu^2)\,D}{EhR^2}\,(\nabla^2 + 1 - \mu)\right)$$

$$\times \left[\frac{1}{R^2}\left(\frac{\delta(\gamma)}{2\pi\,\sin\gamma} - \frac{3}{4\pi}\cos\gamma\right)\right] \qquad (2.149)$$

where again

$$\nabla^2 = \frac{d^2}{d\gamma^2} + \cot\gamma\,\frac{d}{d\gamma}.$$

We proceed in a manner similar to that adopted in the classical theory by expressing the fundamental solution of the transverse displacement $W(\underset{\sim}{x};\underset{\sim}{x}')$ in the equivalent form

$$W(\underset{\sim}{x};\underset{\sim}{x}') = W_1(\underset{\sim}{x};\underset{\sim}{x}') + W_2(\underset{\sim}{x};\underset{\sim}{x}') \qquad (2.150)$$

such as,

$$L_1\,[\,W_1(\underset{\sim}{x};\underset{\sim}{x}')\,] = L_0\,[\,\delta(\underset{\sim}{n} - \underset{\sim}{n}')\,]$$

$$L_1\,[\,W_2(\underset{\sim}{x};\underset{\sim}{x}')\,] = L_0\,[\,-\frac{1}{R^2}\,\frac{3}{4\pi}\cos\gamma\,]. \qquad (2.151)$$

We first consider the particular component W_2 governed by the second of Eqns above

$$L_1 [W_2(\underset{\sim}{x};\underset{\sim}{x}')] = \frac{R^2}{D} (\nabla^2 + 1 - \mu) [1 - C_0 (\nabla^2 + 1 - \mu)] (- \frac{3}{4\pi} \cos\gamma) \tag{2.152}$$

where

$$C_0 = \frac{k_s (1 - \mu^2) D}{EhR^2}.$$

By operating on the right side of Eqn. 2.152 we obtain

$$[1 - C_0 (\nabla^2 + 1 - \mu)] (- \frac{3}{4\pi} \cos\gamma) = - \frac{3}{4\pi} [1 + C_0 (1 + \mu)] \cos\gamma$$

and

$$\frac{R^2}{D} (\nabla^2 + 1 - \mu) \left[- \frac{3}{4\pi} [1 + C_0 (1 + \mu)] \cos\gamma \right] =$$

$$= \frac{3 R^2 (1 + \mu) [1 + C_0 (1 + \mu)]}{4 \pi D} \cos\gamma.$$

Thus Eqn. 2.152 can now be written as

$$(\nabla^2 + 2) [\nabla^2 + \nu (\nu + 1)] [\nabla^2 + \lambda (\lambda + 1)] W_2(\underset{\sim}{x};\underset{\sim}{x}') = 3 C_0' \cos\gamma \tag{2.152'}$$

where

$$C_0' = \frac{3\ R^2\ (1 + \mu)\ [1 + C_0\ (1 + \mu)]}{4\ \pi\ D}.$$

We introduce the function $f_p(\underset{\sim}{x};\underset{\sim}{x}')$ such as

$$(\nabla^2 + 2)\ f_p(\underset{\sim}{x};\underset{\sim}{x}') = 3\ C_0'\ \cos\gamma \tag{2.153}$$

which leads to

$$f_p(\underset{\sim}{x};\underset{\sim}{x}') = -\ C_0'\ [\ 1 + \cos\gamma\ \ln(1 - \cos\gamma)\ ]. \tag{2.154}$$

We express $W_2(\underset{\sim}{x};\underset{\sim}{x}')$ in the form

$$W_2(\underset{\sim}{x};\underset{\sim}{x}') = A_p\ f_p(\underset{\sim}{x};\underset{\sim}{x}') \tag{2.155}$$

and introduce it into Eqn. 2.152' such that

$$[\nabla^2 + \nu(\nu + 1)]\ [\nabla^2 + \lambda(\lambda + 1)]\ (\ A_p\ f_p(\underset{\sim}{x};\underset{\sim}{x}')\ ) = 3\ C_0'\ \cos\gamma \tag{2.156}$$

or

$$[\nabla^2 + \nu\ (\nu + 1)]\ [\nabla^2 + \lambda\ (\lambda + 1)]\ (\ A_p\ \cos\gamma\ ) = \cos\gamma$$

which results to

$$A_p\ \Big[\ [-\ 2 + \nu\ (\nu + 1)]\ [-\ 2 + \lambda\ (\lambda + 1)]\ \Big]\ \cos\gamma = \cos\gamma$$

and finally,

$$A_p = \frac{1}{[\nu\ (\nu + 1) - 2]\ [\lambda\ (\lambda + 1) - 2]}. \tag{2.157}$$

Thus, according to Eqn. 2.155 we can write

$$\begin{aligned} {}_2(\underset{\sim}{x};\underset{\sim}{x}') &= - A_p\ C_0'\ [\ 1 + \cos\gamma\ \ln(1 - \cos\gamma)\ ] \\ &= - T_1\ [\ 1 + \cos\gamma\ \ln(1 - \cos\gamma)\ ] \end{aligned} \tag{2.158}$$

where

$$T_1 = \left(\left[\mathrm{Re}(\nu(\nu + 1) - 2) \right]^2 + \left[\mathrm{Im}(\nu(\nu + 1) - 2) \right]^2 \right)^{-1} \cdot C_0'. \tag{2.159}$$

We now consider the first of Eqns. 2.151 which governs the contribution of the Delta function distribution onto the transverse displacement W and express $W_1(\underset{\sim}{x};\underset{\sim}{x}')$ in the form

$$W_1\ (\underset{\sim}{x};\underset{\sim}{x}') = L_0[\ U_s(\underset{\sim}{x};\underset{\sim}{x}')\ ] \tag{2.160}$$

provided that the introduced scalar function $U_s(\underset{\sim}{x};\underset{\sim}{x}')$ satisfies

$$L_1[\ U_s(\underset{\sim}{x};\underset{\sim}{x}')\ ] = \frac{\delta(\gamma)}{2\pi R^2 \sin\gamma} \tag{2.161}$$

or

$$(\nabla^2 + 2)\ [\nabla^2 + \nu(\nu + 1)\ ]\ [\nabla^2 + \lambda(\lambda + 1)\ ]\ U_s(\underset{\sim}{x};\underset{\sim}{x}') = \frac{\delta(\gamma)}{2\pi R^2 \sin\gamma}.$$

With similar procedures and arguments utilized in the classical theory approach, we retain only those independent solutions of the homogeneous form of Eqn. 2.161 that have singular characteristics at a single point on the complete sphere. This leads to the following expression for the scalar function U_s

$$U_s(\underset{\sim}{x};\underset{\sim}{x}') = A_2\ P_\nu(-\cos\gamma) + A_3\ P_\lambda(-\cos\gamma) \tag{2.162}$$

where A_2 and A_3 are complex conjugate arbitrary constants. The evaluation of the constants is dictated by the requirement that the particular solution of U_s satisfies Eqn. 2.161 in the vicinity of the pole $\gamma = 0$.

The introduction of an additional auxiliary scalar function $f(\underset{\sim}{x};\underset{\sim}{x}')$ and the application of the divergence theorem in the form of Eqn. 2.24, leads to the evaluation of one of the complex arbitrary constants and which is of the form

$$A_2 = \frac{1}{4\ [\nu(\nu+1) - \lambda(\lambda+1)]\ [2 - \nu(\nu+1)]\ \sin\nu\pi}$$

and

$$A_3 = \text{CONJG}\ [\ A_2\ ]. \tag{2.163}$$

According to Eqn. 2.160 $W_1(\underset{\sim}{x};\underset{\sim}{x}')$ can be written in the form

$$W_1(\underset{\sim}{x};\underset{\sim}{x}') = \frac{R^2}{D}\left[(\nabla^2 + 1 - \mu) - C_0' (\nabla^2 + 1 - \mu)^2 \right] U_s(\underset{\sim}{x};\underset{\sim}{x}')$$

which results to

$$W_1(\underset{\sim}{x};\underset{\sim}{x}') = \frac{R^2}{D}\, 2\, \mathrm{Re}\Big\{[1 - \mu - \nu(\nu+1)]\, A_2 \left[1 - C_0' [1 - \mu - \nu(\nu+1)]\right] \cdot P_\nu(-\cos\gamma) \Big\} \tag{2.164}$$

or

$$W_1(\underset{\sim}{x};\underset{\sim}{x}') = 2\, \mathrm{Re}\Big\{ A_n\, P_\nu(-\cos\gamma) \Big\} \tag{2.164'}$$

where $A_n = \frac{R^2}{D}\left\{[1 - \mu - \nu(\nu+1)]\, A_2 \left[1 - C_0' [1 - \mu - \nu(\nu+1)] \right]\right\}$.

The complete expression of the fundamental solution of the displacement function W will take the form of the sum of the solutions described by Eqns. 2.158 and 2.164. However, since the combined expression is to correspond to the Generalized Green's function of the spherical domain, the restrain condition

$$\iint_\sigma W(\underset{\sim}{x};\underset{\sim}{x}') \cos\gamma \, d\sigma = 0 \tag{2.165}$$

must be met. The above requirement introduces an additional term, which when combined in the expression of $W_2(\underset{\sim}{x};\underset{\sim}{x}')$ leads to

$$W_2 = - T_1 \left[1 + \cos\gamma \ln[1 - \cos\gamma] + B \cos\gamma \right] \tag{2.166}$$

where T_1 is given by Eqn 2.159 and

$$B = \frac{4}{3} - \ln 2. \tag{2.167}$$

Thus the complete expression of the fundamental singular solution or "free space" Green's function for the transverse displacement function W is defined as the sum of Eqns. 2.164 and 2.166.

The remaining auxiliary variables Ψ, Λ, U and Γ are evaluated with the help of the system of equations (A. 31,32,35) and 2. 136 together with the incorporation of the displacement function W derived above. We recall that the secondary system of equations was expressed in terms of the functions W and Ψ through the uncoupled Eqns. 2.135,136. From Eqn. 2.136 we observe that the auxiliary variable Ψ has no dependence on the normal surface traction q_n. For the axisymmetric case the general homogeneous solution of Eqn. 2.136 will take the form

$$\Psi(\underset{\sim}{x};\underset{\sim}{x}') = A_1^{\psi} P_1(\cos\gamma) + A_2^{\psi} Q_1(\cos\gamma) + B_1^{\psi} P_{\omega}(\cos\gamma) + B_2^{\psi} Q_{\omega}(\cos\gamma) \tag{2.168}$$

where

$$\omega\ (\omega + 1) = 2 - \frac{1}{\xi k_s^0} \tag{2.169}$$

and A_1^{ψ} , A_2^{ψ} , B_1^{ψ} , B_2^{ψ} are arbitrary constants.

Eqn. (A.32) can provide the general solution form of the auxiliary variable $\Lambda(\underset{\sim}{x};\underset{\sim}{x}')$ expressed as

$$\Lambda(\underset{\sim}{x};\underset{\sim}{x}') = - k_s^0 (\nabla^2 + 2) \Psi(\underset{\sim}{x};\underset{\sim}{x}')$$

$$= - k_s^0 [2 - \omega(\omega + 1)] \left[B_1^{\psi} P_{\omega}(\cos\gamma) + B_2^{\psi} Q_{\omega}(\cos\gamma) \right]. \qquad (2.170)$$

The requirement, however, of a single singularity in the domain and the elimination of the regular solutions from the expressions for Ψ and Λ yields

$$\Psi(\underset{\sim}{x};\underset{\sim}{x}') = B_1^{\psi} P_{\omega}(-\cos\gamma) \qquad (2.171)$$

and

$$\Lambda(\underset{\sim}{x};\underset{\sim}{x}') = - k_s^0 [2 - \omega(\omega + 1)] B_1^{\psi} P_{\omega}(-\cos\gamma). \qquad (2.172)$$

The incorporation of the final forms of $\Psi(\underset{\sim}{x};\underset{\sim}{x}')$ and $\Lambda(\underset{\sim}{x};\underset{\sim}{x}')$ into the singular solution would require the evaluation of the arbitrary constant B_1^{ψ}, which in turn would have to satisfy a requirement set as a priori. But the only condition variable Ψ must satisfy, besides being a solution of the governing system, is the existence of the Delta function to which it apparently has no relation since it is independent of the normal surface traction. We observe, however, that variables Ψ and Λ are related to the tangential displacement u_{γ}, the rotation of the normal and consequently to the shearing resultant Q_{γ}.

The axisymmetry of the solution reasonably requires that when approaching the pole $\gamma = 0$, the two vectors u_γ and β_γ satisfy

$$\lim_{\gamma\to 0} u_\gamma = \lim_{\gamma\to 0} \left[\frac{dU}{d\gamma} - \Psi R \sin\gamma \right] = 0$$

$$\lim_{\gamma\to 0} \beta_\gamma = \lim_{\gamma\to 0} \left[\frac{d\Gamma}{d\gamma} - \Lambda \sin\gamma \right] = 0. \qquad (2.173)$$

The general expressions for Ψ and Λ contain a logarithmic singularity and their contribution to the limiting value of u_γ and β_γ vanishes since

$$\lim_{\gamma\to 0} [\sin\gamma \Psi] = \lim_{\gamma\to 0} [\sin\gamma \Lambda] = 0. \qquad (2.174)$$

Thus for the axisymmetric case and without any loss of true representation of the system's variables, we can set

$$\Psi(\underset{\sim}{x};\underset{\sim}{x}') = \Lambda(\underset{\sim}{x};\underset{\sim}{x}') = 0. \qquad (2.175)$$

With the elimination of Ψ and Λ from the secondary system of equations, the remaining variables U, Γ and the already defined W are associated through the relations

$$R^2 \nabla^2\Lambda(\underset{\sim}{x};\underset{\sim}{x}') - (1 + \mu) k_s \nabla^2 U(\underset{\sim}{x};\underset{\sim}{x}') + [\nabla^2 - 2 (1 + \mu) k_s] W(\underset{\sim}{x};\underset{\sim}{x}')$$

$$+ \frac{R^2 (1 - \mu^2) k_s}{Eh} q_n = 0$$

$$\left[\nabla^2 + 1 - \mu - \frac{1}{\xi k_s} \right] \Gamma(\underset{\sim}{x};\underset{\sim}{x}') - \frac{W(\underset{\sim}{x};\underset{\sim}{x}')}{\xi R k_s} = 0 \qquad (2.176)$$

$$[\nabla^2 + 1 - \mu] U(\underset{\sim}{x};\underset{\sim}{x}') + [1 + \mu + \frac{1}{k_s}] W(\underset{\sim}{x};\underset{\sim}{x}') + \frac{R}{k_s} \Gamma(\underset{\sim}{x};\underset{\sim}{x}') = 0.$$

We operate onto the first of the equations above with $\nabla^2 + 1 - \mu$ and obtain

$$R [\nabla^2 + 1 - \mu] \nabla^2\Gamma - (1 + \mu) k_s [\nabla^2 + 1 - \mu] \nabla^2 U +$$

$$(\nabla^2 + 1 - \mu) \left[\nabla^2 - 2(1 + \mu)\right] W + (\nabla^2 + 1 - \mu) \left[\frac{R^2 (1 - \mu^2) k_s}{Eh} q_n\right] = 0.$$

From the third of Eqns. 2.176 we deduce

$$(\nabla^2 + 1 - \mu) U = - (1 + \mu + \frac{1}{k_s}) W - \frac{R}{k_s} \Gamma,$$

while from the second equation we obtain

$$(\nabla^2 + 1 - \mu) \Gamma = \frac{W}{\xi R k_s} + \frac{1}{\xi k_s} \Gamma.$$

The linearity of the operators involved in the above expressions lead to the following:

$$\Gamma(\underset{\sim}{x};\underset{\sim}{x}') = -\left[\frac{\xi^2 k_s^2}{R D_3}\nabla^4 + \frac{\xi k_s D_1}{R D_3}\nabla^2 + \frac{D_2}{R D_3}\right] W(\underset{\sim}{x};\underset{\sim}{x}')$$

$$-\frac{\xi^2 k_s^2}{R D_3}(\nabla^2 + 1 - \mu)\left[\frac{R^2 (1 - \mu^2) k_s}{Eh} q_n\right] \qquad (2.177)$$

where

$$D_1 = 1 + 2\xi k_s - \xi k_s^2 (1 - \mu^2)$$

$$D_2 = 1 + (1 + \mu)\xi k_s - 2(1 - \mu^2)\xi^2 k_s^2 \qquad (2.178)$$

$$D_3 = 1 + 2\mu\xi k_s + (\mu^2 - 1)\xi^2 k_s^2.$$

We decompose $\Gamma(\underset{\sim}{x};\underset{\sim}{x}')$ as follows

$$\Gamma(\underset{\sim}{x};\underset{\sim}{x}') = \Gamma_s(\underset{\sim}{x};\underset{\sim}{x}') + \Gamma_r(\underset{\sim}{x};\underset{\sim}{x}') \qquad (2.179)$$

where the subscripts s and r identify the singular and the regular components of (2.177). The regular solution Γ_r is to be derived as the dependence of Γ onto the equilibrating surface traction $q_{n'}$, while Γ_s will be associated with the fundamental singular solution of the transverse displacement W.

The operations in expression 2.177 are being carried out with the help of the following identities:

$$\nabla^2[1 - \cos\gamma \ln(1 - \cos\gamma)] = -3\cos\gamma - 2[1 + \cos\gamma \ln(1 - \cos\gamma)]$$

$$\nabla^2 (\cos\gamma) = - 2 \cos\gamma \tag{2.180}$$

$$\nabla^2 [P_\nu(-\cos\gamma)] = - \nu(\nu + 1) P_\nu(-\cos\gamma)$$

and they lead to the final form of $\Gamma(\underset{\sim}{x};\underset{\sim}{x}')$

$$\Gamma(\underset{\sim}{x};\underset{\sim}{x}') = 2 \, \mathrm{Re}\left[A_n^\Gamma P_\nu(- \cos\gamma)\right] + T_1^\Gamma [1 + \cos\gamma \ln(1 - \cos\gamma)] + C^\Gamma \cos\gamma \tag{2.181}$$

where

$$A_n^\Gamma = - \left[\frac{\xi^2 k_s^2}{R D_3} [\nu(\nu + 1)]^2 - \nu(\nu + 1) \frac{\xi k_s D_1}{R D_3} + \frac{D_2}{R D_3} \right] A_n$$

$$T_1^\Gamma = \left[4 \frac{\xi^2 k_s^2}{R D_3} - 2 \frac{\xi k_s D_1}{R D_3} + \frac{D_2}{R D_3} \right] T_1$$

$$C^\Gamma = \left[\frac{\xi^2 k_s^3 R (1 + \mu) (1 - \mu^2) C_q}{D_3 E h} + \frac{2 \xi k_s D_1 - 4 \xi^2 k_s^2 - D_2}{R D_3} C_p \right]$$

$$C_q = - \frac{3}{4\pi R^2} \tag{2.182}$$

$$C_p = - T_1 B$$

$$B = \frac{4}{3} - \ln 2.$$

Similar procedures to the ones above are used to determine the remaining variable $U(\underset{\sim}{x};\underset{\sim}{x}')$ which is also obtained from Eqns. 2.176. Between these relations $U(\underset{\sim}{x};\underset{\sim}{x}')$ is isolated and expressed in the form

$$U(\underset{\sim}{x};\underset{\sim}{x}') = -(\xi R)\,\Gamma(\underset{\sim}{x};\underset{\sim}{x}') + \left[(1 - 2\xi k_s) + \frac{\xi [2 - (1 - \mu^2) k_s]}{1 - \mu^2} \nabla^2 + \frac{\xi}{1 - \mu^2} \nabla^4 \right] W(\underset{\sim}{x};\underset{\sim}{x}') - \frac{R^2}{Eh} q_n + \frac{\xi k_s R^2}{Eh} (\nabla^2 + 1 - \mu)\, q_n \quad (2.183)$$

which, after the execution of the operations, leads to

$$U(\underset{\sim}{x};\underset{\sim}{x}') = 2\,\mathrm{Re}\left[A_n^U P_\nu(-\cos\gamma)\right] + T_1^U [1 + \cos\gamma \ln(1 - \cos\gamma)] + C^U \cos\gamma \quad (2.184)$$

where

$$A_n^U = -\xi R A_n^\Gamma + \left[1 - 2\xi k_s - \frac{\xi [2 - (1 - \mu^2) k_s]}{(1 - \mu^2)} \nu(\nu + 1) + \frac{\xi}{1 - \mu^2} [\nu(\nu + 1)]^2 \right] A_n$$

$$T_1^U = -\xi R T_1^\Gamma + \left[1 - 2\xi k_s - 2 \frac{\xi [2 - (1 - \mu^2) k_s]}{(1 - \mu^2)} + 4 \frac{\xi}{1 - \mu^2} \right] T_1 \quad (2.185)$$

$$C^U = -\xi R C^\Gamma + C_p - \frac{R^2}{Eh} [1 + \xi k_s (1 + \mu)]\, C_q.$$

Equations (2.166,181,182) relating to W, Γ, and U variables respectively will constitute the basis upon which the complete set of the dependent variables of the system is to be determined. Thus we obtain the tangential displacement u_γ by utilizing its relation to the variable $U(\underset{\sim}{x};\underset{\sim}{x}')$ which yields

$$u_\gamma = \frac{d}{d\gamma} U(\underset{\sim}{x};\underset{\sim}{x}') = - 2\,\mathrm{Re}\left[A_n^U P_\nu^1 (-\cos\gamma) \right] +$$

$$+ T_1^U \left[\frac{\cos\gamma \sin\gamma}{1 - \cos\gamma} - \sin\gamma \ln(1 - \cos\gamma) \right] - C^U \sin\gamma \qquad (2.186)$$

and the angular rotation β_γ from variable $\Gamma(\underset{\sim}{x};\underset{\sim}{x}')$ such as

$$\beta_\gamma = \frac{d}{d\gamma} \Gamma(\underset{\sim}{x};\underset{\sim}{x}') = - 2\,\mathrm{Re}\left[A_n^\Gamma P_\nu^1 (-\cos\gamma) \right] +$$

$$+ T_1^\Gamma \left[\frac{\cos\gamma \sin\gamma}{1 - \cos\gamma} - \sin\gamma \ln(1 - \cos\gamma) \right] - C^\Gamma \sin\gamma \qquad (2.187)$$

while due to axisymmetry

$$u_\eta = \beta_\eta = 0. \qquad (2.188)$$

The shear resultant Q_γ expression follows from Eqn. (A.27) in the form

$$Q_\gamma = \frac{Eh}{2\,(1 + \mu)\,k_s^0} \left[\beta_\gamma + \frac{1}{R} \frac{dW}{d\gamma} \right] \qquad (2.189)$$

and consequently

$$Q_\eta = 0. \qquad (2.189')$$

The kernel expressions for the stress and moment resultants follow from Eqns. (A.23,24)

$$N_\gamma = \frac{Eh}{(1 - \mu^2)\, R} \left[\frac{du_\gamma}{d\gamma} + \mu \cot\gamma\, u_\gamma + (\mu + 1)\, W \right]$$

$$N_\eta = \frac{Eh}{(1 - \mu^2)\, R} \left[\mu \frac{du_\gamma}{d\gamma} + \cot\gamma\, u_\gamma + (\mu + 1)\, W \right] \qquad (2.190)$$

$$M_\gamma = \frac{D}{R} \left[\frac{d\beta_\gamma}{d\gamma} + \mu \cot\gamma\, \beta_\gamma \right]$$

$$M_\eta = \frac{D}{R} \left[\mu \frac{d\beta_\gamma}{d\gamma} + \cot\gamma\, \beta_\gamma \right]$$

and

$$N_{\gamma\eta} = M_{\gamma\eta} = 0. \qquad (2.190')$$

II.2.1.2 IDENTIFICATION OF THE SINGULARITIES

We examine the character of the fundamental singularity in the displacement and stress kernels as $\gamma \to 0$ and evaluate the predictions of the improved theory in the vicinity of the pole. It is to be expected that the differences between the classical and the improved treatments of the shell domain are most pronounced near the point of application of the singular load.

By calculating the limiting values of the Legendre functions associated with the kernels as well as of the elementary functions involved we obtain for the transverse displacement W

$$\lim_{\gamma\to 0} W = 2\,\mathrm{Re}\left\{ A_n \frac{2}{\pi} \sin\nu\pi \left[\lim_{\gamma\to 0} \left(\sin\frac{\gamma}{2} \right) + CP_0(\nu) \right] \right\}$$

$$- T_1 \lim_{\gamma\to 0} [1 + \cos\gamma \ln(1 - \cos\gamma) + B\cos\gamma]$$

or

$$\lim_{\gamma\to 0} W = 2 \left[\frac{2}{\pi} \mathrm{Re}[A_n \sin\nu\pi] - T_1 \right] \lim_{\gamma\to 0} \ln(\sin\frac{\gamma}{2}) + \text{Const.} \qquad (2.191)$$

It is apparent that, while the classical theory analysis predicts a finite response of the transverse displacement W at the point of application of the singular load, according to the improved theory treatment W is unbounded, experiencing a logarithmic singularity in its kernel. This finding, however, is in complete agreement with previous results obtained in other investigations concerning both the shallow and the nonshallow approach of the shell problem.

A detailed evaluation (numerical) reveals that in the limit as $\gamma\to 0$, the displacement variables u_γ and β_γ identically satisfy

$$\lim_{\gamma\to 0} [\, u_\gamma \,] = 0$$

and

$$\lim_{\gamma\to 0} [\, \beta_\gamma \,] = 0. \qquad (2.192)$$

As noted earlier the above two conditions together with the equilibrium requirement around the pole expressed by the integral

$$\lim_{\gamma \to 0} \int_{0}^{2\pi} \left[Q_{\gamma} \cos\gamma + N_{\gamma} \sin\gamma \right] R \sin\gamma \, d\eta = -1 \qquad (2.193)$$

constitute a set of constraints that the fundamental solution must satisfy. It has also been noted that their interaction with the construction of the fundamental singularity, when set as a priori, could lead to an incorrect fundamental solution. Evaluation of the integral shown in Eqn. 2.193 with the help of Eqns. 2.189,190 reveals that the condition is indeed satisfied.

The singularity encountered in the shear resultant kernel Q_{γ} is of the order

$$\lim_{\gamma \to 0} Q_{\gamma} = \frac{2\,Eh}{2\,(1+\mu)\,k_s^0\,R} \left[\mathrm{Re}[A_n \frac{2}{\pi} \sin\nu\pi] - T_1 \right] \lim_{\gamma \to 0} \left(\frac{1}{\gamma} \right). \qquad (2.194)$$

The character of the singularities in the stress and moment resultant kernels is logarithmic, same as in the classical theory analysis, and their limiting value can be simply written as

$$\lim_{\gamma \to 0} \left[N_{\gamma},\ N_{\eta},\ M_{\gamma},\ M_{\eta} \right] = \lim_{\gamma \to 0} \left[A_i \ln\left(\sin \frac{\gamma}{2} \right) + B_i \right] \qquad (2.195)$$

where, A_i and B_i are constants evaluated between the limiting behavior of the Legendre functions and the respective constants associated with the Fundamental Solutions.

We should further note that the state of compression in the vicinity of the load point experienced in the classical theory, $\lim_{\gamma \to 0} N_\gamma = -\infty$, is no longer predicted by the improved theory which, in turn, demonstrates that N_γ approaches $+\infty$. Thus we conclude that, under the influence of a concentrated load applied along the outward normal, the vicinity of the pole is in tension. Such response is expected on the grounds of physical reasoning.

II.2.2 SINGULAR SELF-EQUILIBRATED SOLUTIONS OF A UNIT MOMENT AND A UNIT TANGENTIAL LOAD

The construction of such singular solutions, their properties and their compatibility as fundamental singular solutions have been discussed in the classical theory analysis. As seen, solutions associated with types of loading without axisymmetric nature do not, within the framework of this study, retain the restrictive condition of a single singularity in the complete spherical surface. This is the result of the singular load state required to insure overall equilibrium of the domain.

We again utilize the homogeneous solutions of Eqns. 2.135,136. This implies that all the components of the external force vector are zero. However, the singularities of the general solution of these equations, encountered in the kernels of the transverse displacement W and the auxiliary function Ψ, will be integrated into the solution to yield the singular states associated with the action of concentrated tangential loads and moments.

The general solution for W and Ψ expressed in the rotated geographical system (γ,η) will be of the form

$$W(\underset{\sim}{x};\underset{\sim}{x}') = \Big[A_1 P_1^1(\cos\gamma) + A_2 Q_1^1(\cos\gamma) + B_1 P_\nu^1(\cos\gamma) + B_2 P_\nu^1(-\cos\gamma) + C_1 P_\lambda^1(\cos\gamma) + C_2 P_\lambda^1(-\cos\gamma) \Big] \cos\eta \qquad (2.196)$$

and

$$\Psi(\underset{\sim}{x};\underset{\sim}{x}') = \Big[A_1' P_1^1 (\cos\gamma) + A_2' Q_1^1 (\cos\gamma) + B_1' P_\omega^1 (\cos\gamma) + B_2' P_\omega^1 (-\cos\gamma) \Big] \cos\eta \qquad (2.197)$$

where

$$\omega (\omega + 1) = 2 - \frac{1}{\xi\, k_s^0}$$

$$\omega = -\frac{1}{2} - i\,\rho \qquad (2.198)$$

$$\rho = \frac{1}{2} \left[1 - 4 \left(2 - \frac{12\, R^2}{k_s^0\, h^2} \right) \right]^{\frac{1}{2}}.$$

We should again note that because of the complex conjugate parameters ν and λ, the associate Legendre functions P_ν^1 and P_λ^1 are also complex conjugates. The implication of the above is that, in order for the displacement W to remain a real quantity, the arbitrary constants B_1, B_2 and C_1, C_2 are complex conjugates respectively. Further we notice that the degree of the associate Legendre function P_ω^1 is also complex, although the auxiliary variable Ψ is required to remain real due to its relation to the displacement and stress variables. However, the character of the parameter ω, as discussed in Appendix C, will lead to a special case of Legendre functions which are real for real values of the argument and the parameter ρ while their order consists of integral non-negative values. This implies that the arbitrary constants B_1' and B_2' are real in

nature. In addition, since $P_1^1(\cos\gamma)$ is a regular function everywhere in the domain, its contribution to the solution of the singular system can be eliminated by setting $A_1 = A_1' = 0$ without any loss of generality. The above is justified from the fact that the solutions retained must satisfy the singular state at $\gamma = 0$ and/or at $\gamma = \pi$.

The general expression of the auxiliary variable $\Lambda(\underset{\sim}{x};\underset{\sim}{x}')$ can be deduced from the relation

$$(\nabla^2 + 2)\Psi(\underset{\sim}{x};\underset{\sim}{x}') + \frac{1}{k_s^0}\,\Lambda(\underset{\sim}{x};\underset{\sim}{x}') = 0 \qquad (2.199)$$

which leads to

$$\Lambda(\underset{\sim}{x};\underset{\sim}{x}') = - k_s^0\,(\nabla^2 + 2)\,\Psi(\underset{\sim}{x};\underset{\sim}{x}')$$

or

$$\Lambda(\underset{\sim}{x};\underset{\sim}{x}') = C'\,[\,B_1'\,P_\omega^1(\cos\gamma) + B_2'\,P_\omega^1(-\cos\gamma)\,]\cos\eta \qquad (2.200)$$

where

$$C' = - k_s^0\,[2 - \omega(\omega + 1)]. \qquad (2.201)$$

The remaining auxiliary variables Γ and U can be derived in terms of W, Ψ and Λ. Uncoupling of the operators in Eqns. A.31,32,35 yields for Γ and U variables the expressions:

$$\Gamma(\underset{\sim}{x};\underset{\sim}{x}') = \left[e_1 + e_2\,\nabla^2 + e_4\,\nabla^4\right] W(\underset{\sim}{x};\underset{\sim}{x}') + e_5\,\sin\gamma\,\frac{\partial}{\partial\gamma}\,\Lambda(\underset{\sim}{x};\underset{\sim}{x}') \qquad (2.202)$$

where

$$e_1 = \frac{k_1}{\alpha_\Gamma}\,, \qquad e_2 = \frac{k_2}{\alpha_\Gamma}\,, \qquad e_4 = \frac{k_4}{\alpha_\Gamma}\,, \qquad e_5 = \frac{k_5}{\alpha\Gamma}$$

$$\alpha_\Gamma = R\,[\,1 + 2\,\xi\,k_s\,\mu - (1 - \mu^2)\,\xi^2\,k_s^2\,]$$

$$k_1 = -\,[\,1 + \xi\,k_s\,(1 + \mu) - 2\,(1 - \mu^2)\,\xi^2\,k_s^3\,] \qquad (2.203)$$

$$k_2 = -\,\xi\,k_s\,[\,1 + \xi\,k_s\,(2 - (1 - \mu^2)\,k_s)\,]$$

$$k_4 = -\,\xi^2\,K_s^2$$

$$k_5 = \xi\,k_s^0\,R\,[\,1 + \xi\,k_s\,(1 + \mu)\,].$$

By utilizing the identities

$$\nabla^2\,W(\underset{\sim}{x};\underset{\sim}{x}') = -\Big\{\,2\,A_2\,Q_1^1(\cos\gamma) + \nu(\nu+1)\,[B_1\,P_\nu^1(\cos\gamma) + B_2\,P_\nu^1(-\cos\gamma)] + \lambda(\lambda+1)\,[C_1\,P_\lambda^1(\cos\gamma) + C_2\,P_\lambda^1(-\cos\gamma)]\,\Big\}\cos\eta$$

$$\nabla^4\,W(\underset{\sim}{x};\underset{\sim}{x}') = \Big\{\,4\,A_2\,Q_1^1(\cos\gamma) + (\nu(\nu+1))^2\,[B_1\,P_\nu^1(\cos\gamma) + B_2\,P_\nu^1(-\cos\gamma)] + (\lambda(\lambda+1))^2\,[C_1\,P_\lambda^1(\cos\gamma) + C_2\,P_\lambda^1(-\cos\gamma)]\,\Big\}\cos\eta$$

$$\frac{\partial}{\partial\gamma}\,\Lambda(\underset{\sim}{x};\underset{\sim}{x}') = C'\Big\{-B_1'\,[\,\omega(\omega+1)\,P_\omega(\cos\gamma) + \cot\gamma\,P_\omega^1(\cos\gamma)\,] + B_2'\,[\,\omega(\omega+1)\,P_\omega(\cos\gamma) - \cot\gamma\,P_\omega^1(\cos\gamma)\,]\Big\}\cos\eta$$

we obtain for $\Gamma(\underset{\sim}{x};\underset{\sim}{x}')$

$$\Gamma(\underset{\sim}{x};\underset{\sim}{x}') = \Big\{ \delta_1 A_2 Q_i^1(\cos\gamma) + \delta_2 [B_1 P_\nu^1(\cos\gamma) + B_2 P_\nu^1(-\cos\gamma)] + \delta_3 [C_1 P_\lambda^1(\cos\gamma) + C_2 P_\lambda^1(-\cos\gamma)] + e_5 C' \Big[\sin\gamma\, \omega(\omega+1) [B_2' P_\omega(-\cos\gamma) - B_1' P_\omega(\cos\gamma)] - \cos\gamma [B_1' P_\omega^1(\cos\gamma) + B_2' P_\omega^1(-\cos\gamma)] \Big] \Big\} \cos\eta \qquad (2.204)$$

where

$$\delta_1 = e_1 - 2 e_2 + 4 e_4$$
$$\delta_2 = e_1 - \nu(\nu+1) e_2 + [\nu(\nu+1)]^2 e_4$$
$$\delta_3 = e_1 - \lambda(\lambda+1) e_2 + [\lambda(\lambda+1)]^2 e_4. \qquad (2.205)$$

Similarly, for the remaining auxiliary variable $U(\underset{\sim}{x};\underset{\sim}{x}')$ we deduce the expression

$$U(\underset{\sim}{x};\underset{\sim}{x}') = -\xi R \Gamma(\underset{\sim}{x};\underset{\sim}{x}') + \Big[(1 - 2\xi k_s) + \frac{\xi [2 - (1-\mu^2) k_s]}{1-\mu^2} \nabla^2 + \frac{\xi}{1-\mu^2} \nabla^4 \Big] W(\underset{\sim}{x};\underset{\sim}{x}') - \frac{R}{2} \sin\gamma [(\xi+1) \frac{\partial}{\partial\gamma} (\Lambda(x;x') + \Psi(x;x'))] \qquad (2.206)$$

which can equivalently be written in the form

$$U(\underset{\sim}{x};\underset{\sim}{x}') = \Big\{ e_U^1 A_2 Q_i^1(\cos\gamma) + e_U^2 [B_1 P_\nu^1(\cos\gamma) + B_2 P_\nu^1(-\cos\gamma)] + e_U^3 [C_1 P_\lambda^1(\cos\gamma) + C_2 P_\lambda^1(-\cos\gamma)]$$

$$+ e_0 \left[\sin\gamma\ \omega(\omega+1)\ [\ B_2'\ P_\omega(-\cos\gamma) - B_1'\ P_\omega(\cos\gamma)\ ] \right.$$

$$\left. - \cos\gamma\ [B_1'\ P_\omega^1(\cos\gamma) + B_2'\ P_\omega^1(-\cos\gamma)\ ] \right] - \frac{R}{2} A_2'\ \sin\gamma\ DQ_1^1 \Big)\ \cos\eta \tag{2.207}$$

where

$$e_U^1 = -\xi\ R\ \delta_1 + 1 - 2\ \xi\ k_s - \frac{2\ \xi\ [2 - (1-\mu^2)\ k_s}{1-\mu^2} + \frac{4\ \xi}{1-\mu^2}$$

$$e_U^2 = -\xi\ R\ \delta_1 + 1 - 2\ \xi\ k_s - \frac{\nu(\nu+1)\ \xi\ [2 - (1-\mu^2)\ k_s}{1-\mu^2}$$

$$+ \frac{[\nu(\nu+1)]^2\ \xi}{1-\mu^2} \tag{2.208}$$

$$e_U^3 = \text{CONJG}\ [\ e_U^2\ ]$$

$$e_0 = \xi\ R\ e_5\ C' + \frac{\xi\ R\ C'}{2} + \frac{R}{2}$$

and

$$DQ_1^1 = \frac{d}{d\gamma}\ Q_1^1(\cos\gamma) = -\frac{1}{2}\cos\gamma\ \ln\frac{1+\cos\gamma}{1-\cos\gamma} + 1 + \frac{1}{\sin^2\gamma}. \tag{2.209}$$

The remaining components of the displacement vector u_γ and u_η are deduced from the relations

$$u_\gamma = \frac{\partial}{\partial\gamma}\ U(\underset{\sim}{x};\underset{\sim}{x}') - R\ \sin\gamma\ \Psi(\underset{\sim}{x};\underset{\sim}{x}')$$

and (2.110)

$$u_\eta = \csc\gamma\ \frac{\partial}{\partial\eta}\ U(\underset{\sim}{x};\underset{\sim}{x}'),$$

while the angular rotations of the normal vector β_γ and β_η are derived from the expressions

$$\beta_\gamma = \frac{\partial}{\partial\gamma}\,\Gamma(\underset{\sim}{x};\underset{\sim}{x}') - \sin\gamma\,\Lambda(\underset{\sim}{x};\underset{\sim}{x}')$$

and (2.111)

$$\beta_\eta = \csc\gamma\,\frac{\partial}{\partial\eta}\,\Gamma(\underset{\sim}{x};\underset{\sim}{x}').$$

Substitution into Eqns. 2.110,111 of the the auxiliary variables leads to

$$u_\gamma = \Bigg\{ e_U^1\,A_2\,DQ_i^1 + 2\,\mathrm{Re}\Big[e_U^2\,\{\nu(\nu+1)\,[B_2\,P_\nu(-\cos\gamma) - B_1\,P_\nu(\cos\gamma)]$$

$$- \cot\gamma\,[B_1\,P_\nu^1(\cos\gamma) + B_2\,P_\nu^1(-\cos\gamma)]\}\Big] - \frac{e_0}{\sin\gamma}\,[B_1\,P_\nu^1(\cos\gamma)$$

$$+ B_2\,P_\nu^1(-\cos\gamma)] + [e_0\,\omega(\omega+1) - R]\,\sin\gamma\,[B_1'\,P_\omega^1(\cos\gamma) + B_2'\,P_\omega^1(-\cos\gamma)]$$

$$- \frac{R\,A_2'}{2}\Big[\sin\gamma\,D_2Q_i^1 + \cos\gamma\,DQ_i^1 + 2\sin\gamma\,Q_i^1(\cos\gamma)\Big]\Bigg\}\cos\eta \qquad (2.212)$$

where

$$D_2Q_i^1 = \frac{d^2}{d\gamma^2}\,Q_i^1(\cos\gamma) = \frac{1}{2}\sin\gamma\,\ln\frac{1+\cos\gamma}{1-\cos\gamma} + \cot\gamma - \frac{2\cos\gamma}{\sin^2\gamma} \qquad (2.213)$$

and

$$u_\eta = -\csc\gamma\,U(\gamma)\,\sin\eta$$

$$U(\underset{\sim}{x};\underset{\sim}{x}') = U(\gamma)\,\cos\eta. \qquad (2.214)$$

Similarly for the angular rotations we derive the expressions

$$\beta_\gamma = \Big\{ \delta_1 A_2 DQ_1^1 + 2 \mathrm{Re}\Big[\delta_2 \{\nu(\nu+1) [B_2 P_\nu(-\cos\gamma) - B_1 P_\nu(\cos\gamma)] \cot\gamma [B_1 P_\nu^1(\cos\gamma) + B_2 P_\nu^1(-\cos\gamma)]\} \Big] \tag{2.215}$$

$$+ C' \Big[\frac{e_5}{\sin\gamma} - \{1 + \omega(\omega+1)\} \sin\gamma \Big] [B_1' P_\omega^1(\cos\gamma) + B_2' P_\omega^1(-\cos\gamma)]$$

and

$$\beta_\eta = - \csc\gamma \, \Gamma(\gamma) \sin\eta$$

$$\Gamma(\underset{\sim}{x};\underset{\sim}{x}') = \Gamma(\gamma) \cos\eta. \tag{2.216}$$

Substitution of the displacement and angular rotation vector components into Eqns. (A.23,24,25) will yield the expressions for the stress, moment and shearing stress resultants. Thus, with these last manipulations we have arrived at a general solution state of a complete sphere experiencing the effect of singular loads applied at both of its poles ($\gamma = 0$ and $\gamma = \pi$). These singular loads introduce a state of deformation and stress symmetric with respect to the surface coordinate $\eta = 0$. The character and the physical interpretation of the singularities in the kernel functions of the dependent field variables will again be examined with the introduction of a limiting contour in the vicinity of the poles. This procedure will provide us a clear view as to what physical system the singularities relate to or further, to what system they could relate to if additional limiting constraints are imposed onto the general solution of the system. The singularities will again be evaluated in the form of the two integrals given by Eqns. 2.103,104 in which

equilibrium around the two poles is implemented in the forms of a resultant tangent force and a resultant moment.

In the two sections that follow, the construction of the singular solution states corresponding to the action of (a) a unit concentrated moment, and (b) a concentrated unit tangential force, will be formulated by utilizing the same general singular solution derived subjected to appropriate limiting conditions for each of the two cases.

II.2.2.1 CONCENTRATED UNIT MOMENT SOLUTION

We consider the self-equilibrated singular moment state shown in Fig. 2-6. The physical conditions imposed onto the general solution in order to evaluate the arbitrary constants, which in turn will insure the correspondence of the final solution to the physical situation desired, are the following:

1. Symmetric transverse displacement W with respect to $\gamma = \frac{\pi}{2}$ expressed as $W(\gamma) = W(\pi - \gamma)$.

2. The net normal displacement in the vicinity of the poles should vanish due to the fact that no net forces act along that direction. The condition, similarly with Eqn. 2.122, will be evaluated in the form of the integral

$$\lim_{\substack{\gamma\to 0\\ \gamma\to\pi}} \int_0^{2\pi} \left[W\cos\gamma - u_\gamma \sin\gamma + R \sin\gamma\, \beta_\gamma \right] R \sin\gamma \cos\eta \, d\eta = 0.$$

3. The tangential displacement component in the direction of $\eta = \pm \frac{\pi}{2}$ should vanish as we approach the two poles due to the character of the applied load. We view this condition again in the form of the integral

$$\lim_{\substack{\gamma\to 0\\ \gamma\to\pi}} \int_0^{2\pi} \left[W \sin\gamma + u_\gamma \cos\gamma + u_\eta \right] R \sin\gamma \cos\eta \, d\eta = 0.$$

4. The net angular rotation of the normal in the direction of $\eta = \pm \frac{\pi}{2}$ must also vanish. This condition was not imposed in the classical theory analysis because of the dependence of the angular displacement components onto the displacement vector. Such requirement is expressed in the form of the limiting integral

$$\lim_{\substack{\gamma\to 0\\ \gamma\to\pi}} \int_0^{2\pi} \left[\beta_\gamma \cos\eta + \sec\gamma\, \beta_\eta \sin\beta \right] R \sin\gamma \, d\eta = 0. \qquad (2.217)$$

5. The net resultant moment in the direction of $\eta = 0$ of the internal stresses around a limiting contour, must balance the external couple applied at the pole. This is expressed in the

form of the integral

$$\lim_{\substack{\gamma\to\pi \\ \gamma\to 0}} \int_0^{2\pi} \Big[M_\gamma \cos\eta - M_{\gamma\eta} \cos\gamma \sin\eta - R \sin\gamma \cos\eta \, [Q_\gamma \cos\gamma - N_\gamma \sin\gamma \,] \Big] R \sin\gamma \, d\eta = \pm 1. \tag{2.218}$$

The first of the requirements leads to the condition

$$A_2^m = 0 \tag{2.219}$$

while requirements 2, 3, 4 result in the following system of equations between the arbitrary constants:

$$s(\nu) B_2^m + s(\lambda) C_2 = 0$$

$$e_U^2 s(\nu) B_2^m + e_U^3 s(\lambda) C_2^m + e_0 s(\omega) B_2' + \frac{R}{2} A_2' = 0$$

$$\delta_2 s(\nu) B_2^m + \delta_3 s(\lambda) C_2^m - e_5 C' s(\omega) B_2' = 0$$

$$s(\nu) B_1^m + s(\lambda) C_1 = 0 \tag{2.220}$$

$$e_U^2 s(\nu) B_1^m + e_U^3 s(\lambda) C_1^m - e_0 s(\omega) B_1' + \frac{R}{2} A_2' = 0$$

$$\delta_2\ s(\nu)\ B_1^m + \delta_3\ s(\lambda)\ C_1^m + e_5\ C'\ s(\omega)\ B_1' = 0$$

where the superscript m on the constants denotes their affiliation with the moment solution and

$$s(\nu) = \frac{2}{\pi} \sin\nu\pi \qquad \text{etc.}$$

The last of the requirements provides the following additional relation between the arbitrary constants:

$$\delta_2\ T(\nu)\ B_2^m + \delta_3\ T(\lambda)\ C_2^m + C'\ [e_5\ T(\omega) + \frac{1+\mu}{2}\ s(\omega)]\ (B_2')^m = -\frac{1}{\pi\ D}$$

where (2.221)

$$T(\nu) = \nu(\nu+1)\ \frac{2}{\pi} \sin\nu\pi.$$

Although the same integral must be evaluated at $\gamma = \pi$, the requirement
$W(\gamma) = W(\pi - \gamma)$ implies that

$$B_1^m = B_2^m,$$

$$C_1^m = C_2^m \qquad (2.222)$$

and consequently no additional relation need to be incorporated. However, when such integral is formed, the moment condition at $\gamma = \pi$ is identically satisfied.

The system of equations generated is sufficient and so when solved the arbitrary constants are evaluated. Their particular values reflect the solution of the physical system described in Fig. 2-6. The symmetry of the system about $\gamma = \frac{\pi}{2}$ also yields the following relation

$$(B_2')^m = - (B_1')^m. \qquad (2.222')$$

II.2.2.2 CONCENTRATED UNIT TANGENTIAL LOAD SOLUTION

By using the same general solution we utilize requirements 2, 3, 4 used in the construction of the moment solution. Their evaluation leads to the following set of equations between the constants:

$$A_2^t + s(\nu)\, B_2^t + s(\lambda)\, C_2^t = 0$$

$$A_2^t - s(\nu)\, B_1^t - s(\lambda)\, C_1^t = 0$$

$$e_U^1\, A_2^t + e_U^2\, s(\nu)\, B_2^t + e_U^3\, s(\lambda)\, C_2^t + e^0\, s(\omega)\, (B_2')^t + \frac{R}{2}\, (A_2')^t = 0 \qquad (2.223)$$

$$- e_U^1 A_2^t + e_U^2 s(\nu) B_1^t + e_U^3 s(\lambda) C_1^t - e^0 s(\omega) (B_1')^t + \frac{R}{2} (A_2')^t = 0$$

$$\delta_1 A_2^t + \delta_2 s(\nu) B_2^t + \delta_3 s(\lambda) C_2^t - e_5 C' s(\omega) (B_2')^t = 0$$

$$\delta_1 A_2^t - \delta_2 s(\nu) B_1^t - \delta_3 s(\lambda) C_1^t - e_5 C' s(\omega) (B_1')^t = 0$$

Evaluation of the force resultant around the pole $\gamma = 0$ leads to the relation

$$2 e_U^1 A_2^t + e_U^2 T(\nu) B_2^t + e_U^3 T(\lambda) C_2^t - [e_0 T(\omega) - \frac{1 + \mu}{2} R s(\omega)] (B_2')^t + \frac{\mu R}{2} (A_2')^t = - \frac{1 - \mu^2}{Eh\pi} . \qquad (2.224)$$

It is apparent that one additional condition is needed in order for the system of equations to become complete. However, our desired system must incorporate two additional singular effects, a resultant force $F = 1$ with direction opposite to the one already considered at $\gamma = 0$ and a resultant moment $M = 2 R$, both applied at $\gamma = \pi$. We proceed in the following manner. We recall the behavior of the complete sphere with singularities at both poles encountered in the classical theory analysis. It was shown then that the system was self-equilibrated due to the fact that the singularities of the general solution were translated into physical terms as the system of forces and moments shown in Fig. 2-4. With the above in mind we attempt to evaluate the moment integral at $\gamma = 0$ to correspond to a

resultant moment of intensity $M = R$ and direction similar to the one in Fig. 2-4. Such condition leads to the relation

$$2\,\delta_1\,A_2^t + \delta_2\,T(\nu)\,B_2^t + \delta_3\,T(\lambda)\,C_2^t - C'\,[e_5\,T(\omega) + \frac{1+\mu}{2}\,R\,s(\omega)]\,(B_2')^t = -\frac{1-\mu^2}{Eh\pi}\,. \tag{2.225}$$

The system of eight equations is solved in terms of the arbitrary constants and subsequently the two integrals, the resultant force and the resultant moment, at $\gamma = \pi$ are evaluated. The above test indeed proves that the singular solution derived, in satisfaction of the choice of limiting conditions, describes the physical system of Fig. 2-4. Again, a moment solution needs to be superimposed onto the system just derived in order to achieve the solution state of Fig. 2-5. However, since such moment solution has already been derived in the form of a self-equilibrated pair of unit moments, the superposition approach requires no additional formulation. Thus the kernel functions associated with a unit tangential load applied at an arbitrary point $x'(\phi',\theta')$, or else in the introduced rotated system (γ,η) at $\gamma = 0$ and directed along $\eta = 0$, will be of the form

$$\begin{aligned} W^T(\underset{\sim}{x};\underset{\sim}{x}') &= W^t(\underset{\sim}{x};\underset{\sim}{x}') + R\,W^m(\underset{\sim}{x};\underset{\sim}{x}') \\ u_\phi^T(\underset{\sim}{x};\underset{\sim}{x}') &= u_\phi^t(\underset{\sim}{x};\underset{\sim}{x}') + R\,u_\phi^m(\underset{\sim}{x};\underset{\sim}{x}') \\ N_\phi^T(\underset{\sim}{x};\underset{\sim}{x}') &= N_\phi^t(\underset{\sim}{x};\underset{\sim}{x}') + R\,N_\phi^m(\underset{\sim}{x};\underset{\sim}{x}') \end{aligned} \tag{2.226}$$

etc. In Eqns. 2.226 kernel functions with superscript T (W^T, M_ϕ^T etc.) refer to the singular solutions associated with a unit tangential load. These solutions were constructed from the kernels which result from the general solution by utilizing the arbitrary constants with superscript t (B_2^t, A_2^t etc.) and the moment kernels multiplied by R necessary to eliminate the effect of the concentrated moment of intensity R accompanying the solution of Fig. 2-4. With these last manipulations we have arrived at the complete set of singular solutions for all three types of concentrated loads applied on the middle surface of a closed sphere incorporating into their expressions the effect of transverse shear deformation.

II.2.2.3 IDENTIFICATION OF THE SINGULARITIES

Since the differences between the two theories are expected to occur in the vicinity of the point of application of the singular load, we will consider the behavior of the dependent variables associated with the last two types of loading in the limit as $\gamma \to 0$.

The character of the singularities experienced by the dependent variables as $\gamma \to 0$ is the same for both moment and tangential load solutions. In terms of the displacement vector components we observe similar characteristics to those of the classical theory analysis. Thus, the transverse displacement W vanishes as we approach the point of application, $\lim_{\gamma \to 0} W = 0$, while both tangential displacement components, u_γ and u_η, both are unbounded as a result of logarithmic singularities in their kernels. The same is true for the angular displacements β_γ and β_η which also present logarithmic behavior in the pole vicinity.

The stress and moment resultant components also match the behavior of their counterparts in the classical analysis. All six components present singularities of order $(1/\gamma)$ and some of their limiting values are recorded below:

$$\lim_{\gamma \to 0} N_\gamma^m = \frac{Eh}{(1 - \mu^2)\, R} \left\{ (1 + \mu) \frac{R}{2} (A_2')^m + (1 - \mu) \left[2\, \mathrm{Re}\{ e_U^2\, B_2^m\, T(\nu) \right.\right.$$

$$[2\ CP_1(\nu) - CP_0(\nu)]) \Big] + 2\ \mathrm{Re}[\ e_U^2\ B_2^m\ T(\nu)\ ]$$

$$+ (1 - \mu) \Big[e_0\ (B_2')^m\ T(\omega)\ [\ 2\ CP_1(\omega) - CP_0(\nu)\ ] \Big]$$

$$- \mu\ [\ e_0\ \omega(\omega + 1) - R\ ]\ s(\omega)\ (B_2')^m \Big) \lim_{\gamma \to 0} \left(\frac{1}{\gamma} \right)$$

$$\lim_{\gamma \to 0} N_\eta^m = \frac{Eh}{(1 - \mu^2)\ R} \Big((1 + \mu)\ \frac{R}{2}\ (A_2')^m - (1 - \mu) \Big[2\ \mathrm{Re}(e_U^2\ B_2^m\ T(\nu)$$

$$[\ 2\ CP_1(\nu) - CP_0(\nu)]) \Big] + \mu\ 2\ \mathrm{Re}[\ e_U^2\ B_2^m\ T(\nu)\ ]$$

$$- (1 - \mu) \Big[e_0\ (B_2')^m\ T(\omega)\ [\ 2\ CP_1(\omega) - CP_0(\omega)\ ] \Big]$$

$$- [\ e_0\ \omega(\omega + 1) - R\ ]\ s(\omega)\ (B_2')^m \Big) \lim_{\gamma \to 0} \left(\frac{1}{\gamma} \right)$$

$$\lim_{\gamma \to 0} N_{\gamma\eta}^m = \frac{Eh}{2\ (1 + \mu)\ R} \Big(2\ \mathrm{Re}(e_U^2\ B_2^m\ T(\nu)\ (4\ CP_1(\nu) - 2\ CP_0(\nu)\ ])$$

$$+ e_0\ (B_2')^m\ T(\omega)\ [\ 4\ CP_1(\omega) - 2\ CP_0(\omega)\ ] \Big]$$

$$+ [\ e_0\ \omega(\omega + 1) - R\ ]\ s(\omega)\ (B_2')^m \Big) \lim_{\gamma \to 0} \left(\frac{1}{\gamma} \right)$$

$$\lim_{\gamma \to 0} M_\gamma^m = \frac{D}{R} \Big((1 - \mu) \Big[2\ \mathrm{Re}(\delta_2\ B_2^m\ T(\nu)\ [2\ CP_1(\nu) - CP_0(\nu)]\ ) \Big]$$

$$+ 2\ \mathrm{Re}[\ \delta_2\ B_2^m\ T(\nu)\ ]$$

$$- (1 - \mu) \Big[e_5\ C'\ (B_2')^m\ T(\omega)\ [\ 2\ CP_1(\omega) - CP_0(\omega)\ ] \Big]$$

$$+ \mu\ C'\ [\ e_5\ \omega(\omega + 1) + 1\ ]\ s(\omega)\ (B_2')^m \Big) \lim_{\gamma \to 0} \left(\frac{1}{\gamma} \right)$$

$$\lim_{\gamma\to 0} M^m_{\eta} = \frac{D}{R}\Bigg\{ -(1-\mu)\Big[2\,\mathrm{Re}\{\,\delta_2\, B_2^m\, T(\nu)\,[2\,CP_1(\nu) - CP_0(\nu)]\,\}\Big]$$

$$+ 2\,\mathrm{Re}[\,\delta_2\, B_2^m\, T(\nu)\,]$$

$$+ (1-\mu)\Big[e_5\, C'\, (B_2')^m\, T(\omega)\,[\,2\,CP_1(\omega) - CP_0(\omega)\,]\Big]$$

$$+ C'\,[\,e_5\,\omega(\omega+1)+1\,]\,s(\omega)\,(B_2')^m\Bigg)\lim_{\gamma\to 0}\left(\frac{1}{\gamma}\right)$$

$$\lim_{\gamma\to 0} M^m_{\gamma\eta} = \frac{(1-\mu)\,D}{2\,R}\Bigg\{ 2\,\mathrm{Re}\{\,\delta_2\, B_2^m\, T(\nu)\,(4\,CP_1(\nu) - 2\,CP_0(\nu)\,]\}$$

$$- e_5\, C'\, (B_2')^m\, T(\omega)\,[\,4\,CP_1(\omega) - 2\,CP_0(\omega)\,]$$

$$- C'\,[\,e_5\,\omega(\omega+1)+1\,]\,s(\omega)\,(B_2')^m\Bigg)\lim_{\gamma\to 0}\left(\frac{1}{\gamma}\right) \qquad (2.227)$$

Similar expressions would result for the respective resultant components of the tangential load solution. Their difference with the above expressions will be the partitipation of the additional constant A_2 which in the general solution accompanies the independent solution $Q_1^1(\cos\gamma)$.

The most pronounced difference between the two theories, however, was observed in the character of the singularity in the shear stress resultants Q_γ and Q_η. It was found, in the classical theory approach, that these resultants demonstrate a very strong singular behavior of order $\frac{1}{\gamma^2}$. In the improved theory, however, the singularity involved with the above kernels is logarithmic and thus integrable. We record

below the limiting value of the shear resultant of the unit moment solution:

$$\lim_{\gamma\to 0} Q_\gamma = \frac{Eh}{2(1+\mu)k_s^0} \lim_{\gamma\to 0} \left[A_1^Q \cos\gamma \ln(1 - \cos\gamma) + A_2^Q \ln(1 - \cos\gamma) + A_3^Q \cos\gamma + A_4^Q \right] \tag{2.228}$$

where

$$A_1^Q = -\frac{1}{4\pi} e_5 C' \omega(\omega + 1) (B_2')^m$$

$$A_2^Q = -\frac{1}{2} \mathrm{Re}\{ [\delta_2 + \frac{1}{R}]T(\nu) B_2^m \} - \frac{1}{\pi} e_5 C' \omega(\omega + 1) (B'_2)^m$$

$$A_3^Q = -\frac{1}{\pi} e_5 C' (B_2')^m \omega(\omega + 1) CP_1(\omega)$$

$$A_4^Q = -2 \mathrm{Re}\{[\delta_2 + \frac{1}{R}] T(\nu) CP_1(\nu) B_2^m\} + \frac{1}{\pi} e_5 C' CP_0(\omega) \omega(\omega + 1) (B_2')^m$$

and a similar expression results for the limiting value of Q_η.

Further, we should note that the character and strength of the singularities in all the dependent variable kernels agrees with the singular behavior previously obtained by Kalnins and Wilkinson[24]. The last finding will have great impact in the evaluation of physical problems where integration of the kernels is vital to the analysis. The more detailed consequences of the significance of the character of singularity in the shear resultants will be given in the next two chapters.

CHAPTER III

INDIRECT BOUNDARY INTEGRAL FORMULATION

III.1 MATHEMATICAL STATEMENT AND BASIC FORMULATION

The Boundary Integral or Boundary Element Method has been identified as a very efficient scheme in treating problems of complex nature which are associated with the field of applied mechanics. As already mentioned, the ability of the technique to reduce the dimension of the problem by one is a key characteristic. This translates to the incorporation into the analysis of only the boundary information rather than that of the whole domain.

The starting point of the technique is the availability of the solutions of the governing field equations for unit excitation, or fundamental singular solutions. The physical reasoning behind these singular solutions as well as the direct use of the principle of superposition will constitute the basis of the mathematical model. In the foregoing, the Indirect Boundary Integral Method, IBIM, will be developed as to the Direct BIM. Even though both approaches utilize the same unit solutions, their formulation differs significantly. IBIM, in addition to simple physical reasoning, uses the concept of a "fictitious" system which is embedded onto a complete domain for which the fundamental singular solutions are derived. On the other hand, DBIM requires a more sophisticated approach which is closely

related to Green's second identity and Betti's reciprocal theorem. Besides the fact that DBIM requires, from the nature of the approach, more computational effort, it can become rather cumbersome when dealing with domains governed by higher order differential equations.

We will utilize the particular closed form Fundamental Solutions derived in the previous chapter and the idea of the "fictitious" system under the following guidlines:

a. The "infinite" domain that the fictitious image of the real system is embedded on, in our particular case, is of finite extent. It is necessary, in order for the overall equilibrium to be preserved, to introduce forms of unit excitation with two singularities. It will soon become apparent that we cannot, in general, utilize the complete spherical surface as image of a real system.

b. The linearity of the real system, which allows the principle of superposition to be applied, will give rise to the concept of a fictitious boundary line along which the fictitious load vectors will be applied.

The consequence of the first statement is that only domains of extent equal or smaller than a hemisphere can be evaluated. Since the two poles in the various kernels are π distance apart, the image singularity associated with a point load at $\underset{\sim}{x}'(\phi',\theta')$, where $\phi' > \frac{\pi}{2}$

, will be located at a point on the surface with $\phi_i < \phi'$ and thus it will violate the physics of the effect of a point load (a point load to introduce singular behavior away from the point of its application). However, most of the spherical shell problems with engineering interest correspond to caps with maximum angle span of $\frac{\pi}{2}$. Complete spherical vessels with internal pressure, which acts in the form of normal traction, will not encounter the double pole effect due to the fact that the corresponding singular solution presents unbounded behavior at only one point on the complete spherical surface. The impact of the second statement into the formulation will be explicitly demonstrated when the singular character of the kernels is to be integrated over the boundary.

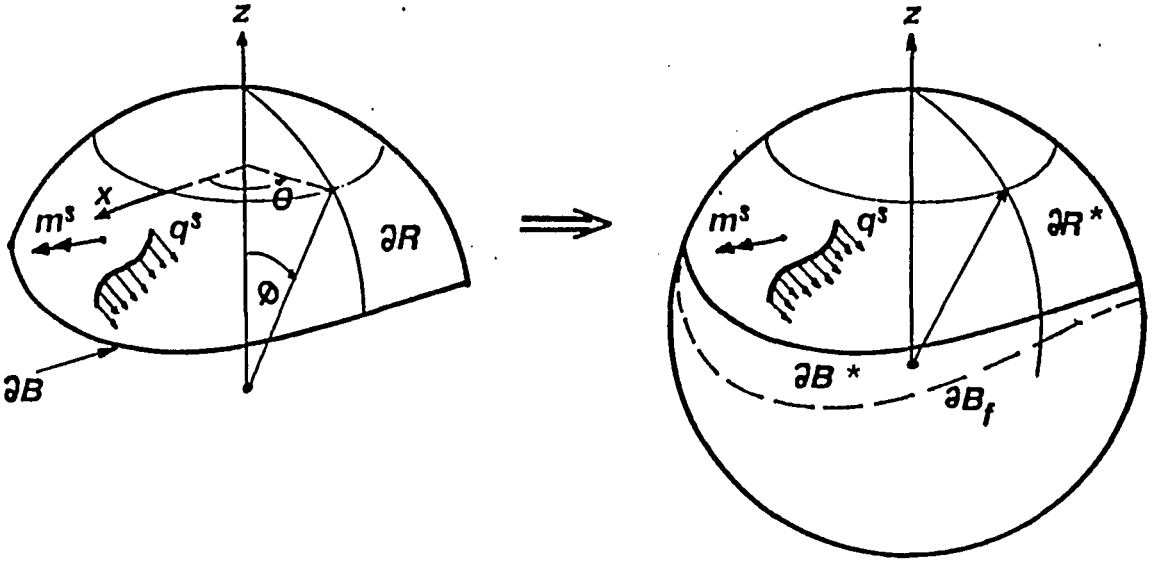

Figure 3-1. Embedding of a real domain onto a complete sphere.

Consider a spherical shell problem whose domain ∂R is a portion of a complete sphere, of size equal or less than a hemisphere, and its boundary ∂B is an arbitrary closed line on the spherical surface. The

domain ∂R is subjected to an arbitrary surface traction vector q^s (with components q_n, q_ϕ and q_θ) and/or surface moment vector m^s, while the boundary ∂B is subject to prescribed boundary conditions. To solve this well posed problem we embed the domain of interest ∂R onto a complete sphere whose singular solutions are available (see Fig. 3-1).

We denote the image domain by ∂R^* and its boundary by ∂B^*. The surface traction vector is then applied to the corresponding points of the new system in the form of an integral effect of unit excitations. According to the nature of the fundamental singularities and singular solutions, equilibrating loads in the forms of either surface traction or point loads will accompany the original surface traction. It is apparent that overall equilibrium of the image domain as well as of the complete sphere is automatically satisfied.

To complete the problem specification we denote $\underset{\sim}{x}(\phi,\theta)$ to be a field point where dependent variables can be evaluated, $\underset{\sim}{x}'(\phi',\theta')$ to be a load point where excitation occurs, $\xi'(\phi',\theta')$ a load point along the boundary ∂B^*, $\underset{\sim}{\xi}(\phi,\theta)$ a point also of the boundary where dependent variables will be evaluated, $\underset{\sim}{n}_s$ and $\underset{\sim}{n}_t$ to be the on-surface unit vectors along the boundary and β_s , β_t the surface angles between the surface coordinate ϕ and the directions of the two unit vectors, as shown in Fig. 3-2.

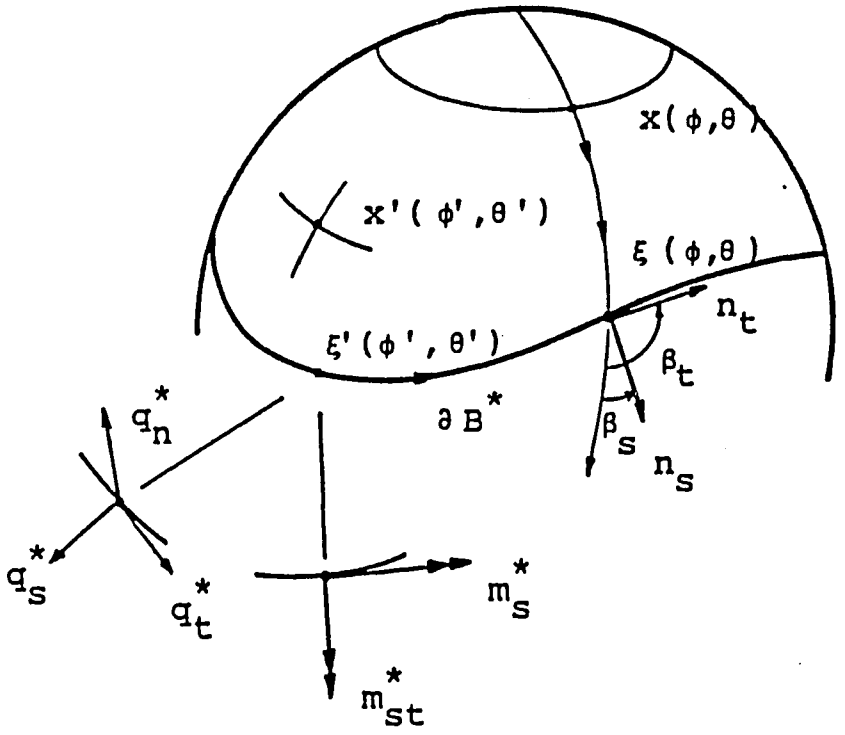

Figure 3-2. Unit boundary vectors and fictitious boundary line tractions.

In order to create the true deformation and stress fields inside the domain, we need to satisfy the prescribed boundary conditions along the surface line ∂B^*. This is accomplished through the introduction of "fictitious" line load vectors applied along ∂B^*. These vectors correspond to normal loads, two tangential loads and either a normal moment vector to the boundary or the normal moment vector together with a twisting couple acting along the ∂B^*.

The required number of such "fictitious" vectors is equal to the number of boundary constraints that need to be satisfied, which in turn is determined by the shell theory used in the mathematical

model. It should be noted that equilibrium of the complete domain is again preserved due to the fact that these load vectors are also expressed in the form of integrals of unit excitation which in itself is self-equilibrated. If we consider an arbitrary field point $\underset{\sim}{x}(\phi,\theta)$, at which we want to determine the displacement components and its stress state, then by the principle of superposition we can express the net effect of the actual surface traction and the fictitious boundary excitation in the form of the integrals

$$W(\underset{\sim}{x}) = \iint_{\partial R} \Big[W^n(\underset{\sim}{x};\underset{\sim}{x}')\, q_n^s(\underset{\sim}{x}') + W_\phi^t(x;x')\, q_\phi^s(\underset{\sim}{x}') + W_\theta^t(\underset{\sim}{x};\underset{\sim}{x}')\, q_\theta^s(\underset{\sim}{x}') + W^m(\underset{\sim}{x};\underset{\sim}{x}')\, m^s(\underset{\sim}{x}') \Big]\, dR$$

$$+ \int_{\partial B} \Big[W^n(\underset{\sim}{x};\underset{\sim}{\xi}')\, q_n^*(\underset{\sim}{\xi}') + W_\phi^t(\underset{\sim}{x};\underset{\sim}{\xi}')\, q_\phi^*(\underset{\sim}{\xi}') + W_\theta^t(\underset{\sim}{x};\underset{\sim}{\xi}')\, q_\theta^*(\underset{\sim}{\xi}') + W_s^m(\underset{\sim}{x};\underset{\sim}{\xi}')\, m_s^*(\underset{\sim}{\xi}') + W_{st}^m(\underset{\sim}{x};\underset{\sim}{\xi}')\, m_{st}^*(\underset{\sim}{\xi}') \Big]\, dB, \qquad (3.1)$$

or similarly for a stress resultant component

$$N_\phi(\underset{\sim}{x}) = \iint_{\partial R} \Big[N_\phi^n(\underset{\sim}{x};\underset{\sim}{x}')\, q_n^s(\underset{\sim}{x}') + N_{\phi,\phi}^t(\underset{\sim}{x};\underset{\sim}{x}')\, q_\phi^s(\underset{\sim}{x}') + N_{\phi,\theta}^t(\underset{\sim}{x};\underset{\sim}{x}')\, q_\theta^s(\underset{\sim}{x}') + N_\phi^m(\underset{\sim}{x};\underset{\sim}{x}')\, m^s(\underset{\sim}{x}') \Big]\, dR$$

$$+ \int_{\partial B} \Big[N_\phi^n(\underset{\sim}{x};\underset{\sim}{\xi}')\, q_n^*(\underset{\sim}{\xi}') + N_{\phi,\phi}^t(\underset{\sim}{x};\underset{\sim}{\xi}')\, q_\phi^*(\underset{\sim}{\xi}') + N_{\phi,\theta}^t(\underset{\sim}{x};\underset{\sim}{\xi}')\, q_\theta^*(\underset{\sim}{\xi}')$$

$$+ N^{m}_{\phi,s}(\underset{\sim}{x};\underset{\sim}{\xi}')\ m^{*}_{s}(\underset{\sim}{\xi}') + N^{m}_{\phi,st}(\underset{\sim}{x};\underset{\sim}{\xi}')\ m^{*}_{st}(\underset{\sim}{\xi}') \Big]\ dB \qquad (3.2)$$

where quantities $q^{s}_{(n,\phi,\theta)}$ and m^{s} correspond to the components of surface traction and surface moment respectively, while $q^{*}_{(n,\phi,\theta)}$ and m^{*}_{s} and m^{*}_{st} represent the components of the fictitious boundary line tractions, normal and twisting line moment vectors respectively. The intensity of these fictitious boundary vectors is unknown. The particular value that these vectors will take at any point along the boundary will guarantee the uniqueness of the problem solution in the sense that the specified boundary conditions of the real problem must be satisfied along ∂B. Thus the net result in terms of a dependent variable is viewed as the integration of the corresponding singular solutions against the unknown forms of the fictitious vectors. The remaining step toward the solution of the problem is to bring the field point to the boundary ∂B [that is $\underset{\sim}{x}(\phi,\theta)\rightarrow\underset{\sim}{\xi}(\phi,\theta)$], see Fig. 3-2, and impose the requirement that the dependent variables evaluated from the superposition principle at $\underset{\sim}{x}(\phi,\theta)$ would now correspond to the respective boundary values. Thus the sample integrals above become

$$W(\underset{\sim}{\xi}) = \iint_{\partial R} \Big[\ W^{n}(\underset{\sim}{\xi};\underset{\sim}{x}')\ q^{s}_{n}(\underset{\sim}{x}') + W^{t}_{\phi}(\underset{\sim}{\xi};\underset{\sim}{x}')\ q^{s}_{\phi}(\underset{\sim}{x}') + W^{t}_{\theta}(\underset{\sim}{\xi};\underset{\sim}{x}')\ q^{s}_{\theta}(\underset{\sim}{x}')$$

$$+ W^{m}(\underset{\sim}{\xi};\underset{\sim}{x}')\ m^{s}(\underset{\sim}{x}') \Big]\ dR$$

$$+ \int_{\partial B} \Big[W^n(\underset{\sim}{\xi};\underset{\sim}{\xi}')\ q_n^*(\underset{\sim}{\xi}') + W_\phi^t(\underset{\sim}{\xi};\underset{\sim}{\xi}')\ q_\phi^*(\underset{\sim}{\xi}') + W_\theta^t(\underset{\sim}{\xi};\underset{\sim}{\xi}')\ q_\theta^*(\underset{\sim}{\xi}')$$

$$+ W_s^m(\underset{\sim}{\xi};\underset{\sim}{\xi}')\ m_s^*(\underset{\sim}{\xi}') + W_{st}^m(\underset{\sim}{\xi};\underset{\sim}{\xi}')\ m_{st}^*(\underset{\sim}{\xi}') \Big]\ dB \qquad (3.3)$$

and similarly

$$N_\phi(\underset{\sim}{\xi}) = \iint_{\partial R} \Big[N_\phi^n(\underset{\sim}{\xi};\underset{\sim}{x}')\ q_n^s(\underset{\sim}{x}') + N_{\phi,\phi}^t(\underset{\sim}{\xi};\underset{\sim}{x}')\ q_\phi^s(\underset{\sim}{x}') + N_{\phi,\theta}^t(\underset{\sim}{\xi};\underset{\sim}{x}')\ q_\theta^s(\underset{\sim}{x}')$$

$$+ N_\phi^m(\underset{\sim}{\xi};\underset{\sim}{x}')\ m^s(\underset{\sim}{x}') \Big]\ dR$$

$$+ \int_{\partial B} \Big[N_\phi^n(\underset{\sim}{\xi};\underset{\sim}{\xi}')\ q_n^*(\underset{\sim}{\xi}') + N_{\phi,\phi}^t(\underset{\sim}{\xi};\underset{\sim}{\xi}')\ q_\phi^*(\underset{\sim}{\xi}') + N_{\phi,\theta}^t(\underset{\sim}{\xi};\underset{\sim}{\xi}')\ q_\theta^*(\underset{\sim}{\xi}')$$

$$+ N_{\phi,s}^m(\underset{\sim}{\xi};\underset{\sim}{\xi}')\ m_s^*(\underset{\sim}{\xi}') + N_{\phi,st}^m(\underset{\sim}{\xi};\underset{\sim}{\xi}')\ m_{st}^*(\underset{\sim}{\xi}') \Big]\ dB \qquad (3.4)$$

where $\int$ is an improper integral due to the singular character of the kernel functions as $\xi \to \xi'$.

For a given shell problem, a set of boundary conditions will be prescribed at every point of the boundary. Thus, according to the mathematical form of the superposition principle expressed above, either four (classical theory) or five (improved theory) simultaneous integral equations will result and subsequently be solved for the unknown intensities of the "fictitious" vectors. It is apparent that once the functional distribution of the line load intensities have been evaluated then backsubstitution into the integral expressions

will produce the value of any dependent variable at interior field points. The mathematical difficulty that such an integral scheme will experience relies upon the fact that the kernel functions are singular and thus the integrands of the integral expressions are unbounded as the field and the load points coincide. In deriving the singular solutions of the shell equations we also identified the character of the singularities in the kernels. Weak singularities, like logarithmic, are integrable and they are not troublesome. Stronger singularities of order ($\frac{1}{\gamma}$) are treated as Cauchy principal values, while even stronger singularities of order ($\frac{1}{\gamma^2}$) are not integrable at all. In Appendix B the common singular integrals encountered in the present analysis are evaluated in closed form. However, the treatment even of weak singularities, when associated with displacement and stresses, on the shell surface is not an easy task. In addition, for the case of the classical theory analysis, the kernels of the shear stress resultants contain singularities of the order ($\frac{1}{\gamma^2}$) and thus any attempt of closed form integration will fail. The means of bypassing the difficulty entirely will be formed upon the following reasoning. If one considers an additional fictitious boundary line ∂B_f^* located away from the actual one and whose points are in a one to one relationship with the points of the boundary line ∂B, or equivalently ∂B^*, then the fictitious line load vectors can be applied along the new line rather than ∂B. The superposition principle can still apply while the evaluation of singular integrals is no longer necessary. This is due to the fact

that the load and the field points on the boundary will never coincide. Theoretically, the position of the auxiliary boundary line is irrelevant to the formulation for as long as the one to one relationship between the points hold. However, when numerical integration rather than exact is to be performed, the choice of the positioning of the auxiliary boundary will be vital to the accuracy of the solution and for that reason further discussion and evaluation is needed. In the next chapter the variation of the solution due to different positions of the auxiliary boundary will be demonstrated and analyzed.

III.2 INTEGRATION PROCEDURES AND NUMERICAL EVALUATION

Theoretically, if closed form integrations of the simultaneous integral equations can be performed, the solution of the particular problem would be exact. However, in practical problems, a closed form solution is almost impossible due to its dependence on the arbitrariness of the boundary geometry and surface traction. Thus, approximations have to be introduced in terms of the treatment of the boundary geometry and the numerical integration procedures. So we expect that the inaccuracies associated with IBIM to be the result of only the degree of approximation set as priori to the analysis.

For the particular case of spherical shell domains the discretization scheme will consider curvilinear boundary elements identified by their midpoints or nodes. The elements involved can be oriented along

four different types of surface lines. These involve boundaries along adjacent circles (ϕ = const.) , meridional circles (θ = constant), arbitrarily oriented great circles and lastly eccentrically located circular contours. We should note that irregular boundary lines will be treated as a sum of portions of great circles, exact equivalent of straight line segments on the plane. The construction of a directory of information for each element as well as the geometric properties and relations are extensively discussed in Appendix B. The intensity of the fictitious line load vectors will be assumed constant over the span of each boundary element. Further, for the case of distributed traction over the surface of the actual domain, the surface will be divided in "rectangular" elements between the ϕ and θ surface coordinates also identified by their middle points. In its general form, for a system of N boundary and M surface elements, the discretized form of the superposition principle, seen in Eqns. 3.1,2, calculating the net effect at a field boundary point $\underset{\sim}{\xi}(\phi,\theta)$, which in fact represents the middle point of one of the boundary elements, will be deduced in the form

$$W(\underset{\sim}{\xi}^i) = \sum_{p=1}^{M} \Big[q_n^s(\underset{\sim}{x}') \int_{\Delta A} W^n(\underset{\sim}{\xi}^i;\underset{\sim}{x}')\, dR_p + q_\phi^s(\underset{\sim}{x}') \int_{\Delta A} W_\phi^t(\underset{\sim}{\xi}^i;\underset{\sim}{x}')\, dR_p$$

$$q_\theta^s(\underset{\sim}{x}') \int_{\Delta A} W_\theta^t(\underset{\sim}{\xi}^i;\underset{\sim}{x}')\, dR_p + m^s(\underset{\sim}{x}') \int_{\Delta A} W^m(\underset{\sim}{\xi}^i;\underset{\sim}{x}')\, dR_p \Big]$$

$$+\sum_{j=1}^{N}\left[\, q_n^*(\underset{\sim}{\xi}')\int_{\Delta S_j} W^n(\underset{\sim}{\xi}^i;\underset{\sim}{\xi}')\,dS_j + q_\phi^*(\underset{\sim}{\xi}')\int_{\Delta S_j} W_\phi^t(\underset{\sim}{\xi}^i;\underset{\sim}{\xi}')\,dS_j\right.$$

$$+ q_\theta^*(\underset{\sim}{\xi}')\int_{\Delta S_j} W_\theta^t(\underset{\sim}{\xi}^i;\underset{\sim}{\xi}')\,dS_j + m_s^*(\underset{\sim}{\xi}')\int_{\Delta S_j} W_s^m(\underset{\sim}{\xi}^i;\underset{\sim}{\xi}')\,dS_j$$

$$\left. + m_{st}^*\int_{\Delta S_j} W_{st}^m(\underset{\sim}{\xi}^i;\underset{\sim}{\xi}')\,dS_j\,\right] \tag{3.5}$$

and similarly

$$N_\phi(\underset{\sim}{\xi}) = \sum_{p=1}^{M}\left[\, q_n^s(\underset{\sim}{x}')\int_{\Delta A} N_\phi^n(\underset{\sim}{\xi}^i;\underset{\sim}{x}')\,dR_p + q_\phi^s(\underset{\sim}{x}')\int_{\Delta A} N_{\phi,\phi}^t(\underset{\sim}{\xi}^i;\underset{\sim}{x}')\,dR_p\right.$$

$$\left. q_\theta^s(\underset{\sim}{x}')\int_{\Delta A} N_{\phi,\theta}^t(\underset{\sim}{\xi}^i;\underset{\sim}{x}')\,dR_p + m^s(\underset{\sim}{x}')\int_{\Delta A} N_\phi^m(\underset{\sim}{\xi}^i;\underset{\sim}{x}')\,dR_p\,\right]$$

$$+\sum_{j=1}^{N}\left[\, q_n^*(\underset{\sim}{\xi}')\int_{\Delta S_j} N_\phi^n(\underset{\sim}{\xi}^i;\underset{\sim}{\xi}')\,dS_j + q_\phi^*(\underset{\sim}{\xi}')\int_{\Delta S_j} N_{\phi,\phi}^t(\underset{\sim}{\xi}^i;\underset{\sim}{\xi}')\,dS_j\right.$$

$$+ q_\theta^*(\underset{\sim}{\xi}')\int_{\Delta S_j} N_{\phi,\theta}^t(\underset{\sim}{\xi}^i;\underset{\sim}{\xi}')\,dS_j + m_s^*(\underset{\sim}{\xi}')\int_{\Delta S_j} N_{\phi,s}^m(\underset{\sim}{\xi}^i;\underset{\sim}{\xi}')\,dS_j$$

$$\left. + m_{st}^*\int_{\Delta S_j} N_{\phi,st}^m(\underset{\sim}{\xi}^i;\underset{\sim}{\xi}')\,dS_j\,\right] \tag{3.6}$$

where $\underset{\sim}{\xi}^i$ represents the middle point of the ith boundary element at which the field variables are evaluated, $\underset{\sim}{\xi}'$ is a load point along the jth boundary element and $\underset{\sim}{x}'$ is a load point of the interior. We should note that the assumption of uniform distribution of the fictitious vectors over each boundary element, simplifies the integrations by reducing the integrands to only the kernel functions rather than their product with the shape function of the vector distributions.

In order to construct the system matrix we consider two arbitrary boundary elements, i and j, and an interior load point $\underset{\sim}{x}'$ as shown in Fig 3-3.

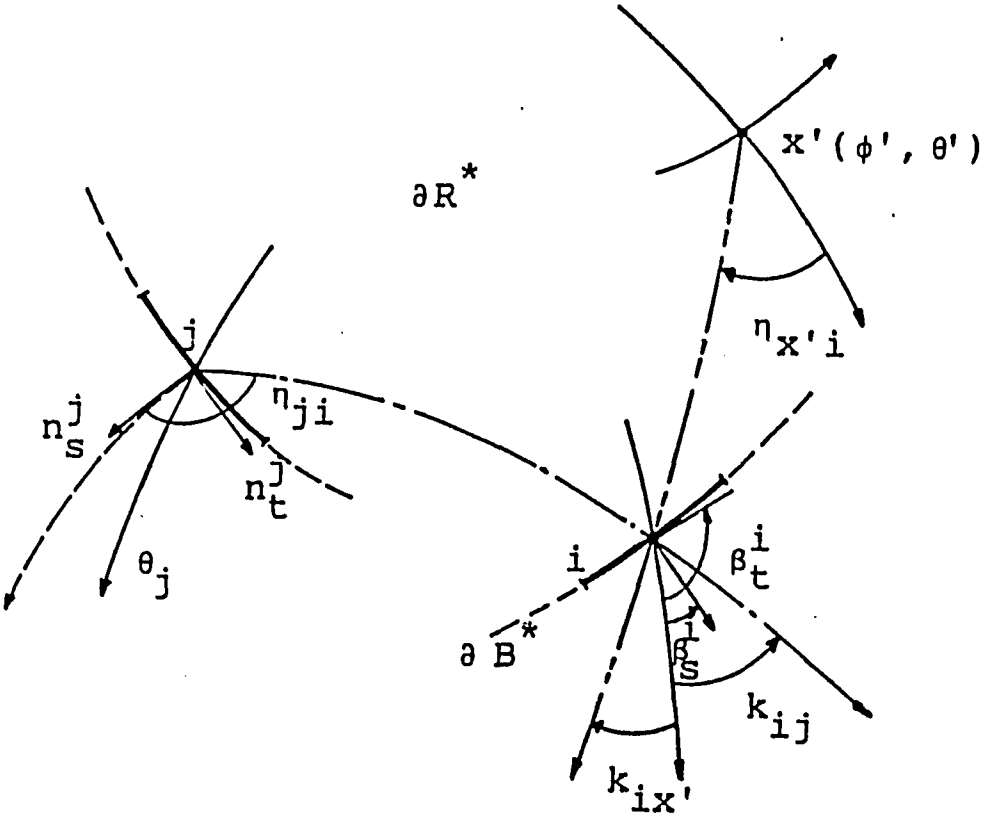

Figure 3-3. Orientation of two arbitrary elements and a field point.

With the discretized form we have reduced the system into the evaluation and subsequently satisfaction of the prescribed boundary constraints at N distinct points of the boundary (the nodes of the elements). Thus, in order for the one to one point relationship to hold, the auxiliary boundary, located at the arbitrary position shown, should also be subdivided into exactly N elements. In Fig. 3-3 above, ϕ and θ are the global surface coordinates, γ and η are the surface coordinates of the local system with pole at the load point $\underset{\sim}{\xi}'(\phi',\theta')$ while β_s and β_t are the angles between the unit vectors $\underset{\sim}{n}_s$ and $\underset{\sim}{n}_t$ and the global coordinate θ of point $\underset{\sim}{\xi}^i(\phi,\theta)$. Because the boundary constraints are expressed along the unit vectors e_s and e_t and the load vectors, except for the one in the normal direction, are accompanied by directional angles at $\underset{\sim}{\xi}'(\phi',\theta')$ and $\underset{\sim}{x}'(\phi',\theta')$, it is necessary to transform stress and displacement vectors from the local to global coordinate systems and visa-versa. Such transformations can be deduced by utilizing the angular relationships

$$\cos\gamma = \cos\phi\,\cos\phi' + \sin\phi\,\sin\phi'\,\cos(\theta - \theta')$$

$$\cos\eta = \frac{\cos\gamma\,\cos\phi' - \cos\phi}{\sin\gamma\,\sin\phi'}$$

$$\sin\eta = \frac{\sin\phi\,\sin(\theta - \theta')}{\sin\gamma} \qquad (3.7)$$

$$\cos k = \frac{\cos\phi' - \cos\phi\,\cos\gamma}{\sin\phi\,\sin\gamma}$$

$$\text{sink} = \frac{\sin\phi' \sin(\theta - \theta')}{\sin\gamma}$$

where k represents the angle between θ and η coordinates measure counter-clockwise as shown in Fig. 3-3. Further, the boundary angles β_s and β_t are calculated for each boundary element and cataloged in its directory. The derivation of their values, which depends on the orientation of the actual boundary line with respect to the global system, is discussed in Appendix B. By focusing attention onto a field point $\underset{\sim}{x}(\phi,\theta)$, whether on the boundary or the interior, at which the displacement vector and stress matrix is to be evaluated, we observe that in order for the dependent variables to be expressed in the global surface coordinates (ϕ,θ) the following transformations must be utilized:

$$\begin{aligned}
u_\phi &= u_\gamma \cos k - u_\eta \sin k \\
u_\theta &= u_\gamma \sin k + u_\eta \cos k \\
\beta_\phi &= \beta_\gamma \cos k - \beta_\eta \sin k \\
\beta_\theta &= \beta_\gamma \sin k + \beta_\eta \cos k \\
Q_\phi &= Q_\gamma \cos k - Q_\eta \sin k \\
Q_\theta &= -Q_\gamma \sin k - Q_\eta \cos k
\end{aligned} \tag{3.8}$$

while the stress and moment resultants are evaluated from the Mohr's circle transformations,

$$
\begin{aligned}
N_{\phi} &= N_{\gamma} \cos^2 k + N_{\eta} \sin^2 k - 2 N_{\gamma\eta} \sin k \cos k \\
N_{\theta} &= N_{\gamma} \sin^2 k + N_{\eta} \cos^2 k + 2 N_{\gamma\eta} \sin k \cos k \\
N_{\gamma\eta} &= (N_{\gamma} - N_{\eta}) \sin k \cos k + N_{\gamma\eta} (\cos^2 k - \sin^2 k) \\
M_{\phi} &= M_{\gamma} \cos^2 k + M_{\eta} \sin^2 k + 2 M_{\gamma\eta} \sin k \cos k \\
M_{\theta} &= M_{\gamma} \sin^2 k + M_{\eta} \cos^2 k - 2 M_{\gamma\eta} \sin k \cos k \\
M_{\gamma\eta} &= - (M_{\gamma} - M_{\eta}) \sin k \cos k + M_{\gamma\eta} (\cos^2 k - \sin^2 k)
\end{aligned}
\tag{3.9}
$$

When the field point $\underset{\sim}{x}(\phi,\theta)$ is taken to the boundary, and since the boundary in itself has an orientation described by the angles β_s and β_t, additional transformation must take place in order for the dependent displacement and stress variables to be expressed along the unit vectors $\underset{\sim}{n}_s$ and $\underset{\sim}{n}_t$. This is necessary due to the fact that prescribed boundary conditions are given along these directions. The new transformation relations at the boundary will be of the form:

$$u_s = u_{\phi} \cos\beta_s + u_{\theta} \sin\beta_s$$

$$u_t = - u_\phi \sin\beta_s + u_\theta \cos\beta_s$$

$$\beta_s = \beta_\phi \cos\beta_s + \beta_\theta \sin\beta_s \qquad (3.10)$$

$$\beta_t = - \beta_\phi \sin\beta_s + \beta_\theta \cos\beta_s$$

$$Q_s = Q_\phi \cos\beta_s + Q_\theta \sin\beta_s$$

and again from Mohr-cirle transformations

$$N_s = N_\phi \cos^2\beta_s + N_\theta \sin^2\beta_s + 2 N_{\phi\theta} \sin\beta_s \cos\beta_s$$

$$N_{st} = - (N_\phi - N_\theta) \sin\beta_s \cos\beta_s + N_{\phi\theta} (\cos^2\beta_s - \sin^2\beta_s) \qquad (3.11)$$

$$M_s = M_\phi \cos^2\beta_s + M_\theta \sin^2\beta_s + 2 M_{\phi\theta} \sin\beta_s \cos\beta_s$$

$$M_{st} = (M_\phi - M_\theta) \sin\beta_s \cos\beta_s + M_{\phi\theta} (\cos^2\beta_s - \sin^2\beta_s).$$

A further simplification in the rigorous analysis is the representation of the fictitious load and moment vectors by statically equivalent forces and moments applied at the middle point of the element they are distributed over. The evaluation of these resultants is given explicitly in Appendix B. Their utilization relies upon the Saint Venant's principle, according to which at some distance away from the loaded element the effect of the distributed

vectors will be the same with the net effect of their statically equivalent counterparts. It was necessary in this analysis to adopt the above procedure due to the involvement of the complex Legendre functions in the mathematical model. These functions can only be evaluated in terms of their hypergeometric series expansion and as a result closed-form evaluation of the integral $\int_{\Delta S_j} H(\underset{\sim}{x};\underset{\sim}{x}')\, dS_j$ will not be practical. As noted in Appendix B, distributed vectors with a certain surface orientation will be represented by concentrated resultant forces in more than one direction. Thus the integration of a kernel function, say $W^n(x;x')$, over the element ΔS_j can be viewed in the form of the following sum:

$$\int_{\Delta S_j} W^n(\underset{\sim}{\xi};\underset{\sim}{\xi}')\, q_n^*(\underset{\sim}{\xi}')\, dS_j = R_{n,n}\, W^n(\underset{\sim}{\xi};\underset{\sim}{\xi}') + R_{n,\phi}\, W^{t,\phi}(\underset{\sim}{\xi};\underset{\sim}{\xi}') + R_{n,\theta}\, W^{t,\theta}(\underset{\sim}{\xi};\underset{\sim}{\xi}') \tag{3.12}$$

where $R_{n,n}$, $R_{n,\phi}$, $R_{n,\theta}$ are the resultant forces of the normal boundary traction q_n^* in all three directions and W^n, $W^{t,\phi}$, $W^{t,\theta}$ are the singular solutions of loads in the respective directions. However, when integrations are to be performed over either the same or neighboring elements, the asymptotic expansions of the Legendre functions may be used instead of the infinite series expansion. Such integrations would present no difficulties worth mentioning other than the singular behavior of the kernels when for one, the auxiliary

and real boundaries coincide, and also the field point is part of the integrating element. Weak singularities such as logarithmic mentioned earlier, and further discussed in Appendix B, are integrated in closed form, while stronger ones, of order $\left(\frac{1}{\gamma}\right)$, are replaced by Cauchy principal-value integrals. Suppose integration is to be performed over the boundary element ΔS_j which includes the boundary point $\underset{\sim}{\xi}^i$, the field point, and the normal resultant to the boundary N_s is to be evaluated at $\underset{\sim}{\xi}^i$, see Fig. 3-4.

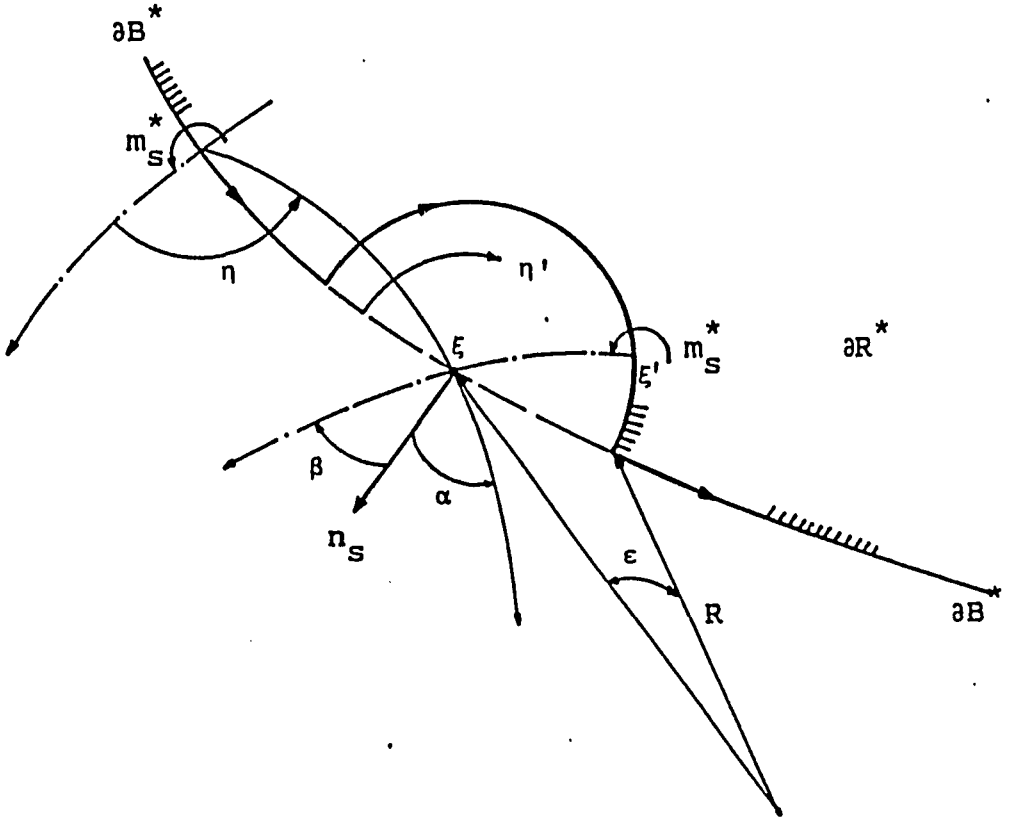

Figure 3-4. Geometry of the auxiliary envelope associated with the evaluation of an improper integral.

If the stress resultant due to the normal moment vector m_s^* is to be evaluated and since the the corresponding kernels contain a strong

singularity, of order ($\frac{1}{\gamma}$), then the following integration procedure is adopted. Normal integration is carried out over the element except for a small neighborhood around point $\underset{\sim}{\xi}^i$, $\pm\epsilon$, where the limiting value of the process as $\epsilon \to 0$ is defined as the principal value of the integral. Thus the complete integral will be of the form

$$N_s^m(\underset{\sim}{\xi}^i) = \lim_{\epsilon\to 0} \int_{\xi_j}^{\epsilon} \left[N_\gamma \cos\alpha^2 + N_\eta \sin\alpha^2 + 2 N_{\gamma\eta} \sin\alpha \cos\alpha \right] dS_j$$

$$+ \lim_{\epsilon\to 0} \int_{\epsilon}^{2\pi} \left[N_\gamma \cos\beta^2 + N_\eta \sin\beta^2 + 2 N_{\gamma\eta} \sin\beta \cos\beta \right] R \sin\epsilon \, d\eta'$$

$$+ \lim_{\epsilon\to 0} \int_{\epsilon}^{\xi_{j+1}} \left[N_\gamma \cos\alpha^2 + N_\eta \sin\alpha^2 + 2 N_{\gamma\eta} \sin\alpha \cos\alpha \right] dS_j \qquad (3.13)$$

where α and β are the angles associated with the orientation of the unit vector $\underset{\sim}{n}_s$ and the stress resultant vector at $\underset{\sim}{\xi}^i$.

Similar procedures are adopted in the discretization of the surface where again the effect of distributed traction over a surface element is replaced by the statically equivalent force system applied at the middle point of the element. If integrations over an element that contains the field point is to be performed, we note that the strong singularity ($\frac{1}{\gamma}$) becomes "weak" and presents no difficulty.

The final step consists of the formation and solution of the system matrices. Eqns. 3.3,4 represent the transverse displacement and the normal stress resultant at a node $\underset{\sim}{\xi}^i$. For a well set physical problem, either four or five system variables will be specified at each such node and consequently a set of four or five integral expressions for each node will result. The only unknowns of the system are the intensities of the fictitious load vectors over each element. Thus for a number of N boundary elements a coefficient matrix of size (4N x 4N), or (5N x 5N), will result representing the system matrix. After the integrations or their equivalent substitutes are performed, the coupled integral system reduces to a system of simultaneous linear algebraic equations which in turn is solved for the values of the unknown intensities. The construction of the main matrix and the contribution of the surface excitation is discussed further in Appendix B.

Obviously, backsubstitution of the fictitious boundary load distributions into Eqns. 3.3,4, or any other equivalent expression, will determine the value of any field variable in the interior or the boundary of the domain.

CHAPTER IV

NUMERICAL RESULTS AND DISCUSSION

Having derived the singular solutions which are associated with all the types of surface excitation that a shell surface could experience, the Indirect Boundary Integral formulation is utilized to illustrate the use of the above solutions and also to clarify the behavior of spherical shells. Our intention is to demonstrate the response of a spherical shell under the influence of concentrated loads and moments and to obtain a clear picture of the effects of the different boundary constraints. We are also interested in evaluating and comparing the two shell theories. We expect that the differences in the shell response to be most pronounced in the vicinity of the singular loads. Further, the performance of the developed numerical scheme will be compared in terms of accuracy and efficiency with the available analytical solutions and also with the corresponding finite element solution.

The different combinations of boundary conditions that often arise in the analysis of shells and which have been incorporated into the numerical scheme, are listed below. As noted earlier, the differences between the two theories are also encountered in the number of the constraints along the boundary. The classical approach requires that four independent field variables must be prescribed along a boundary edge, while improved theory sets the requirement to five. For

example, for a boundary portion having a_s = constant, normal and tangent(on-surface) unit vectors $\underset{\sim}{n}_s$ and $\underset{\sim}{n}_t$ respectively, the following conditions may be prescribed:

a. Clamped edge:

Classical theory: W, u_s, u_t, β_s

Improved theory : W, u_s, u_t, β_s, β_t

b. Simply supported edge:

Classical theory: W, u_s, u_t, M_s

Improved theory : W, u_s, u_t, M_s, β_t

c. Simply supported,free to move in the normal direction:

Classical theory: u_s, u_t, M_s, V_s

Improved theory : u_s, u_t, M_s, M_{st}, Q_s

d. Free edge:

Classical theory: N_s, T_{st}, M_s, V_s

Improved theory : N_s, N_{st}, M_s, M_{st}, Q_s

where V_s and T_{st} are the Kirchoff's shearing stress resultants given by:

$$V_s = Q_s + \frac{1}{A_t} \frac{\partial M_{st}}{\partial \alpha_t}, \quad T_{st} = N_{st} + \frac{M_{st}}{R_t}.$$

The need of using the improved theory over the classical counterpart is no more obvious than in the case of a free edge. The classical approach relies upon the St. Venant's principle and its approximation implies a redistribution of stress in the vicinity of the edge. However, results obtained by the classical analysis for stress concentration around openings and stress intensity in the neighborhood of cracks could be misleading. Overall, it is not clear which is in fact the better theory of the two. It is known, though, that each theory has its own spectrum and domain of applicability.

In what follows a number of spherical shell problems are evaluated and compared with the analytical and finite element solutions. The types of problems chosen reflect the effects of the different boundary constraints, the various concentrated surface loads and also the characteristic differences of the two shell theories. The implications of Kircoff's shearing stress resultants are viewed through the numerical evaluation of a stress concentration shell problem with the parallel analysis of the finite element method, the classical theory and the improved theory model.

Lastly, the effects of openings and cracks are studied with the analysis of corresponding physical systems.

IV.1 PROBLEM OF A CLAMPED SPHERICAL CAP SUBJECTED TO A CONCENTRATED POINT LOAD AT ITS APPEX. IBIM, FEM AND ANALYTICAL SHALLOW SOLUTION COMPARISON

The first of the example problems concerns the classical problem of a spherical cap loaded with a point load at the appex and subjected to clamped boundary. This problem was evaluated by Reissner[1] using the classical approach of the shallow theory of shells. The shell problem, shown in Fig. 4-1, used in the evaluation of the numerical results, has the following properties:

Radius R = 10 in., thickness h = .171127 in, E = 30 x 10^6 psi, μ = 0.25 and it is subjected point load P = 1 lb acting outward. The tabulated data of the transverse displacement W show the very good agreement between the "exact" solution, the Boundary Integral technique and the FEM. It should again be noted that the shallow treatment gives a very good approximation to the actual response whenever the assumption of shallowness is valid. The stress resultant $N_{\theta\theta}$ and moment resultant $M_{\theta\theta}$ as well as the surface displacement component u_ϕ are compared between BIM and FEM treatments. We observe that the agreement in the results is excellent. The remaining element resultants are also tabulated for the BIM solution only. It should be mentioned that based upon results, not shown here, Reissner's shallow solution approach can provide good approximate results even outside the so considered shallow region of the shell.

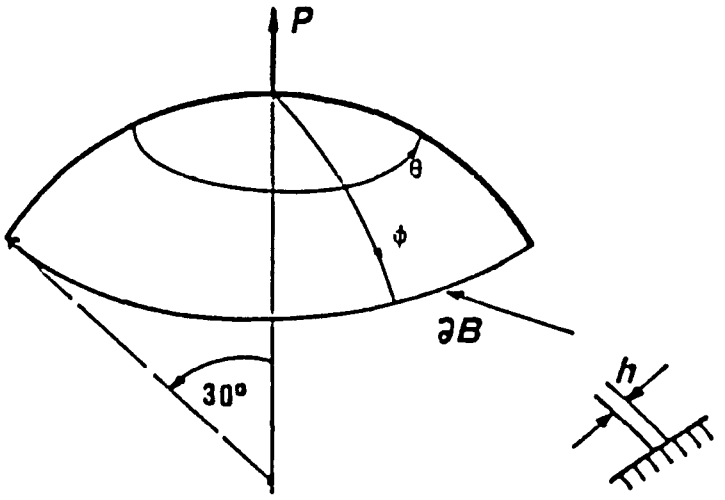

Figure 4-1. Clamped spherical cap with a point load at its appex.

Table 4-1. Comparison of exact, IBIM and FEM solutions on the radial displacement W of a clamped spherical cap subjected to a point load at the appex.

	RADIAL DISPLACEMENT W x 10^{-3} in		
ϕ-Degrees	B I M	F E M	SHALLOW SOLUTION
1	.4387	.4405	.4322
2	.3945	.3963	.3883
3	.3425	.3442	.3366
4	.2889	.2906	.2836
5	.2372	.2389	.2325
6	.1895	.1913	.1856
7	.1469	.1486	.1437
8	.1098	.1115	.1074
9	.0783	.0799	.0766
10	.0520	.0537	.0511
11	.0307	.0323	.0304
12	.0137	.0153	.0139
13	.0006	.0021	.0013
14	-.0097	-.0076	-.0081
15	-.0163	-.0147	-.0148
16	-.0210	-.0195	-.0192
17	-.0238	-.0224	-.0218
18	-.0251	-.0237	-.0229
19	-.0251	-.0238	-.0228
20	-.0241	-.0229	-.0217
21	-.0223	-.0213	-.0200
22	-.0199	-.0190	-.0177
23	-.0171	-.0163	-.0150
24	-.0140	-.0134	-.0122
25	-.0108	-.0103	-.0093
26	-.0076	-.0073	-.0065
27	-.0047	-.0046	-.0040
28	-.0023	-.0022	-.0019
29	-.0006	-.0006	-.0005
30	0.0000	0.0000	0.0000

Table 4-2. Comparison of IBIM and FEM solutions on the meridional displacement of a clamped spherical cap subjected to a point load at the appex.

DISPLACEMENT $u_\phi \times 10^{-6}$ in		
ϕ -Degrees	B I M	F E M
1	-.0486	-.0485
2	-.0913	-.0913
3	-.1265	-.1265
4	-.1535	-.1536
5	-.1727	-.1729
6	-.1847	-.1851
7	-.1906	-.1910
8	-.1911	-.1916
9	-.1873	-.1879
10	-.1801	-.1808
11	-.1704	-.1712
12	-.1588	-.1597
13	-.1461	-.1470
14	-.1327	-.1337
15	-.1191	-.1202
16	-.1055	-.1067
17	-.0924	-.0937
18	-.0799	-.0812
19	-.0682	-.0695
20	-.0574	-.0587
21	-.0475	-.0487
22	-.0386	-.0398
23	-.0307	-.0318
24	-.0238	-.0248
25	-.0179	-.0188
26	-.0129	-.0136
27	-.0087	-.0093
28	-.0054	-.0057
29	-.0025	-.0027
30	0.0000	0.0000

Fig. 4-1b

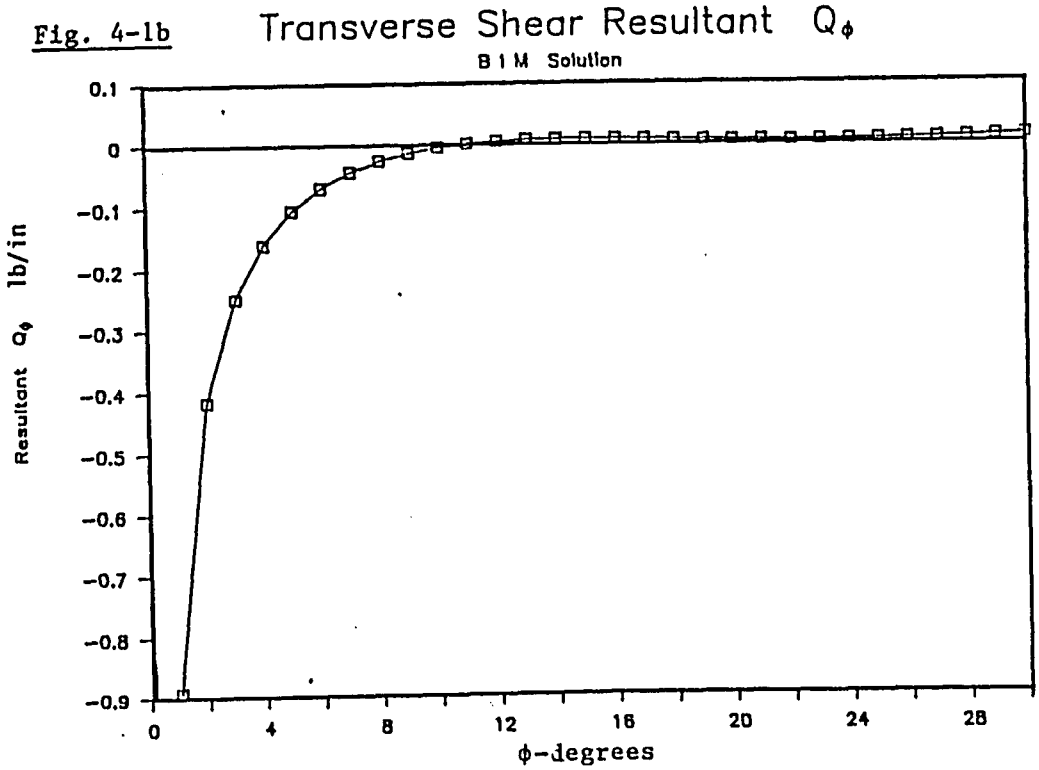

Fig. 4-1c : Stress Resultant $N_{\phi\phi}$

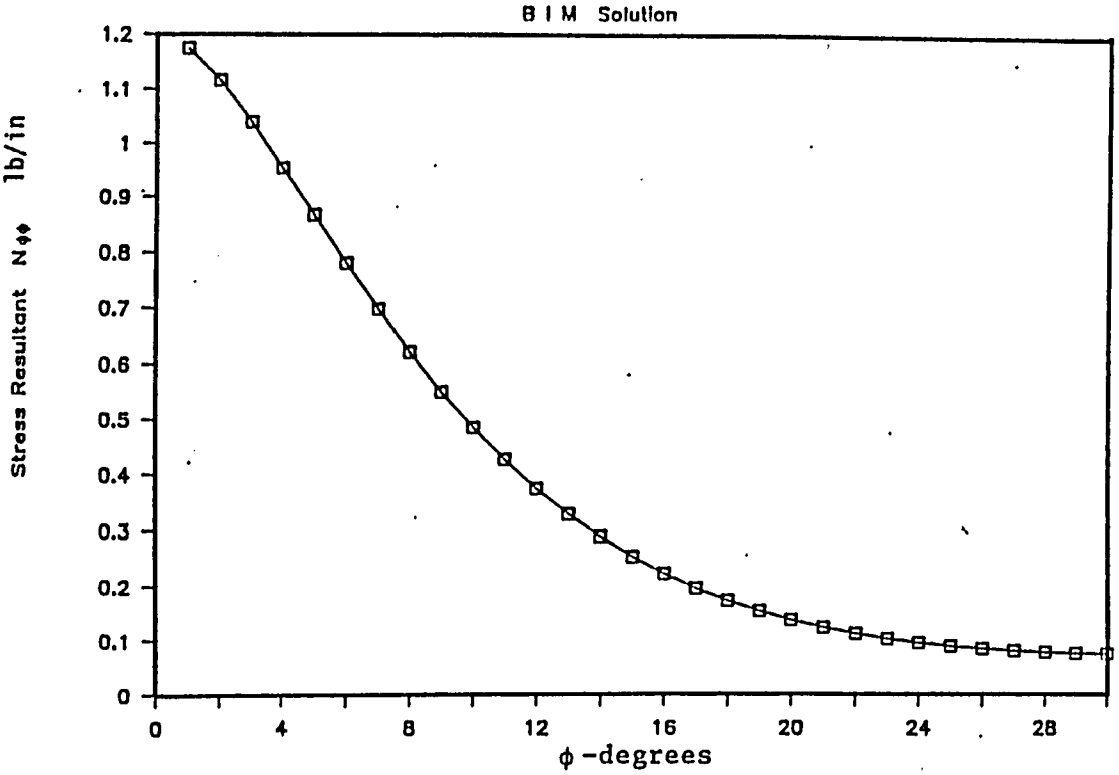

Fig. 4-1d : Stress Resultant $N_{\theta\theta}$

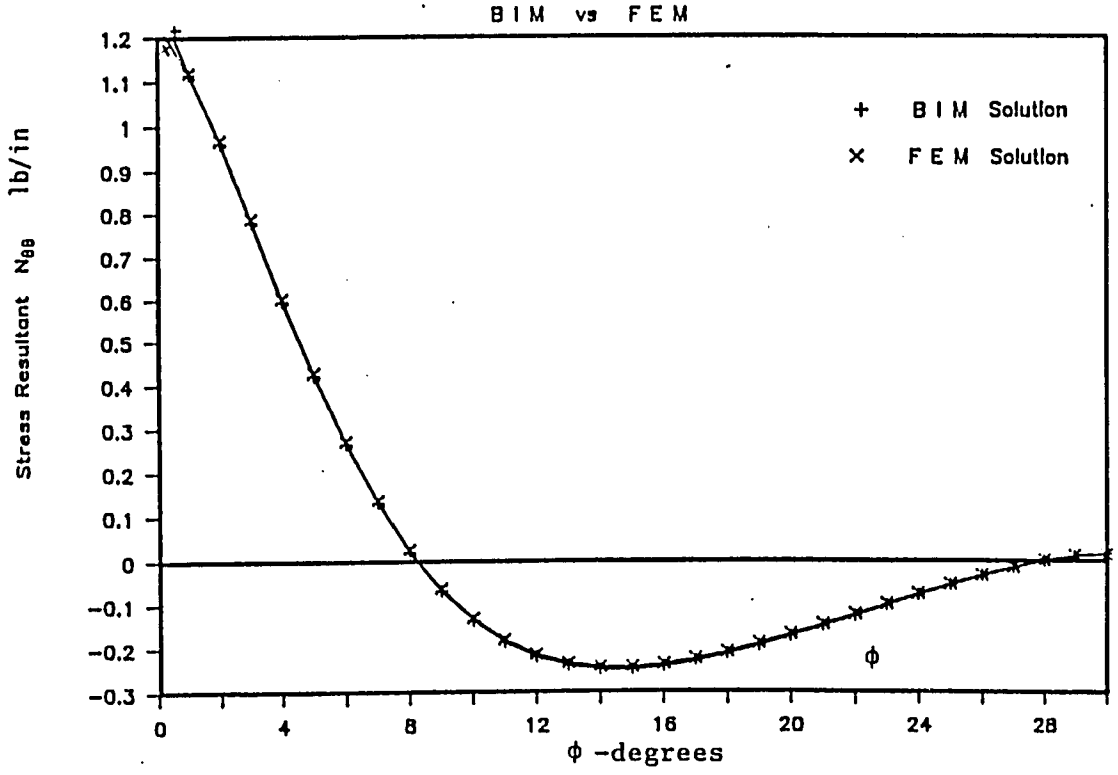

Fig. 4-1e : Moment Resultant $M_{\phi\phi}$

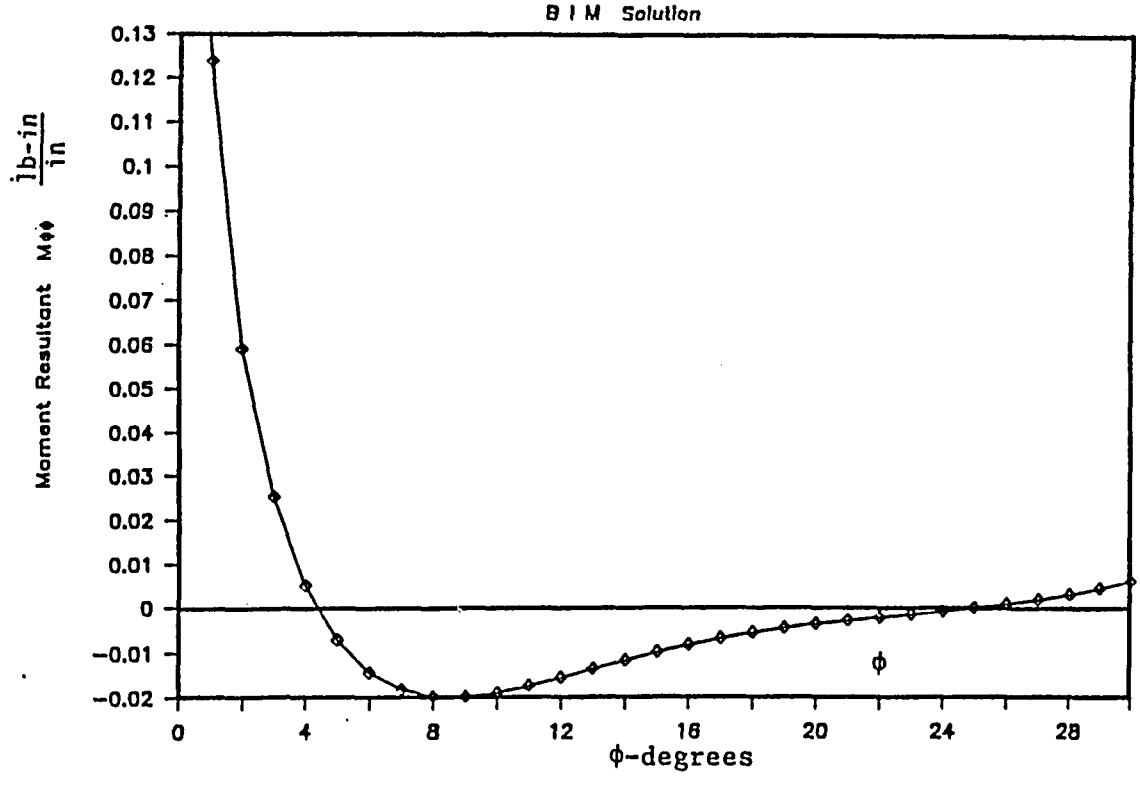

Fig. 4-1f : Moment Resultant $M_{\theta\theta}$

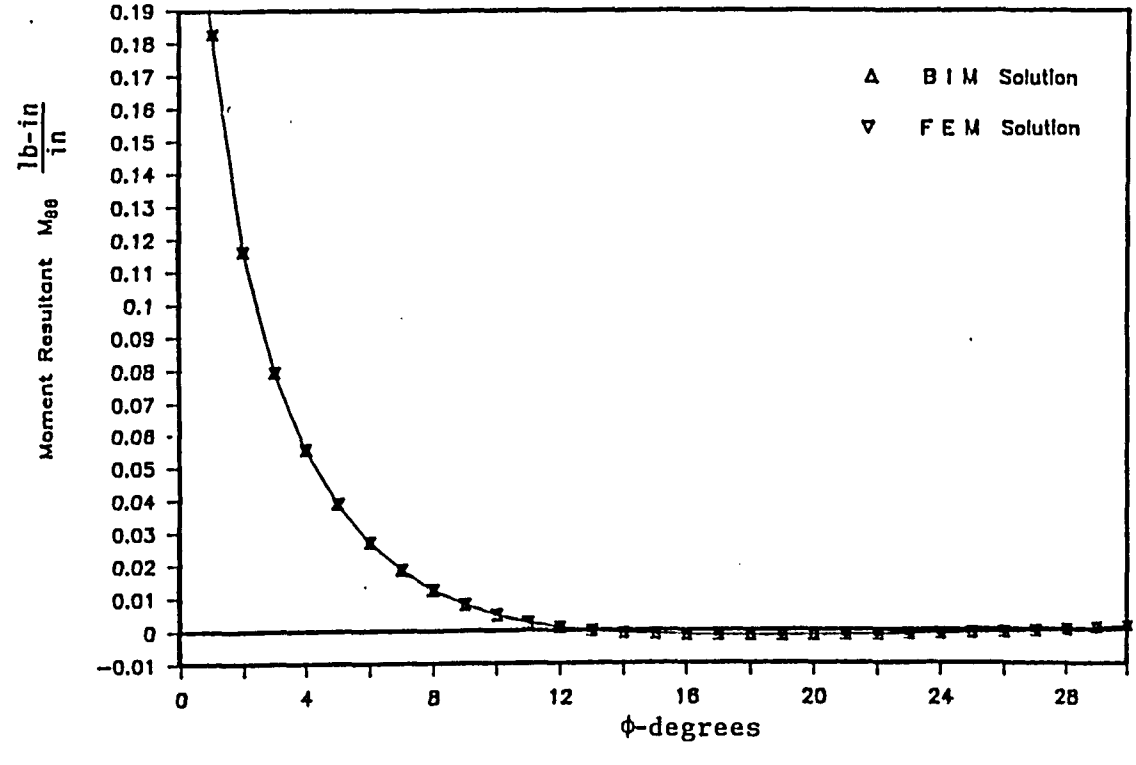

IV.2 PROBLEM OF A SPHERICAL CAP LOADED WITH A POINT LOAD AT THE APPEX AND SUBJECTED TO (a) SIMPLY SUPPORTED AND (b) FREE TO MOVE IN THE RADIAL DIRECTION BOUNDARY CONDITIONS

Consider a spherical cap with extent of 30 degrees, loaded with a point load $P = 1$ lb at the appex acting outward for the case of a simply supported boundary, as shown in Fig. 4-2a, and inward for the free to move in the radial direction edge, as seen in Fig. 4-2i. The shell is of radius $R = 10$ in, thickness $h = 0.5$ in, $E = 30 \times 10^6$ psi and Poisson's ratio $\mu = 0.3$. The problem is solved by both methods, BIM and FEM, and comparative tabulation is presented in terms of the radial displacement, the meridional displacement, the stress resultant $N_{\theta\theta}$ and the moment resultant $M_{\theta\theta}$. The results of the stress resultant $N_{\phi\phi}$, moment resultant $M_{\phi\phi}$ and shear resultant Q_{ϕ} are also displayed for the BIM solution.

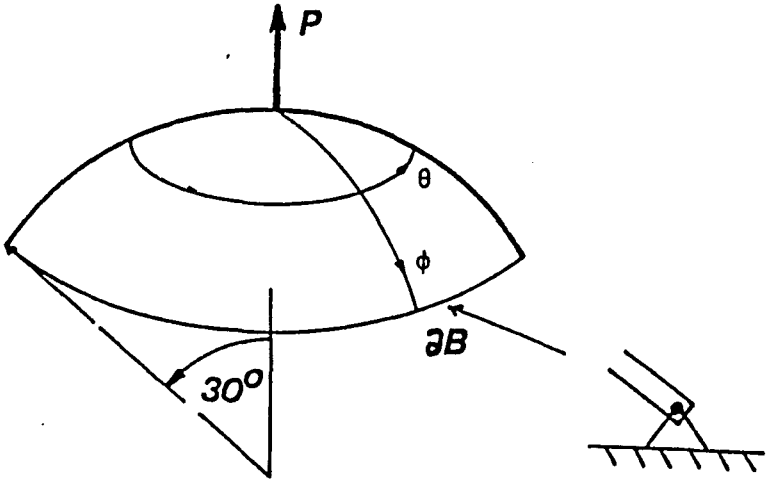

Figure 4-2a : Simply supported spherical cap with a point load at its appex.

Fig. 4-2b :

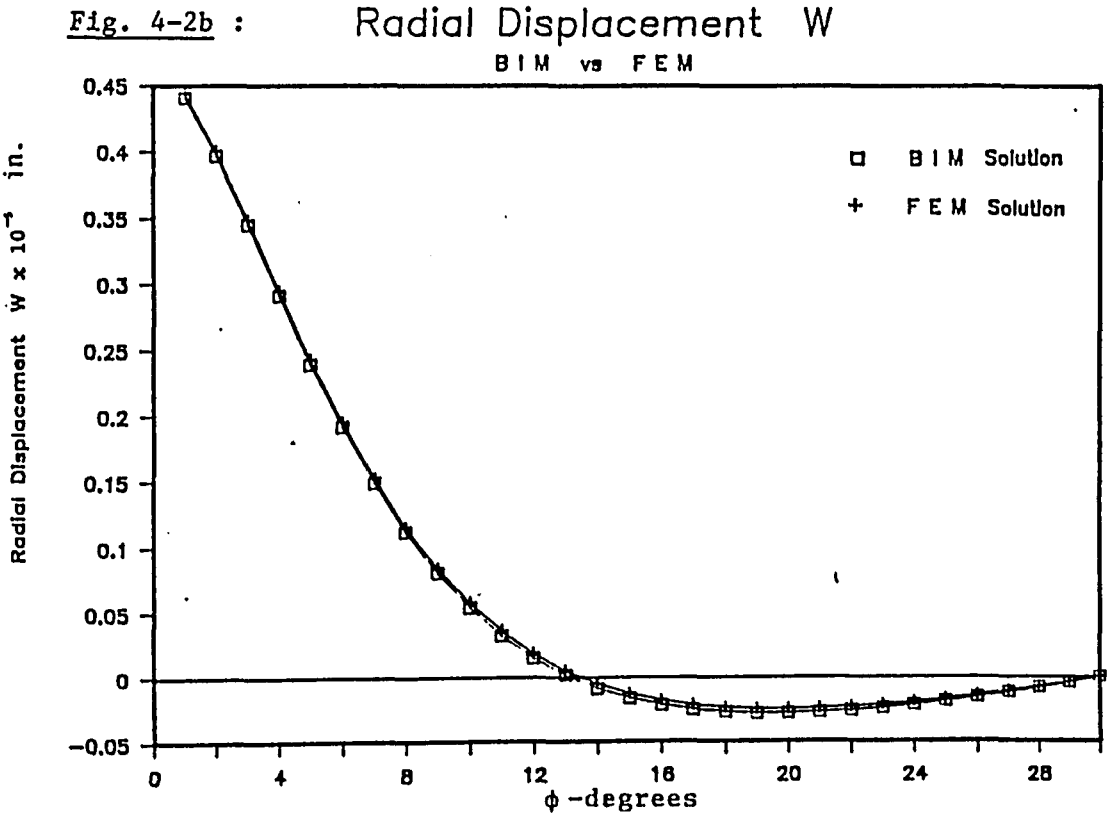

Fig. 4-2c : Meridional Displacement u_ϕ

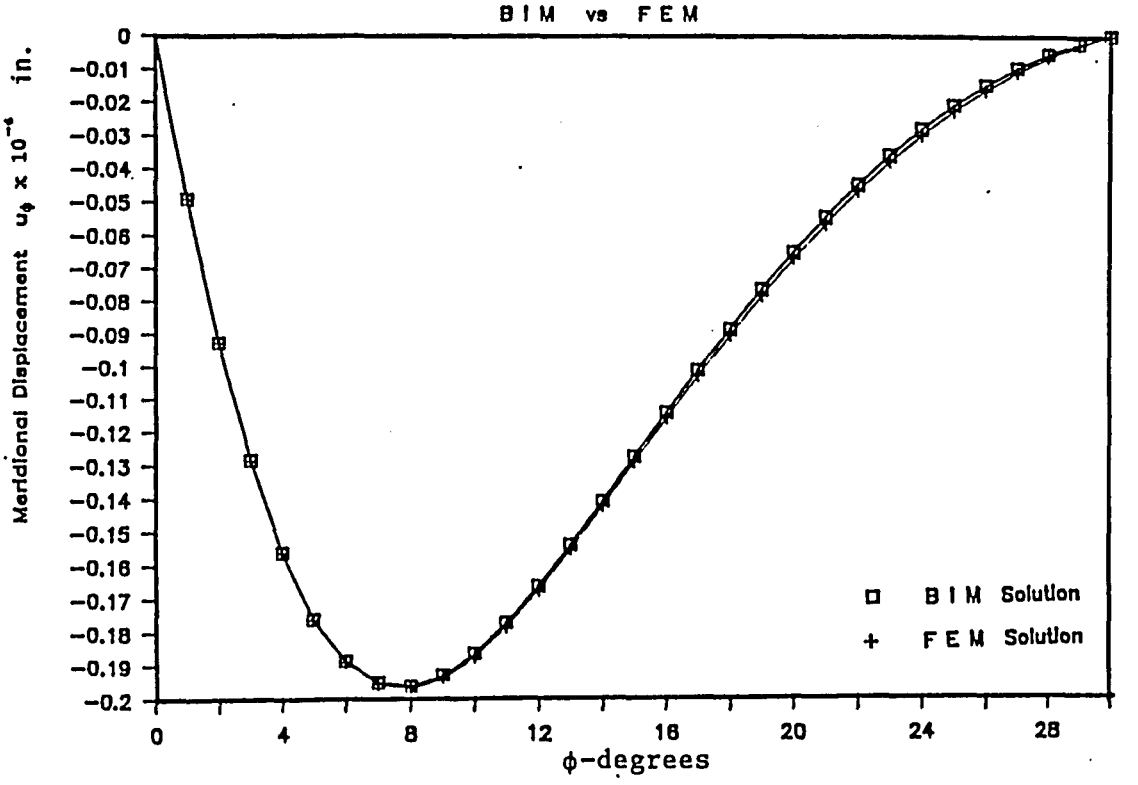

Fig. 4-2d : Transverse Shear Resultant Q_ϕ

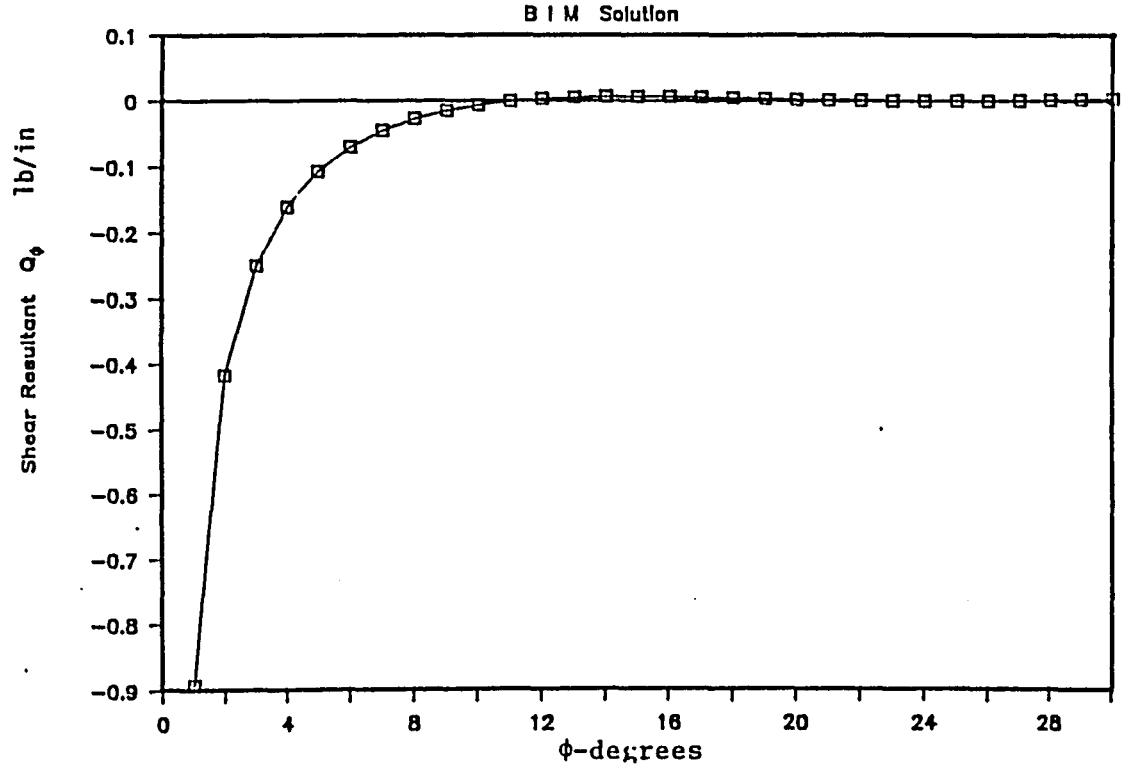

Fig. 4-2e :

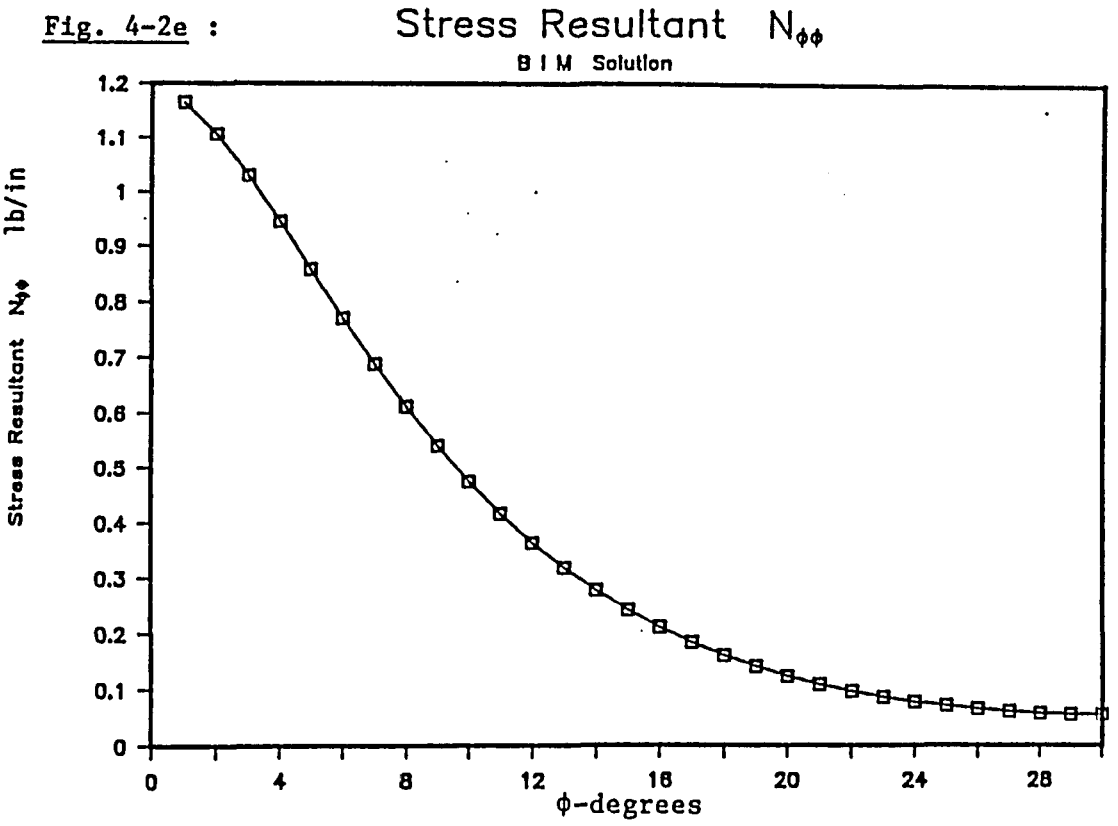

Fig. 4-2f :

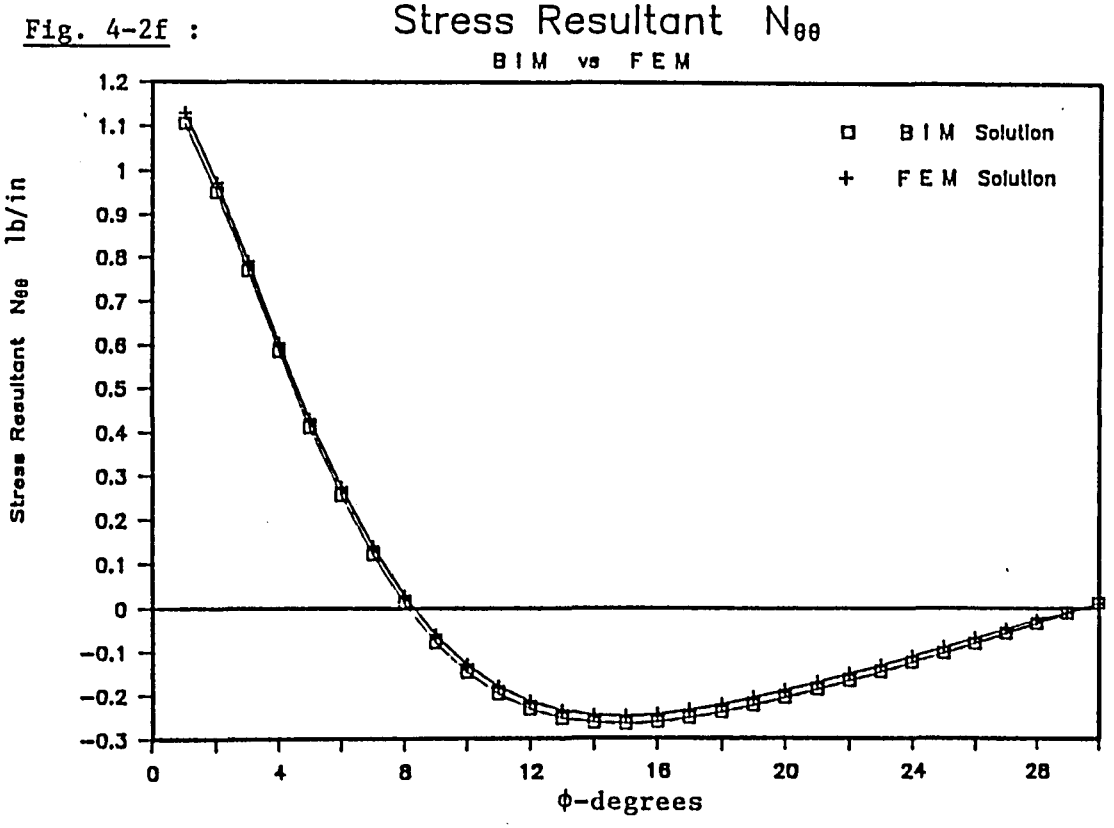

Fig. 4-2g :

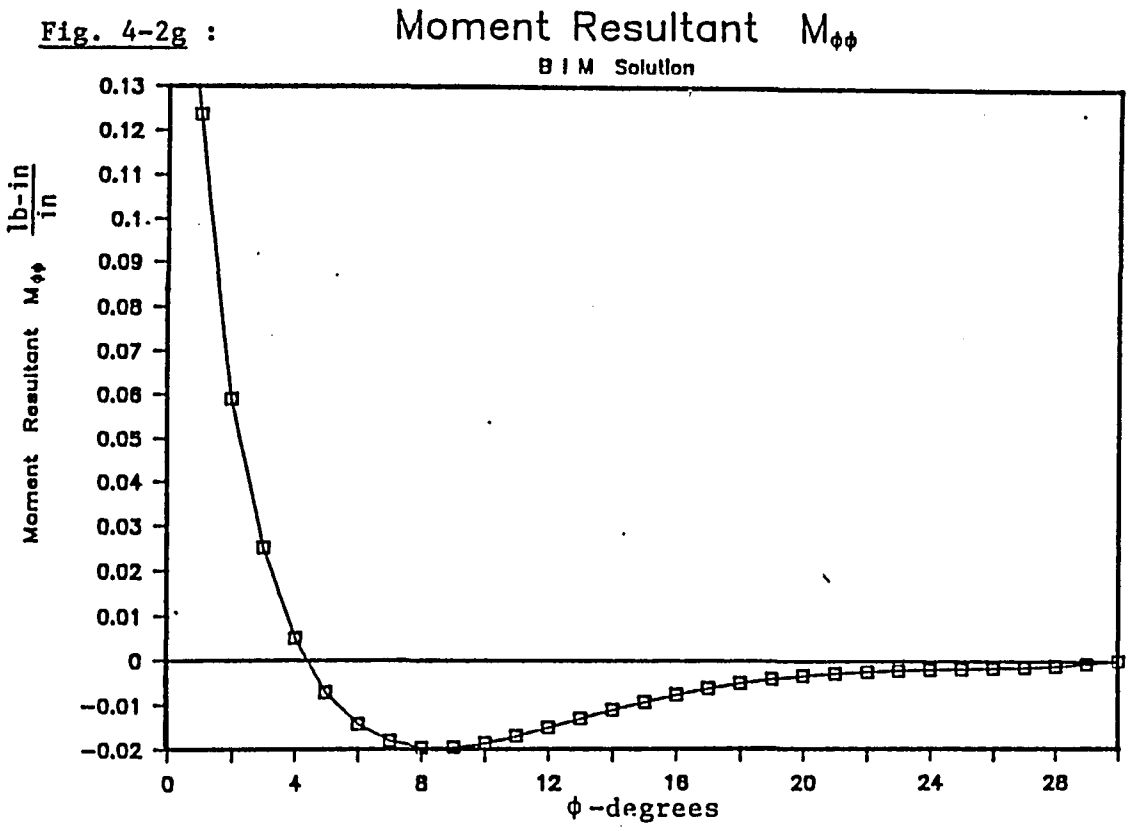

Fig. 4-2h :

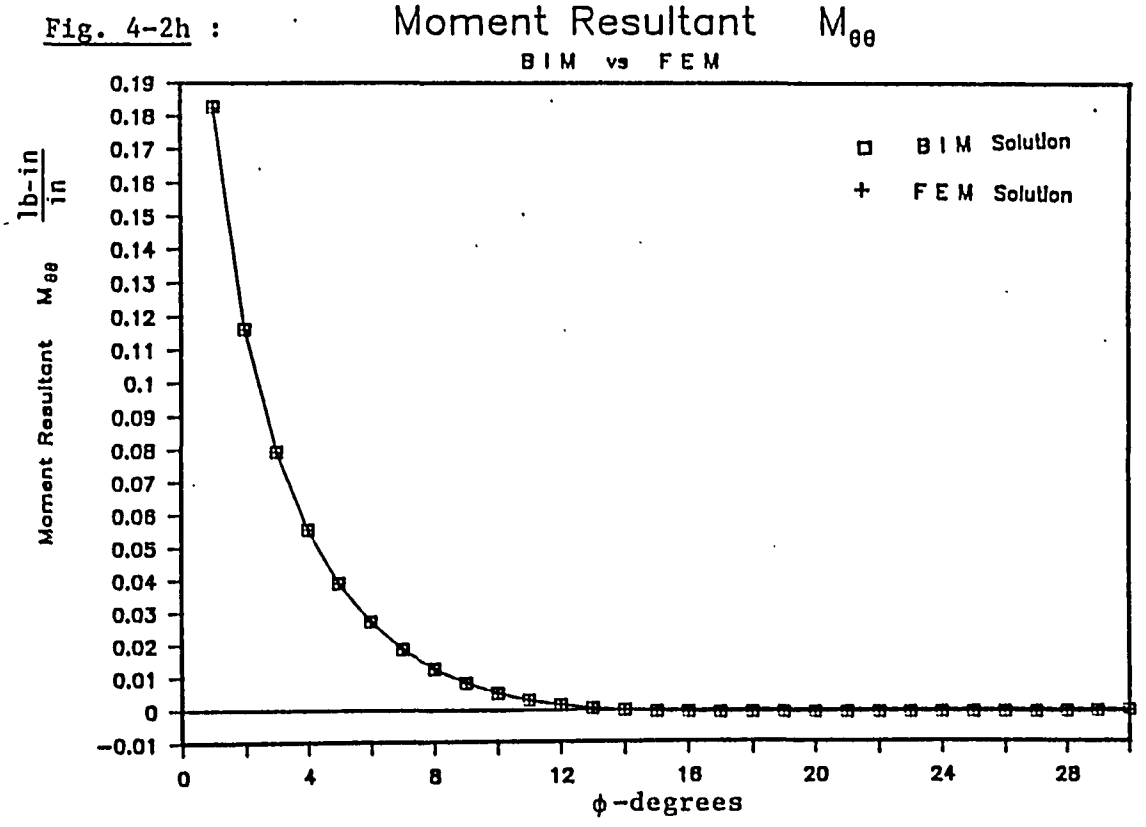

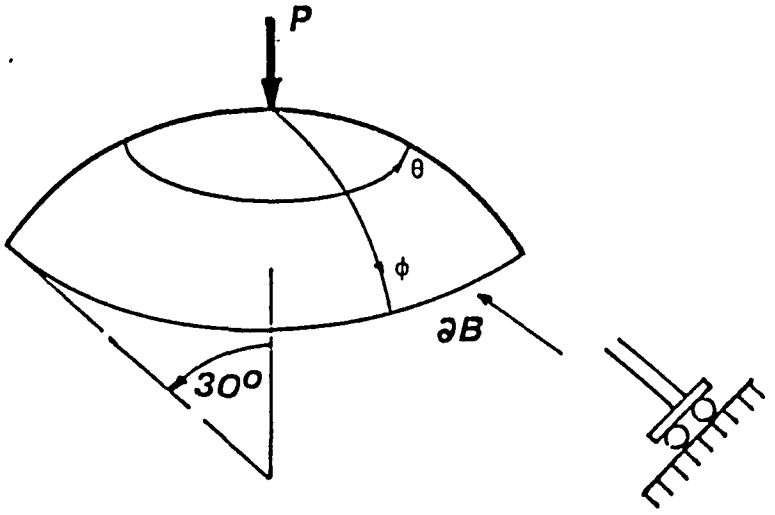

Fig. 4-2i : Spherical cap free to move in the normal direction loaded with a point load at its appex.

Fig. 4-2j :

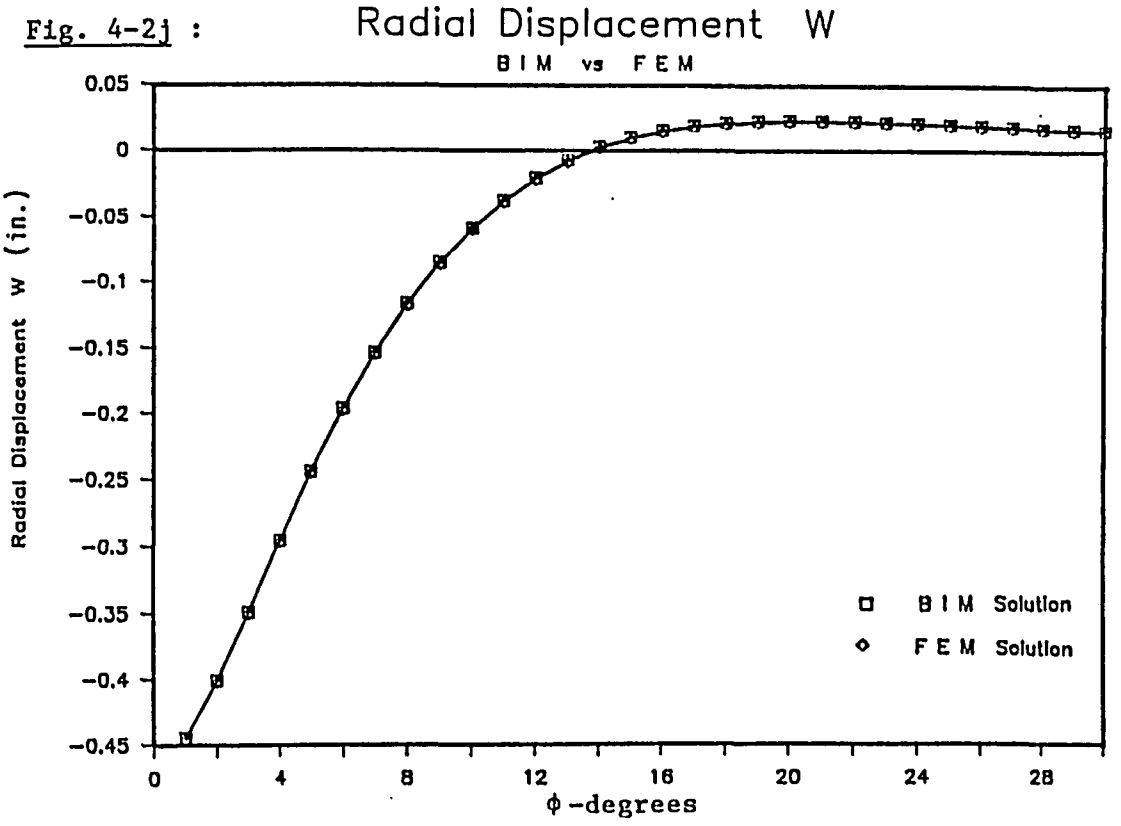

Fig. 4-2k : Meridional Displacement u_ϕ

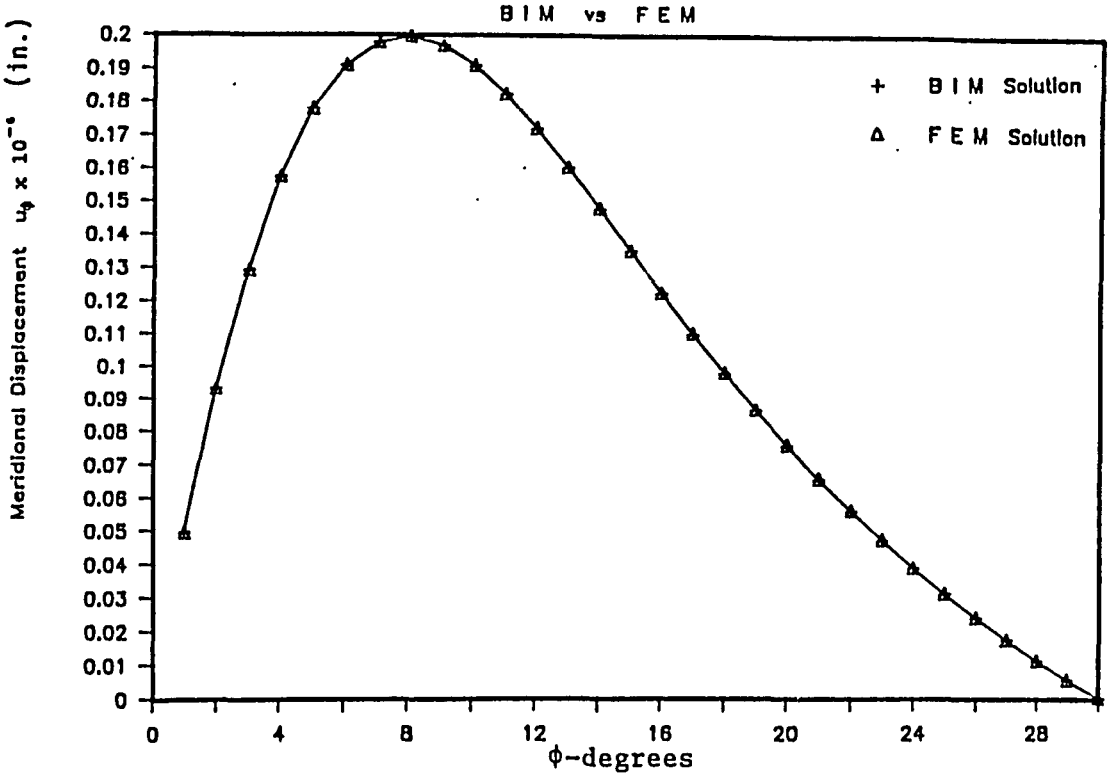

Fig. 4-21 : Transverse Shear Resultant Q_ϕ

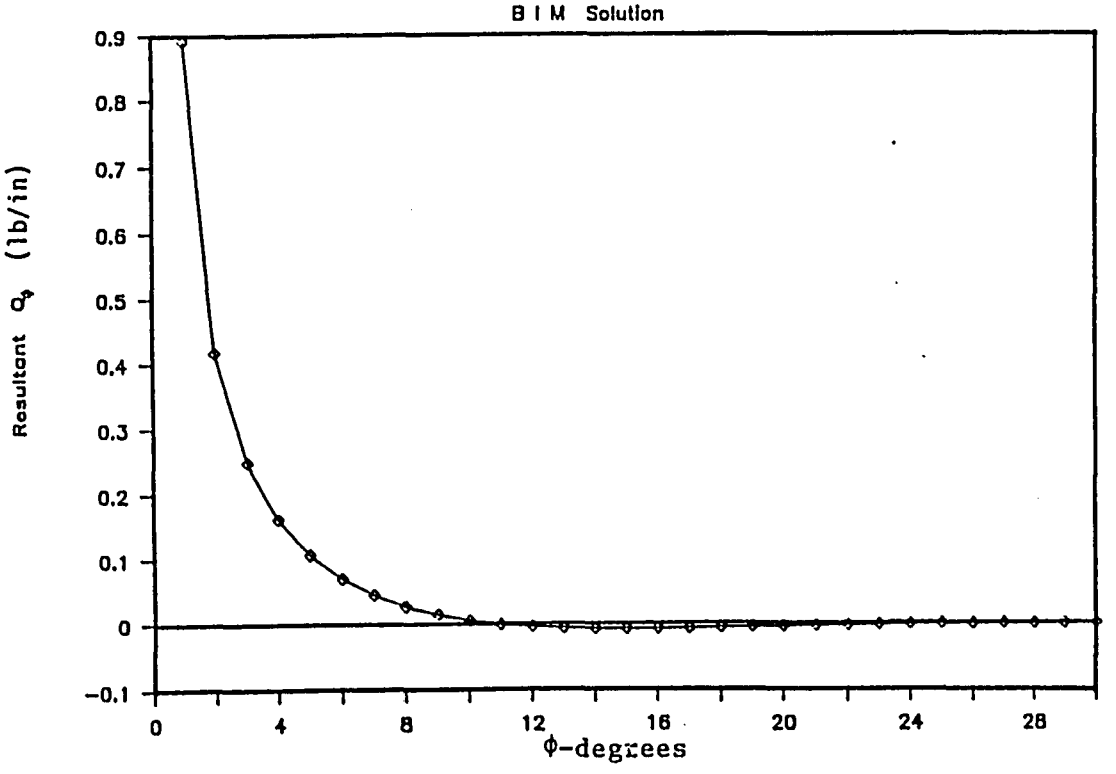

Fig. 4-2m :

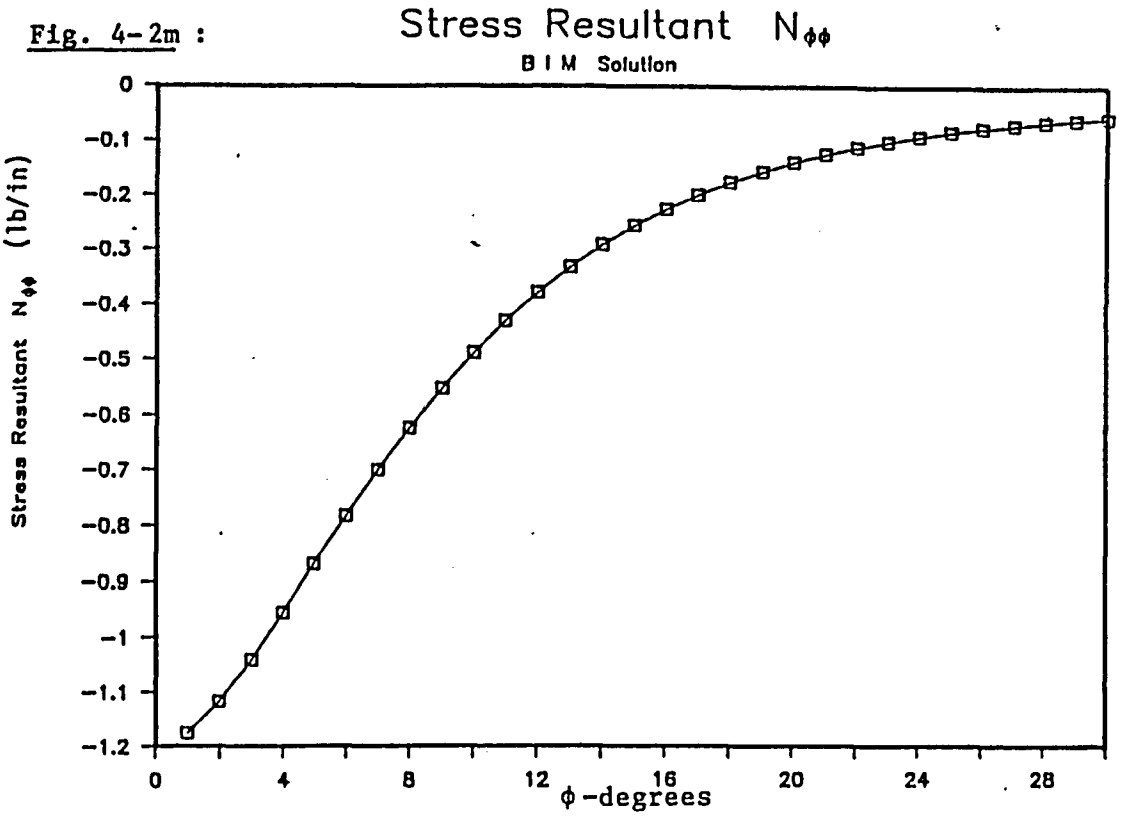

Fig. 4-2n :

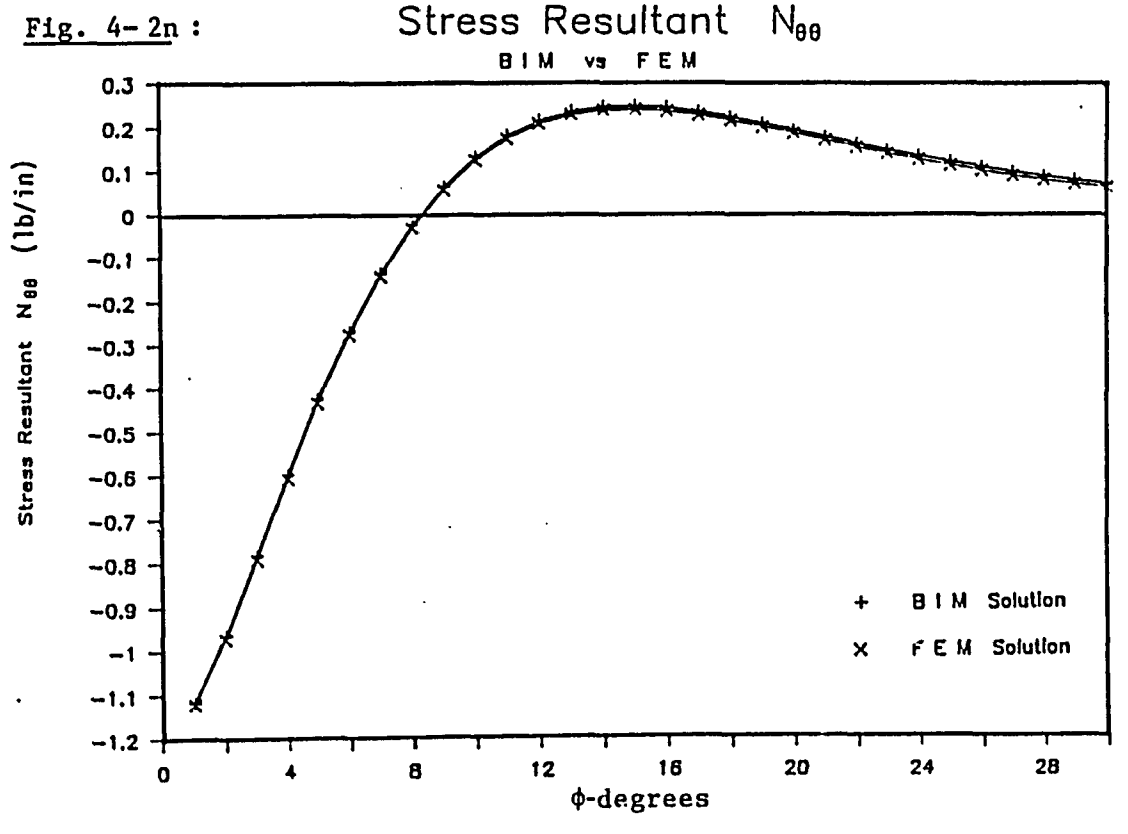

Fig. 4-2o :

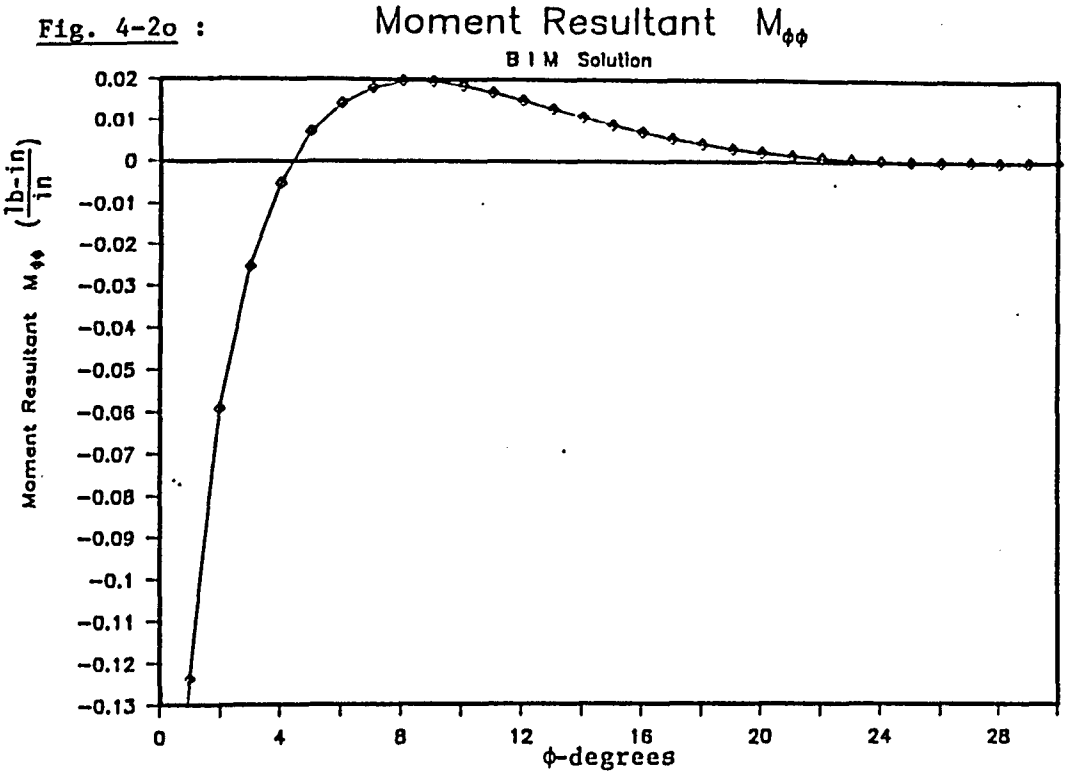

Table 4-3. Comparison of IBIM and FEM solutions on $M_{\theta\theta}$ of a free to move in the radial direction spherical cap subjected to a point load at the appex.

ϕ- DEGREES	B I M	F E M	$(\frac{lb\text{-}in}{in})$
1	-.18271	-.18240	
2	-.11603	-.11592	
3	-.07930	-.07924	
4	-.05541	-.05540	
5	-.03884	-.03882	
6	-.02701	-.02703	
7	-.01851	-.01850	
8	-.01236	-.01236	
9	-.00797	-.00797	
10	-.00486	-.00486	
11	-.00270	-.00270	
12	-.00124	-.00125	
13	-.00030	-.00030	
14	.00027	.00027	
15	.00059	.00059	
16	.00074	.00073	
17	.00077	.00076	
18	.00073	.00072	
19	.00065	.00065	
20	.00056	.00055	
21	.00046	.00046	
22	.00037	.00037	
23	.00029	.00029	
25	.00023	.00023	
26	.00019	.00019	
27	.00016	.00016	
28	.00014	.00014	
29	.00012	.00013	
30	.00012	.00011	

The detailed evaluation and comparison demonstrates not only the excellent agreement in the results of IBIM and FEM, but also displays the similarities in the shell response for the three different types of boundary constraints. The differences are concentrated in the vicinity of the boundary. Because of the all-around axisymmetry in all three shell problems studied so far, the finite element model utilized the axisymmetric conical shell element . This procedure reduced the problem to a line of elements and consequently allowed finer discretization. However, such model could only provide the two displacement components and the stress and moment resultants in the θ-direction. It is observed that the more discetized the finite element model became, the better was the agreement between the two solutions. In later section the computational effort will be compared and analyzed. However, despite the fact that the FEM model used above can provide very reliable results, it cannot evaluate, as it is, the complete stress field. For such case, higher order elements need to be utilized. This results in increased computational effort.

IV.3 PROBLEM OF A CLAMPED SPHERICAL SHELL SUBJECTED TO A POINT LOAD AWAY FROM ITS APPEX.

A shell problem solved analytically by Wilkinson and Kalnins[23] is considered. The particular problem, shown in Fig. 4-3, is portion of a sphere with 60-degree opening, clamped at the boundary and subjected to an outward point load $P = 1$ lb at a 30-degree angle away from the appex. The geometric and material properties are: $R = 10$ in, $h = 0.5$ in, $E = 30 \times 10^6$ psi and $\mu = 0.3$. The displacement and stress field is evaluated along $\theta = 0^0$ and $\theta = \pi$.

Figures 4-3c to 4-3f demonstrate the state of bending and membrane stress as predicted by the classical theory analysis. Thus compressive membrane stresses are experienced at the vicinity of the point of application, see Fig. 4-3c and Fig. 4-3d, while bending stresses inrease along the positive axis as the singular point is approached. In terms of comparison of the results with the available analytical solution, the only profound difference occurs in the moment resultant $M_{\phi\phi}$ and near the boundary of the shell. In order to evaluate the apparent disagreement, the finite element analysis was utilized. The auxiliary approach revealed, as seen in Fig. 4-3f, that indeed the IBIM model led to the correct solution.

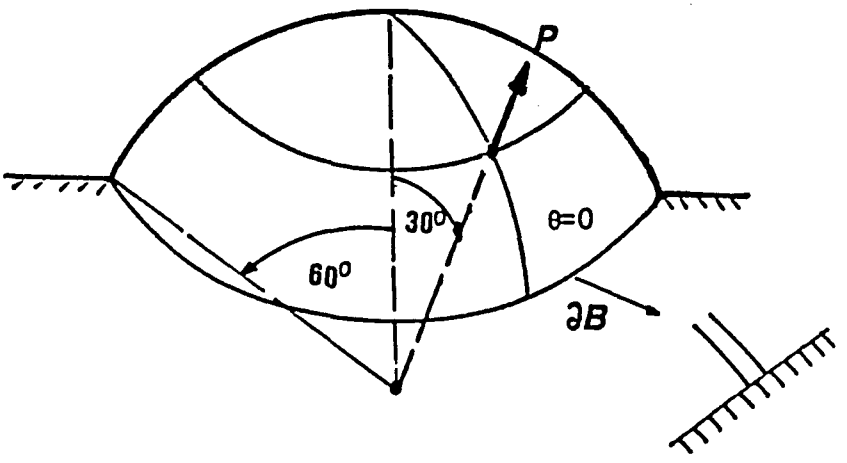

Fig. 4-3 : Clamped spherical cap subjected to a point load away from the appex.

Fig. 4-3b :

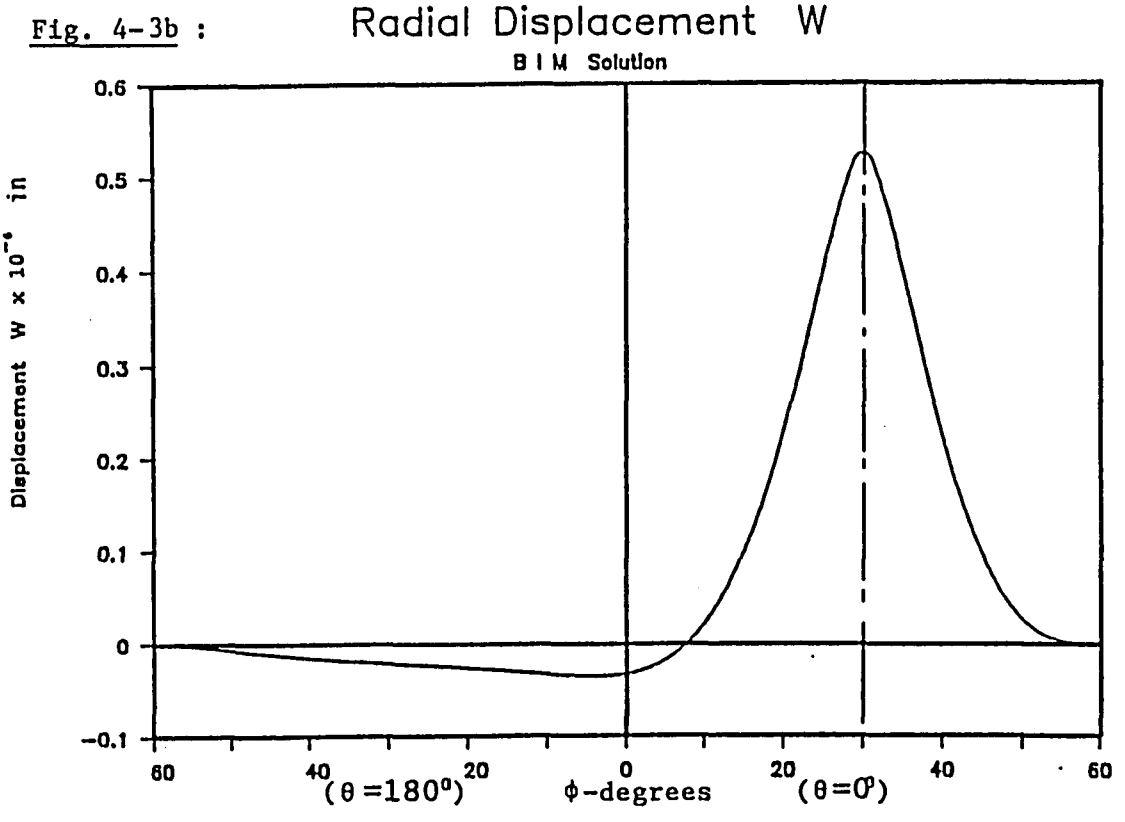

Fig. 4-3c :

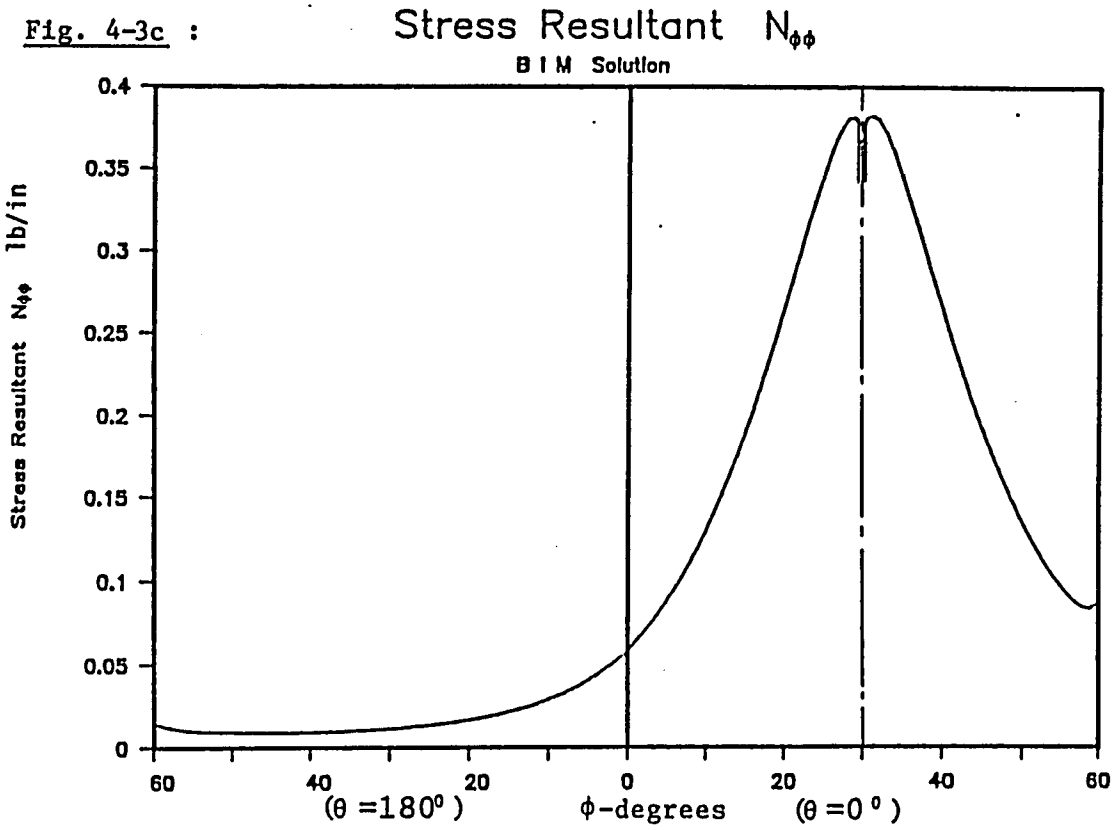

Fig. 4-3d :

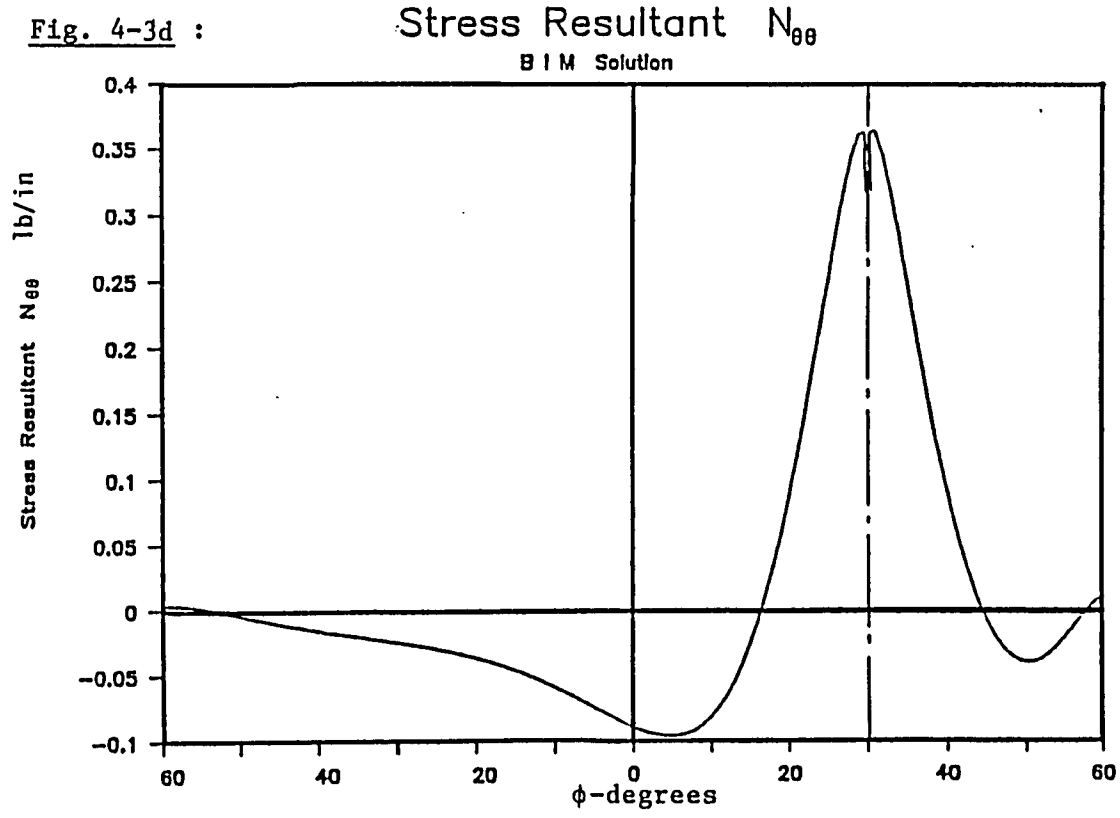

Fig.4-3e :

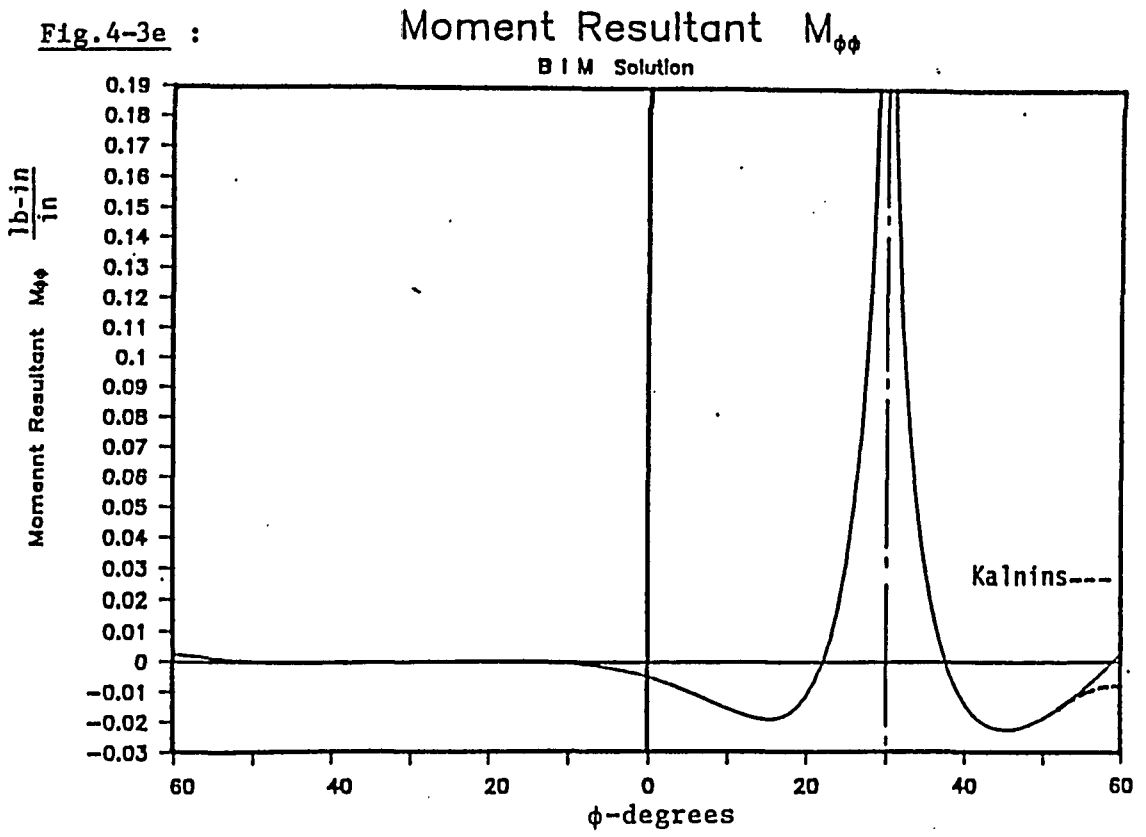

Fig. 4-3f :

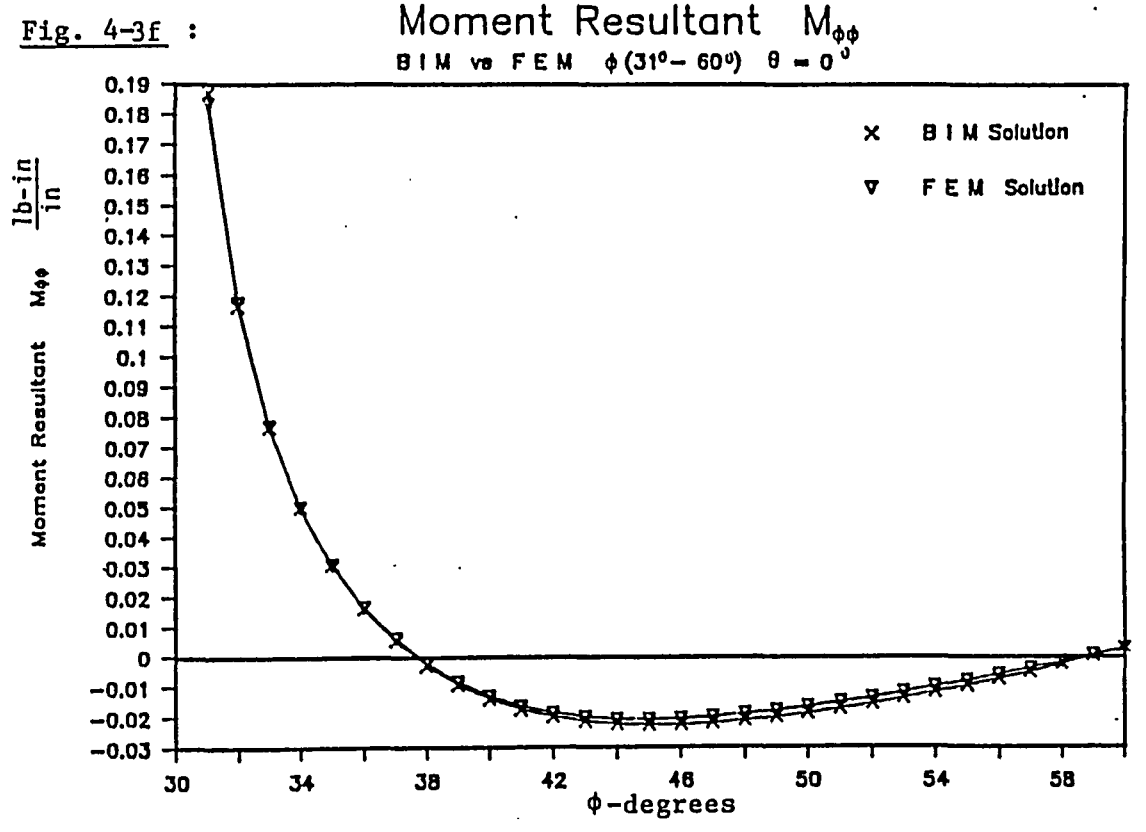

IV.4 PROBLEM OF A CLAMPED SPHERICAL CAP SUBJECTED TO A CONCENTRATED MOMENT AT ITS APPEX. IBIM AND FEM COMPARISONS.

The deformation and stress field produced by a concentrated moment M = 1 lb-in applied at the appex of a clamped spherical cap is demonstrated in this example. The concentrated moment acts along the surface coordinate $\theta = 0^0$ and the boundary angle is $\phi_B = 30^0$. The shell has R = 10 in., h = .5 in., E = 30 x 10^6 psi and $\mu = 0.3$. The example problem is treated by both numerical techniques, BIM and FEM. Since all-around axissymetry is no longer valid, the finite element model was computationally more involved. Quadrilateral shell elements were used to discretize half of the domain (solution is axisymmetric with respect to $\theta = 0^0$). The numerical results of the displacement components are tabulated in Tables 4-4 and 4-5, while the stress and moment resultants are plotted in Fig. 4.4b-4e. The presense of singular terms in the BIM stress and moment resultant expressions introduces the disimilar behavior around the point of application demonstrated more profoundly in Fig. 4.4b.

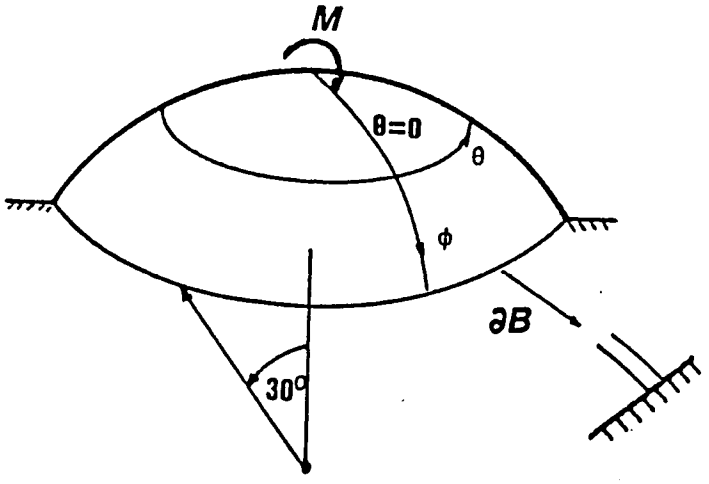

Fig. 4-4 : Clamped spherical cap subjected to a concentrated moment at the appex.

Table 4-4. Comparison of IBIM and FEM solutions on the radial displacement of a clamped spherical cap subjected to a concentrated moment at the appex.

RADIAL DISPLACEMENT W x 10^{-6} in($\theta=0^{\circ}$)

φ- Degrees	B I M	F E M
0	0.0000	0.0000
1	-.1030	-.1030
2	-.1503	-.1505
3	-.1774	-.1777
4	-.1920	-.1925
5	-.1981	-.1987
6	-.1980	-.1987
7	-.1935	-.1943
8	-.1857	-.1865
9	-.1755	-.1764
10	-.1638	-.1646
11	-.1510	-.1519
12	-.1376	-.1385
13	-.1241	-.1250
14	-.1107	-.1115
15	-.0976	-.0983
16	-.0851	-.0857
17	-.0732	-.0738
18	-.0621	-.0626
19	-.0518	-.0523
20	-.0424	-.0429
21	-.0340	-.0344
22	-.0266	-.0268
24	-.0201	-.0203
25	-.0145	-.0147
26	-.0099	-.0100
27	-.0062	-.0063
28	-.0034	-.0035
29	-.0015	-.0015
30	0.0000	0.0000

Table 4-5. Surface displacements of IBIM and FEM solutions for a clamped spherical cap subjected to a concentrated moment at the appex.

	$u_\phi \times 10^{-7}$ in ($\theta = 0^0$)		$u_\theta \times 10^{-7}$ in ($\theta = 90^0$)	
ϕ-Degrees	B I M	F E M	B I M	F E M
1	-.2970	-.3026	.3168	.3246
2	-.2854	-.2902	.3180	.3243
3	-.2645	-.2687	.3125	.3177
4	-.2390	-.2429	.3034	.3079
5	-.2114	-.2150	.2921	.2959
6	-.1834	-.1867	.2795	.2827
7	-.1558	-.1589	.2660	.2687
8	-.1293	-.1323	.2520	.2542
9	-.1046	-.1074	.2377	.2395
10	-.0820	-.0844	.2233	.2247
11	-.0614	-.0637	.2090	.2102
12	-.0432	-.0453	.1949	.1958
13	-.0274	-.0293	.1811	.1818
14	-.0139	-.0155	.1676	.1681
15	-.0026	-.0040	.1545	.1549
16	.0064	.0052	.1418	.1421
17	.0135	.0125	.1295	.1297
18	.0188	.0179	.1176	.1178
19	.0223	.0216	.1061	.1063
20	.0243	.0238	.0950	.0951
21	.0249	.0246	.0843	.0844
22	.0244	.0242	.0740	.0740
23	.0229	.0228	.0639	.0640
24	.0207	.0206	.0541	.0542
25	.0178	.0178	.0446	.0448
26	.0145	.0145	.0354	.0355
27	.0109	.0110	.0263	.0264
28	.0072	.0072	.0174	.0175
29	.0035	.0035	.0086	.0087
30	0.0000	0.0000	0.0000	0.0000

R = 10 in h = 0.5 in E = 30×10^6 μ = 0.3

Fig. 4-4b :

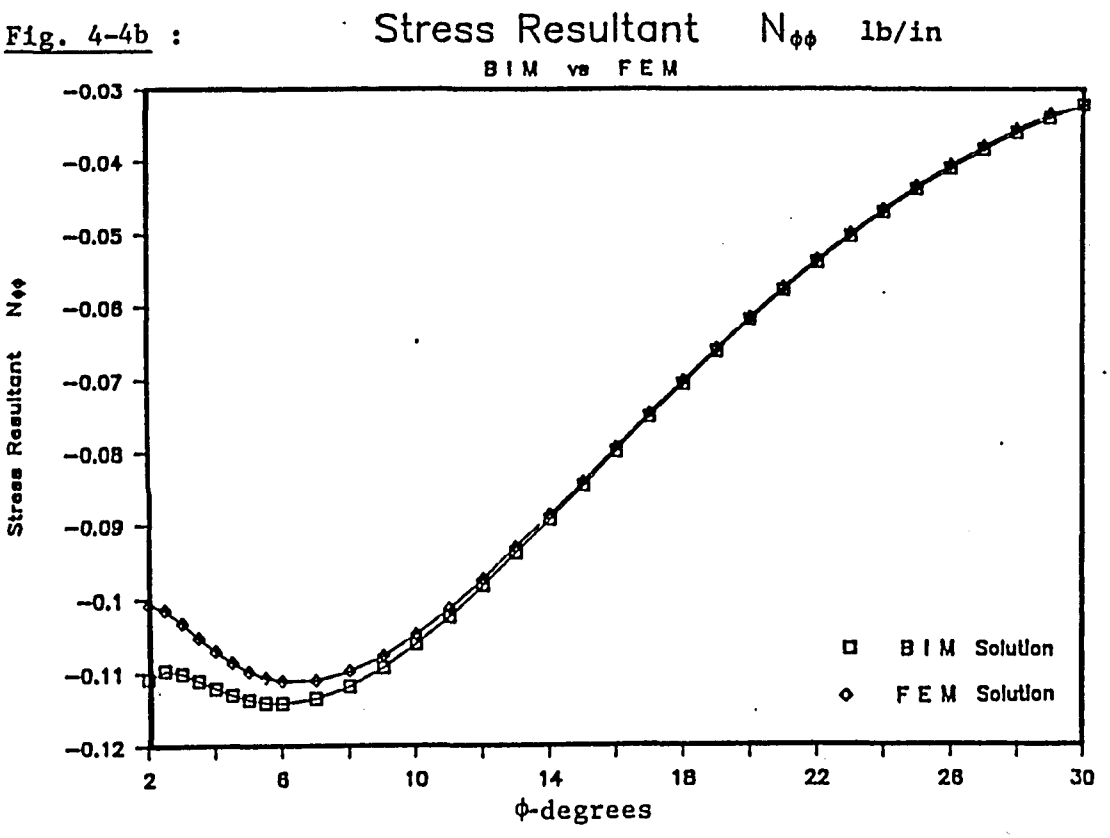

Fig. 4-4c :

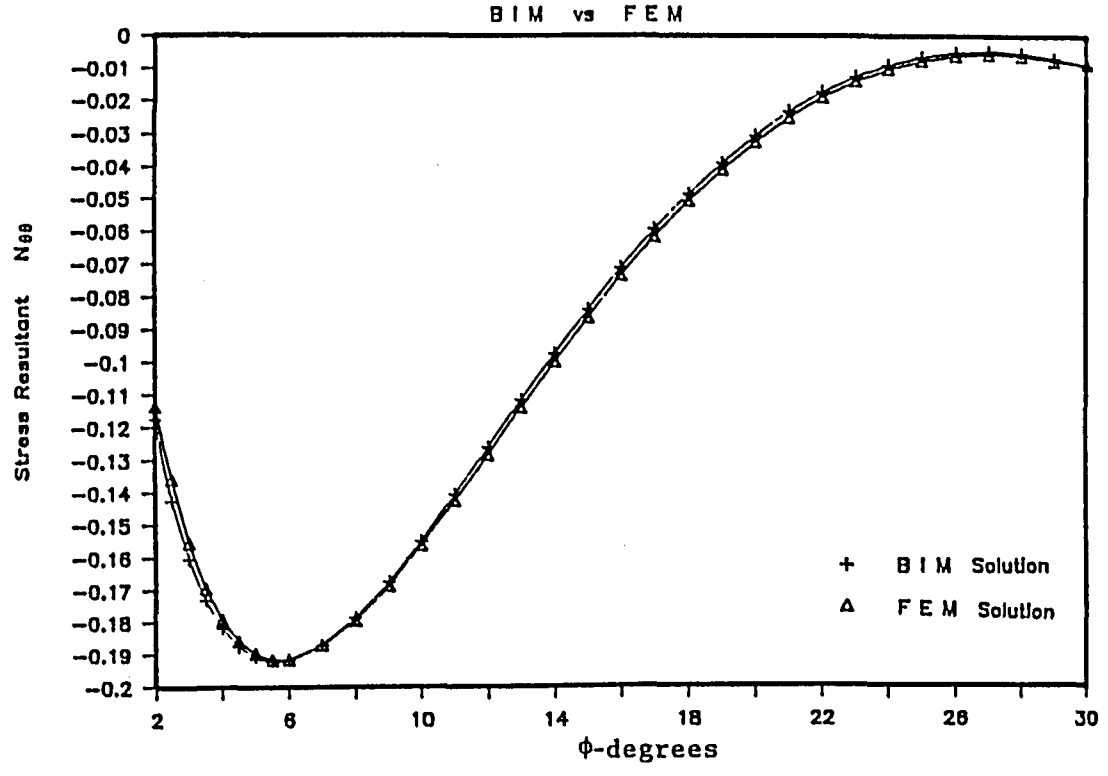

Fig. 4-4d : Moment Resultant $M_{\phi\phi}$ $\frac{\text{lb-in}}{\text{in}}$

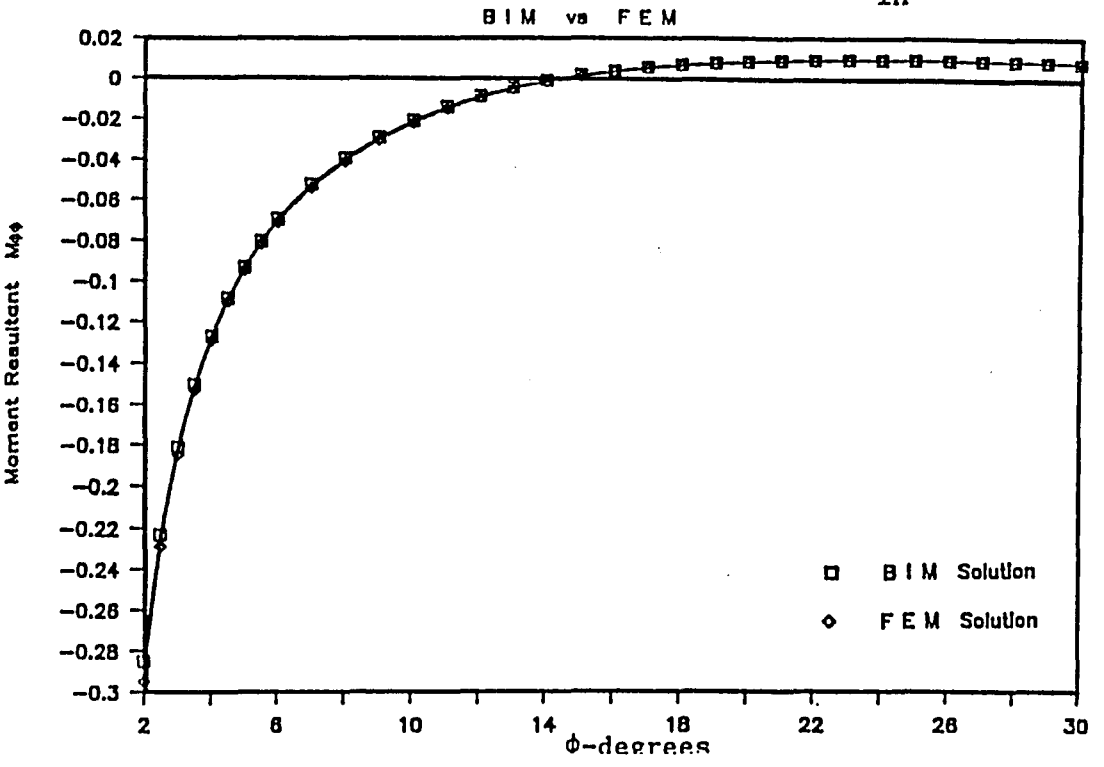

Fig. 4-4e : Moment Resultant $M_{\theta\theta}$ $\frac{\text{lb-in}}{\text{in}}$

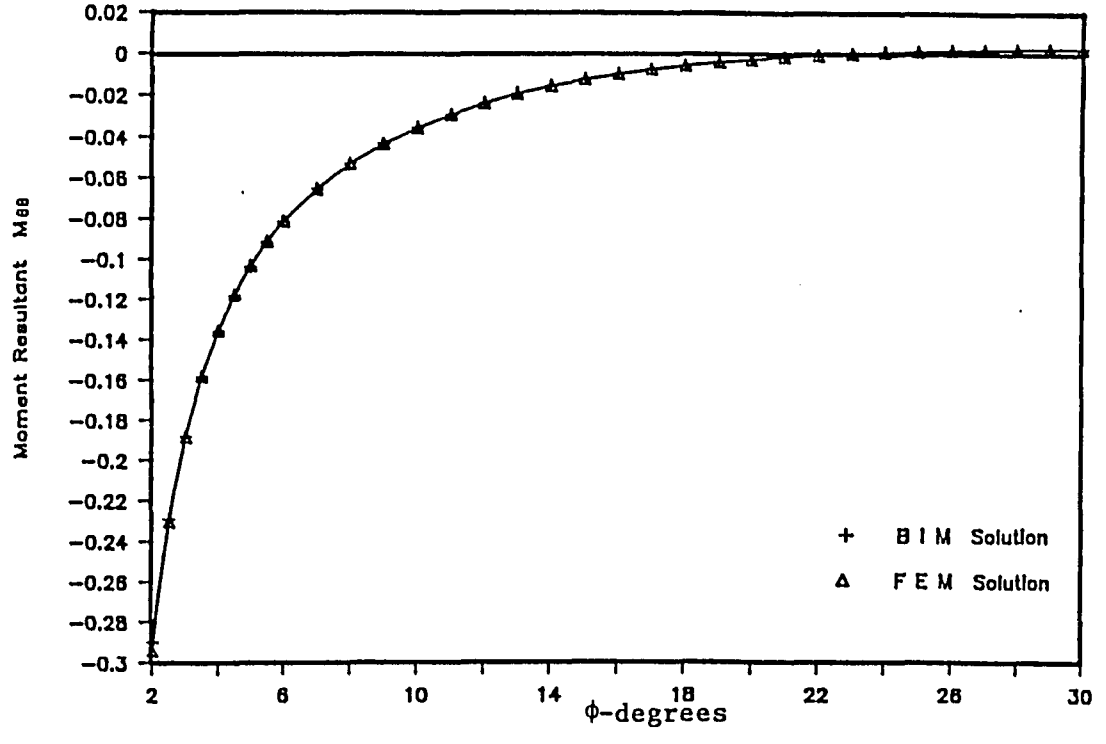

It is interesting to note that while identical results are obtained for all three displacement components, see Tables 4-4 and 4-5, and moment resultants, see Fig. 4-4d and 4-4e, differences in the shell response are observed in the membrane stress resultants shown in Fig. 4-4b and 4-4c. It is further noted that away from the point of application of the singular moment all the components of stress are identical. The differences between IBIM and FEM in the stress resultant expressions is the result of the singular character of the corresponding kernels of the IBIM analysis. The shallow shell solution presented by Lucasiewcz[15] predicts that both stress resultants will go to zero at the appex of the shell.

IV.5 PROBLEM OF A CLAMPED SPHERICAL CAP SUBJECTED TO A CONCENTRATED TANGENTIAL LOAD AT THE APPEX. COMPARISON OF IBIM AND FEM SOLUTIONS.

A similar shell problem (see Fig.4-5) is evaluated for the case of a concentrated tangential load applied at the appex along $\theta = 0^{o}$. The various displacement and stress resultant components are plotted in Fig. 4.5b-5h. Again, quadrilateral shell elements were used to discretize half of the shell domain in the finite element model. We are interested, as in the previous problems, in the justification of the derived form of the singular solutions corresponding to the particular type of surface loading.

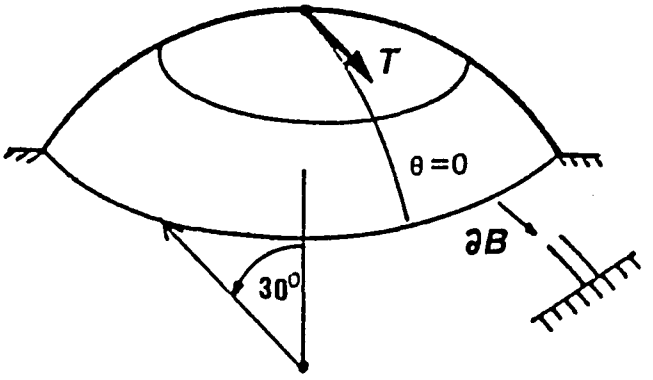

Fig. 4-5 : Clamped spherical cap subjected to a concentrated tangential load at the appex.

Fig. 4-5b :

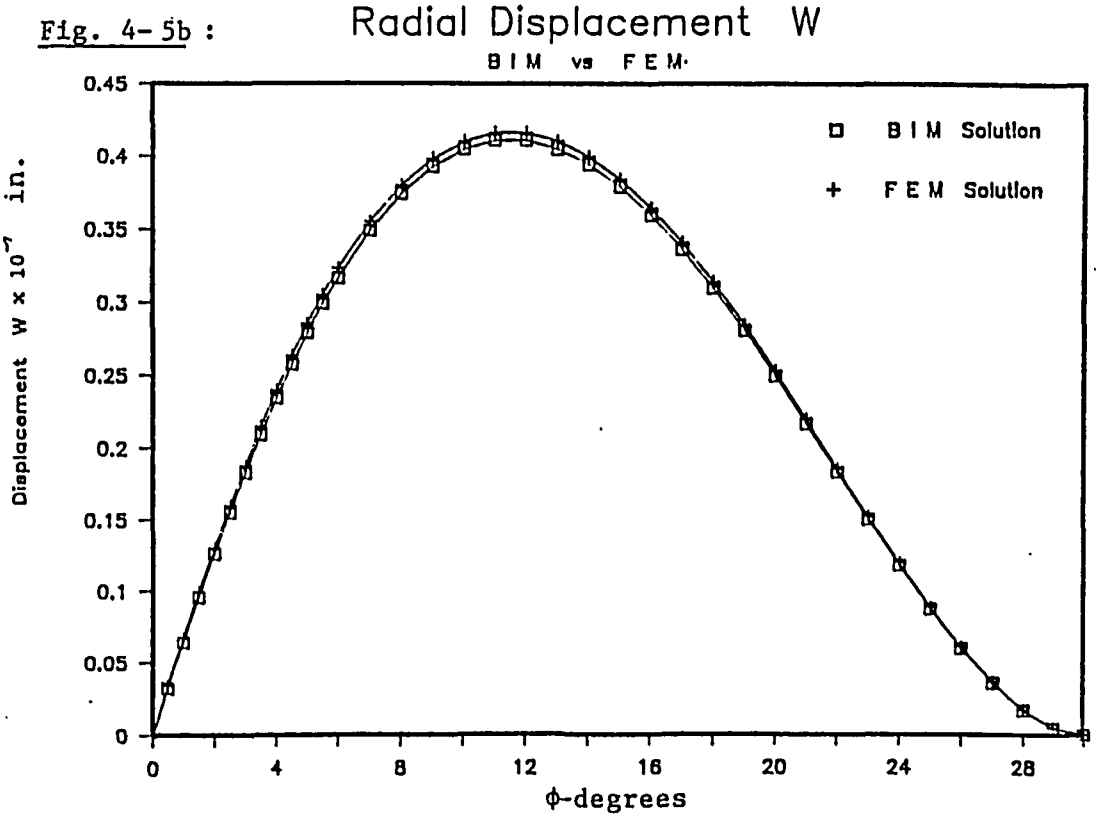

Fig. 4-5c : Meridional Displacement u_ϕ ($\theta = 0°$)

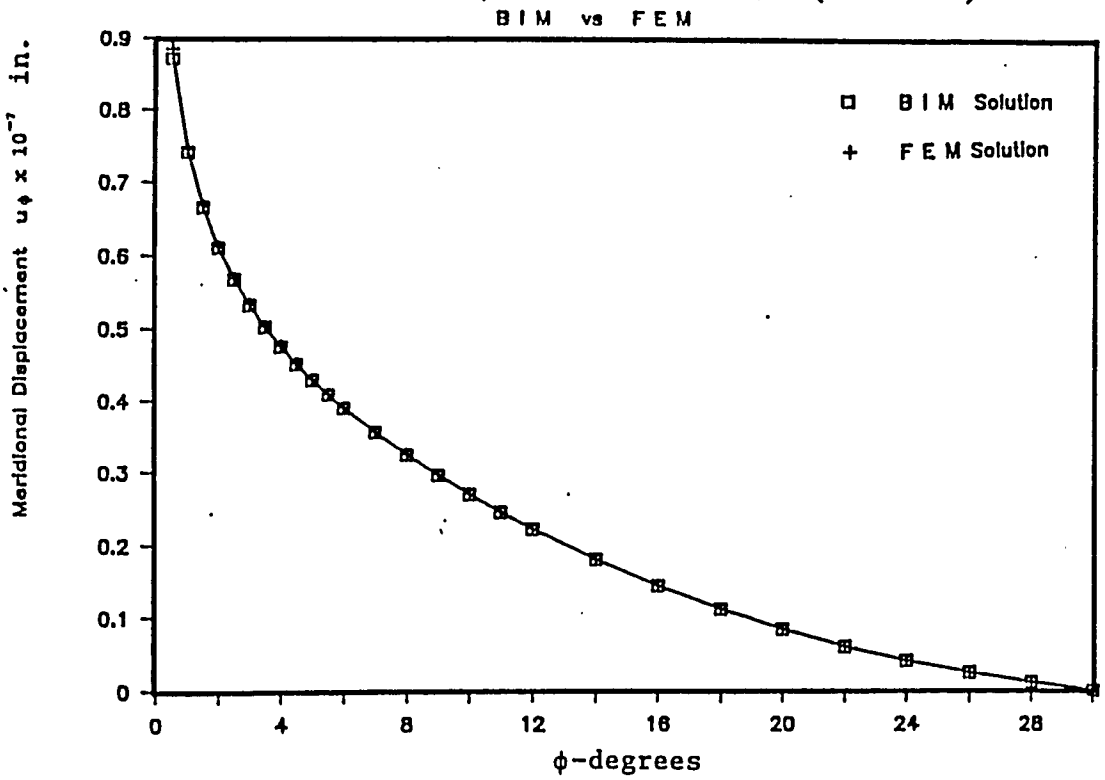

Fig. 4-5d : Tangential Displacement u_θ ($\theta = 90°$)

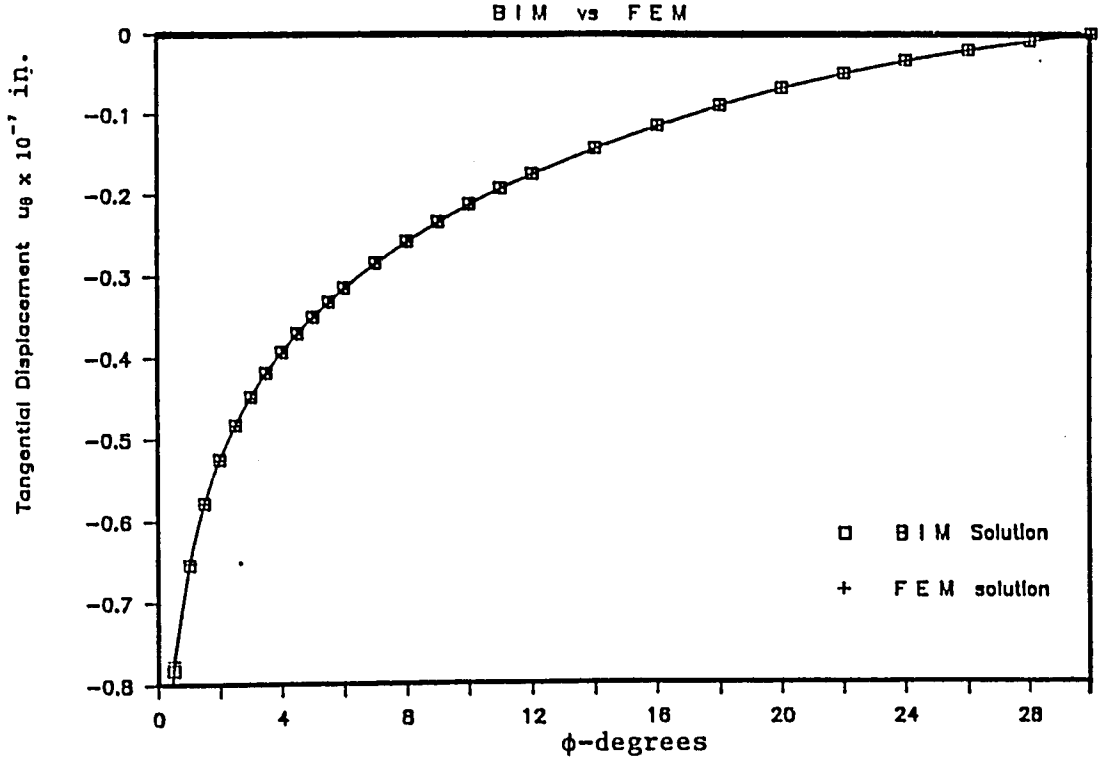

Fig. 4-5e :

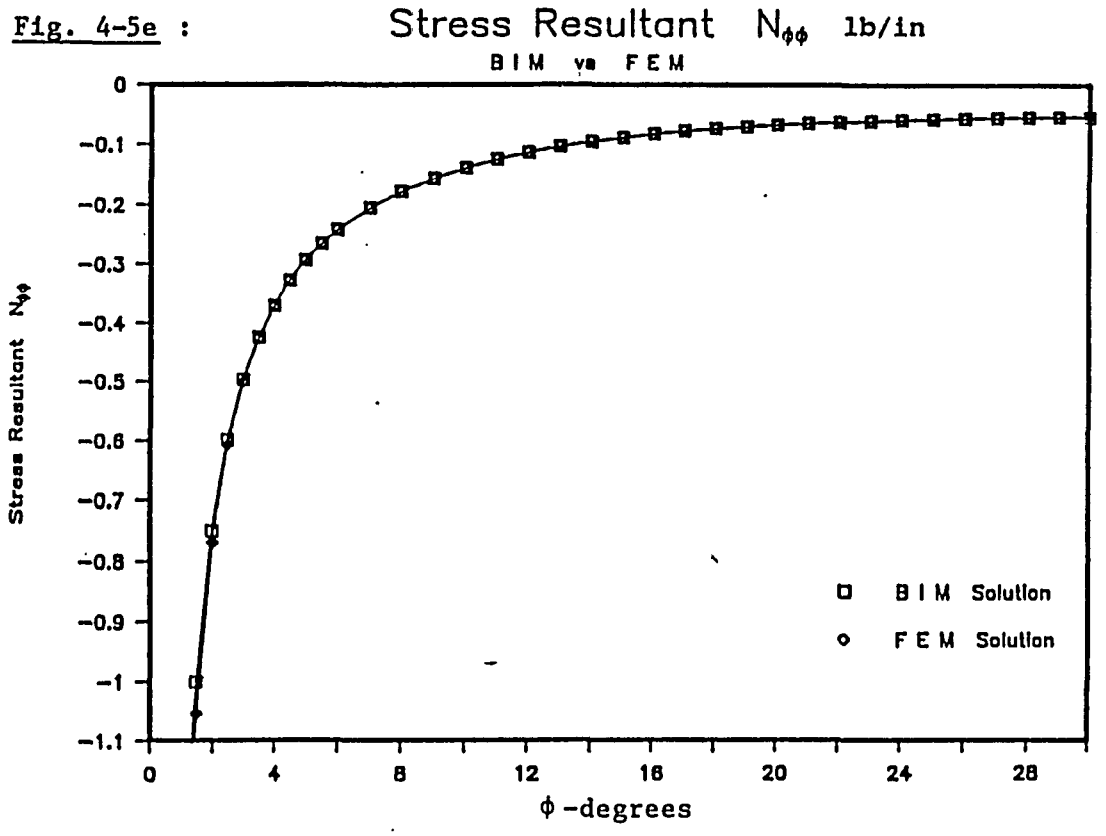

Fig. 4-5f :

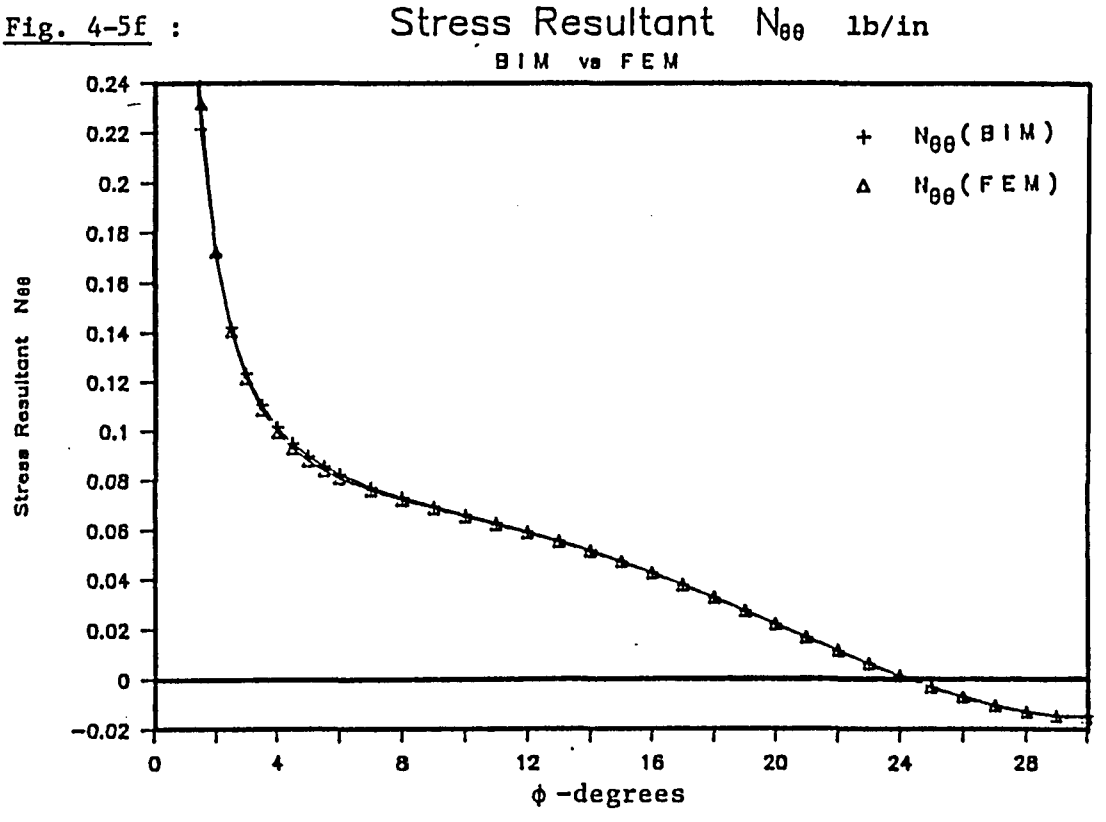

Fig. 4-5g : Moment Resultant $M_{\phi\phi}$ $\frac{\text{lb-in}}{\text{in}}$

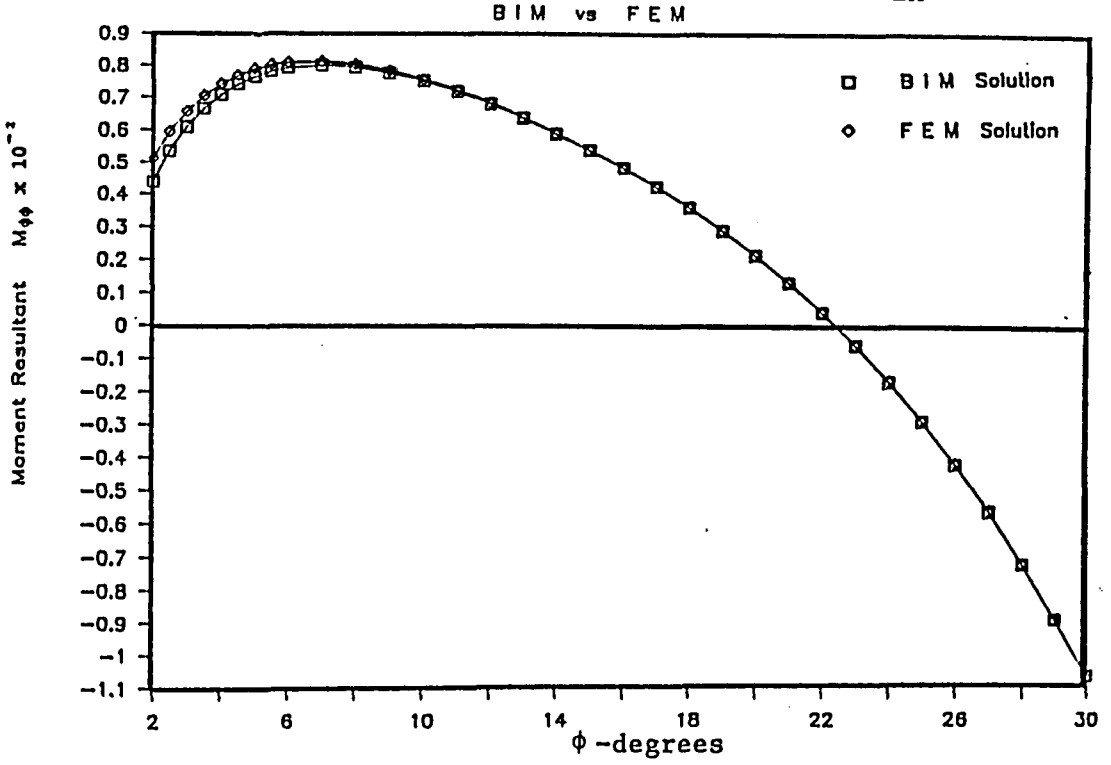

Fig. 4-5h : Moment Resultant $M_{\theta\theta}$ $\frac{\text{lb-in}}{\text{in}}$

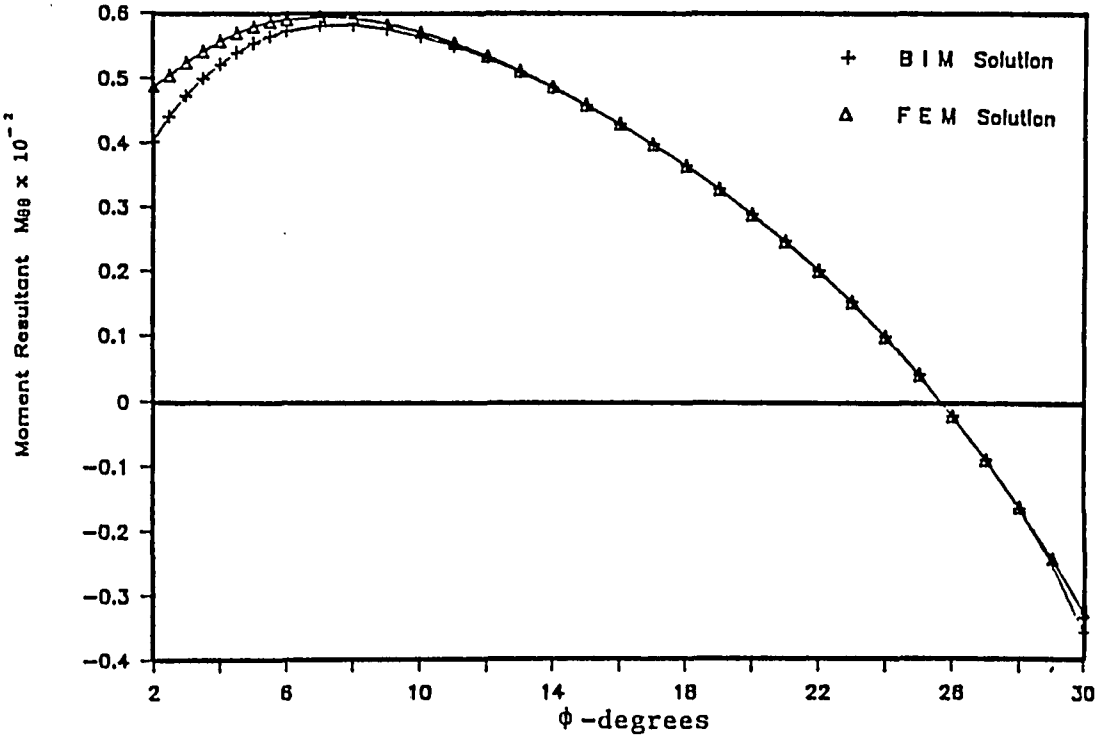

The displacement components are plotted in Fig. 4-5b to 4-5d. These figures demonstrate excellent agreement throughout the extent of the spherical cap. Excellent agreement is also obtained for the membrane stress resultants, see Fig. 4-5e and 4-5f, with slight deviations near the singular load. Far more noticable deviations are experienced by the moment resultants in the vicinity of the shell appex. However, the solutions become identical as one moves away from the pole. Such differences near the singular load occur as a result of the singular character of the kernels in the IBIM.

IV.6 PROBLEM OF COMPARISON OF CLASSICAL AND IMPROVED THEORY OF SHELLS FOR THREE TYPES OF CONCENTRATED SURFACE EXCITATION.

In the foregoing, a clamped spherical cap of 30-degree opening and with $R = 10$ in, $h = 0.5$ in, $E = 30 \times 10^6$ and $\mu = 0.3$ will be subjected to a normal point load, a concentrated moment and a tangential load at its appex. Our intention in this set of problems is to verify the improved theory mathematical model and also to demonstrate the differences of the two theories. It is expected that the two approaches differ in the vicinity of the point of application and reach identical distributions away from it. Table 4-6 represents the comparison of the two theories for the case of a normal point load at the appex. Fig. 4.6a-f correspond to the comparison for the case of a concentrated moment and lastly Fig. 4.6g-l represent the comparison of the shell response for the tangential load excitation.

Table 4-6. Comparison of displacement solutions of a clamped spherical cap. Classical and Improved theories.

	CLASSICAL SOLUTION		IMPROVED SOLUTION	
Degrees	W x 10^{-6} in.	u_ϕ x 10^{-7} in.	w	u_ϕ
1	0.43883	-0.04775	0.44149	-0.04824
2	0.41630	-0.09150	0.41716	-0.09208
3	0.38742	-0.13061	0.38735	-0.13112
4	0.35498	-0.16449	0.35436	-0.16487
6	0.28614	-0.21575	0.28502	-0.21578
8	0.21900	-0.24546	0.21781	-0.24516
10	0.15847	-0.25586	0.15742	-0.25530
12	0.10708	-0.25021	0.10625	-0.24950
14	0.06584	-0.23220	0.06524	-0.23143
16	0.03475	-0.20551	0.03435	-0.20478
18	0.01321	-0.17364	0.01294	-0.17300
20	0.00087	-0.13964	-0.00010	-0.13911
22	-0.00609	-0.10599	-0.00626	-0.10558
24	-0.00706	-0.74550	-0.00723	-0.74240
26	-0.00483	-0.04641	-0.00499	-0.04620
28	-0.00164	-0.02185	-0.00176	-0.02173
30	0.00000	0.00000	0.00000	0.00000

Fig. 4-6a :

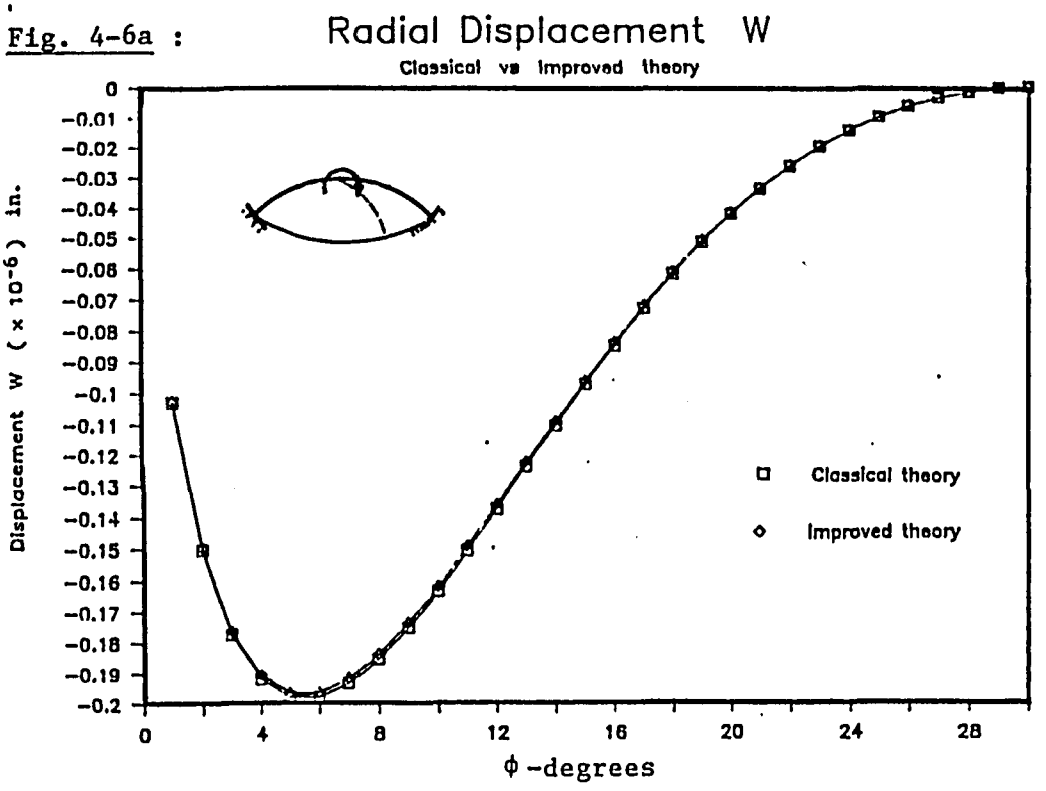

Fig. 4-6b :

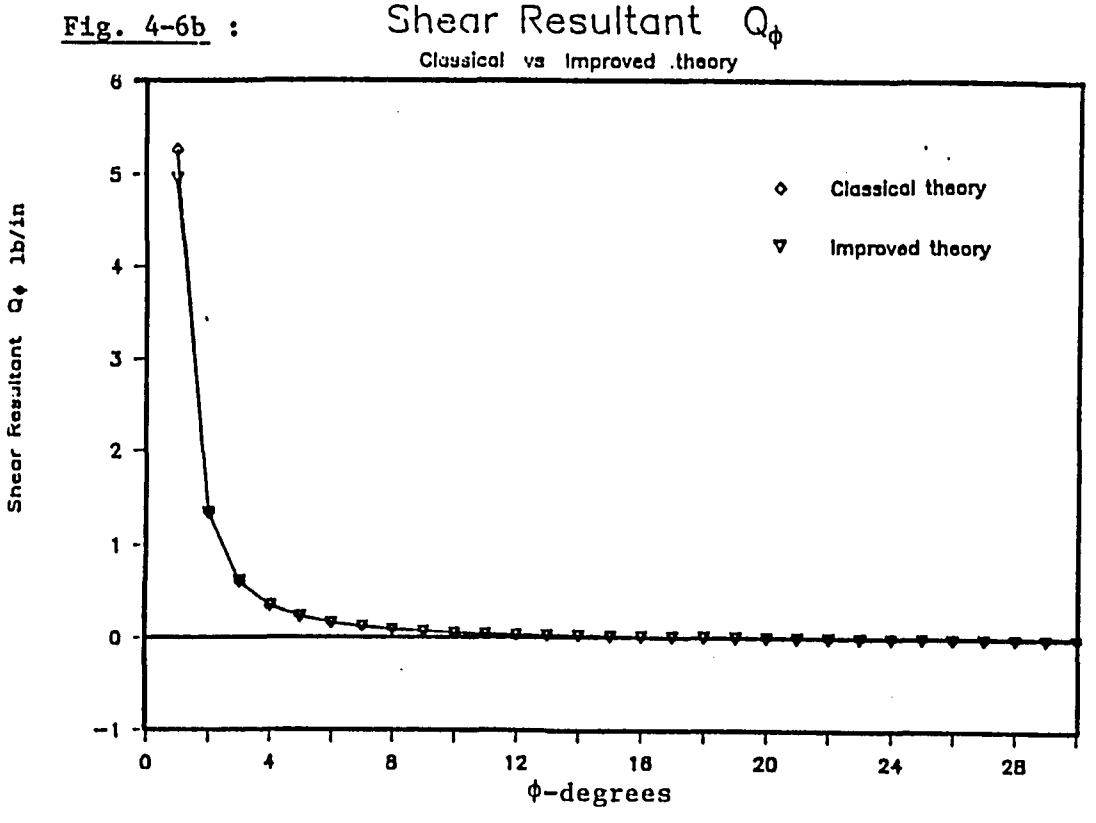

Fig. 4-6c :

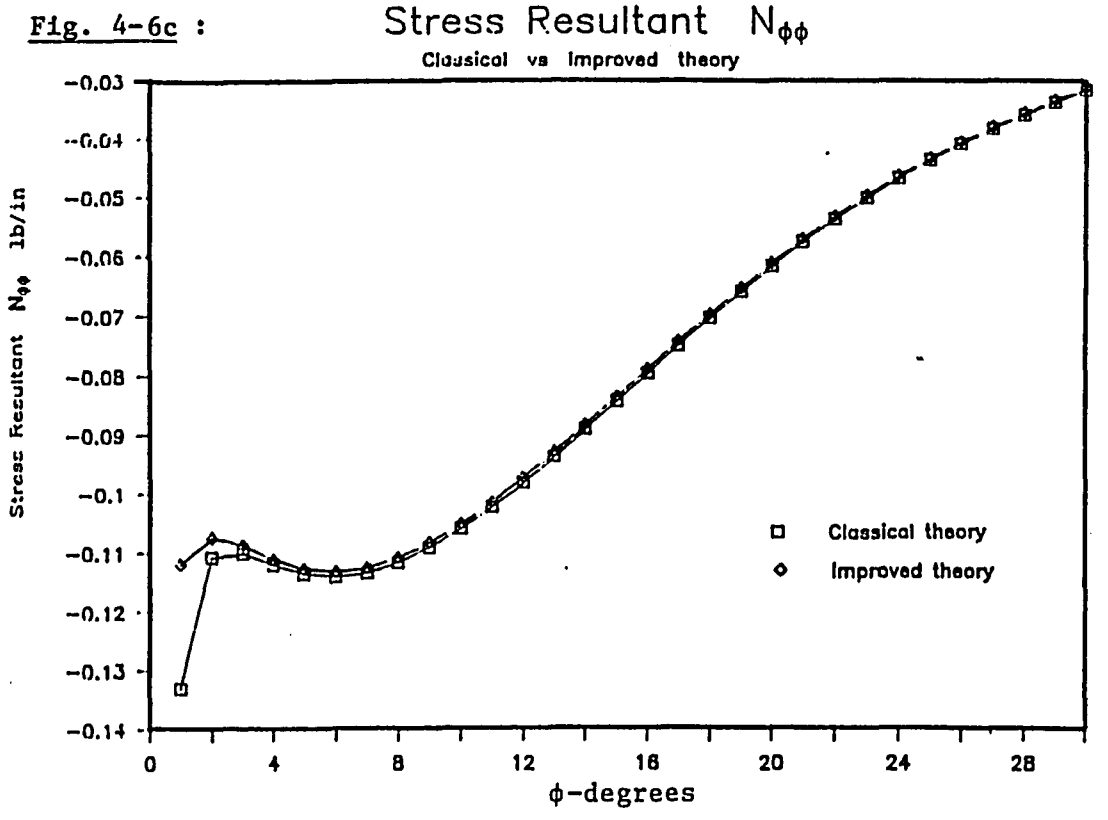

Fig. 4-6d :

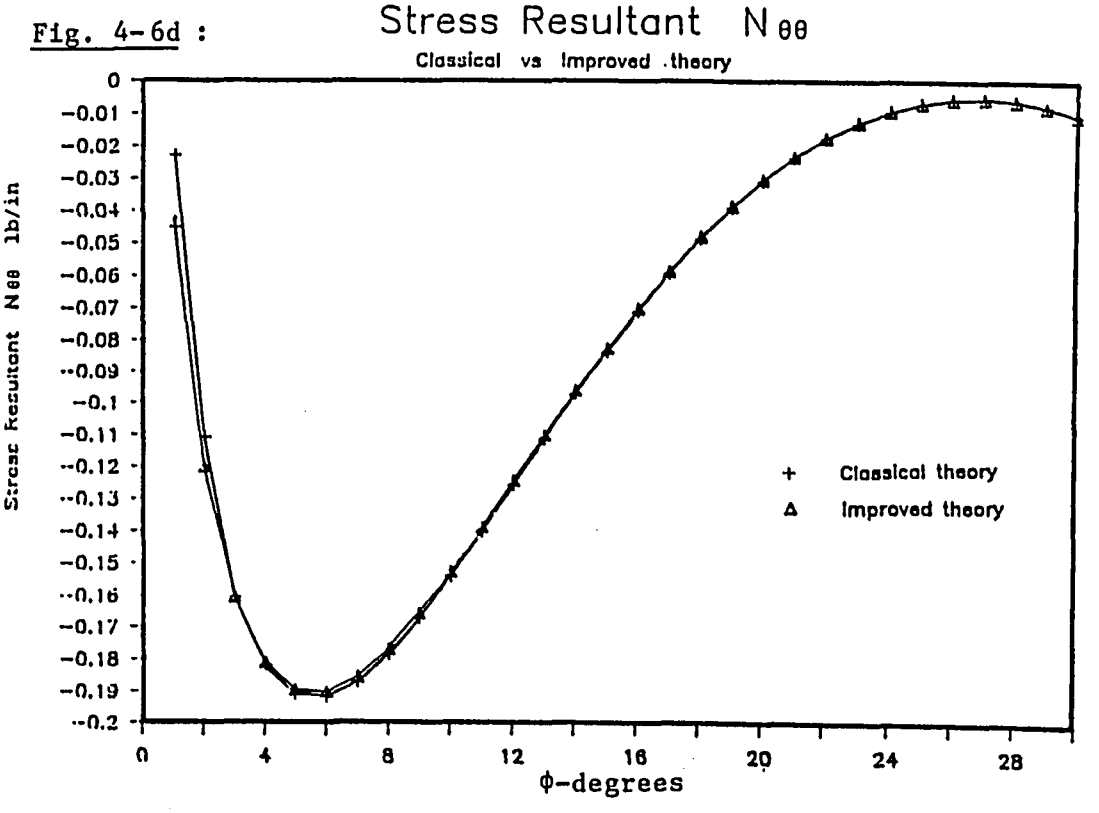

Fig. 4-6e :

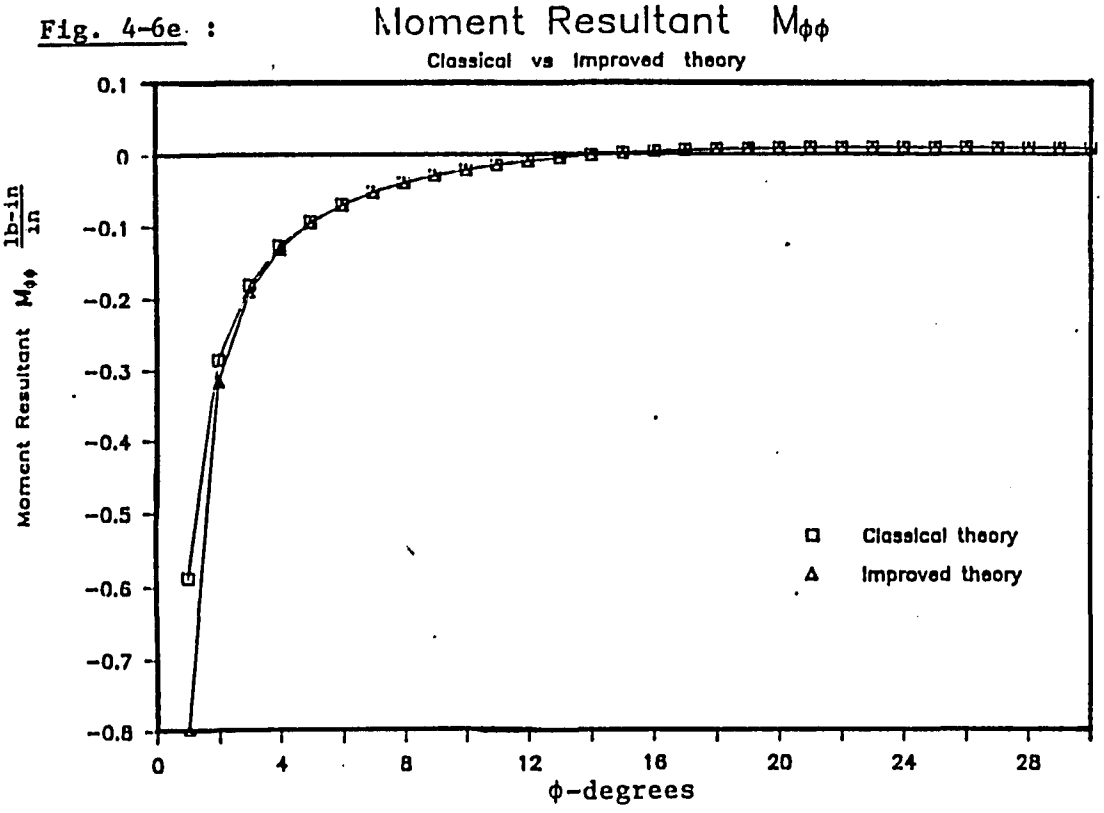

Fig. 4-6f :

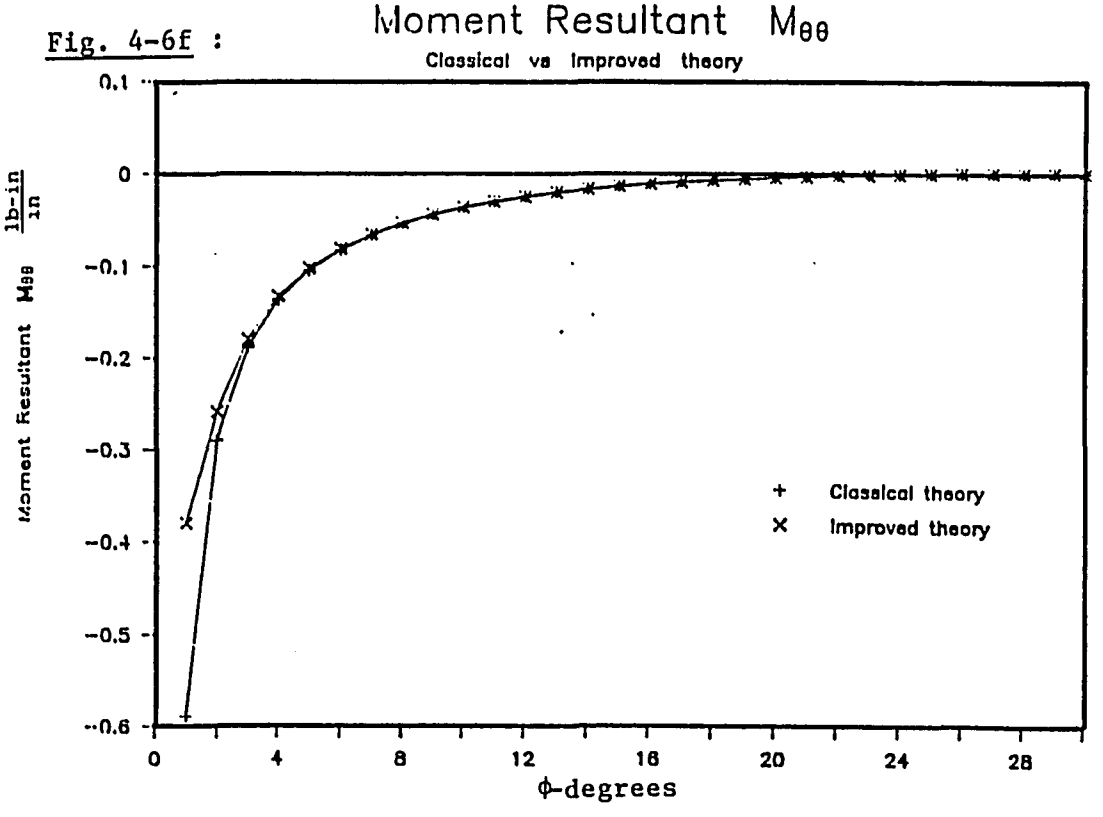

Fig. 4-6g : Radial and Meridional Displacements

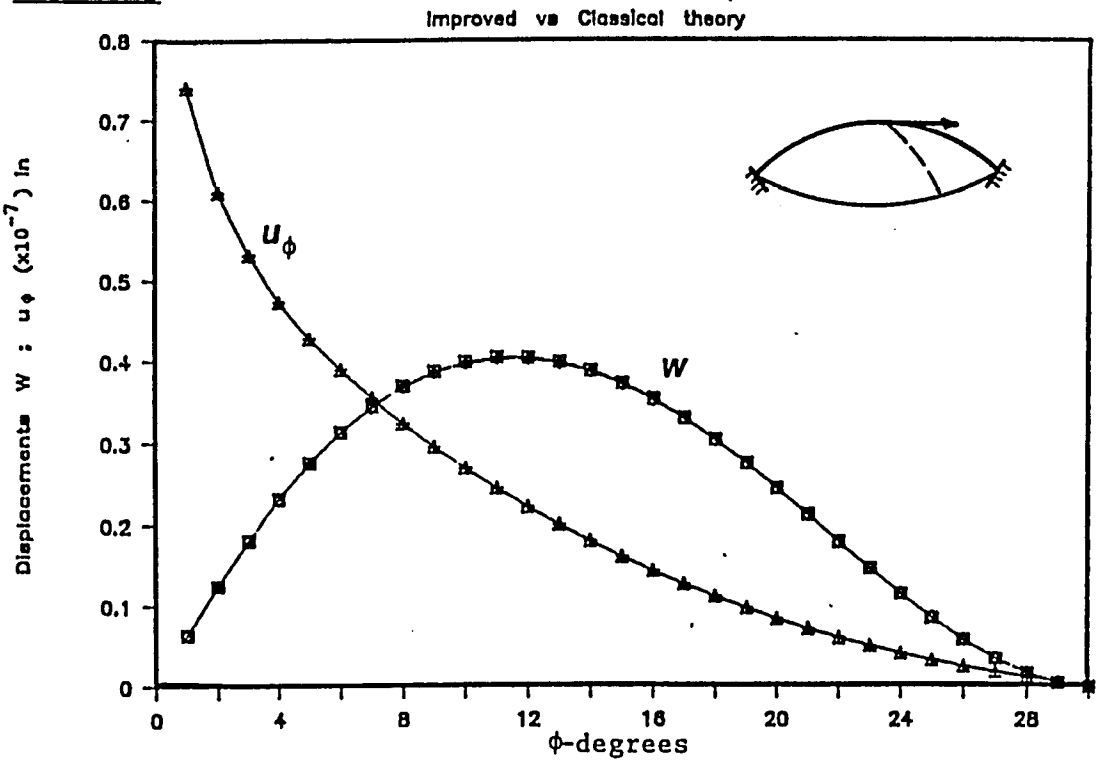

Fig. 4-6h : Shear Resultant Q_ϕ

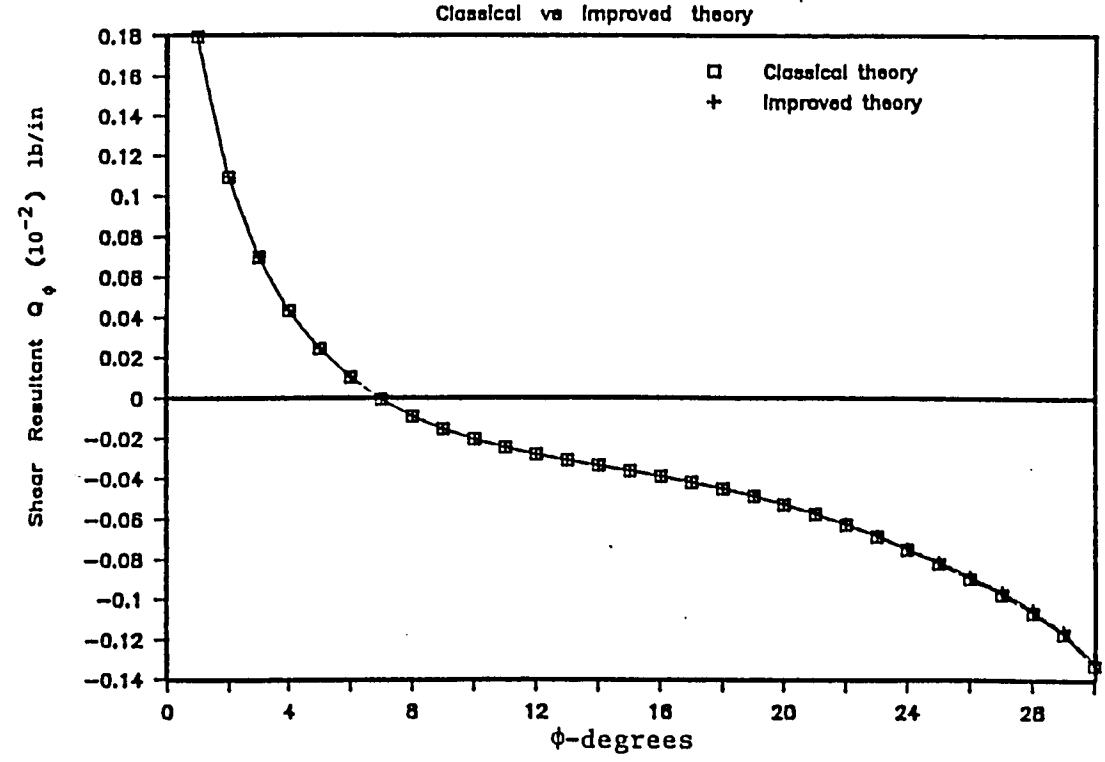

Fig. 4- 6i :

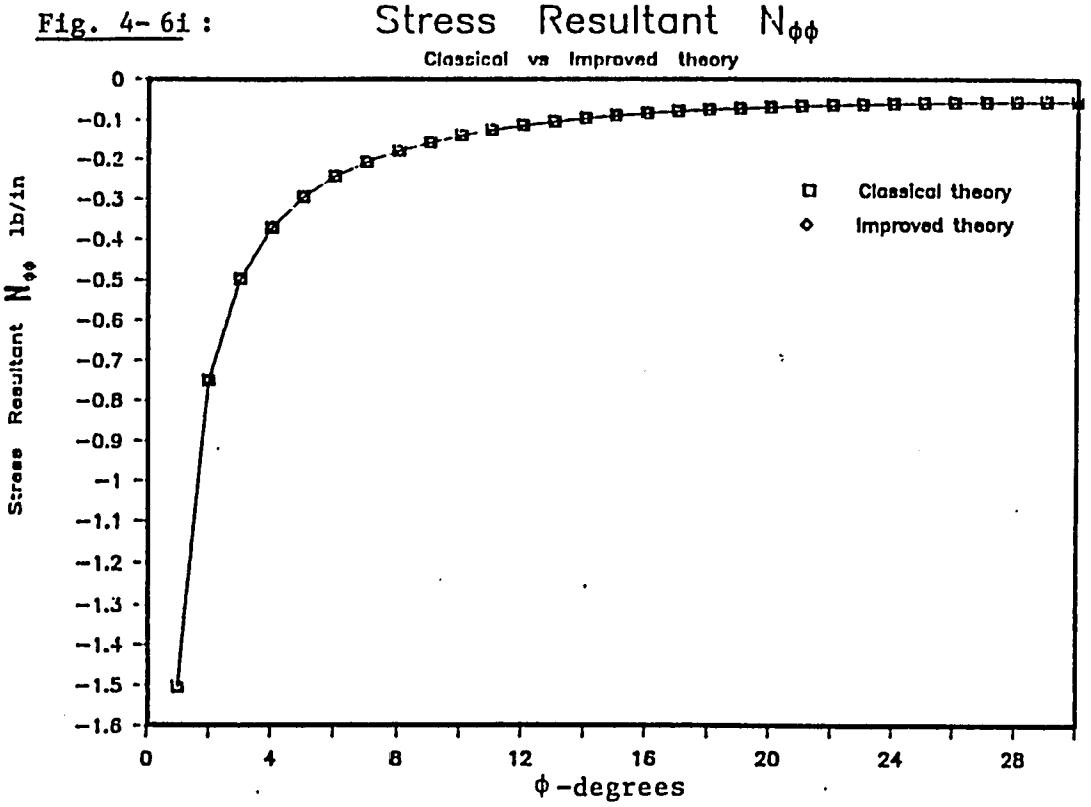

Fig. 4- 6j :

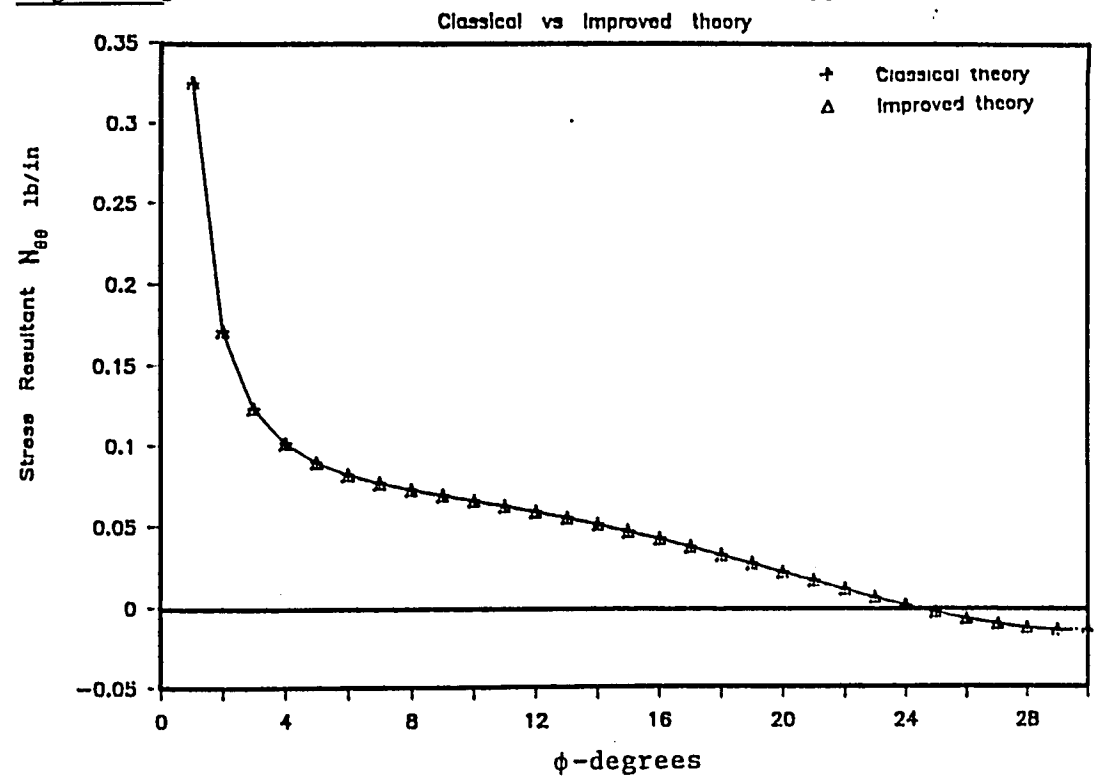

Fig. 4-6k : Moment Resultant $M_{\phi\phi}$

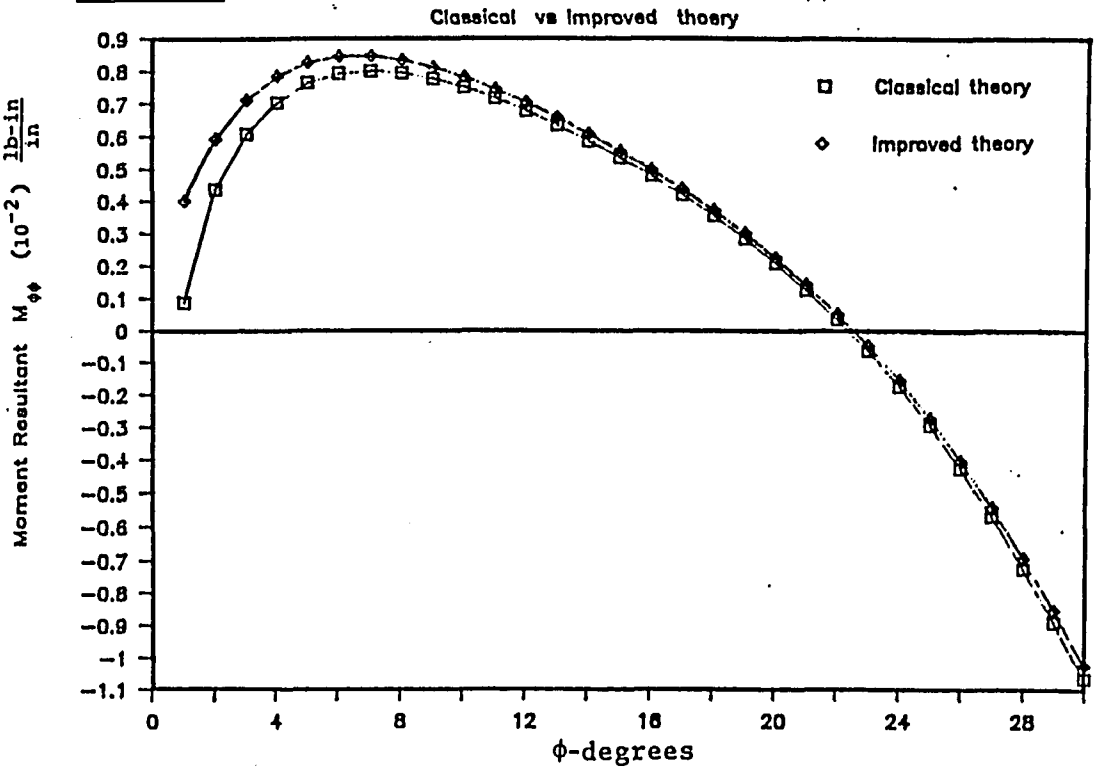

Fig. 4-6l : Moment Resultant $M_{\theta\theta}$

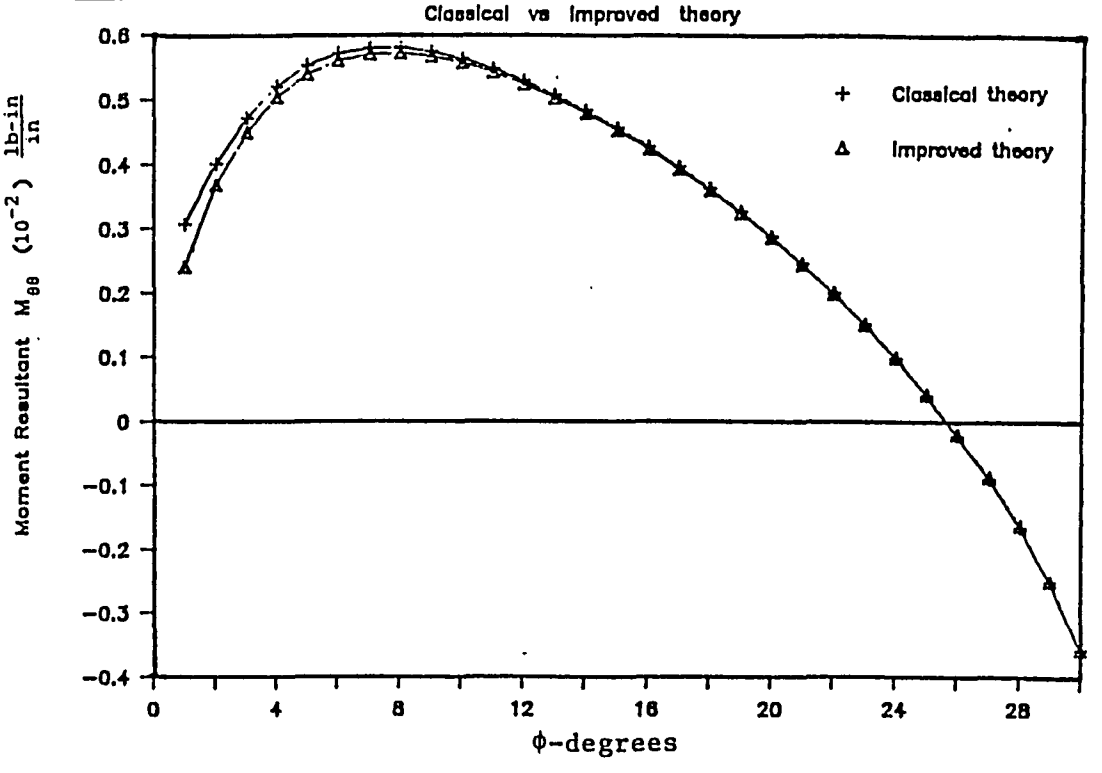

The differences in the response of the shell between the two theories are primarily due to the character of the singularities in the corresponding kernels. We recall the behavior of the shell under the action of a point load predicted by the different theories: The classical theory approach predicts that the vicinity of the load is in compression while the improved theory predicts tension for the same region. Consequently the transverse displacement function W experienced logarithmic singularity at the point of application for the improved analysis. The remaining stress and displacement variables, for the case of the normal load, contained the same order of singularity in their expressions. From the numerical tabulation in Table 6-6, we observe the differences in the displacement values. The remaining field variables presented identical distribution throughout the shell domain.

For the case of a concentrated moment, the radial displacement results are identical, see Fig. 4-6a, while the stress and moment resultants differ considerably in the vicinity of the singular load, see Fig. 4-6b to 4-6g. We focus attention at Fig. 4-6b displaying the transverse shear resultant Q_{ϕ}. The classical analysis predicts a very strong singular character of the order $(1/\gamma^2)$ while the improved theory introduces a logarithmic singularity in the kernel. Fig. 4-6b clearly indicates that the classical theory value is higher than the one obtained by the improved analysis.

Comparison of the response of the shell under the action of a concentrated tangential load, see Fig. 4-6h to 4-6l, reveals that

except for the two moment resultants $M_{\phi\phi}$ and $M_{\theta\theta}$, the results are almost identical. The incorporation of the transverse shear into the mathematical model seems to have a profound influence on the bending solution which is dominant in the neighborhood of the concentrated excitation. As it has been clearly indicated by the comparative results for all three types of loading, the membrane solution is almost uneffected by the the incorporation of the shear effect into the analysis.

It should be stated that our intentions, in this close examination and comparison of the solutions of the two theories, are to justify the correctness of the singular solutions of the improved theory. To that extend, we believe that the mathematical formulation of our investigation indeed led to the correct form of the singular solutions. The domain of application of the different theories, however, cannot be deduced from the above evaluation but rather from a two-directional approach that considers physical reasoning at the vicinity of the singularity as well as implementation of the effect of the boundary constraints. In addition, it should be stated that, in general, is not clear as to which of the two theories describes the shell field more accurately. The most distinct deviations are expected to appear along boundaries and their vicinities with free edge conditions and especially when stress concentration is a dominant issue.

IV.7 THE PROBLEM OF THE EFFECT OF AN OPENING ON THE STRESS AND DISPLACEMENT FIELDS. COMPARISON OF CLASSICAL, IMPROVED AND FINITE ELEMENT ANALYSES.

In the problem that follows, the effect of a circular opening with free edge conditions onto the stress and displacement field, is studied. Special attention is paid on the stress and displacement distribution over the free edge. We are interested in the comparison of the classical and improved theory results at the free edge because of the different assumptions utilized by the two theories. We recall that the classical theory analysis introduces the Kirchoff's effective shearing resultants and it is reasonable to expect greater differences than the ones encountered so far.

We consider a spherical shell bounded by two parallel circles, see Fig.4-7, and subjected to a point load acting along the outward normal. Along with the two theories the above shell problem is also evaluated with the finite element analysis.

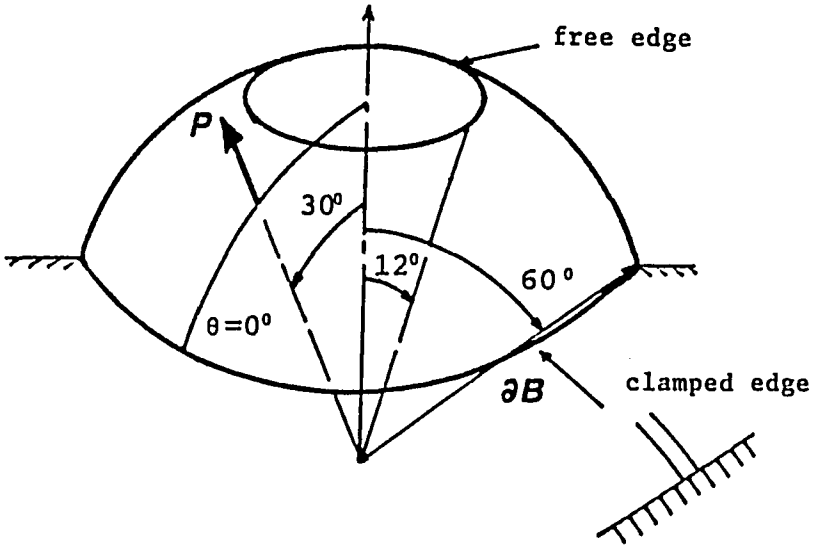

Figure 4-7. A spherical shell with two boundaries (one clamped and one free) subjected to a point load.

Fig. 4-7b : Radial Displacement ($\theta = 0°$)

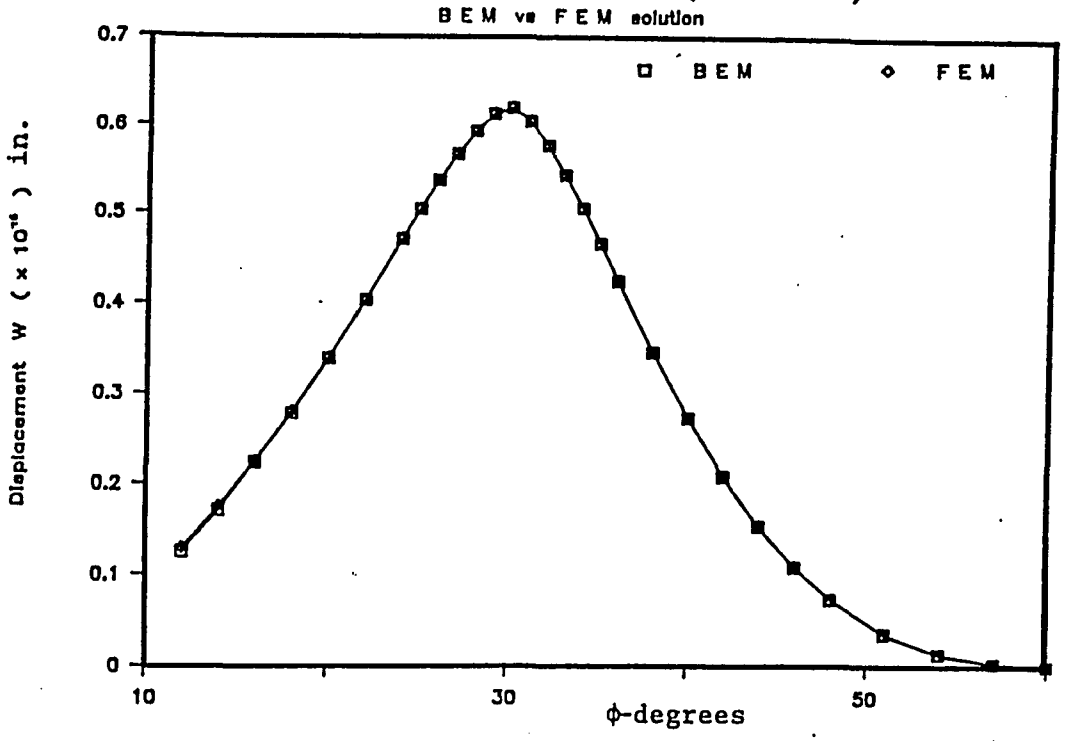

Fig. 4-7c : Meridional Displacement u_ϕ ($\theta = 0°$)

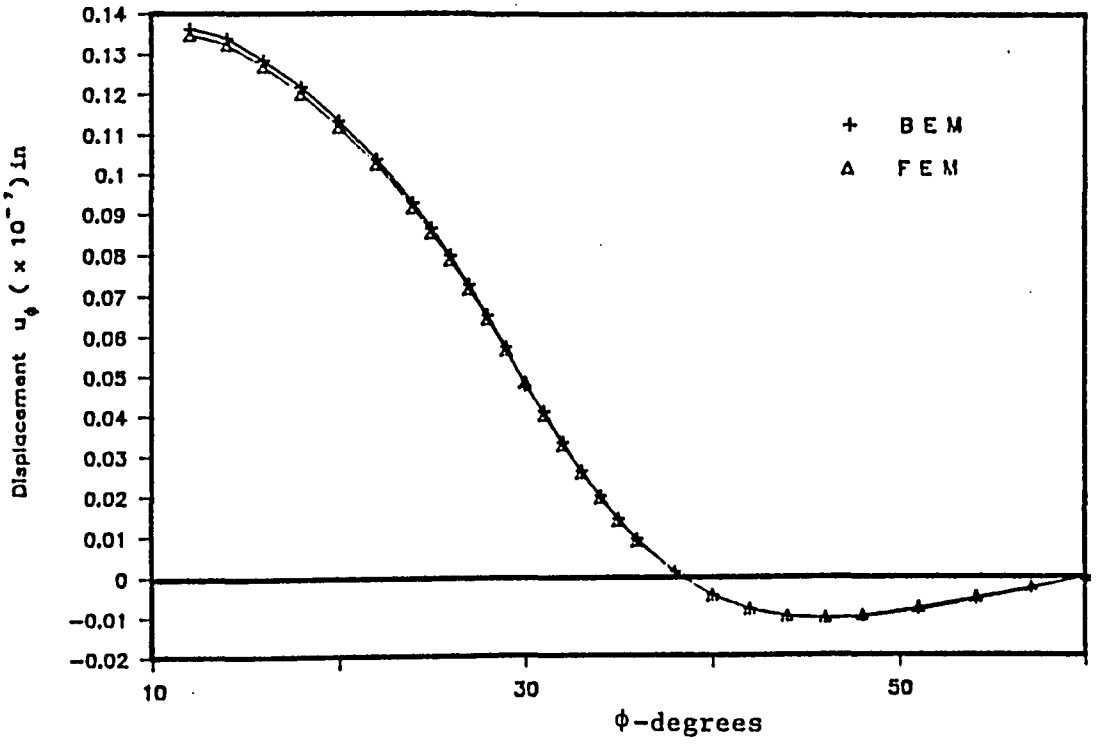

Fig. 4-7d : Stress Resultant $N_{\phi\phi}$ ($\theta = 0°$)

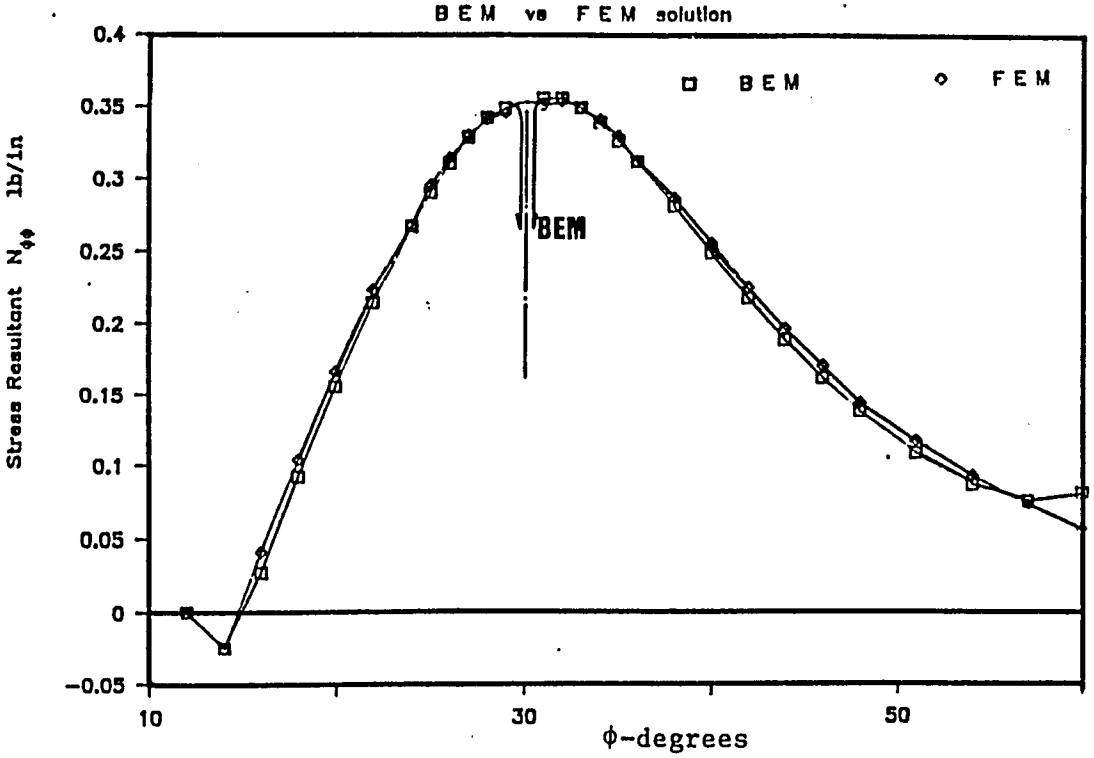

Fig. 4-7e : Stress Resultant $N_{\theta\theta}$ ($\theta = 0°$)

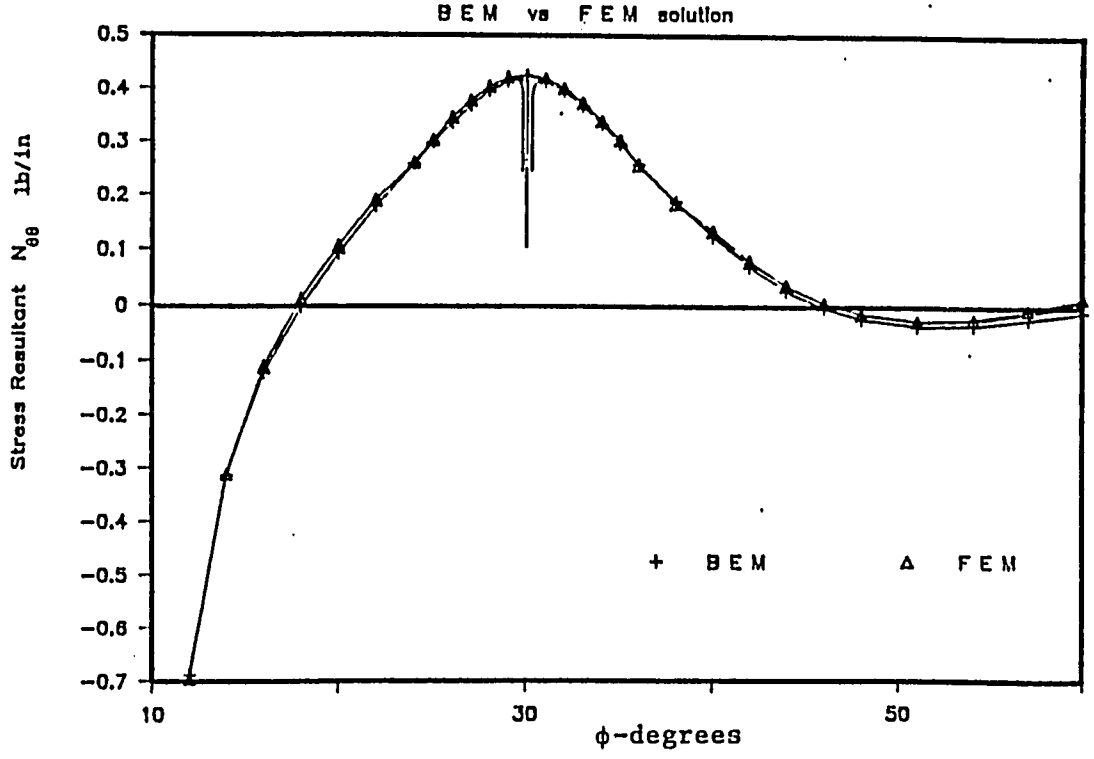

Fig. 4-7f : Moment Resultant $M_{\phi\phi}$ ($\theta = 0°$)

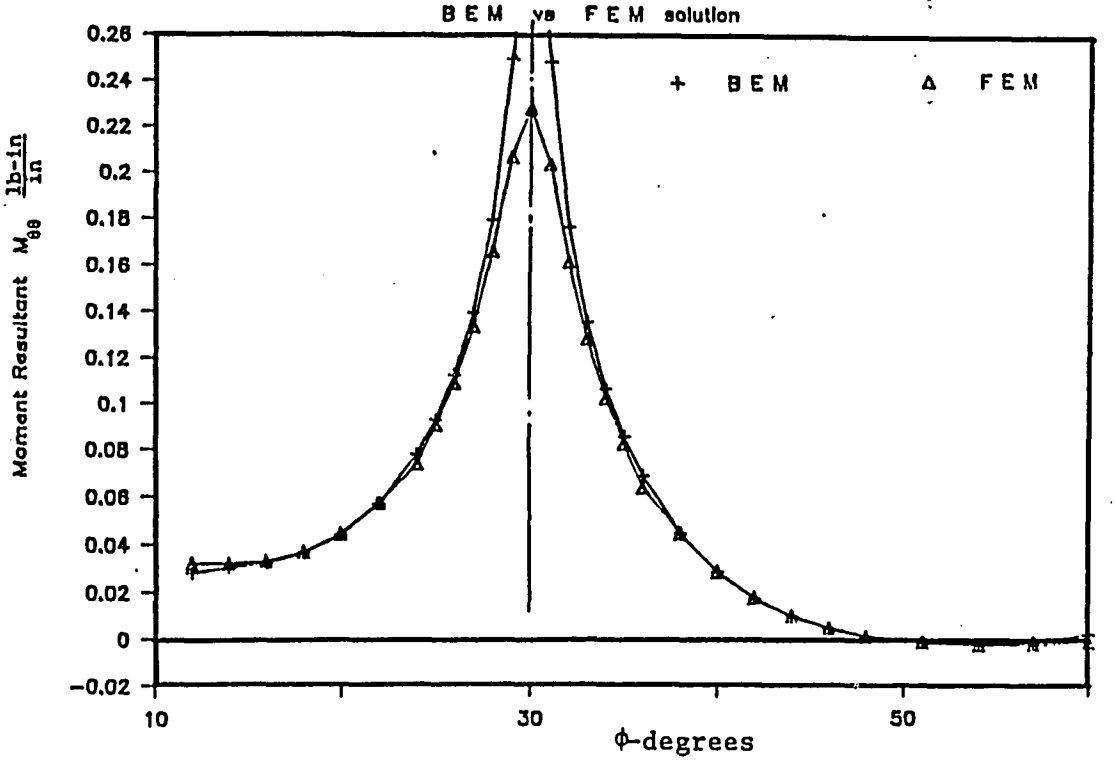

Fig. 4-7g : Moment Resultant $M_{\theta\theta}$ ($\theta = 0°$)

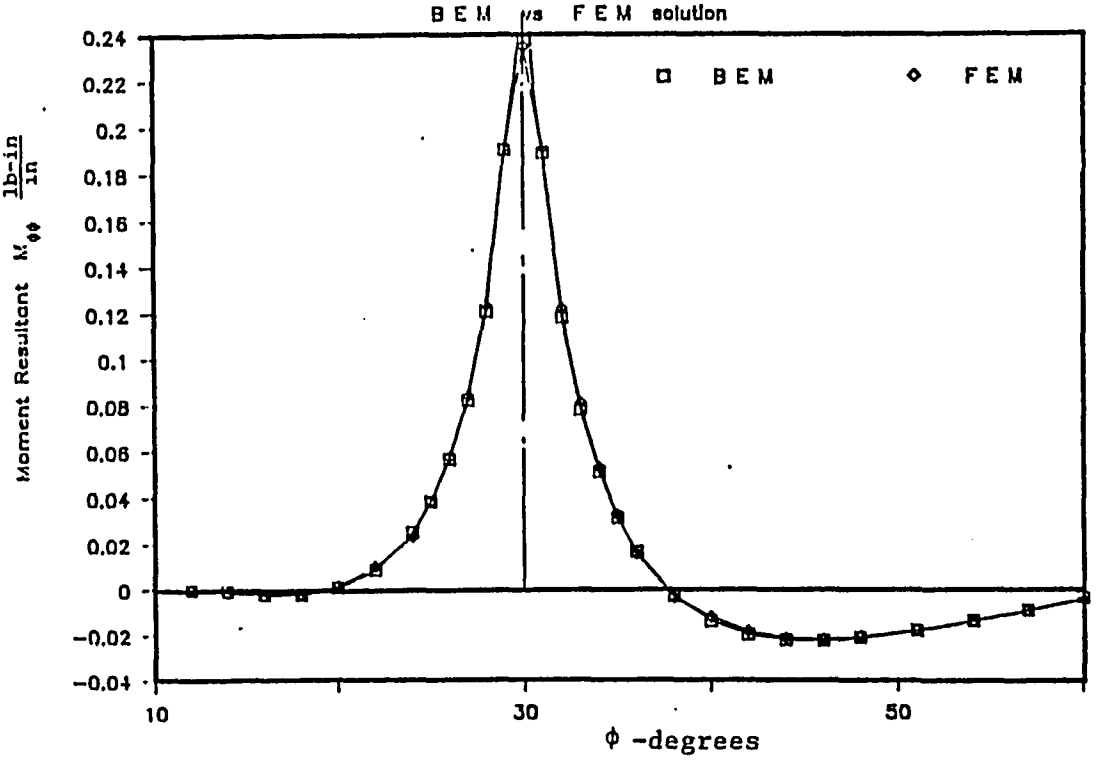

Fig. 4-7h : Radial Displacement W . (ϕ = 12°)

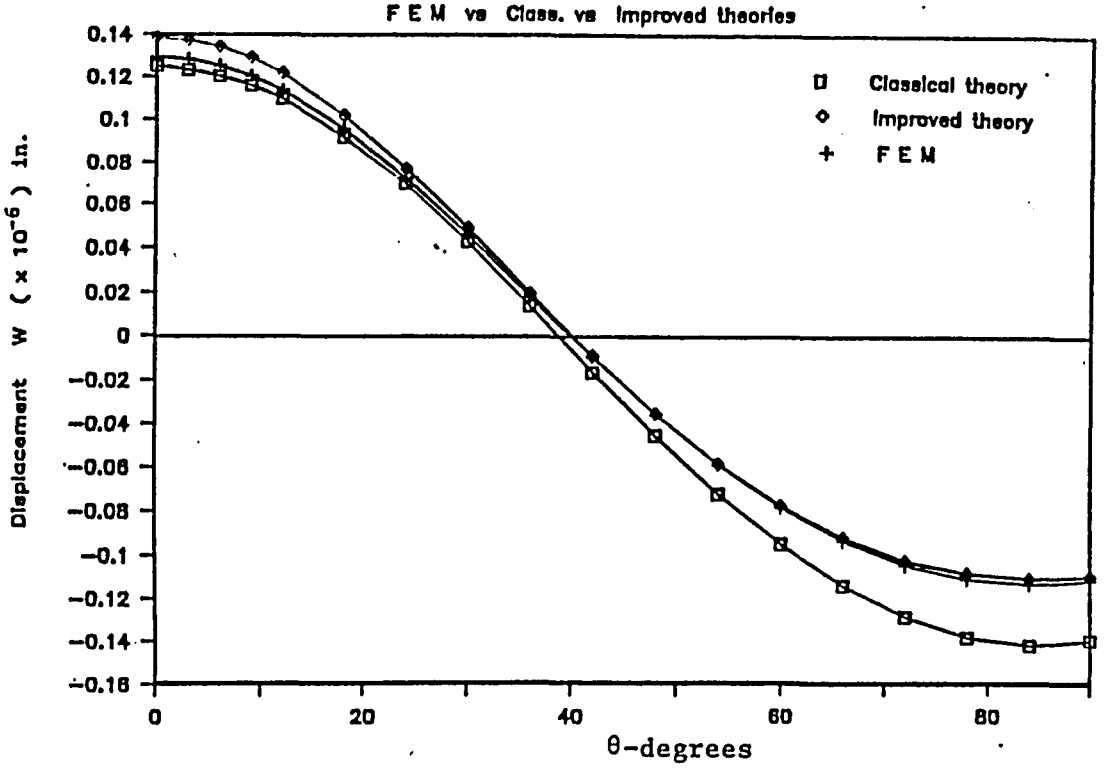

Fig. 4- 7i : Meridional Displacement u_ϕ (φ = 12°)

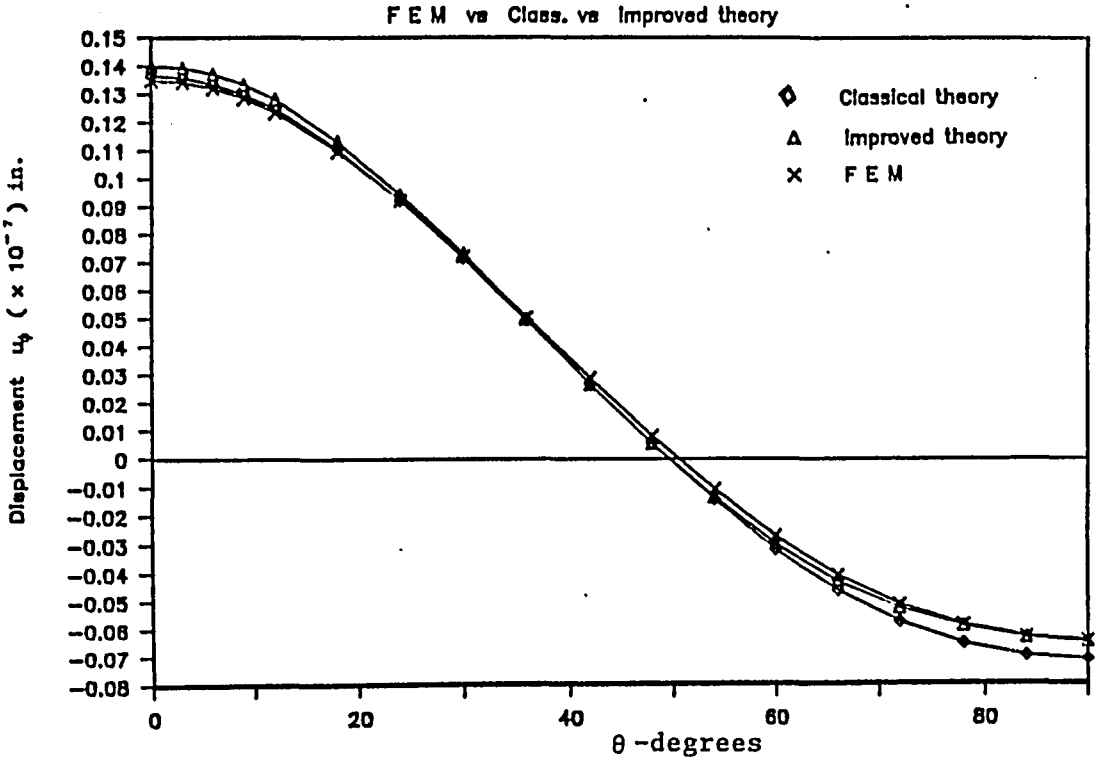

Fig. 4- 7j : Tangential Displacement ($\Phi = 12°$)

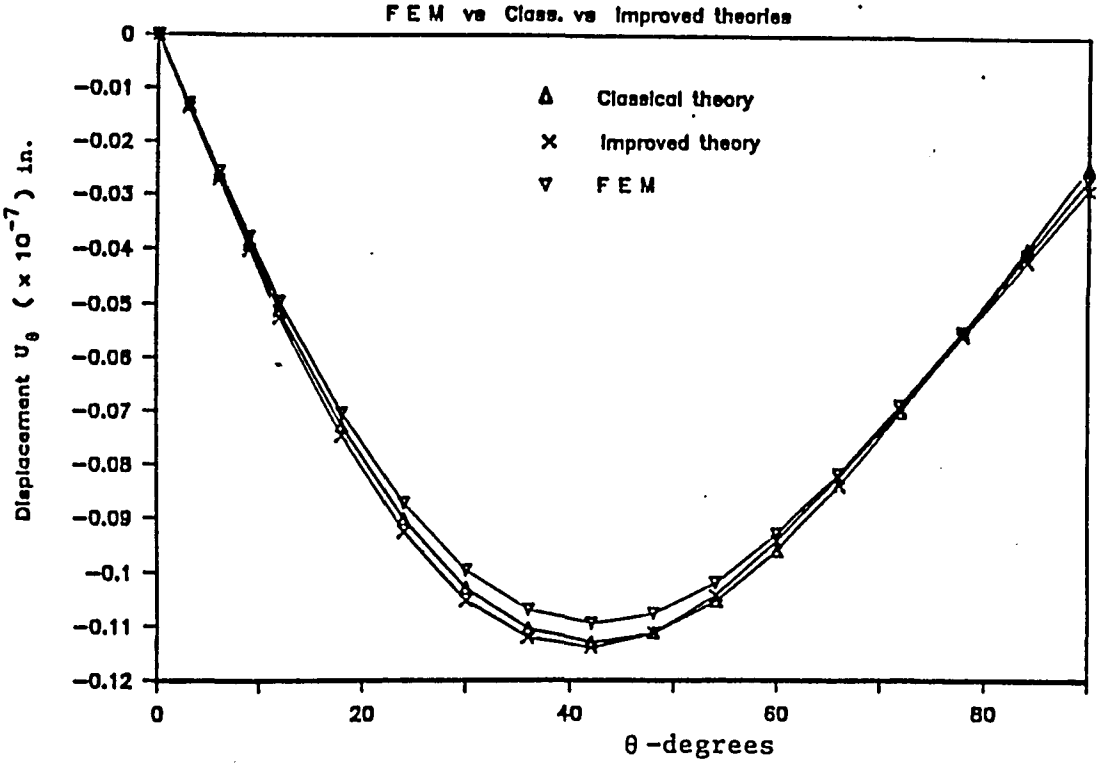

Fig. 4-7k : Stress Resultant $N_{\theta\theta}$ ($\phi = 12^\circ$) lb/in

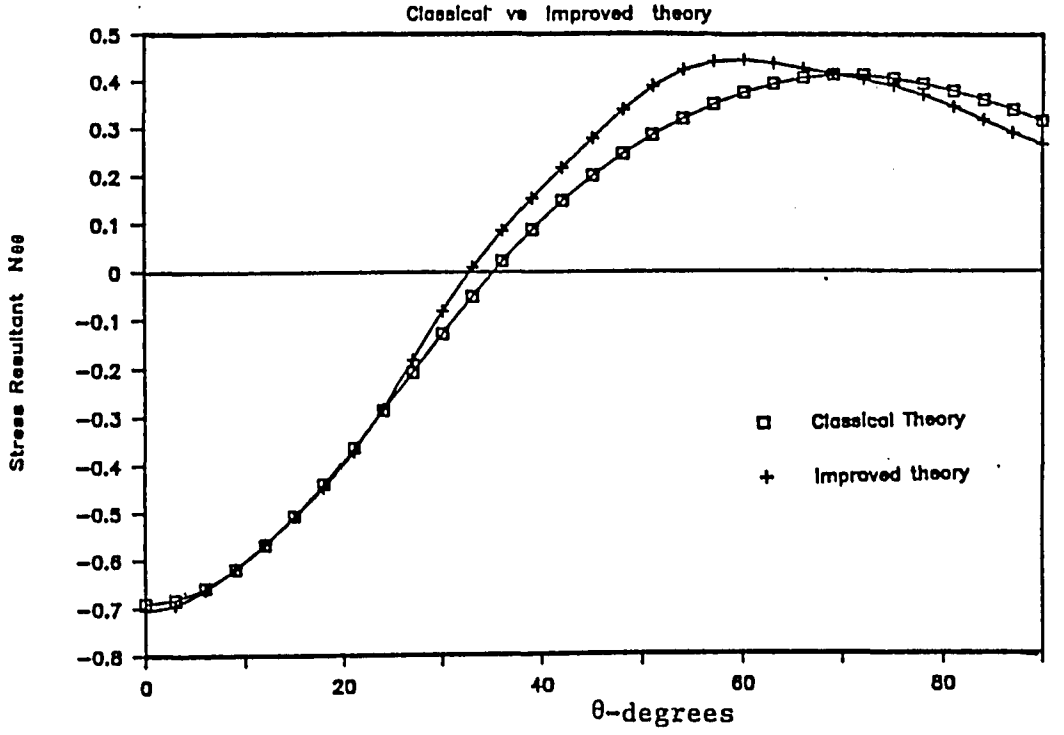

In Fig. 4-7b to 4-7g the stress and displacement fields produced by the classical analysis, along $\theta = 0^{o}$, is plotted and compared with the corresponding finite element results. The differences between the two approaches are of no significant value in that region, except for the behavior of the stress and moment resultants near the load point. In the vicinity of the load the stress and moment resultants of the Boundary Integral analysis are unbounded while the finite element results for the same variables are finite. We focus attention on the results obtained along the free edge. Fig. 4-7h to 4-7j present a comparison of the displacement field along the circular free edge for the two shell theories and the finite element analysis. The striking differences occur in the radial displacement results shown in Fig. 4-7h. It is observed that in the part of the contour nearer to the point load there is excellent agreement between the classical and the finite element solutions. In the same region the improved theory predicts higher values for the displacement. However, as we move along the contour the classical theory results deviate from their finite element counterparts which in turn coincide with those of the improved theory. The apparent behavior is the result of the Kirchoff's effective shearing resultants introduced along the edge. In Fig. 4-7k the nonvanishing stress resultant $N_{\theta\theta}$ is compared for the two theories. The difference in the behavior of the above variable is indicative of the important role that boundary constraints play in the response of the shell problem.

IV.8 ON THE PROBLEM OF A SPHERICAL SHELL CONTAINING A THROUGH CRACK

The limits of applicability of the singular solutions and the numerical scheme that has been developed are tested in terms of the solution of the problem described in Fig. 4-8. The choice of the shell parameters are chosen to coincide with those used by Delale F. and Erdogan F.[30]. Their solution was evaluated analytically using the shallow shell theory approach. The shell is of radius R = 10 in., h = 0.489897948 in. and the angular opening of the crack is ϕ_{cr} = 14.1788183°. The above choice sets a/h = 5 (same as in [30]) and the Poisson's ratio is μ = 1/3. We consider the case of the crack surface subjected to uniform membrane loading $N_{\theta\theta} = h\sigma_m$ = 1 lb/in.

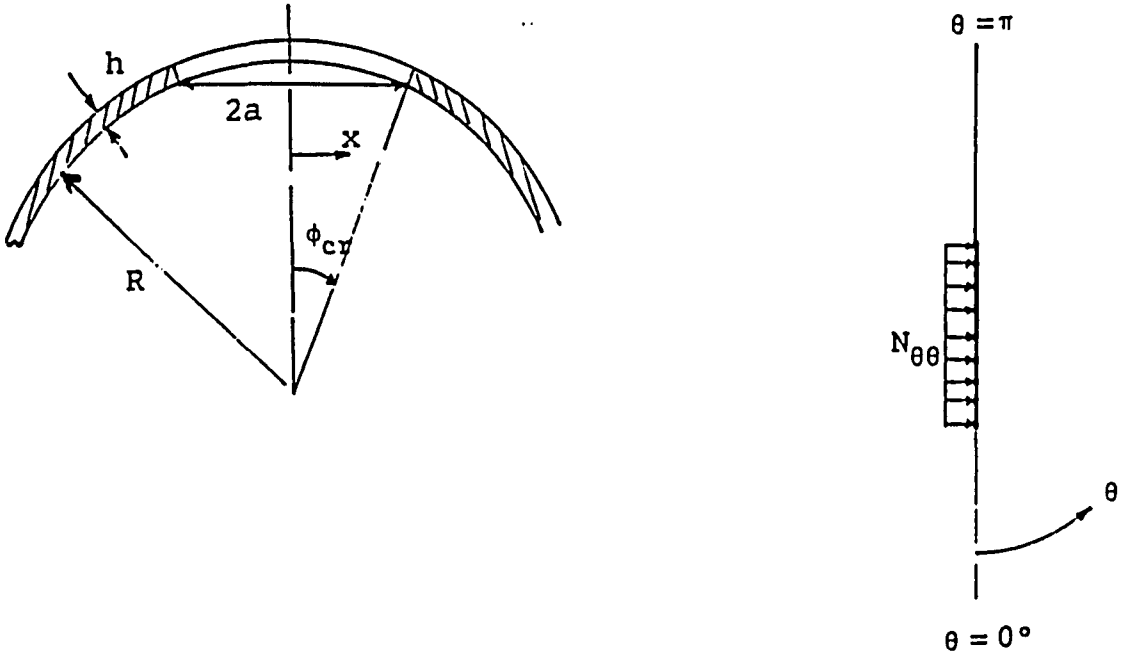

Figure 4-8. A spherical shell with a through crack at the appex. The crack surface is loaded with compressive edge traction.

The IBIM model is described in Fig. 4-8b and it considers a boundary of axisymmetry at $\theta = 0^0$ and $\theta = \pi$. The effect of additional boundary away from the region is eliminated since our interest is focused in the neighborhood of the crack.

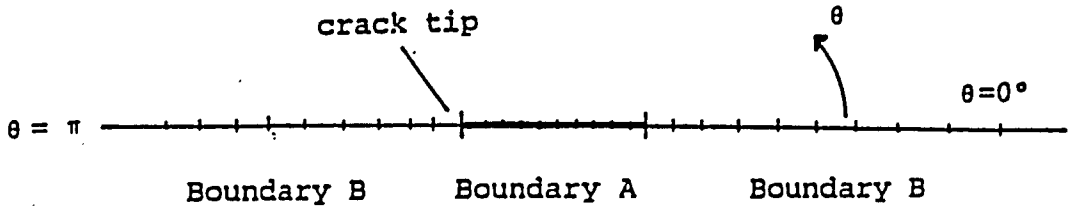

Boundary A : $M_{\theta\theta} = Q_\theta = N_{\phi\theta} = M_{\phi\theta} = 0$, $N_{\theta\theta} \neq 0$

Boundary B : $Q_\theta = N_{\phi\theta} = M_{\phi\theta} = \beta_\theta = u_\theta = 0$

Figure 4-8b. IBIM modeling of the crack region.

The IBIM is capable of describing the displacement and stress fields around and over the crack surface. For reasons of comparison the out-of-plane displacement is evaluated and compared with the results obtained in [30]. Such comparison is given in Fig. 4-8c. According to the shallow solution, the shell bulges out around the crack but at some distance away from the tip the displacement becomes negative. The IBIM results show close agreement with the analytical results with the exception that the displacement turns negative in the vicinity of the crack tip. In order to explore the above deviation, driven by the notion that the crack considered above is big, we considered a very similar problem in which the angular opening of the crack is of $\phi_{cr} = 6^0$. In Fig.4-8d we observe that the displacement turns negative some distance ahead of the crack tip.

Figure 4-8c : Out-of-plane crack surface displacement

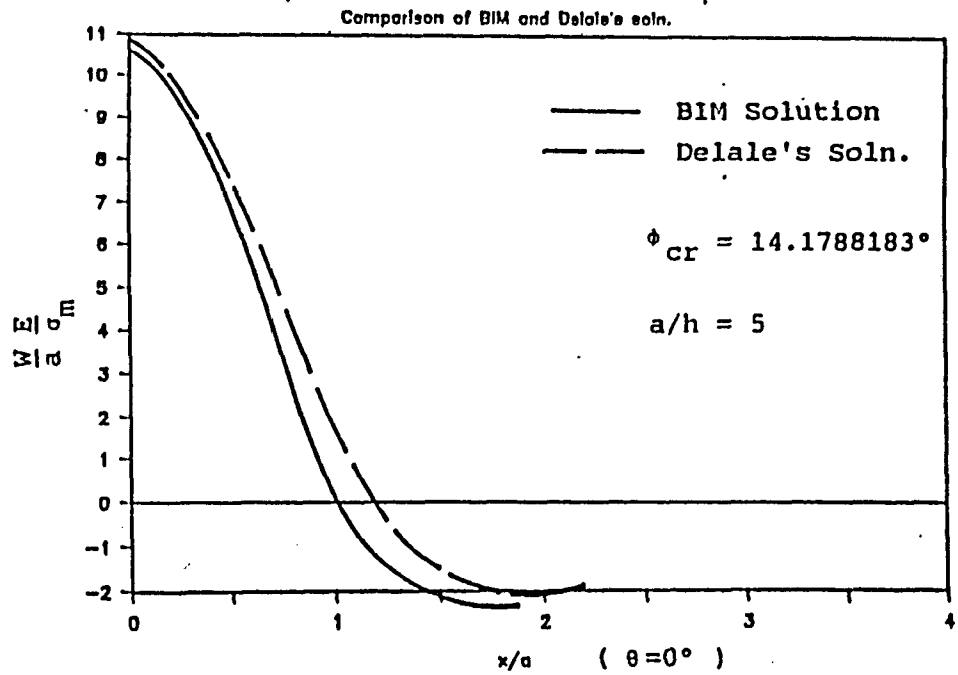

Figure 4-8d: Radial Displacement of the Crack Region

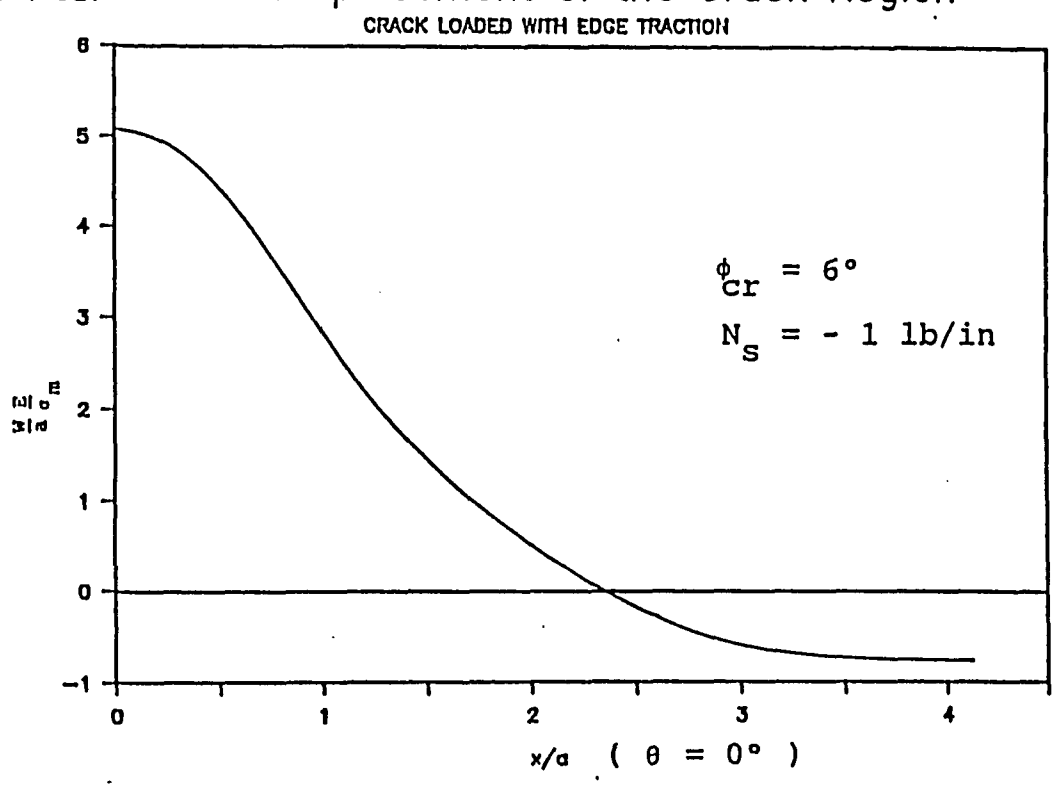

It should be noted that the above evaluation utilized the same IBIM routine, used to evaluate all the previous problems, and introduced no additional parameters that would either imply or incorporate the presense of a crack tip. Because it is expected that the stress distribution near the crack tip have asymptotic character, we evaluated the stress resultants in that region in order to see how sensitive the routine in understanding the presense of a singular stress field. Fig. 4-8e demonstrates that the IBIM approach indeed provides the expected asymptotic behavior.

Figure 4-8e : Stress Resultant $N_{\phi\phi}$ near crack tip

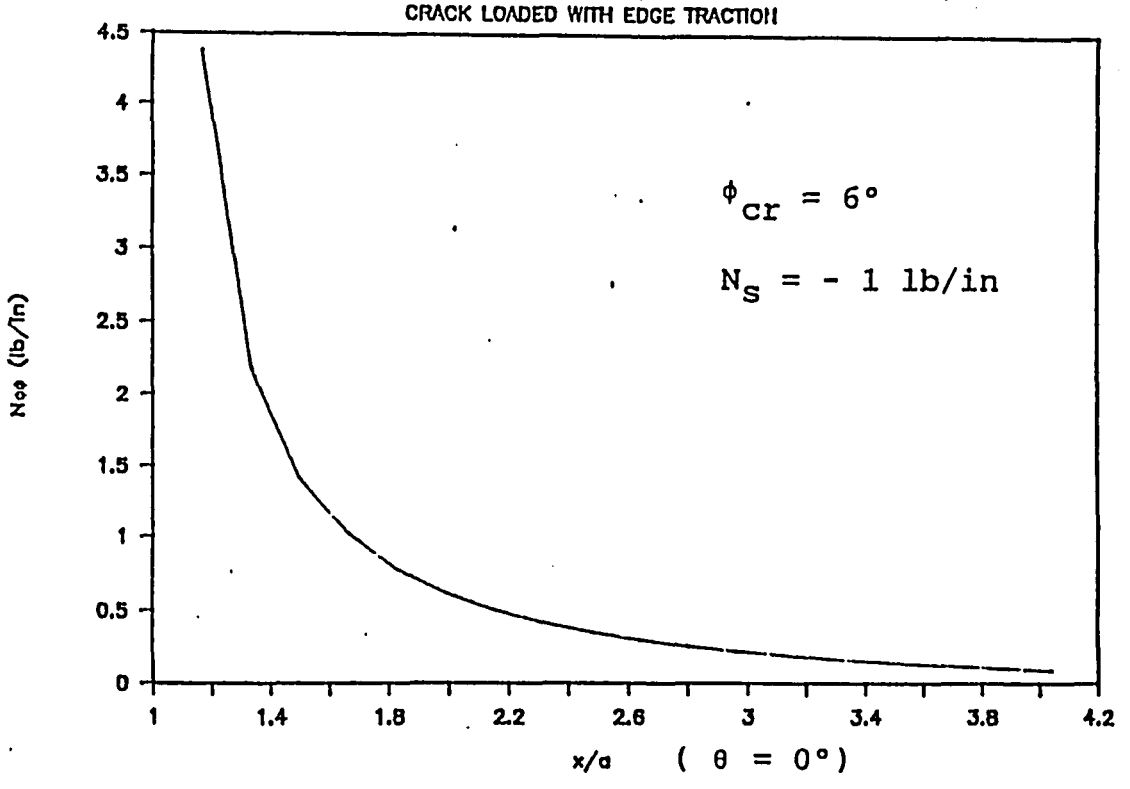

IV.9 EFFECT OF THE "FICTITIOUS" BOUNDARY ON THE NUMERICAL EVALUATION

Except for the crack problem where closed-form singular integrations were performed over the boundary elements, in all previous problems, the Boundary Integral model incorporated the idea of the "fictitious" boundary to avoid integration over singular points. We should recall that the shear resultant kernels of the classical theory, for the cases of concentrated moments and tangential forces, display a non-integrable singularity of the order ($\frac{1}{\gamma^2}$) and as a consequence of that approximate integration techniques need to be utilized.

From the mathematical point of view, for as long as the actual and fictitious boundaries do not intersect and a one to one point relationship exists, the position of the fictitious boundary is irrelevant. However, since a discrete number of points represent the complete boundary, the position of the auxiliary boundary ∂B_f indeed effects the problem solution inside the real domain. We also expect that the number of boundary elements effects the accuracy of the final solution. To observe the variations of the solution inside the real domain introduced by the number of elements and the position of the fictitious boundary, we considered a clamped spherical cap subjected to a point load $P = 1$ lb at the appex and tabulated the values of the displacement components as well as the circumferential stress resultant and stress couple at various points inside the domain. These values are compared with the corresponding finite element solution. From the results presented in Tables 4-7 and 4-8,

in which N refers to the number of elements and $\Omega = \pi/40$ represents the angular distance of the position of the auxiliary boundary from the real one, we observe that the variation of the position is more critical than the variation of the number of boundary elements.

Table 4-7. Effect of the fictitious boundary and the number of boundary elements on the displacement solution of a spherical shell problem. IBIM and FEM comparison.

N	ΔB^*	6°	12°	18°	24°	30°
		W($\times 10^{-6}$ in)				
40	Ω	.2831	.10456	.01154	-.00770	.000
	$\frac{3}{2}\Omega$	.28786	.10842	.01399	-.00687	.000
	2Ω	.29516	.11440	.01783	-.00550	.000
30	Ω	.28340	.10495	.01195	-.00742	.000
	$\frac{3}{2}\Omega$	.28790	.10855	.01412	-.00677	.000
	2Ω	.29520	.11445	.01787	-.00547	.000
FEM	Solution	.2961	.1152	.01831	-.00534	.000
		u ($\times 10^{-7}$ in)				
40	Ω	-.2144	-.2479	-.1711	-.07279	.000
	$\frac{3}{2}\Omega$	-.2165	-.2514	-.1748	-.07516	.000
	2Ω	-.2196	-.2568	-.1807	-.07900	.000
30	Ω	-.2146	-.2484	-.1718	-.07370	.000
	$\frac{3}{2}\Omega$	-.2165	-.2515	-.1750	-.07540	.000
	2Ω	-.2196	-.2568	-.1807	-.07910	.000
FEM	Solution	-.2199	-.2574	-.1814	-.07950	.000

Table 4-8. Effect of the fictitious boundary and the number of boundary elements on the stress solution of a spherical shell problem. IBIM and FEM comparison.

$N_{\theta\theta}$ lb/in

N	ΔB^*	6°	12°	18°	24°	30°
	Ω	.2138	.0497	-.0148	-.000168	.02660
40	$\frac{3}{2}\Omega$	.2200	.0548	-.0113	.00220	.02932
	2Ω	.2293	.0628	-.00567	.0032	.03123
	Ω	.2142	.0500	-.0145	-.0015	.02294
30	$\frac{3}{2}\Omega$	.2201	.0550	-.01109	.0034	.02835
	2Ω	.2294	.0628	-.00561	.00326	.03123
FEM Soln		.2303	.06310	-.00566	.00303	.03183

$M_{\theta\theta}$ $\frac{\text{ib-in}}{\text{in}}$ $(\times 10^{-1})$

	Ω	.6199	.1231	-.0215	-.0296	.0437
40	$\frac{3}{2}\Omega$	.6222	.1290	-.0197	-.0292	.03727
	2Ω	.6256	.1288	-.0169	-.0284	.03309
	Ω	.6138	.1230	-.0214	-.0291	.05594
30	$\frac{3}{2}\Omega$	.6221	.1254	-.0197	-.0290	.04133
	2Ω	.6256	.1288	-.0169	-.0284	.03423
FEM Soln		.62578	.12909	-.01665	-.0284	.03213

We should emphasize that the FEM numerical results do not correspond to the exact solution and so the tabulated values should not lead to the conlusion that better results, at times, are obtained with less elements over the boundary.

The variation of the number of elements, however, has a far more drastic effect in the amount of computational time needed for the evaluation of a particular problem. Because the system matrix of the boundary integral model is always fully populated and its size is determined according to the scheme (4N x 4N) or (5N x 5N), an increase in the number of elements does not translate into linear increase of the respective computer time but in a rather exponential type change. Thus, for the sample problem used earlier we record the following CPU times associated with the boundary subdivisions:

ELEMENTS	CPU sec.
20	62
30	108
40	256

CHAPTER V

CLOSURE

V.1 CONCLUSIVE REMARKS AND FUTURE DEVELOPMENTS

A new derivation of the singular solutions of the nonshallow theory of spherical shells and the development of the corresponding Indirect Boundary Integral Method has been presented. The undertaking of such effort was very much influenced by the fact that better mathematical descriptions of the the actual physical problems, when utilized in numerical routines, can provide a very close approximation to the exact solution. The BIM indeed satisfies the above statement since its mathematical model is derived directly from the exact governing differential system. Its implementation requires the existence of the field singular solutions. In the area of shell theory, and spherical shell in particular, many previous works have focused on the action of concentrated forces and moments. The complexity of the governing differential system, however, limited their application to arbitrary shell problems and as a result the number of complete solutions is minimal.

It was our intention to obtain the mathematical model of the response of a spherical shell under the influense of surface unit excitation and further to utilize the mathematical solution into an efficient

numerical scheme. Our approach in satisfying the goals of the proposed research consisted of two major steps.

The closed-form singular solutions, Green's functions, for a self equilibrated complete spherical shell were obtained in Chapter II, where the complete mathematical analysis is presented. In the process of the derivation we were able to evaluate and discuss the differences of the two shell theories, classical and improved, and draw a clear picture of the intricacies associated with their application on physical shell problems. Thus, complete singular solutions for the case of concentrated unit normal load, unit tangential load and concentrated surface moment are derived in closed form.

Secondly, the unique character of the derived singular solutions, direct consequence of the self-equilibration requirement to which they are attached, was utilized in the Indirect Boundary Integral numerical scheme that is presented in Chapter III. The particular formulation of IBIM, new in the area of shell theory, was designed to facilitate a number of different classes of problems that could arise within the framework of the nonshallow theory of spherical shells. The newly introduced mathematical and numerical formulation was tested and justified in Chapter IV with the solution of a number of representative problems. The comparison of the IBIM with the available analytical solutions as well as numerical solutions, evaluated by using the ANSYS finite element code, have clearly

demonstrated the validity of both, the mathematical and numerical models that we have developed.

We believe that the goals set in proposing the investigation and analysis of the spherical shell problem have been accomplished. The contribution of the work is not solely based on the derivation and construction of the closed-form singular solutions, but also on the designing and formulation of a new very flexible and efficient numerical approach. Even though the static analysis is reasonably complete, future works could utilize the basic principles to include additional effects into the mathematical model of the shell. Such effects, as rotary inertia and thermal interaction, would expand the applicability range of the computational shell theory in the modern technical world. It could be argued that already developed numerical techniques have the ability of solving complex physical problems. We believe, however, that the key characteristics of the Boundary Integral analysis, beeing directly related to the governing differential system and having the ability to reduce the problem dimensions by one, do provide room for the partitipation of its numerical scheme into the computational community of applied mechanics.

V.2 OVERALL COMPARISON OF IBIM AND FEM

It is apparent from the tabulated and plotted numerical data that the agreement between the two numerical schemes is excellent. The differences that occur are concentrated in the vicinity of point

loads. These differences are the direct effect of the singular character of the variable kernels incorporated in the boundary integral analysis. However, we can argue that since the singular solutions utilized are exact, the BIM solution is closer to the actual shell response except for the vicinity of the load point. The above statement was justified by the observation that with finer finite element model the two solutions converged even further. In terms of CPU time, design flexibility and construction of the particular discretization model, we observed the following:

When dealing with an all-around axisymmetric shell problem and requiring a rather quick look at the shell behavior, not considering the complete stress matrix, FEM analysis seems to be more efficient since it is evaluated with the use of conical element. However, when all around axisymmetry is no longer present and in addition detailed study of the response is required, the BIM is far superior in terms of model construction, CPU time and design flexibility. This is primarily due to the fact that the bulk of the work in the BIM analysis is concentrated in the treatment of the boundary of the shell problem. It would be unfair to compare the CPU times involved in a strict form because the two analyses were evaluated in different computer operating systems. Nevertheless, a rough estimation of the CPU time required by both approaches revealed that for the case of all around axisymmetry, FEM required only 54 sec while IBIM used about 108 sec for a 30-element boundary. The picture was drastically reversed when instead of the axisymmetric conical elements, quadrilateral shell elements were used in the construction of the

finite element model. The CPU time of FEM climbed to 34 minutes while the IBIM used the same amount of CPU time. The approximate ratio of the speed of the two operating systems is about 4:1 in favor of the system running the IBIM code.

APPENDIX A

GOVERNING EQUATIONS OF THE MIDDLE SURFACE OF A THIN NONSHALLOW SPHERICAL SHELL

In the following, the system of governing equations for a thin spherical shell is deduced for both the classical as well as the improved theory of shells. The improved theory incorporates the effect of the transverse shear into the analysis.

The well known basic equations of equilibrium of the shell element are the same for both theories and they are recorded in this section. The primary system of equations is reduced, following the procedure of Berry[19] for the classical theory, to a secondary system of two equations governing the transverse displacement W and an auxiliary function, while the same primary system will be reduced, using Prasad's[25] approach for the improved theory, to a secondary system of three uncoupled equations associated with the transverse displacement W and two auxiliary variables.

A-1 THE EQUILIBRIUM OF A SHELL ELEMENT

Consider a spherical shell defined by the coordinate system (ϕ,ϑ), shown in Fig. A-1, with Young's modulus E, Poisson's ratio μ, thickness h and middle-surface radius R. An element separated from

the shell with the positive convention of the displacements and the element stress and moment resultants is shown in Fig. A-1.

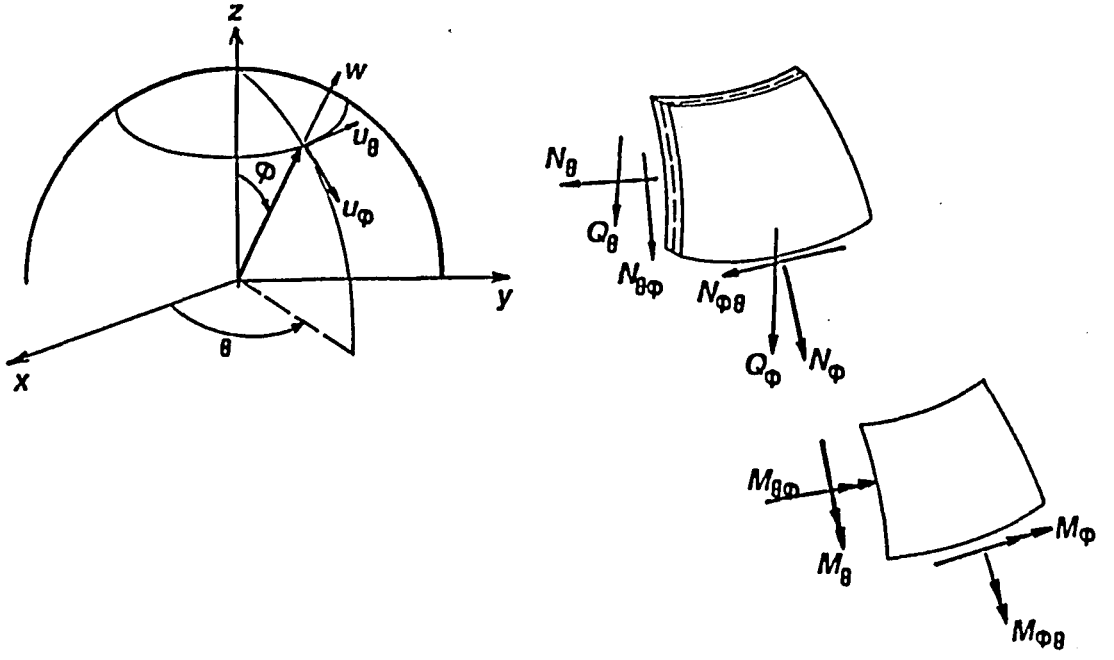

Figure A-1. Geometry of a spherical surface and orientation of the shell element variables.

The equations of equilibrium of the shell element may be written in the form :

$$\frac{1}{R}\left(\frac{\partial N_\phi}{\partial \phi} + Q_\phi + \cot\phi\,(N_\phi - N_\theta) + \csc\phi\,\frac{\partial N_{\phi\theta}}{\partial \theta}\right) + q_\phi = 0$$

$$\frac{1}{R}\left(\frac{\partial N_{\phi\theta}}{\partial \phi} + 2\,N_{\phi\theta}\cot\phi + \csc\phi\,\frac{\partial N_\theta}{\partial \theta} + Q_\theta\right) + q_\theta = 0 \qquad \text{(A.1)}$$

$$\frac{1}{R}\left(\frac{\partial Q_\phi}{\partial \phi} + \cot\phi\,Q_\phi - (N_\phi + N_\theta) + \csc\phi\,\frac{\partial Q_\theta}{\partial \theta}\right) + q_n = 0.$$

The above relations express the condition that the resultant vector of all internal and external forces acting on the element of the shell must vanish.

The condition for the vanishing of the resultant moment leads to the following relations :

$$\frac{1}{R}\left(\frac{\partial M_{\phi\theta}}{\partial\phi} + 2\,M_{\phi\theta}\cot\phi + \csc\phi\,\frac{\partial M_{\theta}}{\partial\theta}\right) - Q_{\theta} = 0$$

$$\frac{1}{R}\left(\frac{\partial M_{\phi}}{\partial\phi} + (M_{\phi} - M_{\theta})\cot\phi + \csc\phi\,\frac{\partial M_{\phi\theta}}{\partial\theta}\right) - Q_{\phi} = 0 \qquad \text{(A.2)}$$

While the relation

$$N_{\phi\theta} - N_{\theta\phi} + \frac{1}{R}(M_{\phi\theta} - M_{\theta\phi}) = 0 \qquad \text{(A.3)}$$

is identically satisfied as a result of the symmetry of the stress tensor (that is, $\tau_{12} = \tau_{21}$, where τ corresponds to the shear stress) which, for the case of a spherical shell, implies that $N_{\phi\theta} = N_{\theta\phi}$ and $M_{\phi\theta} = M_{\theta\phi}$.

The stress variables in Eqs. (A.1)-(A.3) are defined as:

N_{ϕ}, N_{θ}, $N_{\phi\theta}$ are the membrane stress resultants;

M_{ϕ}, M_{θ}, $M_{\phi\theta}$ are the moment resultants and

Q_{ϕ}, Q_{θ} are the transverse shear resultants.

Finally, q_{ϕ} , q_{θ} and q_{n} are the components of the external force vector along the ϕ, θ and normal directions respectively.

By confining ourselves to the linear theory of thin shells, we can express the components of displacement of an arbitrary point of the shell in terms of the displacement of its corresponting point on the middle surface according to the relations,

$$u_\phi(\zeta) = u_\phi + \zeta\ \beta_\phi$$
$$u_\theta(\zeta) = u_\theta + \zeta\ \beta_\theta \qquad \text{(A.4)}$$
$$W(\zeta) = W + c\ (\ \zeta\ W' + \frac{1}{2}\ \zeta^2\ W''\ )$$

where u_ϕ, u_θ and W are the components of the displacement vector in ϕ, θ and normal directions respectively of a point on the reference surface, W' and W'' are derivatives of ζ and they represent contributions to a nonvanishing transverse normal strain, β_ϕ and β_θ are the angular displacements of the normal to the middle surface, ζ is the distance from the middle surface and c is a tracer that takes the value of $c = 0$ for the classical theory and the value of $c = 1$ for the improved theory. For the classical theory where the transverse shearing strains $\gamma_{\phi n}$ and $\gamma_{\theta n}$ are neglected, the angular displacements β_ϕ and β_θ can be expressed in terms of the displacement variables in the form

$$\beta_\phi = \frac{1}{R}\ (\ u_\phi - \frac{\partial W}{\partial \phi}\ )$$
$$\beta_\theta = \frac{1}{R}\ (\ u_\theta - \csc\phi\ \frac{\partial W}{\partial \theta}\ ). \qquad \text{(A.5)}$$

The above relations do not hold in the improved theory analysis where β_ϕ and β_θ remain independent of the displacement functions. In addition, for thin shells, the tracer $c = 1$ of the improved theory can be set equal to zero implying that the effect of the transverse normal stress is neglected (in other words, $W' = W'' = 0$), while the effect of the transverse shear is retained.

The strain functions can be calculated from the displacement relations (see Love[31]) and take the form

$$\epsilon_\phi = \frac{1}{R}\left(\frac{\partial u_\phi}{\partial \phi} + W \right)$$

$$\epsilon_\theta = \frac{1}{R}\left(\csc\phi \frac{\partial u_\phi}{\partial \theta} + u_\phi \cot\phi + W \right) \qquad \text{(A.6)}$$

$$\epsilon_{\phi\theta} = \frac{1}{R}\left(\frac{\partial u_\theta}{\partial \phi} - u\theta \cot\phi + \csc\phi \frac{\partial u_\phi}{\partial \theta} \right)$$

while the curvature functions k_ϕ , k_θ and τ are expressed in terms of the angular displacements and given by

$$k_\phi = \frac{1}{R}\frac{\partial \beta_\phi}{\partial \phi}$$

$$k_\theta = \frac{1}{R}\left(\csc\phi \frac{\partial \beta_\theta}{\partial \theta} + \cot\phi\, \beta_\phi \right) \qquad \text{(A.7)}$$

$$\tau = \frac{1}{R}\left(\frac{\partial \beta_\theta}{\partial \phi} + \csc\phi \frac{\partial \beta_\phi}{\partial \theta} - \cot\phi\, \beta_\theta \right).$$

Between the six deformation variables described by Eqs. (A.6) and (A.7) three differential relations of compatibility exist. The one relation utilized in this analysis is recorded below and is written in the form

$$\frac{\partial}{\partial\phi}\left(\sin\phi\,\frac{\partial\epsilon_{\phi\theta}}{\partial\theta}\right)-\frac{\partial}{\partial\phi}\left(\sin^{2}\phi\,\frac{\partial\epsilon_{\theta}}{\partial\phi}\right)+\frac{\partial^{2}\epsilon_{\phi}}{\partial\theta^{2}}-\sin\phi\cos\phi\frac{\partial\epsilon_{\phi}}{\partial\phi}$$

$$+2\sin^{2}\phi\,\epsilon_{\phi}-\frac{\sin^{2}\phi}{R}\left(\nabla^{2}+2\right)W. \qquad (A.8)$$

Because of the assumption that the shell is thin we can consider the transverse stress σ_{rr} negligible and write the remaining stresses in the form:

$$\sigma_{\phi}=\frac{E}{1-\mu^{2}}\left(\epsilon_{\phi}+\mu\,\epsilon_{\theta}\right)\quad,\quad\sigma_{\theta}=\frac{E}{1-\mu^{2}}\left(\epsilon_{\theta}+\mu\,\epsilon_{\phi}\right)$$

$$\sigma_{\phi\theta}=\frac{E}{2(1+\mu)}\,\epsilon_{\phi\theta}. \qquad (A.9)$$

When the stresses are integrated over the thicness of the shell they yield the various stress and couple resultants expressed as:

$$N_{\phi}=\frac{Eh}{1-\mu^{2}}\left(\epsilon_{\phi}+\mu\,\epsilon_{\theta}\right)\quad,\quad N_{\theta}=\frac{Eh}{1-\mu^{2}}\left(\epsilon_{\theta}+\mu\,\epsilon_{\phi}\right)$$

$$N_{\phi\theta}=\frac{Eh}{2(1+\mu)}\,\epsilon_{\phi\theta} \qquad (A.10)$$

and

$$M_\phi = D\,(\,k_\phi + \mu\, k_\theta\,) \quad , \quad M_\theta = D\,(\,k_\theta + \mu\, k_\phi\,)$$

$$M_{\phi\theta} = \frac{D(1-\mu)}{2}\,\tau \tag{A.11}$$

where D denotes the stiffness constant defined by

$$D = \frac{Eh^3}{12(1-\mu^2)}\,. \tag{A.12}$$

The changes of curvature k_ϕ , k_θ and twist τ can be expressed as

$$k_\phi = k_\phi^0 + \frac{\epsilon_\phi}{R} \quad , \quad k_\theta = k_\theta^0 + \frac{\epsilon_\theta}{R}$$

$$\tau = \tau^0 + \frac{\gamma_{\phi\theta}}{R} \tag{A.13}$$

where

$$k_\phi^0 = -\frac{1}{R^2}\left(\frac{\partial^2 W}{\partial\phi^2} + W\right)$$

$$k_\theta^0 = -\frac{1}{R^2}\left(\csc^2\phi\,\frac{\partial^2 W}{\partial\theta^2} + \cot\phi\,\frac{\partial W}{\partial\phi} + W\right) \tag{A.14}$$

$$\tau^0 = \frac{2}{R^2}\csc\phi\left(\cot\phi\,\frac{\partial W}{\partial\theta} - \frac{\partial^2 W}{\partial\phi\,\partial\theta}\right).$$

The above relations yield the following equivalent expressions for the moment resultants

$$M_\phi = D\,(\,k_\phi^0 + \mu\, k_\theta^0\,) + \frac{h^2}{12R}\,N_\phi$$

$$M_\theta = D\,(\,k_\theta^0 + \mu\, k_\phi^0\,) + \frac{h^2}{12R}\,N_\theta \tag{A.15}$$

$$M_{\phi\theta} = \frac{D(1-\mu)}{2} \tau^{0} + \frac{h^2}{12R} N_{\phi\theta}.$$

The resultants of the shear stresses $\sigma_{\phi n}$ and $\sigma_{\theta n}$ which do not vanish in the improved theory analysis will take the form

$$Q_{\phi} = \left[\frac{Eh}{2(1+\mu)k_s^0} \right] \left(\beta_{\phi} + \frac{1}{R} \frac{\partial W}{\partial \phi} \right)$$

$$Q_{\theta} = \left[\frac{Eh}{2(1+\mu)k_s^0} \right] \left(\beta_{\theta} + \frac{1}{R \sin\phi} \frac{\partial W}{\partial \theta} \right) \qquad \text{(A.16)}$$

where k_s^0 is an averaging shear coefficient that results from the parabolic representation of the shear stresses over the shell thickness. It can assume the value of 5/6 obtained by Reissner[3] for the improved theory of plates and was confirmed by Naghdi[6] for the improved theory of shells. We should note that in the classical theory analysis the integrals of the stresses $\tau_{\phi n}$ and $\tau_{\theta n}$, which have been neglected within the framework of the theory, will result to nonvanishing shearing stress resultants Q_{ϕ} and Q_{θ}. The apparent contradiction is explained based upon the satisfaction of the equilibrium of the shell element. Thus, the representation of such resultants will be derived directly from the equilibrium equations (A.1) and (A.2).

A-2 REDUCTION OF THE SYSTEM OF EQUATIONS

A-2a CLASSICAL THEORY

We consider a spherical shell domain subjected only to normal surface traction q_n. Within the scope of this analysis the rotations of the normal to the middle surface vector $\underset{\sim}{n}$ denoted as β_ϕ and β_θ will be expressed in terms of the components of dispacement vector. This implies that the uknown variables of the system reduce by two, which in turn reduce the order of the governing differential system also by two. Their dependance onto the displacement functions is demonstrated by Eqs. A.5. When the appropriate expressions of the moment resultants are introduced into the moment equilibrium relations, yield the form of the shearing stress resultants which are given by

$$Q_\phi \left(1 + \frac{h^2}{12R^2} \right) = - \frac{D}{R^3} \frac{\partial}{\partial \phi} \left(\nabla^2 + 2 \right) W$$

$$Q_\theta \left(1 + \frac{h^2}{12R^2} \right) = - \frac{D}{R^3} \frac{1}{\sin\phi} \frac{\partial}{\partial \theta} \left(\nabla^2 + 2 \right) W \qquad \text{(A.17)}$$

where

$$\nabla^2 = \frac{\partial^2}{\partial \phi^2} + \cot\phi \frac{\partial}{\partial \phi} + \csc^2\phi \frac{\partial^2}{\partial \theta^2}$$

In the analysis that is to follow we can can safely assume that $1 + \frac{h^2}{12R^2} \approx 1$ whenever it is appropriate to do so.

The first two of the equilibrium equations can be satisfied with the introduction of a stress function F relating to the stress resultants through the relations below:

$$N_{\phi} = \frac{1}{R^2}\left[\csc^2\phi\,\frac{\partial^2 F}{\partial\theta^2} + \cot\phi\,\frac{\partial F}{\partial\phi} + F + \frac{D}{R}\left(\nabla^2 + 2\right) W\right]$$

$$N_{\theta} = \frac{1}{R^2}\left[\frac{\partial^2 F}{\partial\phi^2} + F + \frac{D}{R}\left(\nabla^2 + 2\right) W\right] \qquad \text{(A.18)}$$

$$N_{\phi\theta} = \frac{1}{R^2}\left[\cos\phi\,\csc^2\phi\,\frac{\partial F}{\partial\theta} - \csc\phi\,\frac{\partial^2 F}{\partial\phi\,\partial\theta}\right].$$

When these relations are introduced into the third of the equilibrium equations we obtain a coupled differential equation in terms of the transverse displacement W and the stress function F in the form

$$\left(\nabla^2 + 2\right)\left[\left(\nabla^2 + 2\right) W + \frac{R}{D} F\right] = \frac{R^4}{D} q_n. \qquad \text{(A.19)}$$

From the compatibility relationship we obtain the second coupled equation relating W and F

$$\frac{1}{R^2}\nabla^2\left(\nabla^2 + 2\right) F - \frac{Eh}{R}\left(\nabla^2 + 2\right) W = R\left(\mu - 1\right) q_n. \qquad \text{(A.20)}$$

The coupled system of equations is uncoupled resulting into two equations governing W and F and the end result of the process is

$$\left(\nabla^2 + 2\right)\left[\nabla^4 + 2\nabla^2 + \frac{EhR^2}{D}\right] = \frac{R^4}{D}\left(\nabla^2 + 1 - \mu\right) q_n \qquad \text{(A.21)}$$

and

$$(\nabla^2 + 2) F = \frac{D}{R} \left[\frac{R^4}{D} q_n - (\nabla^2 + 2)^2 W \right] . \quad (A.22)$$

The differential equation (A.21) governs the transverse displacement W of a spherical shell loaded with normal surface traction. We should also note that the order of the governing system [Eqs. (A.21) and (A.22)] is eight and that is the result of the dependence of the rotations onto the displacement vector of the system.

A-2b IMPROVED THEORY

The primary system of equations of the improved theory, which governs the components of the displacement vector W , u_ϕ , u_θ and the angular rotations of the normal vector to the middle surface β_ϕ and β_θ, will be reduced to a secondary system. The new governing system will be expressed in terms of auxiliary variables which are introduced to simplify the analysis. The choice of the auxiliary variables and the adopted procedure follow the guidlines set by Prasad[25]. The objective of this analysis is to reduce the system to a set of coupled differential operators which, when solved, will lead to the determination of the five displacement unknowns of the system.

The various resultants introduced in Eqs. (A.1) and (A.2) can be expressed in terms of the displacement functions in the form

$$N_\phi = \frac{Eh}{(1-\mu^2)R}\left[\frac{\partial u_\phi}{\partial\phi} + W + \mu\left(u_\phi \cot\phi + \csc\phi \frac{\partial u_\theta}{\partial\theta} + W\right)\right]$$

$$N_\theta = \frac{Eh}{(1-\mu^2)R}\left[\mu\left(\frac{\partial u_\phi}{\partial\phi} + W\right) + u_\phi \cot\phi + \csc\phi \frac{\partial u_\theta}{\partial\theta} + W\right] \qquad \text{(A.23)}$$

$$N_{\phi\theta} = \frac{Eh}{2(1+\mu)R}\left[\frac{\partial u_\phi}{\partial\theta}\csc\phi + \frac{\partial u_\theta}{\partial\phi} - \cot\phi\, u_\theta\right]$$

$$M_\phi = \frac{D}{R}\left[\frac{\partial\beta_\phi}{\partial\phi} + \mu\left(\frac{\partial\beta_\theta}{\partial\theta}\csc\phi + \cot\phi\,\beta_\phi\right)\right]$$

$$M_\theta = \frac{D}{R}\left[\mu\frac{\partial\beta_\phi}{\partial\phi} + \frac{\partial\beta_\theta}{\partial\theta}\csc\phi + \cot\phi\,\beta_\phi\right] \qquad \text{(A.24)}$$

$$M_{\phi\theta} = \frac{(1-\mu)D}{2R}\left[\frac{\partial\beta_\theta}{\partial\phi} + \frac{\partial\beta_\phi}{\partial\theta}\csc\phi - \beta_\theta\cot\phi\right]$$

$$Q_\phi = \frac{Eh}{2(1+\mu)k_s^0}\left[\beta_\phi + \frac{1}{R}\frac{\partial W}{\partial\phi}\right]$$

$$Q_\theta = \frac{Eh}{2(1+\mu)k_s^0}\cdot\left[\beta_\theta + \frac{1}{R\sin\phi}\frac{\partial W}{\partial\theta}\right]. \qquad \text{(A.25)}$$

We should note from Eqs. (A.25) that the shear resultants are proportional to the shear strains defined by the combined terms

$$\beta_\phi + \frac{1}{R}\frac{\partial W}{\partial\phi} \quad \text{and} \quad \beta_\theta + \frac{1}{R\sin\phi}\frac{\partial W}{\partial\theta}. \qquad \text{(A.26)}$$

Thus, while in the classical theory analysis the shear resultants were retained only for equilibrium purposes, in the improved theory, by incorporating the the transverse shear effect, we related the shear resultant directly to the field variables assuming a linear

transverse shear stress-strain relationship across the thicness h of the shell. The distribution of shear stress, however, has been assumed parabolic over the thickness and thus leading to the characteristic value of the coefficient $k_s^0 = \frac{6}{5}$.

The components of the displacement vector as well as the angular rotations of the normal are expressed in terms of the auxiliary variables in the form

$$u_\phi = \frac{\partial U}{\partial \phi} - R\,\Psi \sin\phi$$

$$u_\theta = \frac{\partial U}{\partial \theta} \csc\phi \qquad \text{(A.27)}$$

$$\beta_\phi = \frac{\partial \Gamma}{\partial \phi} - \Lambda \sin\phi$$

$$\beta_\theta = \frac{\partial \Gamma}{\partial \theta} \csc\phi \qquad \text{(A.28)}$$

When Eqs. (A.27) and (A.28) are introduced into the expressions of the stress, moment and shear resultants, given by Eqs. (A.23)-(A.25), and then in turn substituted into the equilibrium equations, Eqs. (A.1)-(A.2), yield a set of differential operators in terms of the auxiliary functions and the transverse displacement W. By setting the tangential components of the external force vector, q_ϕ and q_θ, equal to zero we obtain from the second of Eqs. (A.1)

$$(\nabla^2 + 1 - \mu) U - \left[\frac{(1+\mu)}{2} \frac{\partial \Psi}{\partial \phi} R \sin\phi + 2\,\Psi\, R \cos\phi \right]$$

$$+ \left(1 + \mu + \frac{1}{k_s} \right) W + \frac{R}{k_s} \Gamma = 0. \qquad (A.29)$$

By differentiating the relation above with coordinate ϕ and subtracting it from the first of Eqs. (A.1) we obtain the second coupled differential equation which is written as

$$\left(\nabla^2 + 2 \right) \Psi + \frac{1}{k_s} \Lambda = 0. \qquad (A.30)$$

Proceeding in the same fashion, we obtain, after substitution and differentiation, from Eqs. (A.2) two additional coupled differential operators in the form

$$\left[\nabla^2 + 1 - \mu - \frac{1}{\xi k_s} \right] \Gamma - \left[\frac{(1+\mu)}{2} \frac{\partial \Lambda}{\partial \phi} \sin\phi + 2 \Lambda \cos\phi \right] - \frac{W}{ERk_s} = 0 \qquad (A.31)$$

and

$$\left(\nabla^2 + 2 - \frac{1}{\xi k_s} \right) \Lambda = 0. \qquad (A.32)$$

Finally, from the third of Eqs. (A.1) we obtain after substitution

$$R \nabla^2 \Gamma - (1+\mu) k_s \nabla^2 U + \left[\nabla^2 - 2 (1+\mu) k_s \right] W$$

$$- R \left(2 \cos\phi + \sin\phi \frac{\partial}{\partial \phi} \right) \left[\Lambda - (1+\mu) k_s \Psi \right] + \frac{(1-\mu^2)R^2}{Eh} k_s q_n = 0 \qquad (A.33)$$

where

$$k_s = \frac{2\,k_s^0}{1-\mu}$$

$$\xi = \frac{h^2}{12R^2} \qquad \text{(A.33a)}$$

$$\nabla^2 = \frac{\partial^2}{\partial\phi^2} + \cot\phi\,\frac{\partial}{\partial\phi} + \frac{1}{\sin^2\phi}\,\frac{\partial^2}{\partial\theta^2}$$

We notice the coupling between the transverse displacement W and the auxiliary functions in three of the resulted coupled equations and also the special relation between Λ and Ψ variables. The objective of the analysis is to be able to reduce the complex system into uncoupled equations governing the system variables. This can be obtained by utilizing the five differential equations as well as the linearity of the various operators involved. We proceed by operating onto Eqn. (A.32) with the linear operator $L_1 = \frac{1}{k_s}\,[\nabla^2 + 1 - \mu)$. Because of the linearity of the operators, we observe the identity

$$(1+\mu)\,k_s\,L_1\,[\nabla^2] = (1+\mu)\,k_s\,\nabla^2\,[L_1]. \qquad \text{(A.34)}$$

Equation (A.29) may assume the equivalent expression

$$k_s\,L_1\,U = \left[\frac{(1+\mu)}{2}\,\frac{\partial\Psi}{\partial\phi}\,R\sin\phi + 2\,\Psi\,R\cos\phi\right] - \left(1+\mu-\frac{1}{k_s}\right)W - \frac{R}{k_s}\,\Gamma. \qquad \text{(A.29')}$$

With the substitution of Eqn. (A.29') and with the help of the identity (A.34), the operated form of Eqn. (A.32) yields the expression

$$\frac{R}{k_s}\left[(\nabla^2+1-\mu) (\nabla^2\Gamma) \right] - (1+\mu)\nabla^2 \left[\left(\frac{(1+\mu)}{2} \frac{\partial\Psi}{\partial\phi} R \sin\phi + 2 R \Psi \cos\phi \right) - (1+\mu+\frac{1}{k_s}) W - \frac{R}{k_s}\Gamma \right] + \frac{1}{k_s} (\nabla^2+1-\mu) \left[(\nabla^2-2(1+\mu)k_s) W \right] - \frac{R}{k_s} (\nabla^2+1-\mu) \left[(2\cos\phi + \sin\phi \frac{\partial}{\partial\phi}) (\Lambda - (1+\mu)k_s \Psi) \right] + (\nabla^2+1-\mu) \left[\frac{(1-\mu^2)R^2}{Eh} q_n \right] = 0. \qquad (A.35)$$

The relation above can be written in the following equivalent form

$$\frac{R}{k_s}\left[(\nabla^2 + 1 - \mu) (\nabla^2 \Gamma) \right] + (1 + \mu) [1 + \mu + \frac{1}{k_s}] \nabla^2 W + (1 + \mu) \frac{R}{k_s} \nabla^2 \Gamma + \frac{1}{k_s} (\nabla^2 + 1 - \mu) [\nabla^2 - 2 (1 + \mu) k_s] W + (\nabla^2 + 1 - \mu) \left[\frac{(1 - \mu^2) R^2}{Eh} q_n \right] = 0 \qquad (A.36)$$

With the introduction of the operator $L_2 = -\frac{1}{\xi} [1 - \xi k_s(\nabla^2 + 1 - \mu)]$ into Eqn. (A.36), along with

$$\frac{L_2}{k_s}\Gamma = \left[\frac{(1 + \mu)}{2} \frac{\partial\Lambda}{\partial\phi} \sin\phi + 2 \Lambda \cos\phi \right] + \frac{W}{\xi R k_s} \qquad (A.37)$$

yields the expression

$$\frac{R}{k_s} L_2 [(\nabla^2 + 1 - \mu) \nabla^2 \Gamma] - \frac{R}{k_s} [(\nabla^2 + 1 - \mu) \nabla^2] L_2 \Gamma$$

$$= R \left[(\nabla^2 + 1 - \mu) \nabla^2 (\frac{(1+\mu)}{2} \frac{\partial \Lambda}{\partial \phi} \sin\phi + 2 \Lambda \cos\phi) \right]$$

$$+ \frac{1}{\xi k_s} [\nabla^2 + 1 - \mu) \nabla^2 W. \qquad (A.38)$$

With the help of Eqn. (A.38) after substitutions of equivalent terms and manipulations of the expression , Eqn. (A.36) will govern the transverse displacement function W alone. The final form of the governing equation is expressed as

$$\nabla^6 W + p_4 \nabla^4 W + p_2 \nabla^2 W + p_0 W - L_0 q_n = 0 \qquad (A.38)$$

where

$$p_4 = 3 - \mu - (1 - \mu^2) k_s$$

$$p_2 = \frac{1 - \mu^2}{\xi} + 2 (1 - \mu) + k_s (1 - \mu^2) (\mu - 3) \qquad (A.39)$$

$$p_0 = \frac{2 (1 - \mu^2)}{\xi} - 2 (1 - \mu) (1 - \mu^2) k_s$$

and

$$L_0 = [- \frac{1}{\xi} (1 - \xi k_s (\nabla^2 + 1 - \mu))] (\nabla^2 + 1 - \mu) \left[\frac{(1 - \mu^2) R^2}{Eh} \right]$$

(A.40)

Equation (A.38) governs the transverse displacement W of a spherical domain under the action of normal surface traction q_n, while q_ϕ =

$q_\theta = 0$. The complete system of governing relations has been reduced to three equations which relate to W and the auxiliary variables Ψ and Λ . The order of the complete system is now ten and it is due to the implementation into the analysis of the shear coefficient. The shear effect, as noted earlier, helped introduce rotations of the normal independent of the displacement vector and which in effect represent the two additional variables of the system.

APPENDIX B

COMPUTER IMPLEMENTATION OF THE BOUNDARY INTEGRAL SCHEME

The mathematical formulation developed has demonstrated the behavior of thin elastic spherical shells under static loads. The analytical solutions encountered, however, can only facilitate a limited class of shells under an arbitrary system of static loads. The analysis of shell domains in particular, and systems in general, of arbitrary plan form under such loadings constitutes the rule rather than the exeption in modern technology. The availability of several numerical methods helped develope procedures for the solution of the most general problems which could arise within the framework of the theory of thin shells. The full potential, however, of such methods can only be recognized by the efficient interaction of the mathematical solution and the implemented computer program.

In what follows, the principles of an Indirect Boundary Integral program formulated upon the introduction of geometries of physical systems will be outlined.

B-1 AN OUTLINE OF THE STRUCTURE OF A BOUNDARY INTEGRAL PROGRAM

In constructing the Boundary Integral program the logical steps used in all analyses, which utilize the approach, are implemented in the following sequence:

1. Introduction of the parameters of the system and the external inputs

2. Generation of the input data associated with the boundary geometry and its discretization as well as the discretization of the domain.

3. Integration of the kernel functions against the shape functions chosen for the boundary and surface elements to generate the matrices of the system.

4. Solution of the system of equations which have been assembled in fashion as to satisfy the prescribed boundary conditions. Such solution will provide the intensities of the fictitious boundary vectors introduced to ensure the satisfaction of the boundary constraints.

5. Backsubstitution of the fictitious vectors into the integrals to obtain the values of the dependent variables at interior points.

B-2 GENERATION OF INPUT DATA

For the case of a shell domain describing a physical problem, a directory of information must be constructed that will reflect the particularities of the specific problem. This directory will incorporate the boundary conditions along different portions of the boundary, their geometry as well as the spacial orientation of the unit vectors, the accuracy of the solution associated with the number of subdivisions along the boundary and the form of the shape functions assumed over the discretized boundary. In addition to the boundary, information will be cataloged for the domain itself by specifying the type of surface traction applied and the discretization of the surface into elements.

B-2a COORDINATE TRANSFORMATION

Consider the spherical shell shown in Fig. B-1 where its middle surface is described by the cartesian coordinate system (x,y,z).

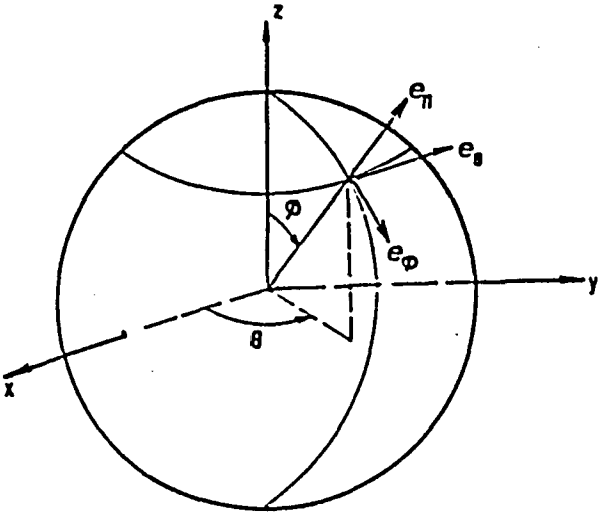

Figure B-1. Surface spherical coordinates and unit vectors.

The parametric representation of the unit vectors e_n , e_ϕ and e_θ can take the form

$$
\begin{aligned}
e_n &= \sin\phi \cos\theta \; i + \sin\phi \sin\theta \; j + \cos\phi \; k \\
e_\phi &= \cos\phi \cos\theta \; i + \cos\phi \sin\theta \; j - \sin\phi \; k \\
e_\theta &= - \sin\theta \; i + \cos\theta \; j
\end{aligned}
\qquad \text{(B.1)}
$$

where ϕ and θ are the surface coordinates.

Thus a vector on the spherical surface with orientation in terms of the surface coordinates can equivalently be oriented in the (x,y,z) coordinate system utilizing Eqns. B.1.

Consider another cartesian coordinate system designated as (x^*,y^*,z^*) with an orientation shown in Fig. B-2.

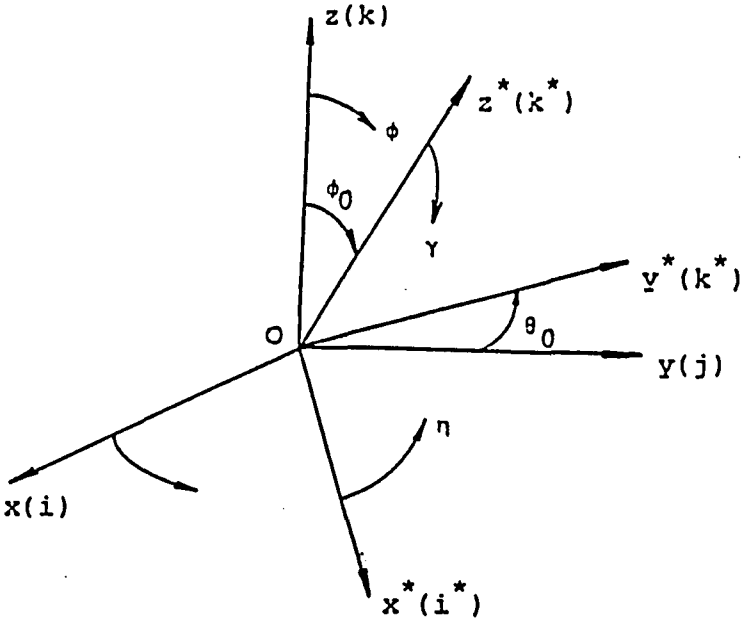

Figure B-2. Fixed and rotated cartesian systems.

The spherical surface can now be described by the primed cartesian system or by the new surface coordinates γ and η . Note that $\gamma = 0$ at $\phi = \phi_0$ and $\eta = 0$ at $\theta = \theta_0$. A transformation matrix L can now be constructed that will enable a vector in the primed cartesian system to be oriented in the unprimed coordinate system. Such a matrix can be expressed in the form:

$$L = \begin{matrix} \cos\theta_0 \cos\phi_0 & -\sin\phi_0 & \cos\theta_0 \sin\theta_0 \\ \sin\theta_0 \cos\phi_0 & \cos\theta_0 & \sin\theta_0 \sin\phi_0 \\ -\sin\phi_0 & 0 & \cos\phi_0 \end{matrix} \qquad (B.2)$$

The matrix L satisfies the relation

$$L\, u^* = u \qquad (B.3)$$

where

$$u^* = a\, i^* + b\, j^* + c\, k^*$$
$$u = A\, i + B\, j + C\, k \qquad (B.4)$$

On the other hand in order to transform a vector originally oriented in the (x,y,z) coordinate system to its equivalent vector in the (x^*,y^*,z^*) system,the transformation matrix

$$L^* = \begin{matrix} \cos\theta_0 \cos\phi_0 & \sin\theta_0 \cos\phi_0 & -\sin\phi_0 \\ -\sin\theta_0 & \cos\theta_0 & 0 \\ \cos\theta_0 \sin\phi_0 & \sin\theta_0 \sin\phi_0 & \cos\phi_0 \end{matrix} \qquad (B.5)$$

should be utilized. Thus matrix L^* satisfies the relation

$$L^* u = u^* . \tag{B.6}$$

B-2b BOUNDARY AND SURFACE DISCRETIZATION

Let us consider an arbitrary portion of a boundary on the spherical surface shown in Fig. B-3.

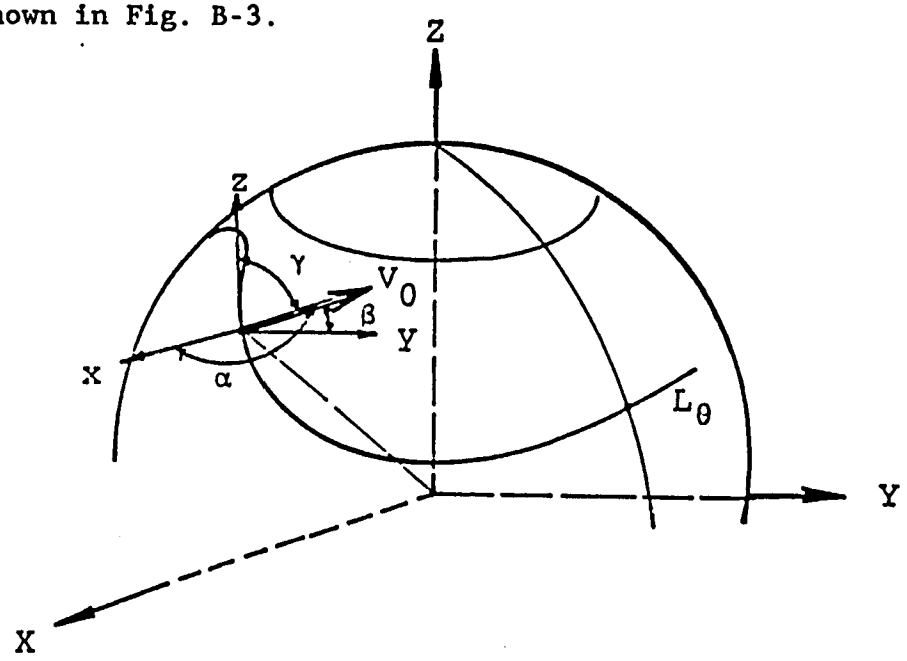

Figure B-3. Geometry of a surface line and spatial orientation of an arbitrary surface vector.

The equation of the surface line segment L_0 expressed in terms of the surface coordinates ϕ and θ is desired. Such representations can often be obtained through rotations of the fixed frame coordinate system (x,y,z). In addition, relationships between different sets of surface coordinates, such as (ϕ,θ) and (γ,η), can provide the

equation of the surface line L_0 in terms of ϕ and θ. Together with the geometry of the surface line the orientation of surface vectors, such as $V_0(\cos\alpha i, \cos\beta j, \cos\gamma k)$, applied along L_0 is also required. Such orientations of vectors can be obtained by utilizing the transformation matrices in Eqns B.2 and B.5. The availability of the surface line geometry and the spacial description of the boundary vectors will make their integration over the boundary segment possible. These boundary vectors will correspond to load, displacement or stress vectors along a real spherical shell boundary. The relationships between the different sets of surface coordinates will be constructed from the transformation matrices as well as from spherical trigonometric relations. Such trigonometric relations are associated with the properties of spherical triangles which in turn are deduced from the intersection of three arbitrary great circles. We should note that portions of great circles on the spherical surface are the equivalent of straight line segments on the plane. For the spherical triangle shown in Fig. B-4

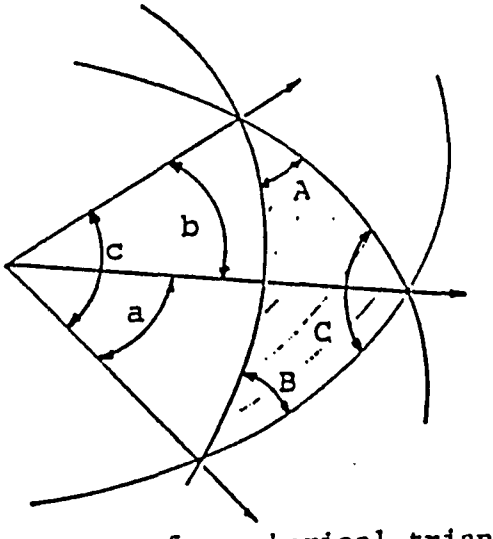

Figure B-4. Geometry of a spherical triangle.

the following relations hold between the parameters:

$$\frac{\sin a}{\sin A} = \frac{\sin b}{\sin B} = \frac{\sin c}{\sin C} \qquad \text{(LAW OF SINES)}$$

$$\cos a = \cos b \cos c + \sin b \sin c \cos A \tag{B.7}$$

$$\cos A = - \cos B \cos C + \sin B \sin C \cos a$$

$$\tan \frac{b+c}{2} \cos \frac{B+C}{2} = \tan \frac{a}{2} \cos \frac{B-C}{2}$$

$$\tan \frac{b-c}{2} \sin \frac{B+C}{2} = \tan \frac{a}{2} \sin \frac{B-C}{2} \tag{B.8}$$

$$\tan \frac{B+C}{2} \cos \frac{b+c}{2} = \cot \frac{A}{2} \cos \frac{b-c}{2}$$

$$\tan \frac{B-C}{2} \sin \frac{b+c}{2} = \cot \frac{A}{2} \sin \frac{b-c}{2}.$$

The analytical representation of four types of surface lines will be derived. These will correspond to boundaries coincident with the principal surface coordinates ($\alpha_1 = \beta$ = const. and $\alpha_2 = \theta$ =const.), boundaries along arbitrarily oriented great circles and boundaries of elliptically located circular contours. Irregular boundary shapes will be treated as a sum of portions of great circles (equivalent of

representation of an arbitrary line on the plane by a sum of straight line segments).

CASE A: Consider the line segment AB being part of a great circle oriented along the surface coordinate γ with $\eta = \eta_0$ = constant for all its points and associated with the rotated cartesian system (x^*,y^*,z^*) as shown in Fig. B-5.

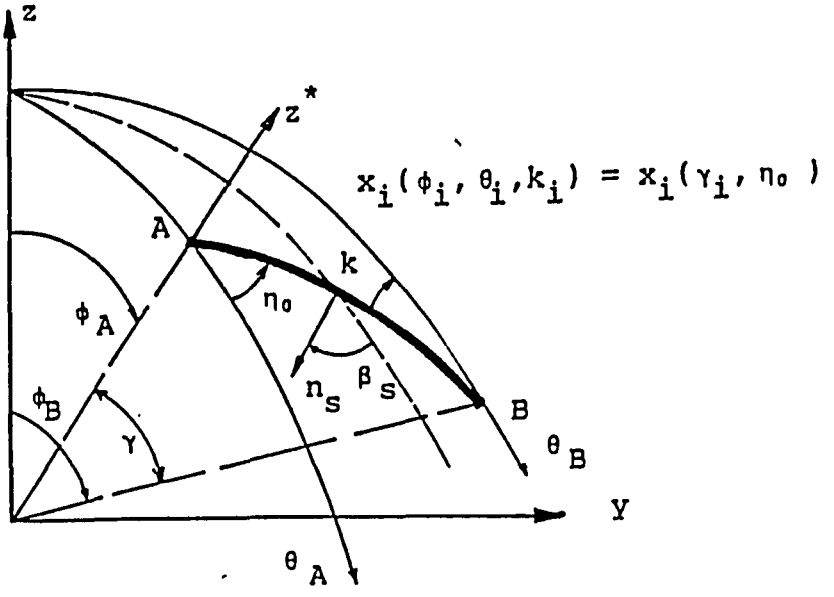

Figure B-5. Portion of an arbitrary great circle.

The trigonometric relations between the surface coordinates (ϕ,θ) and (γ,η) are:

$$\cos\eta_0 = \frac{\cos\phi_a \cos\gamma - \cos\phi_b}{\sin\phi_a \sin\gamma}$$

$$\cos\eta_0 = \frac{\sin\phi_a \sin(\theta_b - \theta_a)}{\sin\gamma} \qquad \text{(B.9)}$$

$$\cos\gamma = \cos\phi_a\cos\phi_b + \sin\phi_a\sin\phi_b\cos(\theta_b - \theta_a)$$

The fixed-space surface coordinates (ϕ,θ) of a point $\underset{\sim}{x}_i$ along the surface line segment AB can be obtained through the relations

$$\tan\left[\frac{(\theta_i-\theta_a)+k_i}{2}\right] = \cot\frac{\pi-\eta_0}{2}\cos\frac{\gamma_i-\phi_a}{2} \Big/ \cos\frac{\gamma_i+\phi_a}{2}$$

and

$$\tan\left[\frac{(\theta_i-\theta_a)-k_i}{2}\right] = \cot\frac{\pi-\eta_0}{2}\sin\frac{\gamma_i-\phi_a}{2} \Big/ \sin\frac{\gamma_i+\phi_a}{2} \qquad (B.10)$$

which lead to

$$(\theta_i-\theta_a)+k_i = 2\tan^{-1}[\,A\,]$$

and

$$(\theta_i-\theta_a)-k_i = 2\tan^{-1}[\,B\,] \qquad (B.11)$$

where quantities A and B above correspond to the right side of Eqns. B.10 respectively. Finally one may easily obtain from Eqns. B.11 for θ_i

$$\theta_i = \theta_a + \tan^{-1}[\,A\,] + \tan^{-1}[\,B\,] \qquad (B.12)$$

and consequently for ϕ_i from Eqn (B.9)

$$\phi_i = \cos^{-1}[\,\cos\gamma_i\cos\phi_a + \sin\gamma_i\sin\phi_a\cos(\,\pi-\eta_0\,)\,]. \qquad (B.13)$$

If β_i represents the angle between ϕ_i and the normal $\underset{\sim}{n}_s$ to the boundary in the tangential sense measured CCW from ϕ_i then one may write

$$\beta_i = \frac{\pi}{2} - k_i \tag{B.14}$$

while k_i is deduced from Eqns (B.11).

Thus for a portion of the boundary along a great circle the discretization will take place over the new coordinate γ while $\eta = \eta_0$ = constant.

CASE B: We consider a point $\underset{\sim}{x}_i$ located along the "circular" contour shown in Fig. B-6, with surface coordinates in the rotated system (x^*, y^*, z^*) given by $\gamma_i = \gamma_a$ and η_i.

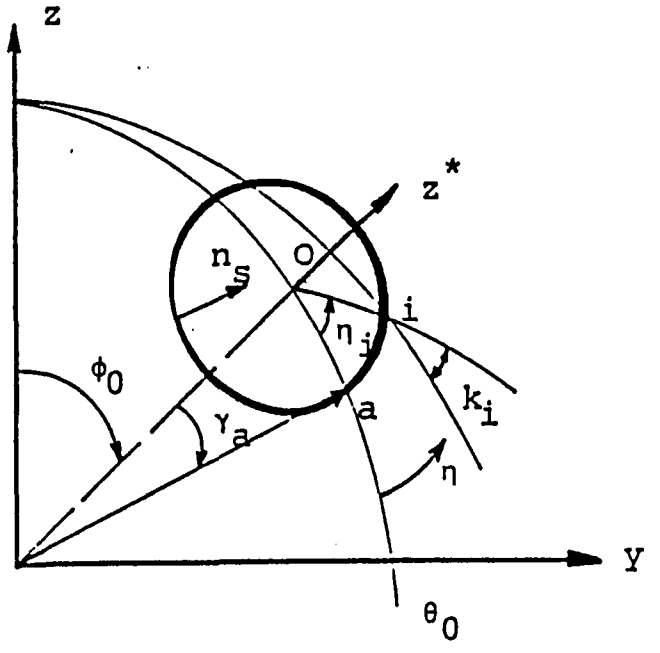

Figure B-6. Arbitrary circoular contour on the spherical surface

The fixed-space surface coordinates (ϕ,θ) of $\underset{\sim}{x}_i$ will be governed by the relations,

$$\phi_i = \cos^{-1}[\ \cos\gamma\ \cos\phi_0 + \sin\gamma\ \sin\phi_0\ \cos(\ \pi - \eta_i\ ) \qquad (B.15)$$

and

$$\tan\left[\ \frac{(\theta_i-\theta_0) + k_i}{2}\ \right] = \cot\frac{\pi - \eta_i}{2}\ \cos\frac{\gamma - \phi_0}{2}\ /\ \cos\frac{\gamma + \phi_0}{2} \qquad (B.16)$$

$$\tan\left[\ \frac{(\theta_i-\theta_0) - k_i}{2}\ \right] = \cot\frac{\pi - \eta_i}{2}\ \sin\frac{\gamma - \phi_0}{2}\ /\ \sin\frac{\gamma + \phi_0}{2}$$

yielding for θ_i

$$\theta_i = \theta_0 + \tan^{-1}[\ A\ ] + \tan^{-1}[\ B\ ]. \qquad (B.17)$$

The angle β_i between ϕ_i and $\underset{\sim}{n}_s^i$ can be deduced from the relation

$$\beta_i = \pi + k_i. \qquad (B.18)$$

Thus the discretization of such contour will take place along the η-coordinate of the rotated system.

CASE C & D: These two cases correspond to boundaries along $\phi = \phi_0 =$ const. and $\theta = \theta_0 =$ const. respectively. Since such boundary lines are expressed in terms of the principal surface coordinates no special treatment is required.

The analysis above provided the closed-form relations between points along specific contours. Such relations, vital to the integration of line vectors with both magnitude and spacial orientation, together with the transformation equations can provide the matrix of specified

points. These points are usually the middle points or nodes of the boundary elements where the boundary conditions must be satisfied. Thus, the properties of each element will be carried by the element node. The specification of the boundary type and consequently the utilization of the above analysis will yield a discretized boundary. Thus, for an arbitrary boundary, constrained with different sets of boundary conditions along its span, the key points will be recognized. The interval between two consecutive such points will corespond to a type of geometric boundary (four types are included in the discretization analysis). The number of subdivisions for each boundary segment will be incorporated and the portion will be divided into that many elements. By utilizing the relations which provide the surface coordinates of arbitrary points, the location of the nodes of the elements in terms of the global surface coordinates will be obtained and cataloged. The orientation of the boundary, as seen from the global frame, with respect to the actual domain will provide the orientation of the surface unit vectors of each node. As mentioned earlier, boundaries of irregular shape will be approximated with portions of great circles between selected points. The numbering of the elements, and consequently of the nodes, will be global, while the sequence of the different segments is insignificant for as long as the boundary coditions that exist for each node follow the same sequence. The last statement is of critical importance since it dominates the procedure of the construction of the system matrix and it will be discussed in that section.

The subdivision of the domain will only occur when distributed surface traction applies at the surface of the domain. For the case of concentrated loads applying on it the only information needed to be cataloged is the surface coordinates, the type, the strength and the direction of the singular load. For the case of surface traction, the domain is subdivided into elements in an effort to integrate the effect of the traction into the system equations. However, such discretization will not lead to an increase of the matrix but rather introduce the effect of the full surface traction vector at each boundary node.

The types of surface traction introduced in this analysis inlude normal surface load, wind load and own weight. Subdivisions of the surface can only be performed in domains bounded by the principal coordinates of the surface. The effect of the traction over each element will be the effect of its equivalent concentrated vector applied at the middle point of the surface element. Such equivalent concentrated vectors will be obtained by utilizing the relations governing the orintations of surface vectors and provided by the transformation matrices introduced earlier.

B-3 INTEGRATION OF THE KERNEL FUNCTIONS ALONG THE BOUNDARY

The implementation of the Boundary Integral Scheme requires the construction of the system matrices. Such matrices are constructed in a manner which enforces the satisfaction of the specified conditions

along the boundary. The system will be solved to determine the values of the fictitious load vectors applied at the boundary. The number of boundary constraints required will determine the number of such unknown vectors and thus the size of the system. The contribution of both the real surface load vectors and the fictitious boundary vectors is demonstrated in the following expression

$$Y(\underset{\sim}{x}) = \iint_R Y^i(\underset{\sim}{x};\underset{\sim}{x}')\ q_s^i\ dR + \oint_{\partial B} Y^i[\ \underset{\sim}{x}\ ;\ \underset{\sim}{x}'(B)\ ]\ (\ q_B^*\ )^i\ \partial B \qquad (B.19)$$

where

$Y(\underset{\sim}{x})$ - a system variable, such as displacement or stress, at a field point $\underset{\sim}{x}(\phi,\theta)$

$Y^i(\underset{\sim}{x};\underset{\sim}{x}')$ - is the kernel function (fundamental solution) of the variable $Y(\underset{\sim}{x})$ associated with the field point $\underset{\sim}{x}(\phi,\theta)$ and a load point $\underset{\sim}{x}'(\phi',\theta')$

q_s^i - the surface traction vector

$[\ q_B^*\ ]^i$ - fictitious load vectors applied along the boundary

R - spherical shell domain

∂B - boundary of the domain R.

$x'(B)$ - load point at the boundary

We should note that if closed form integrations are performed, the integral equations that result from Eqn. B.19 can provide the exact answer to the particular problem. However, such closed form solutions

are rarely possible and instead the boundary integral equations become discretized and take the form

$$Y(\underset{\sim}{x}) - \sum_{p=1}^{M} \left[\int_{\Delta A_p} Y^i(\underset{\sim}{x};\underset{\sim}{x}')\ q_s^i\ dR_p \right] + \sum_{j=1}^{N} \left[\int_{\Delta S_B} Y^i[\underset{\sim}{x};\underset{\sim}{x}'(B)]\ [q_B^*]^i\ dS_j \right] \tag{B.20}$$

where

M = number of surface elements

N = number of boundary elements.

Special attention is focused onto the discretized closed boundary integral, which is now expressed as the sum of the integrals over each boundary element. The fictitious load vectors correspond to line tractions in the normal and the two tangential directions and also normal and twisting line moment vectors. The normal line moment is directed along the on-surface normal vector to the boundary line while the line twisting moment applies along the boundary line and only when the improved theory is in use. The task of the scheme is to effectively integrate the product of the kernel and load functions over each element utilizing the directory of information established for each such element. For this analysis the intensity of the unknown vectors will be constant over each element and thus the shape funtion will be unity. Further, for reasons of simplification of the integration process, the line vectors will be replaced by a statically equivalent system of resultant forces applied at the node of each element. It is necessary to incorporate such approach because

of the particularities of the kernel functions. These kernels are mainly expressed in terms of complex Legendre functions which in turn are evaluated from the infinite hypergeometric series. Integrations will only be performed over the same or neighboring elements where the Legendre functions can be expressed asymptotically.

Consider the load and moment tractions shown in Fig.B-7 and the unit vectors associated with an arbitrary point $\underset{\sim}{x}_j$ and the middle point $\underset{\sim}{x}_m$ of the element (i,i+1).

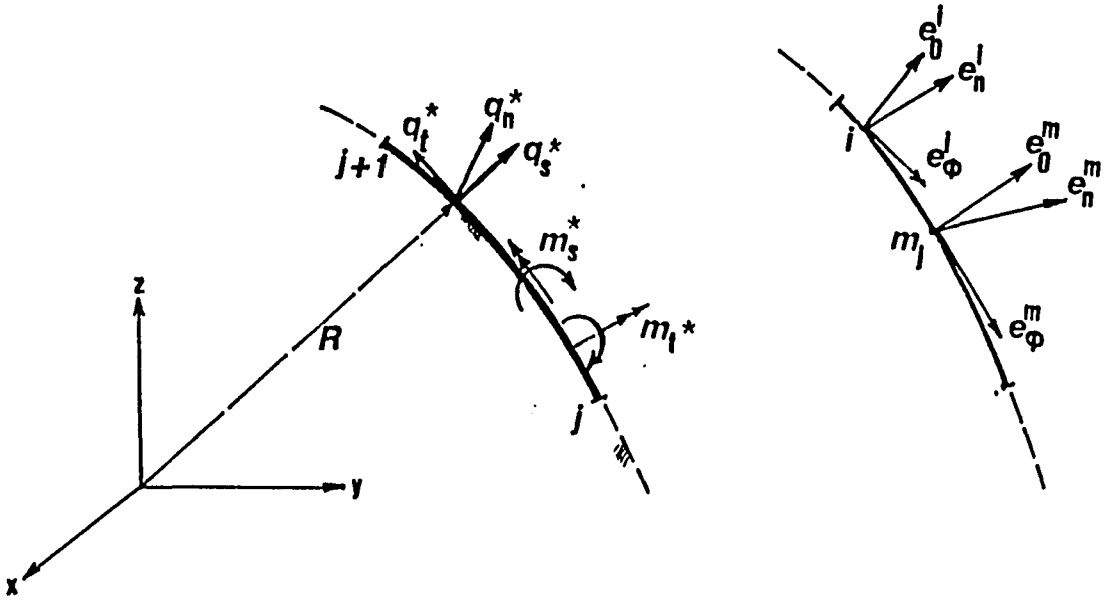

Figure B-7. Fictitious load and unit vectors of a boundary element.

The resultant of a line vector along the element is simply the integration of its inner product with the unit vector at $\underset{\sim}{x}_m$. Thus, for the four types of boundary we obtain a set of resultant forces designated by $R_{\rho 1;\rho 2}$, where the first subscript denotes the direction

of the resultant and the second denotes the direction of the distributed vector. We examine the four cases separetly:

CASE I: For an element along ϕ = constant $\phi(i) = \phi(i+1) = \phi_m$ and

$$dS_B = R \sin\phi_m \, d\theta$$

Hence

$$R_{n,n} = 2 R q_n \sin\phi_m [\cos^2\phi_m (\theta_m-\theta_i) + \sin^2\phi_m \sin(\theta_m-\theta_i)]$$

$$R_{\phi,n} = 2 R q_n \sin^2\phi_m \cos\phi_m [\sin(\theta_m-\theta_i) - (\theta_m-\theta_i)]$$

$$R_{\theta,n} = 0$$

$$R_{n,\phi} = 2 R q_\phi \sin^2\phi_m\cos\phi_m [\sin(\theta_m-\theta_i) - (\theta_m-\theta_i)]$$

$$R_{\phi,\phi} = 2 R q_\phi \sin\phi_m [\cos^2\phi_m\sin(\theta_m-\theta_i) + \sin^2\phi_m(\theta_m-\theta_i)]$$

$$R_{\theta,\phi} = 0 \qquad \text{(B.21)}$$

$$R_{n,\theta} = 0$$

$$R_{\phi,\theta} = 0$$

$$R_{\theta,\theta} = 2 R q_\theta \sin\phi_m \sin(\theta_m-\theta_i)$$

$$M_{s,s} = 2 R m_s \sin\phi_m \sin(\theta_m-\theta_i)$$

$$M_{t,s} = 0$$

$$M_{t,t} = 2 R m_t \sin\phi_m [\cos^2\phi_m\sin(\theta_m-\theta_i) + \sin^2\phi_m(\theta_m-\theta_i)]$$

$$M_{s,t} = 0$$

$$M_{n,t} = 2\ R\ m_t\ \sin^2\phi_m\ \cos\phi_m\ [\ \sin(\theta_m-\theta_i) - (\theta_m-\theta_i)\ ]$$

where $M_{\rho 1,\rho 2}$ are the resultants of the moment vectors.

CASE II: For a boundary element along $\theta_B = \text{const.} = \theta_m$, $dS_B = R\ d\phi$ and hence,

$$R_{n,n} = 2\ R\ q_n\ \sin(\phi_m-\phi_i)$$
$$R_{\phi,n} = R_{\theta,n} = 0$$

$$R_{n,\phi} = R_{\theta,\phi} = 0$$
$$R_{\phi,\phi} = 2\ R\ q_\phi\ \sin(\phi_m-\phi_i) \qquad \text{(B.22)}$$

$$R_{n,\theta} = R_{\phi,\theta} = 0$$
$$R_{\theta,\theta} = 2\ R\ q_\theta\ (\phi_m-\phi_i)$$

$$M_{s,s} = 2\ R\ m_s\ \sin(\phi_m-\phi_i)$$
$$M_{t,s} = M_{s,t} = M_{n,t} = 0$$
$$M_{t,t} = 2\ R\ m_t\ (\phi_m-\phi_i)\simeq$$

CASE III: For a boundary element along a great circle other than the principle ones and surface coordinates in the (γ,η) system, $\eta_i = \eta_m = \text{const.}$ and $dS_B = R\ d\gamma$.

Hence

$$R_{n,n} = 2\,R\,q_n \sin(\gamma_m-\gamma_i)$$

$$R_{s,n} = R_{t,n} = 0$$

$$R_{n,s} = R_{t,s} = 0$$

$$R_{s,s} = 2\,R\,q_s\,(\gamma_m-\gamma_i)$$

(B.23)

$$R_{n,t} = R_{s,t} = 0$$

$$R_{t,t} = 2\,R\,q_t \sin(\gamma_m-\gamma_i)$$

$$M_{s,s} = 2\,R\,m_s \sin(\gamma_m-\gamma_i)$$

$$M_{t,t} = 2\,R\,m_t\,(\gamma_m-\gamma_i)$$

$$M_{s,t} = M_{t,s} = M_{n,s} = M_{n,t} = 0$$

where s and t are the orientations of the unit vectors as shown in Fig.B-8.

CASE IV: For a boundary element along a "circular" path as shown in Fig.B-9 together with the orientation of the tangent unit vectors e_s and e_t, $\gamma_i = \gamma_m$ = constant and $dS_B = R \sin\gamma_m d\eta$.

Hence

$$R_{n,n} = 2\,R\,q_n \sin\gamma_m \left[\cos^2\gamma_m(\eta_m-\eta_i) + \sin^2\gamma_m \sin(\eta_m-\eta_i) \right]$$

$$R_{s,n} = 2\,r\,q_n \sin^2\gamma_m \cos\gamma_m \left[\sin(\eta_m-\eta_i) - (\eta_m-\eta_i) \right]$$

$$R_{t,n} = 0$$

$$R_{n,s} = 2\,R\,q_s \sin^2\gamma \cos\gamma_m \left[\sin(\eta_m-\eta_i) - (\eta_m-\eta_i) \right]$$

$$R_{s,s} = 2\,R\,q_s \left[\cos^2\gamma_m \sin\gamma_m \sin(\eta_m-\eta_i) + \sin^2\gamma_m (\eta_m-\eta_i) \right]$$

(B.24)

$$R_{t,s} = R_{s,t} = R_{n,t} = 0$$

$$R_{t,t} = 2\,R\,q_t \sin\gamma_m \sin(\eta_m-\eta_i)$$

$$M_{s,s} = 2\,R\,m_s \sin\gamma_m \sin(\eta_m-\eta_i)$$

$$M_{s,t} = M_{t,s} = M_{n,s} = 0$$

$$M_{t,t} = 2\,R\,m_t \left[\cos^2\gamma_m \sin\gamma_m \sin(\eta_m-\eta_i) + \sin^2\gamma_m (\eta_m-\eta_i) \right]$$

$$M_{n,t} = 2\,R\,m_t \sin^2\gamma_m \cos\gamma_m \left[\sin(\eta_m-\eta_i) - (\eta_m-\eta_i) \right].$$

B-3a EVALUATION OF SINGULAR INTEGRALS

When integration of the kernel function against the load vector is to take place over an element which contains the field point as well as the load point, particular attention is paid to those kernels that contain singularities. The singular behavior of the kernels results from their association with the Legendre functions (see App.C). The order of the singularity, however, will determine wether a kernel function is integrable or not. The strongest singularity encountered in the analysis is of the order $1/\gamma^2$ and is found in the shear resultant of the classical theory. Singular integrals involving such function cannot be evaluated in closed form. Further, weaker singularities can in fact be evaluated either in closed form or as Cauchy principal values. Such integrals that are encountered in the analysis are listed below:

$$I_1 = \int_{\Delta S_B} \frac{1}{\sin\gamma} \, dS_B$$

$$I_2 = \int_{\Delta S_B} \cos\gamma \, \ln(1 - \cos\gamma) \, dS_B \qquad \text{(B.25)}$$

$$I_3 = \int_{\Delta S_B} \ln(1 - \cos\gamma) \, dS_B$$

Integral I_1 posseses a strong singularity and its evaluation will be in terms of the principal value of the integral. That value will be

determined with the help of an envelope, shown in Fig.3-4, by approaching the singular point at the boundary from inside.

We should also stress the importance of the boundary angles as well as the directional angles of the kernels. This particular point is extensively discussed in Chapter 3. Thus for the envelope shown, the integration of a kernel $K(\underset{\sim}{x};\underset{\sim}{x}')$ over the element ΔS_i can be written in the equivalent form

$$\int_{S_i} K(\underset{\sim}{x};\underset{\sim}{x}')\, dS_i = \int_{\Delta S_i} K_S\,(\underset{\sim}{x};\underset{\sim}{x}')\, dS_i + \int_{\Delta S_i} K_R\,(\underset{\sim}{x};\underset{\sim}{x}')\, dS_i \qquad (B.26)$$

where

K_S - singular part of the kernel

K_R - regular part of the kernel.

Also

$$\int_{\Delta S_i} K_S\,(\underset{\sim}{x};\underset{\sim}{x}')\, dS_i = \lim_{\epsilon\to 0} \int_{\gamma_i'}^{\epsilon} K_S(\underset{\sim}{x};\underset{\sim}{x}')\, dS_i + \lim_{\epsilon\to 0} \int_{0}^{2\pi} K_S(\underset{\sim}{x};\underset{\sim}{x}')\, dS_\epsilon$$

$$+ \lim_{\epsilon\to 0} \int_{\epsilon}^{\gamma_{i+1}'} K_S(\underset{\sim}{x};\underset{\sim}{x}')\, dS_i \qquad (B.27)$$

where

$$dS_\epsilon = R \sin\gamma'\, d\epsilon \qquad (B.28)$$

The remaining two integrals are weak and can be evaluated in closed form. Thus, for a boundary element along either θ = const. or η =

determined with the help of an envelope, shown in Fig.3-4, by approaching the singular point at the boundary from inside.

We should also stress the importance of the boundary angles as well as the directional angles of the kernels. This particular point is extensively discussed in Chapter 3. Thus for the envelope shown, the integration of a kernel $K(\underset{\sim}{x};\underset{\sim}{x}')$ over the element ΔS_i can be written in the equivalent form

$$\int_{S_i} K(\underset{\sim}{x};\underset{\sim}{x}')\, dS_i = \int_{\Delta S_i} K_S\,(\underset{\sim}{x};\underset{\sim}{x}')\, dS_i + \int_{\Delta S_i} K_R\,(\underset{\sim}{x};\underset{\sim}{x}')\, dS_i \qquad (B.26)$$

where

K_S - singular part of the kernel

K_R - regular part of the kernel.

Also

$$\int_{\Delta S_i} K_S\,(\underset{\sim}{x};\underset{\sim}{x}')\, dS_i = \lim_{\epsilon\to 0} \int_{\gamma_i'}^{\epsilon} K_S(\underset{\sim}{x};\underset{\sim}{x}')\, dS_i + \lim_{\epsilon\to 0} \int_{0}^{2\pi} K_S(\underset{\sim}{x};\underset{\sim}{x}')\, dS_\epsilon$$

$$+ \lim_{\epsilon\to 0} \int_{\epsilon}^{\gamma_{i+1}'} K_S(\underset{\sim}{x};\underset{\sim}{x}')\, dS_i \qquad (B.27)$$

where

$$dS_\epsilon = R \sin\gamma'\, d\epsilon \qquad (B.28)$$

The remaining two integrals are weak and can be evaluated in closed form. Thus, for a boundary element along either θ = const. or η =

$$dS_B = R \sin\phi_B \, d\theta$$

$$\cos\gamma = \cos\phi_B^2 + \sin\phi_B^2 \cos(\theta_m - \theta). \tag{B.31}$$

Thus,

$$I_2 = \int_{-\Delta\theta}^{\Delta\theta} \cos\gamma \ln(1-\cos\gamma) \sin\phi_B \, R \, d\theta$$

$$= 4 R \sin\phi_B \ln[\sin\phi_B] \, (\Delta\theta - \sin^2\phi_B \sin(\Delta\theta))$$

$$+ R \sin\phi_B \int_{-\Delta\theta}^{\Delta\theta} \ln(1-\cos\theta') \, d\theta' - R \sin^3\phi_B \int_{-\Delta\theta}^{\Delta\theta} \cos\theta' \ln(1-\cos\theta') \, d\theta'$$

(B.32)

where $\Delta\theta = \theta_m - \theta_i$ and the two integrals above were evaluated previously.

Further we should note that when integrations of the kernels are to be performed over surface elements that contain both the field and the load point, the singularities up to the order $1/\gamma$ are all weak and can be integrated with no difficulties.

B-4 ASSEMBLY AND SOLUTION OF THE SYSTEM EQUATIONS

The first step toward the solution is to effectivly assemble a system of linear algebraic equations, which will substitute for the integral equations of the system, incorporating the boundary information for the particular problem. Thus for N discrete boundary elements and

n number of specified conditions we can express the governing system in the form of the matrix relation

$$L\,\psi^{*} + S = BC \qquad \text{(B.33)}$$

where

- L = nN x nN fully populated system matrix associated with the integrations of the fundamental solutions.
- ψ^{*} = nN x 1 vector of the fictitious boundary loads
- S = nN x 1 vector whose elements correspond to the accumulated effect of the known surface traction ψ at each node
- BC = nN x 1 vector of the specified boundary conditions at the N nodes (the number is four per element for the classical theory and five for the improved theory).

In relating two arbitrary elements on the discretized boundary, designated by i and j where i is the element where the constraints must be satisfied and j is the element loaded with the fictitious line loads, the following parameters are identified:

$G_{i,j} = \int_{\Delta S_j} K^{t}\,(\,x_i\,;\,x_j\,)\,dS_j$, where K^{t} refers to the fundamental solution associated with a field variable, such as displacement or stress, specified at the boundary node i and represents the effect of the fictitious load vector of type t distributed over the element j.

$[\ \psi^*(j)\ ]$ - intensity of the fictitious load vector over the jth boundary element and of type t.

$S_k\ (i)$ - accumulated effect of the known surface tractions at node i in reference to the field variable specified as the kth boundary condition.

$BC_k\ (i$ - specified kth boundary condition at the ith node.

Thus if $K^t(x_i;x_j)$ is the fundamental solution of the transverse displacement and t refers to the normal load vector, then

$$\int_{\Delta S_j} K^t(x_i;x_j)\ dS_j = \int_{\Delta S_j} W^n(x_i;x_j)\ dS_j. \qquad (B.34)$$

However, since the integration for the case when $i \neq j$ has been replaced by the effect of the resultant forces applied at the jth node, the integral expression will take the equivalent form

$$\int_{\Delta S_j} W^n\ dS_j = R_{n,n}\ W^n + R_{n,\phi}\ W^{t,\phi} + R_{n,\theta}\ W^{t,\theta} \qquad (B.35)$$

where

W^n - fundamental solution of W due to normal load

$W^{t,\phi}$ - fundamental solution of W due to a tangential load

position of the actual domain in reference to each boundary segment and the different sets of boundary conditions as well as the values of these constraints at the boundary. Further the external forces applied over the domain are read together with their intensities and surface coordinates. Lastly the field points, at which the stress and displacement matrices are to be calculated, are read and stored in an array. The last input is a counter that controls the stress and displacement output.

The program can facilitate four different boundary geometries and five different sets of boundary conditions. These include constraints of fixed, simply supported, free to rotate, free edge and symmetric boundaries. For the specisl case of a crack problem, which falls under the free edge boundary constraint, a special counter is read indicating that attention is to be paid to the element neighboring the crack tip.

B-5b PROCESSING OF INPUT DATA AND EXECUTION

The different boundaries are discretized using the relations introduced earlier in this section and the coordinates of the nodes as well as the orientation of the unit vectors at each node are calculated and entered into the element directory. Also the resultant forces over each element are calculated and stored. When the element directory is completed, the construction of the system matrix begins.

The elements of the system matrix are generated by means of Eqns.(B-[33-35]). A special subroutine has been designed that minimizes the computer time needed to evaluate the complex Legendre Functions.

The completion of the matrix L is followed by the implimentation of the subroutine SSLAE designed to solve a general system of simultaneous linear algebraic equations by means of Gauss-elimination with complete pivoting. The output of the subroutine SSLAE is stored in an array and utilized, together with the external force system, to calculate stresses and displacements at interior points. The stress matrix consists of eight stress resultants while the displacement calculations include all three components.

APPENDIX C

PROPERTIES OF LEGENDRE FUNCTIONS

The Legendre functions aresolutions of the Legendre differential equation

$$(1-z^2)\,\frac{d^2w}{dz^2} - 2z\frac{dw}{dz} + [\ \nu\ (\ \nu + 1\ ) - \mu^2\ (1-z^2)^{-1}\ ] = 0 \qquad (C.1)$$

with parameters ν , μ unrestricted complex numbers.

We seek the properties of the solution of Eqn.(C.1) for the case of variable z beeing real and between -1 and +1. In this case the fundamental system of solutions are denoted by $P_\nu^\mu\ (\ x\ )$ and $Q_\nu^\mu\ (\ x\ )$ [or also by $P_\nu^\mu\ (\cos\phi)$ and $Q_\nu^\mu\ (\cos\phi)$ with $0 \le \phi \le \pi$]. They are called Legendre functions of the first and second kind respectively. It is most efficient, in terms of the numerical evaluation, to express the Legendre functions in terms of hypergeometric functions which, in turn, can be calculated from their infinite series expansion. Thus for the case of integer values of μ, for $\mu \ge 1$ the functions are noted as associated Legendre functions, their evaluation is obtained according to the relation

$$\Gamma\ (\nu\text{-}m\text{+}1)\ m!\ P_\nu^m\ (x) = (-2)^{-m}\ \Gamma\ (\nu\text{+}m\text{+}1)\ (1-x^2)^{\frac{1}{2}m}$$

$$X\ \ F(\ 1\text{+}m\text{+}\nu,\ m\text{-}\nu;\ 1\text{+}m;\ \frac{1\ -\ x}{2}\ ) \qquad (C.2)$$

where

$$F\ (\ a,\ b\ ;\ c\ ;\ y\ ) = \frac{\Gamma(c)}{\Gamma(b)\Gamma(a)} \sum_{n=0}^{\infty} \frac{\Gamma(a+n)\ \Gamma(b+n)}{\Gamma(c+n)} \frac{y^n}{n!} \qquad (C.3)$$

and $\Gamma\ (\ s\ )$ is the Gamma function of a complex argument s.

Except for the case $\nu = 1$ the Legendre functions of the second kind were used as First kind functions according to the identity

$$P_\nu^\mu(-x) = P_\nu^\mu(x)\ \cos[\pi\ (\nu + \mu)]\ -\ 2\ \pi^{-1}\ Q_\nu^\mu(x)\ \sin\ [\pi\ (\nu+\mu)]. \qquad (C.4)$$

The evaluation of the Legendre functions ($\mu = 0$) of the first kind will be obtained from special forms which converge most rapidly in the vicinity of the points $\phi = 0,\ \pi/2$, and π and it will serve both $P_\nu(\cos\phi)$ and $P_\nu(-\cos\phi)$ when the appropriate intervals are switched. Thus for points near $\phi = 0$, we use

$$P_\nu(\cos\phi) = F\ (\ -\nu,\ \nu+1;\ 1;\ \sin^2\ \frac{\phi}{2}\ ). \qquad (C.5)$$

For points near $\phi = \pi\ /2$, we use

$$P_\nu(\cos\phi) = \frac{\Gamma\left(\frac{\nu+1}{2}\right)\ \cos(\nu\pi/2)}{\pi^{1/2}\ \Gamma\left(\frac{\nu}{2}+1\right)}\ F\left(\frac{\nu+1}{2},\ -\frac{\nu}{2};\ \frac{1}{2};\ \cos^2\phi\right) \qquad (C.6)$$

$$+\ \frac{2x\Gamma\left(\frac{\nu}{2}+1\right)\ \sin(\nu\mu/2)}{\pi^{1/2}\ \Gamma\left(\frac{\nu+1}{2}\right)}\ F\left(\frac{\nu}{2}+1,\ \frac{1\ -\ \nu}{2};\ \frac{3}{2};\ \cos^2\phi\right)$$

and for points near $\phi = \pi$, we use

$$\frac{\pi}{\cos \nu\pi} P_\nu(\cos\phi) = \left[\log\frac{1+x}{1-x} + \psi(\nu+1) + \psi(-\nu) + 2\,C\right] F\left[-\nu,\ \nu+1;\ 1;\ \frac{1+x}{2}\right]$$

$$- 2 \sum_{r=0}^{\infty} \frac{(-\nu)_r (\nu+1)_r}{(r!)^2} \left(\frac{1+x}{2}\right)^r \left[\sum_{\alpha=1}^{r} \frac{1}{\alpha}\right] \qquad (C.7)$$

where $x = \cos\phi$, $\psi(...)$ denotes the logarithmic derivative of the Gamma function, C is the Euler's constant or else defined as $C = \psi(1)$ and $(\nu)_r$ is defined by

$$(\nu)_r = \nu\ (\nu+1).....(\nu+r-2)(\nu+r-1). \qquad (C.8)$$

The associated Legendre functions and their derivatives are calculated from the following recursion formulas:

$$P_\nu^1(\cos\phi) = \frac{\nu+1}{\sin\phi}\left[P_{\nu+1}(\cos\phi) - \cos\phi\ P_\nu(\cos\phi)\right] \qquad (C.9)$$

$$P_\nu^m(\cos\phi) = -\,[2(m-1)\cot\phi\ P_\nu^{m-1}(\cos\phi) + (\nu - m + 2)(\nu + m - 1)\ P_\nu^{m-2}(\cos\phi)\,] \qquad (C.10)$$

and they are also valid for the function $P_\nu^m(-\cos\phi)$ for which ϕ is replaced by $\pi - \phi$. The derivatives with respect to ϕ are calculated from

$$\frac{d}{d\phi} P_\nu(\cos\phi) = P_\nu^1(\cos\phi)$$

$$\frac{d}{d\phi} P_\nu(-\cos\phi) = - P_\nu^1(-\cos\phi) \qquad (C.11)$$

$$\frac{d}{d\phi} P_\nu^m(-\cos\phi) = (\nu - m + 1)(\nu + m) P_\nu^{m-1}(\cos\phi) - m \cot\phi \, P_\nu^m(-\cos\phi).$$

A particular case of the Legendre functions is the one of order $\nu = -\frac{1}{2} + i\tau$ which eventhough retains all the properties (except for a number of recursion formulas) of the Legendre functions it is real in the domain -1 to +1 despite the complex parameter ν. For large values of τ the following formulas hold:

$$P^m_{-.5 + i\tau}(\cos\phi) = \frac{\tau^{m-\frac{1}{2}}}{\sqrt{2\pi \sin\phi}} e^{\tau\phi} \left[1 - \frac{m^2 - \frac{1}{4}}{2\tau} \cot\phi + O(\tfrac{1}{\tau^2})\right] \qquad (C.12)$$

and

$$P^m_{-.5 + i\tau}(-\cos\phi) = \frac{\tau^{m-\frac{1}{2}}}{\sqrt{2\pi \sin\phi}} e^{\tau(\pi-\phi)} \left[1 + \frac{m^2 - \frac{1}{4}}{2\tau} \cot\phi + O(\tfrac{1}{\tau^2})\right]. \qquad (C.13)$$

The limiting conditions of the kernels encountered in the analysis are satisfied with the use of the following limiting values of the Legendre functions:

$$\lim_{\phi \to 0} P_\nu(\cos\phi) = 1$$

$$\lim_{\phi\to 0} P_\nu(-\cos\phi) = (2/\pi)\sin\nu\pi\,[\,\psi(\nu+1) + C + \lim_{\phi\to 0}\log\sin(\phi/2)\,] + \cos\nu\pi$$

$$\lim_{\phi\to 0} P_\nu^1(\cos\phi) = -\lim_{\phi\to 0}\nu(\nu+1)\,\phi/2 \qquad (C.14)$$

$$\lim_{\phi\to 0} P_\nu^1(-\cos\phi) = -(2/\pi)\sin\nu\pi \lim_{\phi\to 0}[\,1/\phi - \phi\,\nu(\nu+1)\,(\pi\cot\nu\pi + K)/4\,]$$

$$\lim_{\phi\to 0} Q_\nu(\cos\phi) = -[\lim_{\phi\to 0}\log\sin(\phi/2) + \psi(\nu+1) + C\,]$$

$$\lim_{\phi\to 0} Q_\nu^1(\cos\phi) = \lim_{\phi\to 0}[\,-1/\phi + \phi\,\nu(\nu+1)\,K/4\,]$$

where

$$K = 2\log\sin(\phi/2) + \psi(\nu+2) + \psi(\nu) + 2C - 1. \qquad (C.15)$$

Also from the relationship between $P^m_{-.5+i\tau}(-\cos\phi)$, $P^m_{-.5+i\tau}(\cos\phi)$ and $Q^m_{-.5+i\tau}(\cos\phi)$:

$$P^m_{-.5+i\tau}(-\cos\phi) = \frac{(-1)^m}{\pi}\cosh\tau\pi\,[Q^m_{-.5+i\tau}(\cos\phi) + Q^m_{-.5-i\tau}(\cos\phi)] \qquad (C.16)$$

we obtain the limiting velues of the spherical toroidal functions $P^{m}_{-.5 + i\tau}$ which are also real as seen from the relation above. We should note that in general that the functions of the second kind $Q^{m}_{-.5 + i\tau}(x)$ can assume complex values. However in the interval $-1 \leq x \leq 1$ the functions $P^{m}_{-.5 + i\tau}(-x)$ are defined as solutions of the Legendre equation linearly independent of $P^{m}_{-.5 + i\tau}(x)$ and considered as solutions of the second kind. But it obvious though from the last relation that the final result is real since the quantities inside the brackets are complex conjugates.

REFERENCES

1. Reissner E., "Stresses and Small Displacements of Shallow Spherical Shells, I, II," Journal of Mathematics and Physics, vol. 25, pp. 80-85, 27, pp. 279-300,1947.

2. Reissner E., "On the Determination of Stresses and Displacements for Unsymmetrical Deformations of Shallow Spherical Shells," Journal of Mathematical Physics, vol. 38, pp. 16-35, 1959.

3. Reissner E., "On Bending of Elastic Plates," Quarterly of Applied Mathematics, vol. 5, pp. 55-68, 1947.

4. Reissner E., and Wan F. Y. M., "On the Effect of Transverse Shear Deformability on Stress Concentration Factors for Twisted and Sheared Shallow Spherical Shells," Journal of Applied Mechanics, Vol. 53, pp. 597-601, 1986.

5. Naghdi P. M., "On the Thoory of Thin Elastic Shells," Quarterly of Applied Mathematics, vol.14, pp. 369-380, 1957.

6. Naghdi P. M., "Note on the Equations of Shallow Elastic Shells," Quarterly of Applied Mathematics, Vol. 14, pp. 331-333, 1956.

7. Simmonds G. J., "Green's Functions for Closed Elastic Spherical Shells, Exact and Accurate Asymptotic Solutions," Proceedings of the Koninklijke Nederlandse Academie van Wetenschappen, Series B,

Vol. 71, No. 3, pp. 236-249, 1968.

8. Sanders J. L.,JR and Simmonds J. G., "Concentrated Forces on Shallow Cylindrical Shells," Journal of Applied Mechanics, ASME Paper, No. 70- WA/APM-2, 1970.

9. Simmonds J. G. and Tropf C. G., "The Fundamental (Normal Point Load) Solution for a Shallow Hyperbolic Paraboloidal Shell," Journal of Applied Mathematics, Vol. 27, No.1, pp. 102-120, 1974.

10. Sanders J. L. JR, "Singular Solutions for Shallow Shell Equations," ASME Paper No. 70-WA/APM-1, vol. 37, pp. 361-364, 1970.

11. Flugge W., "Concentrated Forces on Shells," Applied Mechanics-Proceedings of the Eleventh International Congress of Applied Mechanics, Springer-Verlag, pp. 270-276, 1964.

12. Forsberg K. and Flugge W., "Point Load on a Shallow Elliptic Paraboloid," ASME Paper no.66-APM-V, 1966.

13. Flugge W. and Elling R. E., "Singular Solutions for Shallow Shells," International Journal of Solids and Structures, Vol. 8, pp. 227-247, 1972.

14. Flugge W., "Stresses in Shells," Translation, Springer-Verlag, Berlin, Gottingen, Heidelberg, 1960.

15. Lucasiewicz S., "Concentrated Loads on Shallow Spherical Shells," Quarterly Journal of Mechanics and Applied Mathematics, Vol. 20, pp. 293-305, 1967.

16. Chernyshev G. N., "On the action of Concentrated Forces and Moments on an Elastic Thin Shell of Arbitrary Shape," Journal of Applied Mathematics and Mechanics (Prikladnaya Matematika i Mekhanika), Vol. 27, pp. 172-184, 1963.

17. Nordgren R. P., "On the Method of Green's Functions in Thermoelastic Theory of Shallow Shells," International Journal of Engineering Science, Vol. 1, pp. 279-308, 1963.

18. Koiter W. T., "A Spherical Shell Under Point Loads at Its Poles," Progress in Applied Mechanics-The Prager Anniversary Volume, McMillan Company, pp. 155-169, 1963.

19. Berry J. G., "On Thin Hemispherical Shells Subjected to Concentrated Edge Moments and Forces," Proceedings of the 2nd Midwestern Conference on Solid Mechanics, pp. 25-44, 1955.

20. Kalnins A., "On Vibrations of Shallow Spherical Shells," Journal of the Acoustical Society of America, Vol. 33, pp. 1102-1107, 1961.

21. Kalnins A., "Effect of Bending on Vibrations of Spherical Shells," Journal of the Acoustical Society of America, Vol. 36,

pp. 74-81, 1964.

22. Wilkinson J. P. and Kalnins A., "On Nonsymmetric Dynamic Problem of Elastic Spherical Shells," Journal of Applied Mechanics, Vol. 87, Trans. ASME, Vpl. 88, Series E, pp.31-38, 1966.

23. Wilkinson J. P. and Kalnins A., "Deformation of Open Spherical Shells Under Arbitrarily Located Concentrated Loads," Journal of Applied Mechanics, Series E, Paper No. 65-WA/APM-24, pp. 305-312, 1966.

24. Kalnins A., "On Fundamental Solutions and Green's Functions in the Theory of Elastic Plates," Journal of Applied Mechanics, Paper No. 65-WA/APM-23, 1966.

25. Prasad C., "On Vibrations of Spherical Shells," Journal of the Acoustical Society of America, Vol. 36, pp. 489-494, 1964.

26. Copley L. G. and Sanders J. L. JR, "A Longitudinal Crack in a Cylindrical Shell Under Internal Pressure," International Journal of Fracture Mechanics, Vol. 5, pp. 117-131, 1969.

27. Erdogan F. and Kibler J. J., "Cylindrical and Spherical Shells With Cracks," International Journal of Fracture Mechanics, Vol. 5, pp.229-237, 1970.

28. Krenk S., "Influence of Transverse Shear on an Axial Crack in a

Cylindrical Shell," International Journal of Fracture Mechanics, Vol. 14, pp. 123-143, 1978.

29. Delale F. and Erdogan F., "Effect of Transverse Shear and Material Orthotropy in a Cracked Spherical Cap," International Journal of Solids and Structures, Vol. 15, pp. 907-926, 1979.

30. Kraus H., "Thin Elastic Shells," New York, 1972.

31. Love A. E. H., "Mathematical Theory of Elasticity," Fourth Edition, Cambridge University Press, 1927.

32. Novozhilov V. V., "The Theory of Thin Shells," (Translated from the Russian) , P. Noordhoff Ltd.-Groningen-The Nederlands, 1959.

33. Sadegh A. M. and Altiero N. J., "A Boundary Integral Method Applied to the Problem of an Elastic Region Weakened by an Arbitrarily-Shaped Hole," Mechanics Research Communications, Vol. 6(3), pp. 167-175, 1979.

34. Sadegh A. M. and Altiero N. J., "Solution of the problem of a crack in a finite plane region using an Indirect Boundary Integral method." Journal of Engineering Fracture Mechanics, Vol.11, pp. 831-837,1979.

35. Altiero N. J. and Sikarskie D. L., "A Boundary Integral Method Applied to Plates of Arbitrary Plan Form," Computers and

Structures, Vol. 9, pp. 163-168, 1978.

36. Banerjee P. K. and Butterfield R., "Boundary Element Methods in Engineering Science," McGraw Hill Book Company.

37. Magnus W. , Oberhettinger F. and Soni R. P., "Formulas and Theorems for the Special Functions of Mathematical Physics," Third Edition, Springer-Verlag, 1966.

38. Abramowitz M. and Stegum I. A., "Handbook of Mathematical Functions," U.S. Government Printing Office, 1964.

39. Bergman S. and Schiffer M., "Kernel Functions and Elliptic Differential Equations in Mathematical Physics," Academic Press, New York, 1953.

40. Courant R. and Hilbert D., "Methods of Mathematical Physics," Interscience, John Wiley, 1953.